The P-Rex1 Regulator Norbin Suppresses Neutrophil-Dependent Antibacterial Immunity

Chiara Pantarelli

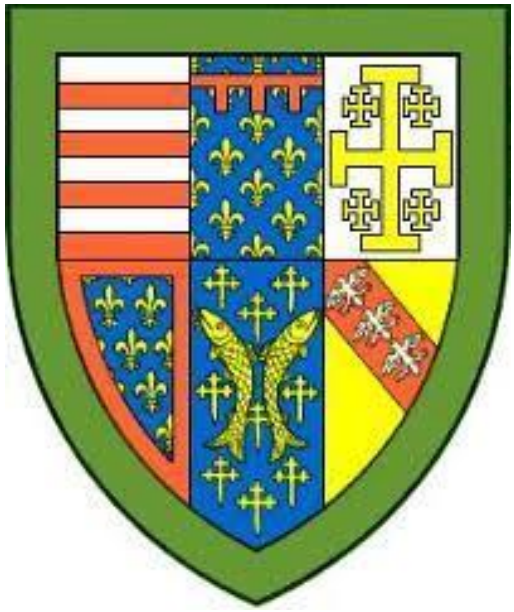

Queens' College

August 2019

This dissertation is submitted to The University of Cambridge
for the degree of Doctor of Philosophy

Welch Group
Signalling Programme
The Babraham Institute
Cambridge
United Kingdom
CB22 3AT

Table of Contents

Declaration

This dissertation is the result of my own work and includes nothing which is the outcome of work done in collaboration except where specifically indicated in the text.

Statement of Length

This dissertation does not exceed the word limit prescribed by the Degree Committee for the Faculty of Biology

Acknowledgements

I owe my gratitude to so many people who have been with me on this scientific and emotional journey over the last four years. It is impossible for me to pick one memory over another or pick out a few people among the many. I will be ever grateful to all whom I have met over these past few years for making my time in Cambridge unforgettable. One person who I will be eternally grateful for is my wonderful supervisor Heidi. If it were not for her, things would have been very different for me. By giving me the opportunity to do my Ph.D. at the Babraham Institute, she has definitely changed my life for good. I thank her for being patient and kind with me, for guiding me and giving me the enthusiasm to undertake this project. She made me love what I was doing, allowing me to swear and cry tears of joy or anger when I was at the bench, and dataset by dataset she gave me the confidence that I could do research. My rollercoaster Ph.D. would have not been the same without the constant support of the past and present lab fellows. Thank you Kirsti, Anna-Karin and Laraine for being my example of scientists with an amazing brain and a big heart; I will never be able to thank them enough for all their personal and professional advice, especially when things went wrong. Thank you to Martin for answering all my questions when I arrived in the Welch lab family. To Elpida, my fellow companion in this whole process, thanks for being there listening to all my struggles, for somehow always looking at the bright side and for never leaving me behind when I was lost. To Polly, who has definitely added highs to these Women in Science Crew. To Simon, for teaching me the beauty of looking deeper, thus expanding myself broader. Thanks to the Signalling family for sharing their considerable knowledge and experience, as well as their genuine interest in my work, making me feel lucky to be part of the bright side of the building. Most of all I feel immensely lucky for having shared a piece of my life with the people I rely on, those I met on the way and those that decided to go (each of them have brought fun and colour into my life). To all, and for all, I am grateful and will never cease to be. To Izzy and Piotr, thanks for all the love, the laughs, the mental support that helped me through the tough months that at the end allowed me to find myself again. To the Carter-Williamson family, thanks for bringing me with you every time I needed a nest, for making me feel that I was not so far from my family afterall. Finally, I have dedicated this thesis to “The Magnificent Seven”, to Marivi’ and Mia for encouraging

me and sharing my happiness over those innumerable video calls throughout the latitude and longitude of this big world.

Acknowledgements of assistance

Initial training in techniques, laboratory practice, and subsequent mentoring

General laboratory techniques – Dr Heidi Welch, Dr Kirsti Hornigold, Dr Anna-Karin Johnsson, Dr Martin Baker (Heidi Welch Lab, Babraham Institute)

In Vivo animal *Streptococcus pneumoniae* model – Dr Anne-Katrien Stark (Klaus Okkenhaug Lab Babraham Institute)

Training in microscopy and image analysis – Simon Walker, Hanneke Okkenhaug (Babraham Institute)

Training in Flow cytometry and flow cytometry analysis – Dr Rachel Walker, Dr Attila Bebes, Dr Rebecca Roberts, Dr Anne-Katrien Stark, Dr Rafeah Alam, Fiorella Cugliandolo

Data obtained from a technical service provider

Statistics – Dr Anne Segonds-Pichon (Babraham Institute Bioinformatics Service)

Mouse genotyping – Transnetyx

Data produced jointly (e.g. where it was necessary or desirable to have two people performing an experiment)

In vivo S. pneumoniae infection experiments were performed with the help of the Biological Support Unit (BSU) from the Import facility of the Babraham Institute Animal House.

Materials provided by someone else

Prex1$^{-/-}$ Prex2$^{-/-}$ mouse strains – Dr Heidi Welch (Babraham Institute)

Anti-Norbin antibodies – Kie Maruyana (National Institute for Physiological Sciences, Japan)

Ncdn$^{fl/fl}$ mice – Akiyoshi Fukamizu (University of Tsukuba, distributed by Riken, Japan)

Streptococcus pneumoniae TIGR4, serotype 4 (University College, London, originally provided by Prof. Jeremy Brown to Dr Anne-Katrien Stark).

Papers published as a result of the work presented in this thesis

See Appendix B

P-Rex1

Hornigold K., Tsonou E., Pantarelli C., Welch HC.
Encyclopedia of Signaling Molecules, 2nd Edition, Editor S Choi. 2018

P-Rex2

Tsonou E., Pantarelli C., Hornigold K., Welch HC.
Encyclopedia of Signaling Molecules, 2nd Edition, Editor S Choi. 2018

Rac-GTPases and Rac-GEFs in neutrophil adhesion, migration and recruitment

Pantarelli C., Welch HC.
European Journal of Clinical Investigation 2018

List of Figures

List of Tables

List of abbreviations

Arp2/3	Actin Related Protein-2/3
ATP	Adenosine Triphosphate
AC	Adenylate Cyclase
AF647	Alexa Fluor 647
Arf	ADP-Ribosylation Factor
APS	Ammonium Persulphate
ANOVA	Analysis of Variance
AUC	Area Under the Curve
BSA	Bovine Serum Albumin
βarr	Beta Arrestin
C5a	Complement component 5a
C5aR	Complement component 5a Receptor
CH	Calponin Homology
CXCR1	CXC Chemokine Receptor 1
CXCR2	CXC Chemokine Receptor 2
CXCR4	CXC Chemokine Receptor 4
DAG	Diacylglycerol
DAPI	4',6-diamidino-2-phenylindole
DEP	Dishevelled, Egl-10 and Pleckstrin domain
DH	Dbl Homology
DOCK	Dedicator of Cytokinesis
DNA	Deoxyribonucleic Acid
dNTP	Deoxyribonucleotide Triphosphate
Dbl	Diffuse B-cell Lymphoma
DHR1	DOCK Homology Region 1
DHR2	DOCK Homology Region 2
DMSO	Dimethyl Sulfoxide
DPBS	Dulbecco's Phosphate-Buffered Saline
DTT	Dithiothreitol
ER	Endoplasmic Reticulum
ELMO	Engulment and Motility
ECL	Enhanced Chemiluminescence
EDTA	Ethylenediaminetetraacetic Acid
EGTA	Ethyleneglycoltetraacetic Acid
ERK	Extracellular Regulated Kinase
FAF-BSA	Fatty Acid Free - Bovine Serum Albumin
FLII	Flightless-1 homolog
FBS	Foetal Bovine Serum
FFA	Free Fatty Acid
FITC	Fluorescein Isothiocyanate
fMLP	N-Formyl Methionyl-Leucyl-Phenylalanine
GAP	GTPase Activating Protein
GEF	Guanine Nucleotide Exchange Factor
GPCR	G Protein-Coupled Receptor
G Proteins	Guanine-Nucleotide Binding Proteins
GDP	Guanosine Nucleotide Diphosphate
GDI	Guanosine Nucleotide Dissociation Inhibitor

GM-CSF	Granulocyte Macrophage-Colony Factor
GRK	G protein-coupled Receptor Kinase
GTP	Guanosine Nucleotide Triphosphate
LPS	Lipopolysaccharides
LFA-1	Lymphocyte Function-associated Antigen-1
LIMK1/2	LIM Kinase
LPA	Lysophosphatidic acid
LTD	Long-Term Depression
LB	Luria Bertiani
HBSS	Hank's Balanced Salt Solution
HEK293	Human Embryonic Kidney 293
Hepes	4-(2-hydroxyethyl)-1-piperazineethanesulfonic acid
HRP	Human Embryonic Kidney 293
ICAM-1	Intercellular Adhesion Molecule-1
PVDF	Immobilon-P Polyvinylidene Fluoride
IP4P	Inositol Polyphosphate 4-Phosphatase
IP_3	Inositol-1,4,5-Trisphosphate
IL-8	Interleukin-8
IP	Inositol Phosphate
IPGTT	Intraperitoneal Glucose Tolerance Test
i.p.	Intraperitoneally
i.v.	Intravenously
JNK	c-Jun N-terminal Protein Kinase
kDa	Kilo Dalton
Mac-1	Macrophage-1 Antigen
MAPK	Mitogen Activated Protein Kinase
mGluR1	Metabotropic Glutamine Receptor-1
mGluR5	Metabotropic Glutamine Receptor-5
mTOR	Mammalian Target of Rapamycin
mTORC1	Mammalian Target of Rapamycin Complex 1
mTORC2	Mammalian Target of Rapamycin Complex 2
NF-κB	Nuclear Factor-kappa-B
PA	Phosphatidic Acid
PAK	p21-Activated Protein Kinase
PAE	Porcine Aortic Endothelial
PAF	Platelet Activating Factor
PBS	Phosphate-Buffered Saline
PE	Phycoerythrin
PH	Pleckstrin Homology
PKB	Protein Kinase B (also known as AKT)
PMA	Phorbol 12-Myristate 13-Acetate
PMSF	Phenylmethylsulfonyl Fluoride
PTEN	Phosphatase and Tensin Homolog Deleted from Chromosome 10
PI	Phosphatidylinositol
PIP_3	Phosphatidylinositol 3,4,5-triphosphate / PtdIns(3,4,5)P_3
PI(3,4)P_2	Phosphatidylinositol 3,4-bisphosphate
PI(4,5)P_2/PIP_2	Phosphatidylinositol 4,5-bisphosphate / PtdIns(4,5)P_2
PREX1	Phosphatidylinositol-3,4,5-trisphosphate-Dependent Rac Exchange Factor 1
PREX2	Phosphatidylinositol-3,4,5-trisphosphate-Dependent Rac Exchange Factor 2

PI3K	Phosphoinositide 3 Kinase
PDK1	Phosphoinositide-Dependent Protein Kinase 1
PCR	Polymerase Chain Reaction
PDZ	Postsynaptic-Density Protein, Discs Large, Zona Occludens-1
PLCβ	Phospholipase-C-β
PKA	Protein Kinase A
PKB/Akt	Protein Kinase B
PKC	Protein Kinase C
PP1α	Protein Phosphatase-1α
PSGL-1	P-Selectin Glycoprotein Ligand-1
Rho	Ras homologous
Ras	Ras Sarcoma
Ran	Ras-Like Nuclear Protein
Rab	Ras-Like Proteins in Brain
ROS	Reactive Oxygen Species
RTK	Receptor Tyrosine Kinase
RGS	Regulator of G Protein Signalling
RNA	Ribonucleic Acid
S1P	Sphingosine-1-Phosphate
S1PR1	Sphingosine-1-Phosphate Receptor
SNP	Single Nucleotide Polymorphism
SDS-PAGE	Sodium Dodecyl Sulphate-Polyacrylamide Gel Electrophoresis
SDF-1α	Stromal cell-Derived Factor-1α
SH2	Src Homology 2
SH3	Src Homology 3
SHP2	Src Homology Region 2 Domain-Containing Tyrosine Phosphatase-2
SEM	Standard Error of the Mean
TEMED	Tetra-Methyl-Ethylenediamine
TBS	Tris Buffered Saline
TBS-T	Tris Buffered Saline - Tween-20
TBE	Tris/Borate/EDTA
TGFβ	Transforming Growth Factor β
TNF-α	Tumour Necrosis Factor-α
TRAIL	TNF-related apoptosis-inducing ligand
v/v	Volume/Volume
w/v	Weight/Volume
WT	Wild Type

Abstract

P-Rex1 is a guanine-nucleotide exchange factor (GEF) that activates the small G protein Rac, thus regulating a wide range of physiological and pathophysiological responses. Neutrophils are leukocytes of the innate immune system in which P-Rex1 regulates several Rac-dependent responses, especially those elicited by GPCR signalling.

The aim of my project was to assess the functional importance of a new interactor of P-Rex1, the GPCR adaptor protein Norbin, in neutrophils.

Norbin is an essential neuronal protein that binds directly to GPCRs, regulating GPCR signalling and trafficking, through unknown mechanisms. Our laboratory recently identified that Norbin stimulates P-Rex1 Rac-GEF activity and promotes P-Rex1 membrane localisation. Furthermore, we showed that Norbin is expressed in myeloid cells. To investigate, we generated mouse strains with conditional deletion of Norbin in myeloid cells and with combined Norbin/Prex1 deficiency.

Unexpectedly, I found increased adhesion, spreading, ROS production and degranulation responses in isolated Norbin-deficient neutrophils. Moreover, Norbin-deficient neutrophils had an increased ROS-dependent capacity to kill *Staphylococcus aureus*. *In vivo*, Norbin deficiency provided increased immunity against pulmonary infection with *Streptococcus pneumoniae*, even in immune-deficient $Prex^{-/-}$ mice. Neutrophil depletion showed that Norbin deficiency renders neutrophils important for combatting this infection. Mostly, Norbin deficiency overrode the functional impairments caused by Prex1 deficiency, although some neutrophil responses remained P-Rex1-dependent. Mechanistically, the Norbin deficiency caused constitutive upregulation of some GPCRs onto the neutrophil surface and promoted the GPCR-dependent activities of Rac and Erk, whereas several other signalling pathways and the surface levels of adhesion molecules were not obviously affected.

Together, my data indicate that the GPCR adaptor and P-Rex1 regulator Norbin plays an important role in suppressing the host defence functions of neutrophils. A subset of Norbin functions are P-Rex1 dependent, whereas others are likely mediated through other regulators of Rac and of Erk, as well as through the control of GPCR trafficking.

Chapter 1 - Introduction

1.1 Neutrophils

Neutrophils are an essential component of the innate immune system and are the first cells recruited to the site of infection. They provide immunity against bacterial and fungal infections, as well as attracting other immune cells to the site of inflammation. This section will summarise our current understanding of neutrophil development: how they are maintained in the circulation, their recruitment into tissues in response to pathogens, and, their functional responses at sites of infection and how they are removed from tissues.

1.1.1 Neutrophil development

Neutrophils are produced in the bone marrow. They are polymorphonuclear leukocytes (PMNs), the most abundant white blood cells in humans, known for their segmented nucleus, for their granules and for being short-lived. Each day, approximately 10^{11} neutrophils are produced under normal conditions (Furze & Rankin, 2008; Manz & Boettcher, 2014). The rate of neutrophil production is highly dynamic, with neutrophil death by apoptosis and immunological stress conditions being the main elements that influence this process. One of the main regulatory factors for tuning the production of neutrophils is granulocyte-colony stimulating factor (G-CSF) (Metcalf, 2007). G-CSF levels are upregulated with neutrophil apoptosis in tissues and reduced when the number of neutrophils in tissues is high (Lieschke et al., 1994; F. L. Liu, Wu, Wesselschmidt, Kornaga, & Link, 1996). Under immunologically stressed conditions (inflammation and infection), neutrophil numbers rise through the increased proliferation and maturation of progenitor cells (granulopoiesis) induced in response to the production of several cytokines, e.g. IL-17 (Cua & Tato, 2010), IL-3 and granulocyte-macrophage colony stimulating factor (GM-CSF) (Skokowa et al., 2006).

Several stages of neutrophil maturation can be distinguished (Figure 1.1), beginning with haematopoietic stem cells (HSCs) in the bone marrow which generate several consecutive mitotic pools of progenitor cells that are decreasingly proliferative and successively more differentiated, namely myeloblast, promyelocyte, myelocyte and band cell stages. These different stages are characterised by the shape of the nucleus, which becomes segmented, and by the increasing number of granule subsets. Key transcription factors in the

development of neutrophils are PU.1, which is required for myeloid lineage commitment, giving rise to both monocytes/macrophages and granulocytes, and C/EBP, which induces the granulocyte lineage, followed by Gfi-1 which confers neutrophil differentiation. The bone marrow also comprises a reserve pool of mature neutrophils, approximately 20 times the number of neutrophils in circulation (Dancey, Deubelbeiss, Harker, & Finch, 1976). These fully differentiated mature neutrophils are defined as the post-mitotic pool, ready for on-demand release (Borregaard, 2010). This terminally differentiated mature neutrophil state cannot be reversed, the cells can only live around one day in the circulation and a few days at most within tissues before progressing to their death, usually by apoptosis (Klausen, Bjerregaard, Borregaard, & Cowland, 2004) (see section 1.1.5).

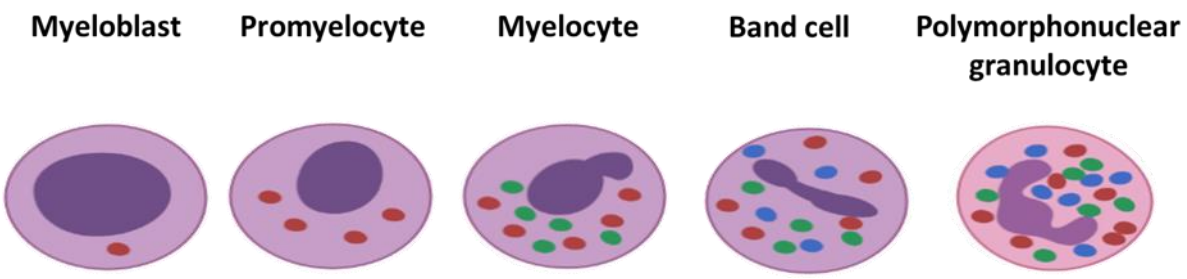

Figure 1.1: Granulocytopoiesis in the bone marrow
Neutrophil maturation from myeloid progenitors to mature neutrophils. The nucleus becomes ingreasingly segmented. The different subsets of neutrophil granules are produced at different stages of maturation, starting with azurophil granules which contain myeloperoxidase (red), followed by specific granules that contrain lactoferrin (green) and finally gelatinase granules (blue). Figure adapted from (Borregaard, 2010).

1.1.2 Overview of neutrophil recruitment

Among leukocytes, neutrophils are the first immune cell population to penetrate the vascular endothelium. Therefore, understanding the signalling mechanism of neutrophil extravasation cascade is critical because it is an initial immune response and also affects the mobilisation of other leukocytes. Mature neutrophils circulate in the blood stream, but upon receiving inflammatory signals, they must adhere to the endothelial vessel wall and transmigrate through it to reach inflamed tissues. In most tissues, the neutrophil recruitment cascade occurs in the following steps: tethering, rolling, adhesion, crawling and, finally, transmigration (Figure 1.2) (Kolaczkowska & Kubes, 2013). There have been a large

number of studies dissecting the multiple steps of neutrophil adhesion and migration across the vessel wall (Filippi, 2019; J. Herter & Zarbock, 2013; Kolaczkowska & Kubes, 2013; Ley, Laudanna, Cybulsky, & Nourshargh, 2007; Nourshargh & Alon, 2014).

Briefly, the initial loose adhesion of neutrophils (tethering) is initiated by changes on the surface of the endothelium in response to a diverse set of inflammatory mediators, including chemoattractants (e.g. IL-8), cytokines (e.g. tumor necrosis factor, TNFα), endotoxins (e.g. lipopolysaccharide, LPS) and growth factors (e.g. granulocyte macrophage-colony factor, GM-CSF). Tethering occurs rapidly (within minutes) and proceeds to selectin-dependent rolling and then integrin-dependent adhesion through the formation of additional bonds between adhesion molecules (mainly selectin and integrins) and ligands on the neutrophil and the vascular endothelium. Once neutrophils are firmly adhered onto the endothelial surface, they undergo spreading and polarisation. These steps are prerequisite for the ability of neutrophils to migrate along the vascular wall to find a suitable place for transmigration (Filippi, 2019).

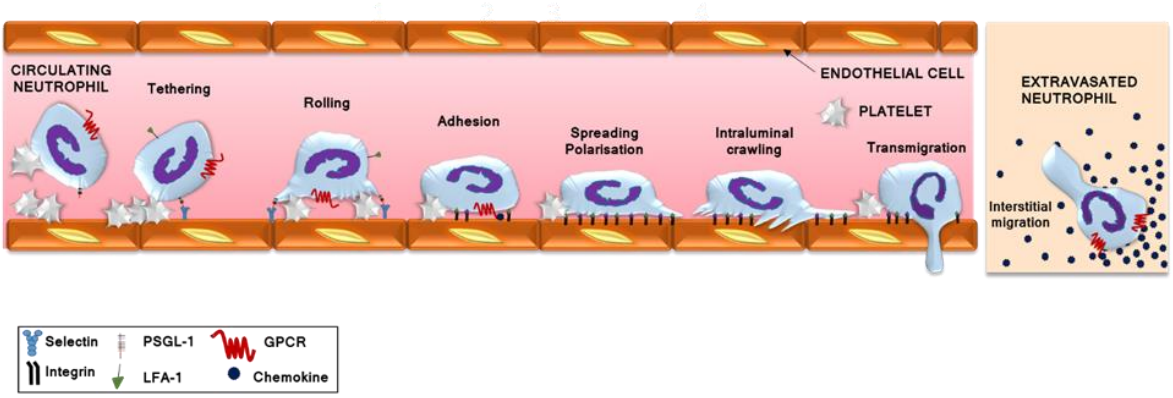

Figure 1.2: Neutrophil Recruitment Cascade
Recruitment of neutrophils from the circulation to sites of inflammation is comprised of several steps: tethering, rolling, adhesion, spreading, polarisation, intravascular crawling and transmigration. Two mechanisms of transmigration are observed: a) paracellular (between endothelial cells) and b) transcellular (through endothelial cells). Rolling is mostly selectin-dependent, whereas adhesion, crawling and transmigration depend on integrin interactions. The extravasated neutrophil in the tissue then follows chemotactic gradients to the site of inflammation or infection, using amoeboid migration that can be integrin-independent. Figure adapted from (Pantarelli & Welch, 2018).

1.1.2.1 Selectin-mediated tethering, rolling and adhesion

According to our current understanding, neutrophils first make temporary and reversible interactions with the endothelial surface. The initial stage requires the interaction of various selectin molecules with their ligands on the interacting cells (McEver & Cummings, 1997; Mocsai, Walzog, & Lowell, 2015; Mueller et al., 2010). Endothelial cells can be activated by pattern-recognition receptor (PRR)-mediated detection of pathogens, the initial host sensors of invading microbes in innate immunity (Janeway & Medzhitov, 2002), as well as cytokines and other inflammatory mediators (such as TNFα and GM-CSF), that increase the expression of adhesion molecules. They upregulate pre-stored P-selectin from secretory granules of the endothelial cell, named Weibel-Palade bodies, by fusing with the plasma membrane within minutes. Another endothelial selectin that contributes to neutrophil rolling, E-selectin, is synthetized *de novo* in response to various pro-inflammatory molecules such as TNFα, IL-1 or LPS (Ley et al., 2007; McEver, 2015; Petri, Phillipson, & Kubes, 2008). E-selectin can be detected on the endothelial surface as soon as 2 hours after the induction of an acute inflammatory response, and its expression usually turns off within 24 hours.

Once on the endothelial surface, P-selectin and E-selectin bind to their glycosylated ligands on neutrophils, including P-selectin glycoprotein ligand 1 (PSGL-1) (Faurschou & Borregaard, 2003; Ley et al., 2007; McEver, 2015; Zarbock, Ley, McEver, & Hidalgo, 2011), leading to the tethering (capturing) of free-flowing neutrophils to the surface of the endothelium and their subsequent rolling along the vessel wall in the direction of blood flow. These two selectins have partially overlapping functions in neutrophil recruitment, but P-selectin is responsible more for the initial tethering and rolling, whereas E-selectin slows the rolling down. To prevent sheer flow in the blood vessel from forcing detachment, neutrophils then begin to firmly adhere to and spread over the endothelium, and this stage is primarily mediated by members of the β2-integrin family.

Over recent years, there is strong evidence that blood platelets are functionally important for neutrophil recruitment during inflammation, by interacting both with circulating neutrophils and with the inflamed vascular endothelium. Inflammatory stimuli promote the interaction of platelets and leukocytes, leading to the formation of platelet-leukocyte conjugates which have been found free flowing in blood, as well as on the

endothelial wall and extravascularly in inflamed tissue, and these conjugates can also can be induced to form *in vitro* (Middleton, Weyrich, & Zimmerman, 2016; Page & Pitchford, 2013; Pitchford, Pan, & Welch, 2017). During neutrophil recruitment, platelets effectively form bridges between neutrophils and vascular endothelial cells by providing additional selectins and integrins, as well as other adhesion molecules (Pitchford et al., 2017). In this manner, platelets are required for neutrophil recruitment in many acute and chronic inflammatory situations, including acute septic, aseptic or allergic pulmonary inflammation, peritonitis, pancreatitis, atherosclerosis, rheumatoid arthritis and encephalomyelitis (multiple sclerosis) (Pitchford et al., 2017).

1.1.2.2 Integrin-dependent firm adhesion and crawling

Rolling and firm adhesion to the vessel wall is achieved by the upregulation of the major neutrophil β2-integrins, macrophage-1 antigen (Mac-1, CD11b/CD18) and lymphocyte function-associated antigen 1 (LFA-1, CD11a/CD18), onto the neutrophil surface. These integrins must become activated from their closed, low affinity state into their open, high-affinity conformation. Various agonists trigger integrin activation in neutrophils, including chemokines such as interleukin 8 (IL-8) and complement component factor 5a (C5a), cytokines such as TNFα and GM-CSF, and the bacterial cell wall component LPS, as well as other bacterial products such as the chemoattractant f-Met-Leu-Phe (N-formyl Met-Leu-Phe peptide, hereafter referred to as fMLP) (Morikis & Simon, 2018).

G protein-coupled receptors (GPCRs) play an important role in neutrophil recruitment by inducing both the upregulation and the high-affinity state of β2 integrins LFA-1 and Mac-1. They bind inflammatory chemokines, such as IL-8, C5a and fMLP. IL-8 is particularly important for neutrophil recruitment as it is immobilised on the luminal side of inflamed vascular endothelial cells, thus providing a ligand for rolling neutrophils, prior to firm adhesion (DiVietro et al., 2001). The GPCR-dependent upregulation and activation of integrins is also called inside-out signalling (Shen, Delaney, & Du, 2012). Once in a high affinity state, the neutrophil integrins bind to ligands such as intercellular cell adhesion molecule-1 (ICAM-1) on the endothelium, resulting in enhanced adhesion and spreading (Ley et al., 2007).

Beside firm adhesion, integrins also initiate intracellular signals in a process known as outside-in signalling. Two Src-like receptor tyrosine kinases, Fgr and Hck are essential for this signalling pathway, as well as phosphoinositide 3-kinase (PI3K) and G-protein regulators such as P-Rex and Vav (see Section 1.5.2) (Abram & Lowell, 2009; L. R. Anderson, Owens, & Naylor, 2014; Fumagalli, Zhang, Baruzzi, Lowell, & Berton, 2007; Kovacs et al., 2014). Neutrophils that lack β2 integrin-mediated outside-in signalling fail to sustain adhesion and detach from the endothelial cells under flow. The importance of integrins for neutrophil recruitment is evident in human deficiencies in the common β-chain subunit of these integrins, also called the CD18 subunit. This is known to prevent extravasation of leukocytes from blood vessels, resulting in a severe immune disorder called leukocyte adhesion deficiency type 1 (LAD-I) (Fagerholm, Guenther, Llort Asens, Savinko, & Uotila, 2019).

Once firmly adhered to the blood vessel wall, the neutrophil polarises and crawls along the intraluminal wall, which is primarily mediated by the β2-integrin Mac-1, in order to find an ideal place for transendothelial migration (Stephens, Milne, & Hawkins, 2008).

1.1.2.3 Leukocyte transmigration and interstitial migration

Neutrophil transmigration occurs either via paracellular (Vestweber, 2007) or transcellular (Carman et al., 2007; Carman & Springer, 2004) migration routes. Mostly, neutrophils transmigrate paracellularly through endothelial cell junctions, which involves the rearrangement of these junctions to facilitate the passage of the neutrophil (DiStasi & Ley, 2009; Muller, 2016). In contrast, transcellular migration involves the migration of neutrophils through the body of endothelial cells and occurs less frequently (Carman & Springer, 2004; Voisin & Nourshargh, 2013). This possibly involves the formation of ICAM-1 dependent intracellular channels (Millan et al., 2006; Yang et al., 2005).

After migrating through the endothelial layer, before entering the tissue, neutrophils encounter the basement membrane and pericytes. The basement membrane is mostly composed of laminin (e.g lamin-8 and -10) and collagen type IV, interconnected by molecules such as nidogen-2 and heparin sulphate proteoglycan. Regions of low extracellular matrix (ECM) density exist, which interestingly co-localize with gaps between adjacent pericytes. Two-photon intravital microscopy, an imaging tool that permits *in vivo* observation of neutrophil extravasation, revealed that neutrophils crawling through gaps

between adjacent pericytes requires β2 integrins (Hyun et al., 2012). Under inflammatory conditions, these gaps enlarge and are used by neutrophils as points of exit to breach the venular wall (Kapur et al., 1999; Proebstl et al., 2012; K. Stark et al., 2013). A recent study, again using two-photon intravital imaging, has observed the existence of selective hotspots for neutrophil transendothelial migration, with coordinated roles for LFA-1 and Mac-1 (Hyun & Choe, 2019). In particular, LFA-1 and Mac-1 control the stages preceding neutrophil protrusion from the endothelial basement membrane and pericyte sheath, i.e. from the point of entry into the endothelial wall up to exit of the endothelial basement membrane and pericyte sheath.

After transmigration, neutrophils migrate by chemotaxis through the interstitial tissue towards the site of inflammation. Both directionality and speed of migration contribute to effective chemotaxis. In fact, neutrophils are the fastest chemotaxing cell in the human body, with reported speeds of 19 ± 6 $\mu m.min^{-1}$ in laboratory settings (Hoang et al., 2013). The generation of polarity and subsequent directional migration are regulated by intracellular signalling pathways in response to the activation of GPCRs by ligands such as fMLP and C5a. The release of Gβγ subunits from activated GPCRs stimulates the production of the lipid second messenger phosphatidyl-inositol (3,4,5)-(trisphosphate) (PIP_3), via the activation of PI3Kγ. This PIP_3 is highly localised towards the source of the chemoattractant, resulting in polarised signalling to Rho-family small G proteins and the actomyosin cytoskeleton, and thus to the formation of a leading edge and polarisation of the cell (G. J. Ferguson et al., 2007). Consequently, this leads to coordinated neutrophil migration via the spatial organisation of Rho-family small G protein activities (see Section 1.3.2.1) (Hawkins, Stephens, Suire, & Wilson, 2010).

1.1.3 Neutrophil effector responses

Once at the site of inflammation, neutrophils can perform a wide variety of effector responses. Here, they release proinflammatory mediators to attract other inflammatory cells and mount effector functions to kill pathogens, including phagocytosis, generation of reactive oxygen species (ROS), release of granules and formation of neutrophil extracellular traps (NETs) (Nauseef & Borregaard, 2014) (Figure 1.3). In addition to the direct killing of pathogens, these combined functions enable neutrophil involvement in progressing

inflammation by stimulating macrophage recruitment, M2 macrophage differentiation (the class of macrophages associated with wound healing and tissue repair) and activation of the adaptive immune system. By influencing these responses, neutrophils also promote other physiological and pathophysiological processes, such as angiogenesis and tumour formation (Selders, Fetz, Radic, & Bowlin, 2017).

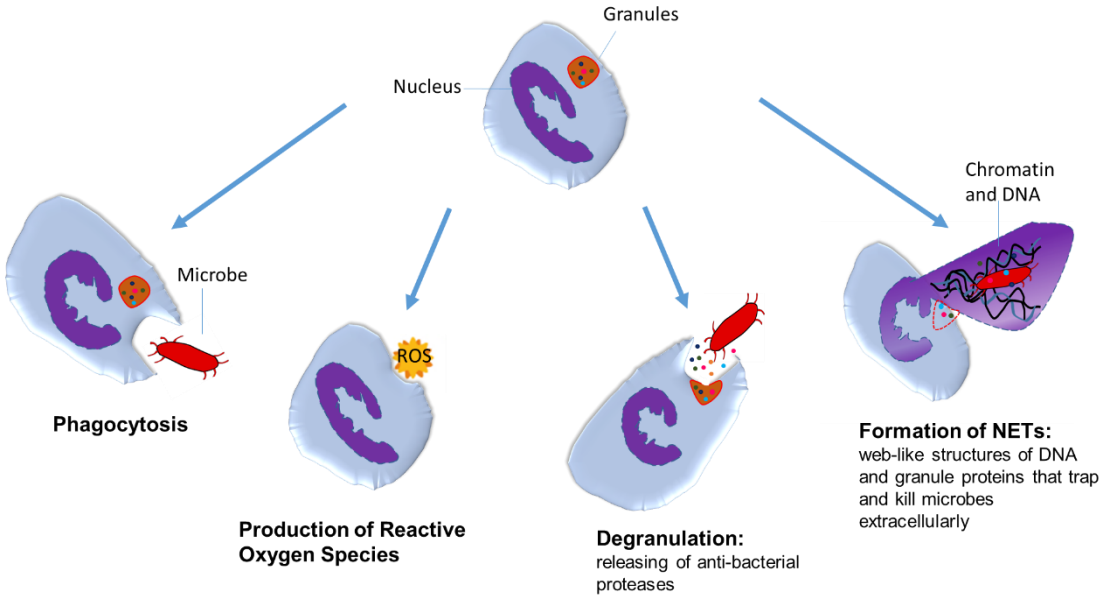

Figure 1.3: Bacterial Killing Mechanisms
Neutrophils are the major phagocyte and the principal effector cell of innate immunity in humans, with a primary role in the clearance of extracellular pathogens. Using a broad array of responses, including cytokine production, the secretion of granules and the formation of ROS and neutrophil extracellular traps (NETs), neutrophils play a crucial role in host defense against bacterial and fungal infections.

1.1.3.1 Bacterial killing mechanism

Neutrophils provide the first line of defence of the innate immune system by phagocytosing, killing, and digesting bacteria and fungi. Phagocytosis is an actin-based process used by neutrophils to clear particles greater than 0.5 µm in diameter (Gordon, 2016). Upon the activation of appropriate receptors, such as integrins and Fcγ receptors (FcR), signalling pathways are activated which lead to phagocytosis (Gu et al., 2003). The mechanism of engulfment can vary depending on the receptor that is activated, for example, the FcRs stimulate the generation of membrane protrusion that form a phagocytic cup (extracellular). In comparison, integrin-mediated phagocytosis involves the particles sinking into the cell rather than the generation of protrusions (intracellular) (Chimini & Chavrier, 2000).

Neutrophils engulf pathogens by phagocytosis and kill them via degranulation and the action of ROS. Neutrophils contain three populations of secretory granules, including azurophil granules which store antimicrobial components such as myeloperoxidase (MPO), lysozyme and defensins. These fuse preferentially with phagosomes (Amulic, Cazalet, Hayes, Metzler, & Zychlinsky, 2012; Benarafa & Simon, 2017; Borregaard, 2010; Faurschou & Borregaard, 2003). The other two types of granules are secondary and tertiary granules, which contain lactoferrin and gelatinase respectively. They can fuse either with the plasma membrane or with the phagosome, depending on the stimulus. The contents of the granules facilitate bacterial death via multiple mechanisms, including the degradation of the bacterial cell wall by lysozyme or the permeabilisation of membrane bilayers and inhibition of DNA synthesis by defensins (Amulic et al., 2012; Borregaard, 2010; Lacy, 2006).

Microbial killing also occurs through the release of ROS into the phagosome or into the extracellular environment. ROS is produced by the Nicotinamide Adenine Dinucleotide Phosphate (NADPH) Oxidase complex (Nox2, also commonly referred to as phagocyte oxidase) which makes superoxide that subsequently forms various ROS, including hydrogen peroxide (H_2O_2) (Dupre-Crochet, Erard, & Nuss, 2013; El-Benna et al., 2016; Paiva & Bozza, 2014). The multicomponent NADPH oxidase enzyme complex contains at least six essential protein components, two in the membrane and four in the cytosol. It comprises of the membrane bound $gp91^{phox}$ and $p22^{phox}$ and the cytosolic subunits $p40^{phox}$, $p67^{phox}$, $p47^{phox}$, and the small GTPase Rac2 (Babior, Lambeth, & Nauseef, 2002). Binding of ligands to GPCRs, toll-like receptors (TLRs) and cytokine receptors (e.g. TNFRs) can prime the cells (see section 1.1.4) for a more robust response of the oxidase complex, by stimulating the fusion of secretory vesicles and granules with the plasma or phagosomal membrane, thus delivering the oxidase components $gp91^{phox}$ and $p22^{phox}$ into these membranes. Upon receptor activation and signalling, the $p47^{phox}$ component is heavily phosphorylated (Heyworth, Shrimpton, & Segal, 1989), and the cytosolic components of the NADPH oxidase complex translocate to the plasma, or phagosomal, membrane forming a functional ROS producing complex (Cross & Segal, 2004; El-Benna et al., 2016; Hallett & Lloyds, 1995). The phosphorylation of $p40^{phox}$ by PKCδ and its binding to the phosphoinositide PI3P are also required for full activation of the oxidase complex (K. E. Anderson et al., 2010). Even in the absence of priming, some receptors are localised constitutively on the neutrophil surface,

such as the GPCRs for IL-8, CXCR1 and CXCR2, which can stimulate the activation of the NADPH oxidase, triggering low levels of ROS production. In contrast to the other oxidase subunits, Rac2 must be activated by GTP-loading in order to form part of the complex. Once assembled, the oxidase complex produces superoxide anions by electron transport from NADPH to O_2, and the superoxide is further converted to other ROS such as H_2O_2 and HOCl, by superoxide dismutase and myeloperoxidase, respectively. The importance of ROS formation in neutrophil function is illustrated in chronic granulomatous disease (CGD), which is caused by mutations in various proteins of the NADPH oxidase complex and is characterised by the inability of phagocytes to kill invading pathogens. This results in patients having severe recurrent fungal and bacterial infections (Dinauer, 2016; O'Neill, Brault, Stasia, & Knaus, 2015).

A third mechanism that neutrophils use to kill pathogens is the more recently identified neutrophil extracellular trap (NET). This involves the secretion of granule proteins and the active release of chromatin via a unique cell death pathway called NETosis (Fuchs et al., 2007). Granule proteins and chromatin together form extracellular fibres which bind bacteria (Brinkmann et al., 2004). The production of ROS is essential for NET formation. Multiple pathways that induce ROS production are known to lead to NETosis, especially those that also mobilise azurophil granules. For example, using a chemical library screen in human neutrophils, Hakkim et al. have shown that the Raf-MEK-ERK pathway is involved in NET formation through activation of the NADPH oxidase (Hakkim et al., 2011). In addition to NETosis, which takes several hours, Kubes et al. have described an alternative mechanism termed “non-lytic NETosis” that leads to the rapid release of NETs within minutes of exposure to *S. aureus*, via the secretion of chromatin and granule contents in the absence of cell death (Pilsczek et al., 2010). Furthermore, the importance of NETs in fighting infections may be illustrated by the increased virulence exhibited by DNase expressing bacteria (Buchanan et al., 2006; Schonrich & Raftery, 2016). The formation of NETs has also been implicated in several pathological conditions, for example the excessive formation of NETs has been linked to several autoimmune diseases, sepsis, and cancer (Jorch & Kubes, 2017; Kaplan, 2013; Khandpur et al., 2013; Saffarzadeh et al., 2012; Yipp et al., 2012).

The non-specific nature of the tools that neutrophils use to clear microorganisms means that these cells can also damage host tissues. During the resolution of inflammation,

neutrophils normally undergo apoptosis and are cleared by macrophages or other phagocytic cells (Haslett, 1999). However, the disruption of this process, by the prevention of apoptosis or due to excessive stimulation, can result in the dysregulation of neutrophil functions leading to ROS- or granule-mediated tissue damage (Kruger et al., 2015; McDaniel, Roy, & Wilgus, 2013; Segel, Halterman, & Lichtman, 2011). As a result, neutrophils are a major cause of tissue damage during inflammatory conditions such as rheumatoid arthritis, bronchiolitis and cystic fibrosis, as well as cardiovascular conditions such as acute myocardial infection and stroke (Cowburn, Condliffe, Farahi, Summers, & Chilvers, 2008). Therefore, investigating how neutrophils are activated and how they can become dysregulated is extremely important to understanding how they can maintain their beneficial roles in microbial killing whilst avoiding tissue damage (Gomez-Moreno, Adrover, & Hidalgo, 2018; Mocsai, 2013; Phillipson & Kubes, 2019; J. Wang, 2018).

1.1.4 Neutrophil priming

One of the mechanisms that allows neutrophils to be rapid effectors of the innate immune response while preventing their inadvertent activation is priming. Neutrophil priming has been extensively described (Guthrie, Mcphail, Henson, & Johnston, 1984), (Condliffe, Chilvers, Haslett, & Dransfield, 1996), (El-Benna, Dang, & Gougerot-Pocidalo, 2008; Wright, Thomas, Moots, & Edwards, 2013) and is defined as an enhanced response to activating stimuli. Exposure to pro-inflammatory cytokines, chemokines, growth factors, lipid-derived signalling molecules, as well as bacterial and viral products, induces neutrophils to transition from a basal into a primed state. Examples of such priming pathways are those mediated by the LPS receptor TLR4 and by receptors for the cytokines TNFα and GM-CSF. Upon exposure to such priming agents, neutrophils undergo a series of phenotypic changes (Miralda, Uriarte, & McLeish, 2017). Those include the shedding of L-selectin, and the fusing of secretory vesicles and granules with the plasma membrane, which leads to increased surface expression of integrin allowing primed cells to adhere to endothelial cells, as well as the upregulation of other surface receptors. These phenotypic changes are associated with the release of granule contents into the extracellular space, including matrix metalloproteases, which facilitate neutrophil migration through tissues by degrading the extracellular matrix. When primed neutrophils encounter bacteria, their microbicidal activities (ROS production, granule release, phagocytosis and NET formation) are increased due to the upregulation in

the number and affinity of receptors on the plasma membrane. Furthermore, priming prolongs neutrophil lifespan by activating anti-apoptotic signal transduction pathways and suppressing the transcription of pro-apoptotic factors.

Initially, priming has been reported as an *in vitro* phenomenon to enhance ROS production (see also section 3.6.2, Chapter Materials and Methods), degranulation, chemotaxis and NET formation, triggered by subsequent stimuli at concentrations that alone would not be sufficient to activate the cells. However, neutrophil priming is clearly also important *in vivo*, as priming agents are released in response to infection, trauma and haemorrhage, and deficiency in priming pathways leads to reduced neutrophil-mediated immunity (Deng et al., 2013; Miralda et al., 2017; Wieland et al., 2005).

1.1.5 Neutrophil lifespan and clearance

The great majority of mature neutrophils reside in the bone marrow. Studies in mice have shown that the half-life of neutrophils under non-inflammatory conditions is regulated by GM-CSF in the bone marrow (Semerad, Liu, Gregory, Stumpf, & Link, 2002). There is controversy in the literature regarding the half-life of neutrophils, and it appears that this is highly dependent on the method used to measure their lifespan (Bekkering, 2013). Several studies have reported that, within the circulation, the lifespan of neutrophils is roughly 12 hours (Basu, Hodgson, Katz, & Dunn, 2002; Summers et al., 2010), whereas one other study claimed that circulatory neutrophils have a lifespan of 5.4 days (Pillay et al., 2010). Although there is some discrepancy between these findings, it is well established that once neutrophils migrate into tissue, they are exposed to survival signals that increase their lifespan to around one week, and disease states can either up- or downregulate lifespan (Tak, Tesselaar, Pillay, Borghans, & Koenderman, 2013).

Neutrophil homeostasis is maintained through a balance of neutrophil production, release from the bone marrow (governed mainly by the opposing actions of CXCR4 and CXCR2) (see sections 1.2.2.3 and 1.2.2.4), and clearance from the circulation (Christopher & Link, 2007; Strydom & Rankin, 2013). Therefore, the homeostatic removal of neutrophils from the circulation must match their production, and this is mediated by macrophages in the liver, bone marrow stroma and the marginal zone of spleen (Gordy, Pua, Sempowski, & He, 2011; Summers et al., 2010). Mechanistically, neutrophil ageing is linked to IL-8 receptor

expression. Indeed, as neutrophils become senescent, expression of CXCR2 decreases, while the expression of CXCR4 increases (Martin et al., 2003; Nagase et al., 2002), thus increasing the responsiveness of the cells to stromal cell-derived factor (SDF-1α), the ligand of CXCR4, and resulting in the homing of senescent neutrophils to the bone marrow. Therefore, CXCR4 is not only a signal to retain new neutrophils in the bone marrow, but also homes the senescent cells back into the bone marrow for destruction. There, the senescent neutrophils undergo apoptosis and are subsequently phagocytosed by stromal macrophages (Bratton & Henson, 2011; Furze & Rankin, 2008). In parallel, phagocytosis of neutrophils in the bone marrow stimulates GM-CSF levels which in turn induces new neutrophil production. In this way, there is a positive feedback loop for neutrophil production, in which, apoptotic neutrophils in the circulation are cleared by the liver and the spleen, whereas senescent neutrophils can migrate into the bone marrow and are cleared there while at the same time stimulating the production of new neutrophils, thus maintaining a homeostatic balance (Furze & Rankin, 2008). Therefore, clearance in the bone marrow leads to new neutrophil production, while clearance in the spleen, liver and tissues reduces tissue damage. Moreover, under steady state conditions, apoptotic neutrophils are also phagocytosed by reticular endothelial macrophages in the spleen and liver, while the production of GM-CSF is suppressed to limit inflammation (Fadok, McDonald, Bratton, & Henson, 1998).

Once neutrophils have completed their anti-pathogen responses at the site of inflammation it is essential that they become apoptotic and are cleared by macrophages, to avoid tissue damage (Soehnlein & Lindbom, 2010). Under normal circumstances, this clearance process initiates a feed forward pro-resolution programme that is characterised by the release of the tissue-repairing cytokines transforming growth factor-β (TGFβ) and interleukin-10 (IL-10). When this clearance does not occur appropriately, neutrophils undergo necrosis and release intracellular contents that can damage the tissue and extend the inflammatory phase. However, neutrophils do not always die at the site where they are recruited. Early evidence suggested that neutrophils accumulating at inflamed sites do not necessarily undergo apoptosis followed by phagocytosis by macrophages (Hughes et al., 1997). Recent studies have shown that neutrophils can leave the site of tissue damage in a process termed reverse migration, which means that interstitial tissue-infiltrated neutrophils migrate away from inflamed sites (Powell et al., 2017). A study combining intravital imaging

and photoactivation techniques also demonstrated that murine neutrophils perform reverse migration from an injury site, moving back into the circulation and eventually homing back into the bone marrow (J. Wang, 2018). Moreover, another process referred to as reverse transendothelial migration (rTEM) has been described which contributes to neutrophil clearance by returning the cells into the blood stream. However, further studies need to be carried out to further clarify the fate of reverse-migrated neutrophil and the regulation of the death process that takes place in the tissues.

1.2 GPCRs and heterotrimeric G proteins

Signalling processes are tightly regulated spatially and temporally, thus integrating a multitude of different pathways and effectors in order to generate specific cell responses and localised effects. In this scenario, Guanine-nucleotide binding proteins (G proteins) are particularly important molecular tools for the coordination and interpretation of the signals provided by the external environment. There are two main classes of G proteins, monomeric G proteins (small G proteins or small GTPases), which will be introduced later in section 1.3, and heterotrimetric G proteins (large G proteins), which signal by coupling to G protein-coupled receptors (GPCRs). Both classes are characterised by their capability of binding GTP and GDP, and switching their state of activity between GTP-bound (active state) and GDP-bound (inactive state). The activation of the two classes of G proteins involves similar mechanisms, and both are important in controlling a wide variety of signalling events.

In this project, I study the regulation of the small G protein Rac and related signalling proteins in neutrophil GPCR signalling pathways, as well as the regulation of the trafficking of GPCRs that signal to Rac. Each of these topics will be introduced in detail in this chapter, beginning with GPCR signalling and trafficking.

1.2.1 G protein-coupled receptors

G protein-coupled receptors (GPCRs) are the largest family of cell surface receptor proteins. They are mainly located at the plasma membrane, and they are characterised by a signature seven transmembrane structure (Pierce, Premont, & Lefkowitz, 2002). They signal through heterotrimeric G proteins, trimeric protein complexes consisting of Gα, Gβ and Gγ subunits,

that are localised on the inner leaflet of the plasma membrane and associated with the GPCRs. GPCRs and the GPCR-coupled heterotrimeric G proteins are important regulators of physiological processes such as vision and smell, behaviour and mood, but also cell density and growth, immune surveillance and inflammation.

The main activation steps of GPCRs and their associated heterotrimeric G proteins have been elucidated in great detail (Lefkowitz, 2013; Pierce et al., 2002). The Gα subunit is a guanine-nucleotide binding protein with GTPase activity, similar to a small G protein. It is bound to GDP in basal conditions, and in response to activation by its GPCR, binds GTP. In humans, 16 different Gα subunits exist, mainly of $G\alpha_{i/o}$, $G\alpha_{s}$, $G\alpha_{q}$ or $G\alpha_{12/13}$-type, which all signal through different downstream effectors. The Gβ and Gγ subunits are a tightly bound dimer with a strong coiled-coil interaction (Sondek, Bohm, Lambright, Hamm, & Sigler, 1996). Under basal conditions, the Gβγ dimer exists in a complex with the GDP-bound Gα subunit. In humans, 6 different Gβ subunits are found and 12 Gγ, giving 72 possible dimer combinations, although not all of these occur. When the GPCR bound to the heterotrimer is activated by agonist binding on the extracellular side, it undergoes conformational change that allows it to act as a GEF to promote the exchange of GDP for GTP on the Gα subunit. This results in a conformational change in Gα, releasing the Gβγ dimer. The separated Gα subunit and Gβγ dimer are now able to interact with their respective effector proteins, leading to downstream signalling events (Lambright et al., 1996). The GTP-bound Gα subunit can interact with regulators of G-protein signalling (RGS) (Chen, Young, & Jones, 2001; Oldham & Hamm, 2008) which act as a GTPase activating protein (GAP), activating the GTPase function of the Gα subunit and resetting the system to basal state, by Gβγ re-associating with the inactive, GDP-bound Gα (Figure 1.4).

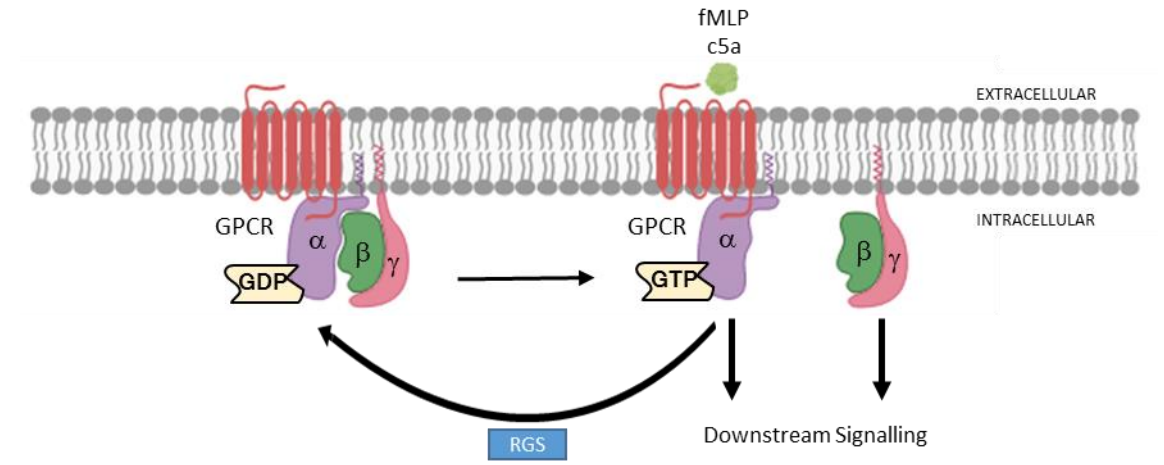

Figure 1.4: Activation cycle of heterotrimetric G proteins
Activation of a GPCR causes the receptor to act as a guanine nucleotide exchange factor (GEF), promoting GDP release from the Gα subunit of heterotrimeric G proteins, allowing GTP to bind. This leads to dissociation of Gα from Gβγ. Both Gα and Gβγ can now interact with effectors to mediate downstream signalling. The system is reset as a Regulator of G protein Signalling (RGS) interacts with the Gα subunit, acting as a GTPase-activating protein (GAP). This facilitates the Gα subunit's GTPase activity, hydrolysing GTP to GDP. The inactive GDP-bound Gα subunit reforms a complex with Gβγ subunits. Figure adapted from (Milligan & Kostenis, 2006).

1.2.1.1 Heterotrimeric G protein signalling pathways

The different classes of heterotrimeric G proteins are defined by their Gα subunits, and broadly speaking, different classes couple to different signalling pathways, although the plasticity and redundancy between these signalling networks is immense. Generally, $G\alpha_s$-type heterotrimeric G proteins are defined by their ability to activate adenylyl cyclase, thus promoting the production of cAMP and activation of PKA, whereas $G\alpha_{i/o}$ type G proteins (which are pertussis toxin, PTX, sensitive) inhibit adenylate cyclase. $G\alpha_q$ type heterotrimeric G proteins are the archetypical activators of phospholipase C β (PLCβ), which produces diacylglycerol (DAG) and inositol 3-phosphate (IP_3) from the membrane lipid phosphatidylinositol 4,5-bisphosphate (PIP_2). DAG then activates PKC, and IP_3 leads to intracellular Ca^{2+} rises (Neves, Ram, & Iyengar, 2002). $G\alpha_{12/13}$ type heterotrimeric G proteins activate RhoA-specific GEFs to modulate the structure of the cytoskeleton (Siehler, 2009). However, all heterotrimeric G proteins tend to signal through multiple pathways, for example most can activate the PLC, PLD, PI3K and Ras/Mek/Erk pathways in more-or-less direct ways. The typical signalling pathways of the different Gα protein families are summarised in Figure 1.5.

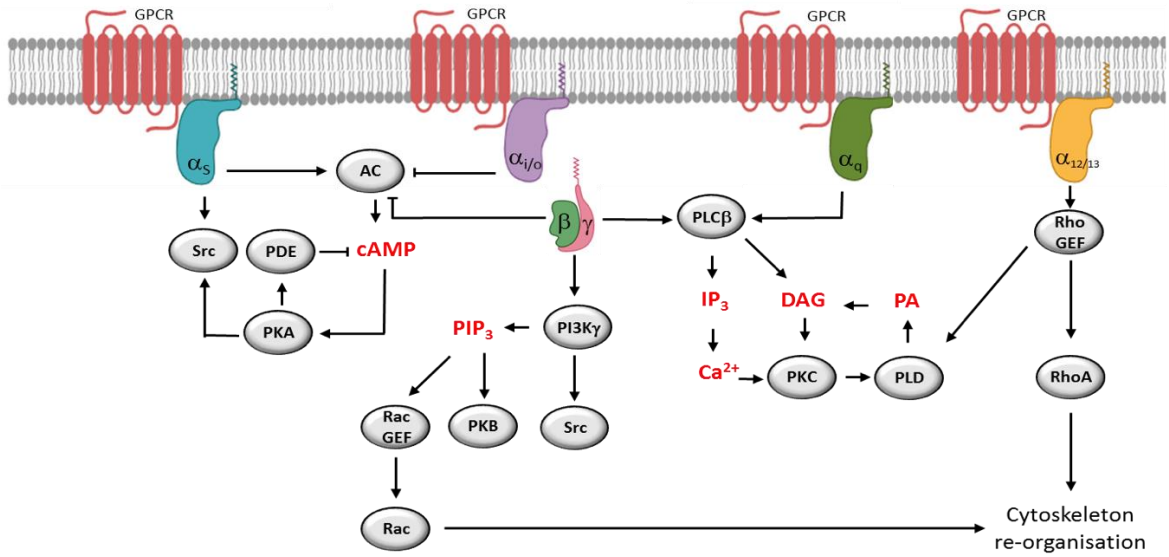

Figure 1.5: Schematic overview of heterotrimeric G protein family signal transduction
Schematic showing characteristic examples of the signalling of different Gα protein families downstream of an activated coupled receptor. $G\alpha_s$ and $G\alpha_{i/o}$ have opposing effects on adenylate cyclase (AC) activity whilst the Gβγ proteins activate PI3Kγ and Rac GEFs, and inhibit AC. The $G\alpha_q$ family signals to activate PLCβ, resulting in the production of IP_3 and DAG from $PI(4,5)P_2$. IP_3 mediates Ca^{2+} rises and DAG activates PKC. The $G\alpha_{12/13}$ family activate Rho-GEFs to stimulate RhoA activity and subsequently cytoskeleton dynamics. Figure adapted from (Yong Huang, Zheng, Su, & Gu, 2009).

1.2.1.2 GPCR trafficking

As GPCRs are enormously important for normal cell function, both their levels and their activity must be tightly controlled. Hence, the regulation of their expression level, their trafficking to and from the membrane, and the mechanisms of their inactivation are equally as important for homeostasis as their activation by agonists. As typical transmembrane proteins, GPCRs are *de-novo* synthesised in the ER and are transported constitutively to the plasma membrane through the Golgi and trans-Golgi network (TGN). For most GPCRs, their activation and signalling at the plasma membrane (as described here above) is followed by desensitisation and then receptor internalisation, particularly upon prolonged agonist-stimulation (S. S. G. Ferguson, 2001; Reiter & Lefkowitz, 2006; Tan, Brady, Nickols, Wang, & Limbird, 2004). Desensitisation and internalisation are controlled by a number of different pathways (DeWire, Ahn, Lefkowitz, & Shenoy, 2007; Drake, Shenoy, & Lefkowitz, 2006; Hanyaloglu & von Zastrow, 2008; Sorkin & von Zastrow, 2009). One of the principal pathways is by members of the G protein-coupled receptor kinase (GRK) family which recognise active GPCRs and phosphorylates serine or threonine residues in the GPCR's

cytoplasmic C-terminus (Reiter & Lefkowitz, 2006). This is followed by recruitment of β-arrestin proteins to the phosphorylated receptor, forming a high affinity interaction. This sterically impedes the coupling of the GPCR to the heterotrimeric G protein (Shenoy & Lefkowitz, 2003), and so the GPCR can no longer transmit downstream signals, which results in fast signal desensitization and is followed by rapid internalization of the receptor (Krupnick & Benovic, 1998; Pitcher, Freedman, & Lefkowitz, 1998). β-Arrestin proteins have a dual role: on the one hand, they lead to signal desensitisation by competing with G proteins for binding to the receptor, on the other hand they promote receptor internalisation by interacting with key proteins such as clathrin adaptor AP2 (Laporte et al., 1999), ADP ribosylation factor 6 (Claing et al., 2001) and clathrin itself (Goodman et al., 1996), leading to clathrin-mediated endocytosis of the GPCR (Doherty & McMahon, 2009; Shenoy & Lefkowitz, 2003). It is important to bear in mind that for some GPCRs, desensitisation can occur in a GRK-independent manner, and phosphorylation of the C terminus may also induce mechanisms of internalisation that are clathrin independent. Internalised GPCRs can follow varying trafficking paths (Irannejad, Tsvetanova, Lobingier, & von Zastrow, 2015; Sorkin & von Zastrow, 2009). However, generally, they are sorted into the endosomal compartment, where they become dephosphorylated. Once the GPCR is dephosphorylated, it may either be recycled to the plasma membrane or be transported to the lysosome for degradation, leading to receptor downregulation (Reiter & Lefkowitz, 2006). While the agonist-induced phosphorylation of GPCRs has been studied in great detail, the mechanisms and outcomes of receptor dephosphorylation are comparatively less well-understood. One study using the Sst2A somatostatin receptor as model has identified protein phosphatase 1β as a major player leading to the disruption of the β-arrestin/GPCR complex (Poll, Doll, & Schulz, 2011). A different study identified protein phosphatase 2A as responsible for the recycling of metabotropic glutamate receptor 1 (mGluR1) (Pandey, Mahato, & Bhattacharyya, 2014), suggesting that there may not be a common dephosphorylation mechanism for all GPCRs, and that similar dephosphorylation events can have different outcomes.

Contrary to the dogma of phosphorylation-dependent receptor desensitisation and switching off by internalisation, in many cases, GPCR internalisation does not attenuate the cellular effects of receptor activation, but instead signalling continues after internalisation

from within the cell, for example in the Golgi apparatus (Godbole, Lyga, Lohse, & Calebiro, 2017). Infact, many recent studies have provided strong evidence that internalised receptors can take part in intracellular signalling events (Calebiro & Godbole, 2018). To complicate matters further, “Hot Spots” on the plasma membrane have recently been identified through single-molecule imaging, where receptors and G proteins are more often found, and therefore, even within the plane of the plasma membrane, there are regions with more or less GPCR signalling (Sungkaworn et al., 2017).

In neutrophils, GPCR trafficking is even more complicated, as many neutrophil GPCRs are stored on the membrane of secretory vesicles and granules that can rapidly fuse with the plasma membrane upon neutrophil priming, allowing the cells to increase their responsiveness to chemotactic cues that are present at sites of *in vivo* inflammation, although other GPCRs are constitutively localised on the neutrophil surface (see section 1.2.2).

Overall it can be stated that membrane trafficking dictates the signalling pattern of GPCRs (Hanyaloglu & von Zastrow, 2008), placing a high importance on elucidating the mechanisms that control this receptor trafficking.

1.2.2 Chemokine receptors in neutrophils

Neutrophil mobilisation from the bone marrow into the blood stream and neutrophil recruitment to sites of inflammation, infection or injury is primarily regulated by chemokines such as C5a, fMLP and IL-8. Upon tissue injury, these chemokines are produced locally by various cell types, including neutrophils, macrophages, fibroblasts, and endothelial cells, or by the pathogens (Abtin et al., 2014; Pober & Sessa, 2007). Neutrophils express more than 30 types of GPCR, which can bind to a broad array of ligands, many of which are chemokines (Lammermann & Kastenmuller, 2019).

Chemokine receptors are typical members of the rhodopsin or serpentine superfamily of GPCRs, with the characteristic seven hydrophobic transmembrane structure. They mediate cellular responses to chemokines, a large family of cytokines which regulate leukocyte trafficking and migration. In addition, “atypical chemokine receptors” also exist, which act as chemokine scavengers to downregulate inflammation (Bachelerie et al., 2014).

Some chemokine receptors pair uniquely with one chemokine ligand, but most are more promiscuous, although restricted to one chemokine group. Major chemokine receptors that control the trafficking and chemotaxis of neutrophils are introduced here. The signalling through these GPCRs, and how these signals guide neutrophil recruitment into the blood stream and into inflamed or infected tissues, has been of interest to the research community for decades.

1.2.2.1 Complement Component 5a Receptor 1

One typical example of chemokine receptors is the Complement Component 5a Receptor 1 (C5aR1), a 351 amino acid GPCR which recognises the 74 amino acid peptide ligand complement component 5a (C5a, which is one of the anaphylatoxins) (Boulay, Mery, Tardif, Brouchon, & Vignais, 1991). This receptor is widely expressed, with high levels in cells of the myeloid linage, including neutrophils and macrophages (Monk, Scola, Madala, & Fairlie, 2007). Importantly for my project, this receptor is found at low levels constitutively at the plasma membrane of basal neutrophils, and is upregulated to the plasma membrane from secretory vesicles and granules upon neutrophil priming (Monari, Kozel, Bistoni, & Vecchiarelli, 2002; Sengelov, 1995).

The crystal structure of C5aR1 has recently been solved at 2.7 Å resolution in complex with a small-molecule antagonist (Robertson et al., 2018). It is similar, overall, to other GPCR receptors, consisting of the canonical seven-transmembrane (TM1–TM7) helix arrangement, except for an extra-helical negative allosteric-binding pocket between transmembrane regions TM3, TM4 and TM5 that is distinct from conventional orthosteric sites for GPCRs antagonists.

C5aR1 primarily couples to $G\alpha_{i/o}$ (Kolev, Le Friec, & Kemper, 2014) and is pre-coupled to the G protein in the absence of C5a ligand (Raffetseder et al., 1996; Siciliano, Rollins, & Springer, 1990). In response to C5a binding, C5aR1 signals through many different pathways, including PI3Kγ, phospholipase-C β, and MEK/ERK (Rabiet, Huet, & Boulay, 2007). PI3Kγ activity is stimulated directly by Gβγ subunits, resulting in the generation of PIP_3 (Stoyanov et al., 1995) and thus PI3K signalling and multiple PI3K-dependent cell responses, including polarisation and migration. Phospholipase-C β is another direct target of Gβγ subunits, and its activation results in the generation of diacylglycerol (DAG), which activates protein kinase

C, and of inositol trisphosphate (IP_3), which stimulates the release of calcium from intracellular stores (Rabiet et al., 2007). The activation of these pathways, along with the C5aR1-mediated activation of kinases such as MEK/ERK, results in adhesion, migration and ROS production by cells such as neutrophils (Rabiet et al., 2007).

As with other GPCRs, the agonist-dependent internalisation of C5aR1 requires the phosphorylation of its cytoplasmic C-terminus, on residues S332, S334 and S338 (Bock et al., 1997; Naik, Giannini, Brouchon, & Boulay, 1997). In response to C5a stimulation, Ca5R1 internalises into endosomes within 5 to 10 minutes (Bock et al., 1997; Naik et al., 1997). The kinases GRK2 and GRK3 mediate the agonist-stimulated phosphorylation of C5aR1 (Langkabel, Zwirner, & Oppermann, 1999; Suvorova, Gripentrog, Oppermann, & Miettinen, 2008). Furthermore, L318 in the C-terminal region also plays an important role in C5Ra1 internalisation, supposedly by stabilising structural elements of the receptor that are important for phosphorylation (Suvorova et al., 2008).

The importance that the C5aR1 receptor plays in the innate immune response is demonstrated by the increased mortality of C5aR1-deficient mice infected with *P. aeruginosa* (Hopken, Lu, Gerard, & Gerard, 1996). Neutrophils lacking C5aR1 also fail to initiate arthritis in the neutrophil-dependent K/BxN serum transfer model of autoimmune rheumatoid arthritis (Monach et al., 2010). A recent follow-up paper has provided new mechanistic insight by showing that C5aR1 cooperates with another neutrophil GPCR, the leukotriene B4 receptor, to recruit neutrophils into the inflamed tissue in this arthritis model (Sadik, Miyabe, Sezin, & Luster, 2018).

1.2.2.2 fMLP Receptor

Two further chemokine receptors expressed by neutrophils bind formylated peptides such as fMLP, which can be derived from bacteria but also from damaged host tissue and are considered potent chemoattractants. FPR1 binds fMLP with high affinity, and FPR2 has lower affinity. FPR1 is expressed at low levels on the surface of basal neutrophils, whereas the bulk of FPR1 is localised on secretory vesicles and various granule subtypes (Rorvig, Ostergaard, Heegaard, & Borregaard, 2013) including azurophil granules (Cowland & Borregaard, 1999; Sengelov, Boulay, Kjeldsen, & Borregaard, 1994), and is rapidly upregulated to the plasma membrane in response to priming with inflammatory stimuli. *In vitro*, these stimuli include

LPS, platelet activating factor (PAF), TNFα and GM-CSF (Hayashi, Means, & Luster, 2003; Kitchen, Rossi, Condliffe, Haslett, & Chilvers, 1996; Oflaherty, Rossi, Redman, & Jacobson, 1991; Sengelov et al., 1994). In response to low doses of stimuli such as PAF, secretory-vesicle FPR1 alone is mobilised; however, in response to powerful stimuli such as phorbol myristate acetate, even azurophil-granule FPR1 also localise to the cell surface (Sengelov et al., 1994). When activated, FPR1 triggers a variety of functions, including chemotaxis, degranulation, ROS production, and phagocytosis (Boulay, Tardif, Brouchon, & Vignais, 1990).

FPR1 has been classically described to play a role in the migration of neutrophils into sites of infection as well as for their killing of microorganisms. Most of the current understanding of this receptor *in vivo* has been obtained through the generation of FPR1 knockout mice (Gao, Lee, & Murphy, 1999). In *L. monocytogenes*-infected FPR1-deficient mice, an increased bacterial load was observed in both the liver and spleen compared to wild-type mice, with reductions in neutrophil migration and ROS production (Gao et al., 1999; M. Y. Liu et al., 2012). Furthermore, *S. pneumoniae*-induced meningeal infection is associated with poorer outcome in FPR1-deficient animals although, interestingly, with a paradoxical increase in neutrophil numbers within the brain that was postulated to be due to the compensatory upregulation of other chemokine receptors (Oldekamp et al., 2014). Finally, FPR1 receptor up-regulation has been described in the circulating neutrophils of patients with emphysema, Crohn's disease, and sepsis (Anton, Targan, & Shanahan, 1989; Stockley, Grant, Llewellynjones, Hill, & Burnett, 1994; Tennenberg & Solomkin, 1988).

1.2.2.3 IL-8 Receptors

IL-8 (CXCL8) was the first chemokine identified as a neutrophil chemoattractant (Yoshimura et al., 1987). It binds to two chemokine receptors expressed on the neutrophil surface in mice, CXCR1 (also known as IL-8 receptor-α) and CXCR2 (IL-8 receptor-β) (Chuntharapai, Lee, Hebert, & Kim, 1994; Sabroe, Williams, Hebert, & Collins, 1997).

CXCR1 binds IL-8 with high affinity, whereas CXCR2 binds IL-8 as well as other ligands, including melanoma growth stimulatory activity GRO/MGSA (CXCL1) (Sabroe et al., 2002), neutrophil activating protein-2 NAP-2 (CXCL7) and epithelial cell-derived neutrophil-activating factor-78 amino acids ENA-78 (CXCL5) (Ahuja, Lee, & Murphy, 1996). Granulocytic-

chemoattractant protein-2 GCP-2 (CXCL6) is an equipotent agonist for both CXCR1 and CXCR2 (Murphy et al., 2000; Wolf et al., 1998). CXCR2 is the major receptor involved in promoting neutrophil mobilisation from the bone marrow into the blood stream, and is also crucial for neutrophil recruitment to sites of inflammation both in humans and mice (Eash, Greenbaum, Gopalan, & Link, 2010; Sabroe, Jones, Whyte, & Dower, 2005). The interaction of these chemokines with CXCR1 and/or CXCR2 triggers the extravasation and subsequent directed migration of circulating neutrophils to injury sites (Martins-Green, Petreaca, & Wang, 2013; Murdoch & Finn, 2000).

IL-8 binding to CXCR1 or CXCR2 leads to the activation of pertussis toxin (Ptx)-sensitive $G\alpha_{i/o}$–type G proteins and their many downstream pathways, including phospholipase C, which, results in the formation of the PKC activator DAG and of IP_3 which elevates the cytosolic calcium concentration (Richardson, Marjoram, Barak, & Snyderman, 2003; Richardson, Pridgen, Haribabu, Ali, & Snyderman, 1998). Unlike several other neutrophil GPCRs, CXCR1 and CXCR2 are constitutively expressed on the plasma membrane rather than being stored in secretory vesicles or granules, presumably to ensure instant activation by immobilised IL-8 on the endothelial surface during neutrophil recruitment. However, like most GPCRs, CXCR1 and CXCR2 are rapidly down-regulated from the neutrophil surface upon activation by IL-8, by clathrin-mediated internalization, which as usual is followed by proteolytic degradation in lysosomes or by recycling back to the neutrophil surface (Samanta, Oppenheim, & Matsushima, 1990). During this process, CXCR2 internalises more rapidly and recovers to normal cell surface levels more slowly than CXCR1 (Barlic et al., 1999; Chuntharapai & Kim, 1995; Feniger-Barish, Ran, Zaslaver, & Ben-Baruch, 1999; Prado, Suzuki, Wilkinson, Cousins, & Navarro, 1996). Furthermore, CXCR2 is special among GPCRs as its proteolytic cleavage upon priming (for example following TNFα stimulation) can shed the receptor from the neutrophil surface (Asagoe, Yamamoto, Takahashi, Suzuka, et al., 1998; Sabroe et al., 2005).

1.2.2.4 SDF-1 Receptor

CXCR4, the receptor for stromal cell-derived factor 1 (SDF-1, CXCL12), is another important chemokine receptor in neutrophils, which plays a key role in maintaining neutrophil homeostasis by counter-acting the effects of CXCR2 in the bone marrow, signalling to

prevent neutrophils from being mobilised prematurely out of the bone marrow into the blood stream (Eash et al., 2010; Link, 2005; von Vietinghoff, Asagiri, Azar, Hoffmann, & Ley, 2010). CXCL12 is constitutively produced in the bone marrow and essential for retaining mature neutrophils there by binding to CXCR4 (De Filippo & Rankin, 2018). High levels of CXCL12 are expressed by 'CXCL12-abundant reticular' (CAR) cells, but also other stromal cells of the bone marrow, including osteoblasts (Strydom & Rankin, 2013; Sugiyama, Kohara, Noda, & Nagasawa, 2006). In neutrophils freshly isolated from bone marrow, the levels of CXCR4 on the cell surface are low and intracellular levels of CXCR4 are high, whereas in medium starved of CXCL12, the cell upregulates CXCR4 onto the surface within hours (De Filippo & Rankin, 2018; Martin et al., 2003). These findings suggested receptor desensitization and internalization in response to constitutively high local concentrations of CXCL12 in the bone marrow microenvironment. Moreover, these data underlined that neutrophils receive constant CXCL12 signals, which position them in the bone marrow, probably by activating integrin-mediated adhesion to stromal cells (Petty, Lenox, Weiss, Poynter, & Suratt, 2009). While high concentrations of CXCL12 retain neutrophils in the bone marrow via CXCR4 signalling, low concentrations of CXCR2 ligands produced by endothelial cells and megakaryocytes facilitate neutrophil mobilisation via CXCR2 (Strydom & Rankin, 2013). This signal balance can be shifted in both directions between retention and mobilisation. GM-CSF treatment or acute inflammation, which increases blood serum levels of GM-CSF and CXCR2 ligands, shifts the balance toward neutrophil mobilisation from the bone marrow (Kohler et al., 2011; Semerad et al., 2002). GM-CSF, can lead both to the downregulation of CXCL12 levels in the bone marrow or enhance the release of CXCR2 ligands from endothelial cells or megakaryocytes. The same shift toward neutrophil mobilisation occurs in mice with conditional gene deletion of CXCR4 or CXCL12 (Eash, Means, White, & Link, 2009; Tzeng et al., 2011).

The plasticity of neutrophil responses to chemotactic cues allows these cells to use various navigation strategies to reach sites of inflammation and infection (Lammermann & Kastenmuller, 2019). Intravital microscopy studies using mice with GPCR-deficient neutrophils and/or use of blocking antibodies has provided insight into how different GPCRs cooperate to arrange the physiological and pathological trafficking paths of neutrophils and has revealed a hierarchy of directional cues. For example, several studies have reported that

over-stimulation of C5aR1 due to high levels of C5a production has major consequences in sepsis and anaphylaxis, and provides a potential therapeutic target for the treatment of acute inflammatory conditions (Czermak et al., 1999; Guo & Ward, 2006; Herrmann et al., 2018; Karasu, Nilsson, Kohl, Lambris, & Huber-Lang, 2019). Moreover, signalling through the fMLP receptor FPR1 has been seen to be required for interstitial chemotaxis in the necrotic zone during a sterile inflammation model of heat-induced liver necrosis, whereas signalling through CXCR2 was shown to be crucial for the extravasation of neutrophils (McDonald et al., 2010). In a mouse skin wound model, the chemokine leukotriene B4 (LTB4), which binds to the GPCR BLT, was shown to be critical for neutrophil infiltration into the inflamed skin, followed by neutrophil swarming which required CXCR2 and fMLP receptors (de Oliveira, Rosowski, & Huttenlocher, 2016).

1.3 Small GTPases

The Ras superfamily of small G proteins consists of 166 human members that regulate a multitude of cellular functions, including cell growth, proliferation, differentiation, morphology, motility and intracellular transport. Most of them can be can be subdivided into five families (Ras, Rab, Arf, Ran and Rho), and specific cellular functions can be assigned to each family. In general terms, the Ras-family regulates gene expression and proliferation, the Rho-family cytoskeletal reorganisation, the Ran-family nucleo-cytoplasmic transport and the Rab and Arf-families direct intracellular vesicle trafficking (Takai, Sasaki, & Matozaki, 2001; Wennerberg, Rossman, & Der, 2005).

1.3.1 Rho GTPases

The Rho-family includes 21 members, including Rac1, RhoA and Cdc42 (Burridge & Wennerberg, 2004). They regulate cytoskeletal organisation, cell adhesion and migration, ROS production, vesicular transport, gene expression and cell division (Nathan, 2006; Weiss, 1989). One of the best-characterised Rho-family functions is their control of cell migration via regulation of the actin cytoskeleton. Rac1, RhoA and Cdc42 regulate the formation of membrane ruffles/lamellipodia, actin stress fibres and filopodia respectively, thus

modulating cell morphology, adhesion and motility (Kay, Langridge, Traynor, & Hoeller, 2008; Ley et al., 2007).

Typically, the activity of Rho-family GTPases is regulated by cycling between an active (GTP-bound) and inactive (GDP-bound) state, under the control of guanine-nucleotide exchange factors (GEFs) and GTPase-activating proteins (GAPs) (Figure 1.6). GEFs catalyse the exchange of GDP for free GTP, which is available in excess in eukaryotic cells, thus activating the small G protein which adopts a conformation that allows it to bind to its downstream effectors. GAPs bind the GTP-bound small G-proteins and stimulate their intrinsic GTPase activity, thus accelerating the hydrolysis of GTP to GDP and Pi, and inactivating the small G protein (Stephens et al., 2008). An extra level of regulation involves the interaction of Rho-GTPases with guanine-nucleotide dissociation inhibitors (GDIs) (Michaelson et al., 2001). GDIs play a dual inhibitory regulatory role by preventing GDP-dissociation (and thus GDP-GTP exchange) from the Rho protein, as well as blocking the translocation of the Rho protein from the cytoplasm to the plasma membrane, thus holding it in an inactive state within the cytoplasm. GDIs prevent Rho proteins from translocating to the membrane by binding with high affinity and so shielding the prenylated C-terminus of the GTPase, which serves to anchor these proteins in the membrane (Michaelson et al., 2001; Moissoglu & Schwartz, 2014).

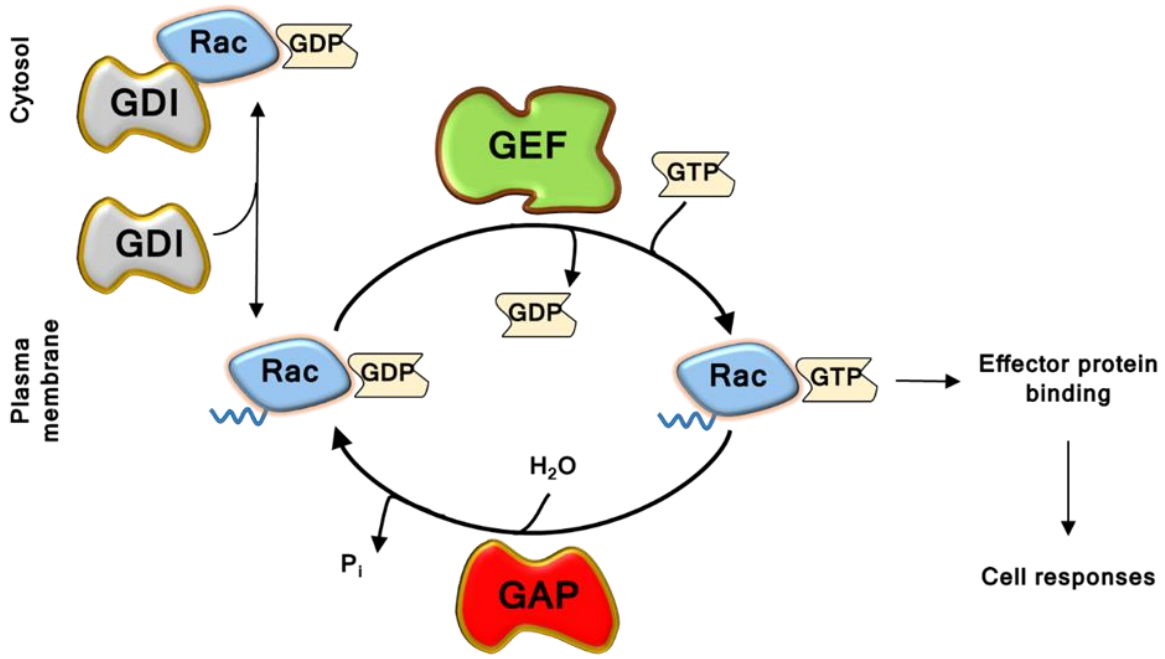

Figure 1.6: Regulation of Rac activity

Diagram representing the regulation of classically regulated Rho family Small G proteins, such as Rac, showing the cycle between the inactive GDP-bound and the active GTP-bound conformation. The activation of the small G protein into its GTP-bound conformation is regulated by the action of a guanine-nucleotide exchange factor (GEF) which catalyses the exchange of GDP for GTP, whereas inactivation is mediated by a GTPase activating protein (GAP) which catalyses the hydrolysis of GTP to GDP. The active form of the small G protein interacts with effectors to mediate downstream signalling. In addition to this, guanine nucleotide dissociation inhibitors (GDIs) sequester inactive Rho-family small G proteins by burying the hydrophobic prenyl modification of the small G protein within a pocket of the GDI, thus promoting their cytosolic localisation. In addition, GDIs inhibit nucleotide dissociation from the G protein. Figure adapted from (Pantarelli and Welch 2018).

1.3.2 Rac GTPases

Rac (Ras-related C3 botulinum toxin substrate) proteins are small G proteins (GTPases) of the Rho family (Heasman & Ridley, 2008; Wennerberg et al., 2005), and consist of four isoforms: Rac1, Rac2, Rac3 and RhoG. The Rac2 and Rac3 isoforms are 92% identical to Rac1 in amino acid sequence (Hajdo-Milasinovic, Ellenbroek, van Es, van der Vaart, & Collard, 2007), whereas RhoG is 72% identical to Rac1 (Wennerberg & Der, 2004). There is also a splice variant of Rac1, Rac1b, which contains a 19 amino acid insertion near the switch II region.

Rac1 and RhoG are both ubiquitously expressed, whereas Rac2 is restricted to cells of the haematopoietic lineage (Wennerberg & Der, 2004), and Rac3 is mainly found in neurons (Haataja, Groffen, & Heisterkamp, 1997). In contrast, Rac1b expression is largely restricted to cancer cells, particularly in breast and colon cancer (Jordan, Brazao, Boavida, Gespach, & Chastre, 1999; Schnelzer et al., 2000). Rac1 and Rac2 differ in the C-terminal region in seven of the fifteen most C-terminal residues, attributing a charge of +7 and +4 for Rac1 and Rac2 respectively (Magalhaes & Glogauer, 2010). It has been proposed that this may result in a different localisation of active Rac1 and Rac2 in neutrophils where Rac1 is localised at the plasma membrane whereas Rac2 localises to internal membranes (Kraynov et al., 2000; Michaelson et al., 2001).

The members of the Rac-like subfamily are classically regulated by GEFs, GAPs and GDIs, as described in section 1.3.1, except that they show relatively high intrinsic GTPase activity, and thus have a propensity to auto-inactivate (Wennerberg & Der, 2004). The only exception is Rac1b, which cannot bind to Rho-GDI and has reduced intrinsic GTPase activity, hence it is mainly bound to the plasma membrane and displays constitutive activity (Fiegen et al., 2004; Matos, Collard, & Jordan, 2003).

1.3.2.1 Rac functions

Rac-GTPases control the structure of the actomyosin cytoskeleton by signalling through several pathways. Active Rac induces lamellipodia formation and membrane ruffling (Machesky & Hall, 1997). Lamellipodia are large sheet-like protrusions attached to the substratum that form at the leading edge of migrating cells. Membrane ruffles are part of

the lamellipodium that have detached from the substratum and folded backwards. The formation of lamellipodia is achieved by Rac through the activation of IRSp53 and WAVE, which couples to the actin-nucleating protein Arp2/3 (Machesky & Insall, 1998; Miki, Suetsugu, & Takenawa, 1998). This results in the formation of actin filaments into a branched network structure at the cell edge. In addition to this, the activation of the protein kinase Pak by Rac can also guide lamellipodia formation by regulating the cofilin-dependent turnover of actin downstream of LIM-kinase activity (N. Yang et al., 1998). Finally, Rac also regulates gene expression through kinases such as Pak and Jnk, which signal to a range of downstream effectors, including transcription factors (Baker, Pan, & Welch, 2016).

1.4 Rac-GEFS

Rac family small G proteins can be activated by two types of guanine nucleotide exchange factors (GEFs), Dbl-type and DOCK-type. Although these GEFs have distinct catalytic domains (DH and DHR2 domains, respectively), they work in a similar way to catalyse the exchange of GDP for GTP, and thus induce the active conformation of Rac, which is able to bind downstream effector proteins and induce a wide variety of cellular functions.

This thesis focuses on Rac-GTPases and the Dbl-type Rac-GEF P-Rex1 in neutrophil responses; therefore, a more extensive description of the roles of these proteins within their pathways can be found in Section 1.5.

1.4.1 P-Rex1

The phosphatidylinositol-3,4,5-trisphosphate-dependent (PREX) protein family consists of P-Rex1, P-Rex2 and the splice variant P-Rex2b. P-Rex1 and P-Rex2 have similar size, 185 kDa and 183 kDa, respectively, whereas the P-Rex2b splice variant is 112 kDa. P-Rex1 was the first of the family to be identified, during a search for factors that activate Rac in response to the second messenger PIP_3 (Welch et al., 2002). Part of this introduction on P-Rex is taken from recent reviews written by our lab, which I co-authored (Hornigold K, 2018 ; Tsonou E, 2018).

1.4.2 P-Rex Structure

P-Rex family GEFs are multi-domain proteins that have a catalytic N-terminal Dbl homology (DH) domain which confers Rac-GEF activity, in tandem with a C-terminally adjacent pleckstrin homology (PH) domain. The DH/PH domain tandem is characteristic for Dbl-type Rho-GEFs (Rossman, Der, & Sondek, 2005). The PH domain of P-Rex1 binds PIP_3 and thereby contributes to membrane attachment. Following the DH/PH domains there are two Dishevelled, EGL-10, Plekstrin (DEP) domains and two Postsynaptic-density protein, Disc large, Zona occludens-1 (PDZ) domains. These domains commonly participate in protein-protein interaction. The C-terminal half of P-Rex1 and P-Rex2 consists of a large inositol polyphosphate 4-phosphatase (IP4P) like domain that lacks phosphatase activity. This last domain is absent in the P-Rex2b splice variant (Figure 1.7). The crystal structure of the P-Rex1 DHPH tandem (Figure 1.8) has recently been solved in complex with constitutively active (G12V) Rac1 (Lucato et al., 2015) or nucleotide-free Rac1 (Cash, Davis, & Tesmer, 2016) and has served as a template for modelling these proteins in complex with Gβγ proteins as well as PIP_3.

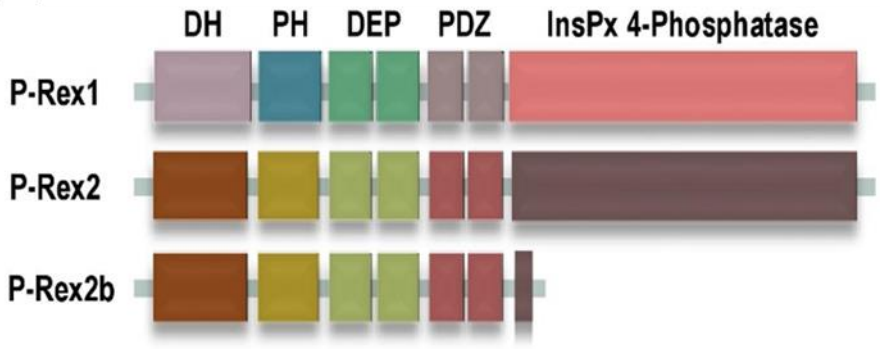

Figure 1.7: Multi-domain structure of P-Rex family Rac-GEFs

PREX1 and PREX2 are Dbl-type Rho-GEFs and share an identical domain structure. At their N-terminus, they have a DH domain, which confers Rac-GEF activity, in tandem with the adjacent PH domain, which binds PIP3 followed by two DEP, and two PDZ protein interaction domains. In their C-terminal half there is an inositol polyphosphate 4-phosphatase (IP4P) domain, which harbours no phosphatase activity and has weak homology between the PREX proteins. PREX2b is a splice variant of PREX2. Figure adapted from (Hornigold K, 2018).

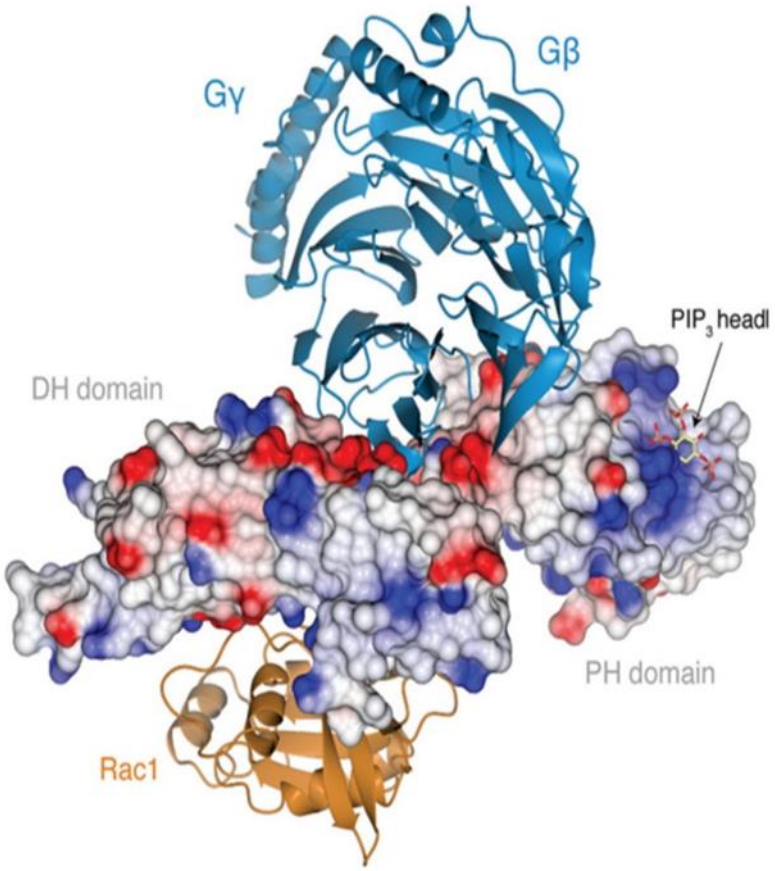

Figure 1.7: Crystal structure of the catalytic core of P-Rex1

Crystal structure of the DHPH domain tandem of P-Rex1 (electrostatic surface view) in complex with Rac1, shown alongside modelling of Gβγ and PIP_3 binding. This research was originally published in the Journal of Biological Chemistry (Lucato et al. 2015 © the American Society for Biochemistry and Molecular Biology) and is reproduced here with kind permission from the authors. The crystal structure confirmed that residues Glu56 and Asn238 in the P-Rex1 DH domain are crucial for Rac1 binding, and that the DH domain is sufficient for catalysis. The modelling suggested furthermore that PIP_3 and Gβγ binding sites are situated away from the Rac1 binding site and that Gβγ contacts both the P-Rex1 DH and PH domains. Cash et al. (2016) reported a similar structure and also crystalized the PH domain in complex with the soluble PIP_3 analogue IP_4, which revealed that Lys280, Arg289, and Lys368 in the PH domain are required for PIP_3 binding.

1.4.3 P-Rex tissue distribution

P-Rex1 was first discovered in neutrophils, where it makes up 0.1% of the cytosolic protein (Welch, Coadwell et al. 2002). However, P-Rex1 is also expressed in other types of leukocytes, like macrophages (Z. Wang, X. Dong, Z. Li, J. D. Smith, & D. Wu, 2008), as well as in platelets (Aslan et al., 2011; Qian et al., 2012a), endothelial cells (Carretero-Ortega et al., 2010) and neurons (Yoshizawa et al., 2005), and at lower levels in many other cell types. Northern blot and western blot studies on mouse tissues have found that P-Rex1 is expressed widely throughout the brain and is also present in bone marrow, thymus, spleen, lymph nodes, and lung (Hill et al., 2005; Welch et al., 2002), whereas P-Rex2 has a more widespread distribution (Donald et al., 2004). In adult mice, western blots studies showed that P-Rex2 protein is abundant in the brain, especially in the Purkinje neurons of the cerebellum, and in the lungs, while a low level of expression is detectable in liver, thymus and spleen (Donald et al., 2008; Hodakoski et al., 2014). However, unlike P-Rex1, P-Rex2 is not detectable in peripheral blood leukocytes (Damoulakis et al., 2014; Lawson, Donald, Anderson, Patton, & Welch, 2011; Welch et al., 2005). Last, P-Rex2b is also absent from leukocytes but is expressed in the heart and in endothelial cells (Donald et al., 2008; Z. Li, Paik, Wang, Hla, & Wu, 2005; Rosenfeldt, Vazquez-Prado, & Gutkind, 2004).

1.4.4 P-Rex1 regulation and binding partners

The structural complexity of P-Rex proteins allows for a number of distinct modes of regulation which have been studied in quite some detail (Hornigold K, 2018).

P-Rex family Rac-GEFs are activated synergistically by PIP_3 and Gβγ subunits via the DHPH tandem, whereas domains in the C-terminal half of the protein have a negative regulatory function, keeping the basal activity of P-Rex low (Barber et al., 2007; Hill et al., 2005). The Gβγ subunit acts through the DH domain to promote P-Rex GEF activity, while PIP_3 binds to the PH domain (Hill & Welch, 2006). However, modelling based on the crystal structure of the DHPH tandem of P-Rex1 indicated that Gβγ proteins may form contacts with elements of both the DH and PH domains (Lucato et al., 2015). Two other proteins are known to have direct positive and negative regulatory roles on both P-Rex1 and P-Rex2 activity, namely activation by PP1α (through dephosphorylation of Ser1165) (Barber et al.,

2007) and inhibition by PKA (through phosphorylation of Ser436) (Chavez-Vargas et al., 2016) (Figure 1.9).

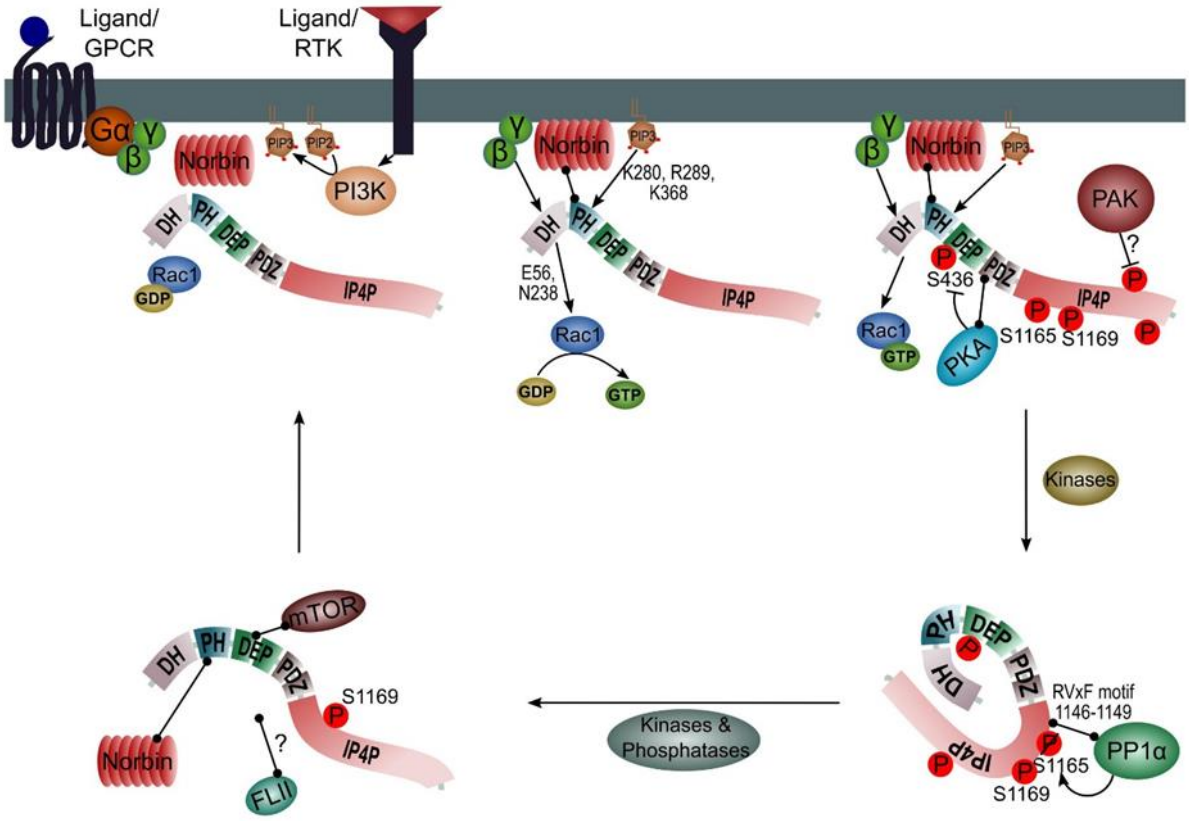

Figure 1.8: Regulation of P-Rex1

In basal cells, P-Rex1 is largely cytosolic and has low catalytic activity, due to intramolecular inhibition. In the cytosol, P-Rex1 binds constitutively to the serine phosphatase PP1α, the GPCR adaptor protein Norbin, the protein kinases PKA and mTOR and the gelsolin superfamily adaptor protein FLII. PP1α binds to the RVXF motif (residues 1146–1149) of P-Rex1 and dephosphorylates Ser1165, which is sufficient to weakly stimulate P-Rex1 Rac-GEF activity. Upon cell stimulation, P-Rex1 is recruited to the plasma membrane, and its GEF activity is stimulated synergistically by interactions with PIP_3 and with Gβγ proteins. The PIP_3 is produced by PI3K activity downstream of various receptor types including receptor tyrosine kinases (RTK). In contrast, the Gβγ proteins are released from activated GPCRs in response to ligand binding. Other mechanisms of P-Rex1 activation include Norbin (described later in section 1.6.2) and PP1α (as described hereinabove), as well as the phosphorylation of Ser1169 by unidentified serine kinases. Negative regulation: PKA binds to the PDZ1 domain and inactivates P-Rex1 by phosphorylating Ser436 in the DEP1 domain, which promotes an inhibitory intramolecular interaction with the catalytic core. In addition, PKA also regulates (possibly indirectly) an intramolecular interaction of the C-terminal half with the catalytic core. The Rac1-GTP-dependent kinase PAK can also phosphorylate P-Rex1 directly (at unknown sites) and inhibits P-Rex1 activity (possibly indirectly) within cells, which led to the proposal of a negative feedback loop involving P-Rex1, Rac1, and PAK to limit P-Rex1 signalling. Figure reproduced from (Hornigold K, 2018).

Moreover, PIP_3 and Gβγ also control the sub-cellular localisation of P-Rex. Under basal conditions, P-Rex1 is located in the cytosol, but in response to PIP_3 and Gβγ production, it translocates to the plasma membrane. Either PIP_3 or Gβγ alone can trigger weak recruitment to the plasma membrane but, as with the stimulation of GEF activity, both stimuli are required to promote robust membrane localisation of the Rac-GEF (Barber et al., 2007; Zhao et al., 2007). Deletion of the DEP tandem, PDZ tandem and IP4P-like domains in P-Rex1 increases translocation to the plasma membrane suggesting that these domains restrict access of the DHPH domain to the membrane, thereby maintaining P-Rex1 in the cytosol under basal conditions. Furthermore, GEF activity is not required for the membrane translocation of P-Rex1, as a GEF-dead E56A/N238A mutant can still translocate (Barber et al., 2007).

Apart from the regulators described above, the number of binding proteins of P-Rex1 identified to date is remarkably small. Only proteins known to bind P-Rex1 directly are mentioned in Figure 1.9. The Vazquez-Prado lab identified the serine kinase mTOR as a direct binding partner of P-Rex1, binding through the DEP domains. Through mTOR, P-Rex1 interacts with both mTOR-containing protein complexes, TORC1, which is central in cell growth, and TORC2 (also known as PDK2), which controls cell morphology and migration. The Malliri lab recently performed a SILAC screen to identify proteins that interact with Rac1 specifically in the presence of P-Rex1. This identified the actin remodelling protein FLII (flightless-1 homolog), a member of the gelsolin superfamily, as a P-Rex1 binding protein (Marei et al. 2016). P-Rex1 bound directly to FLII, independently of its Rac-GEF activity. P-Rex1 interacted with the C-terminal GEL domain of FLII (Figure 1.9), whereas Rac1 bound to the N-terminal LRR domain of FLII. These interactions were important in the regulation of cell contractility.

1.4.5 Functional roles of P-Rex1

In order to study the functional roles of P-Rex family GEFs, our lab has generated Prex1, Prex2 and Prex1/Prex2 knockout mouse strains. All strains are fertile but display several specific phenotypes, which describe the physiological and pathological effects of these proteins, as summarised in this section.

P-Rex1 is highly expressed in leukocytes, and its functions have mostly been studied in neutrophils and macrophages (see section 1.5.1.1). Other roles of P-Rex1 are in melanoblast migration during mouse development (Lindsay et al., 2011; Lindsay et al., 2015), in social behaviours, associated with a role in hippocampal plasticity (J. Li et al., 2015) and, together with P-Rex2, in motor coordination, associated with the control of synaptic plasticity in cerebellar Purkinje neurons (Donald et al., 2008; Jackson, Welch, & Bellamy, 2010).

Knockdown of endogenous P-Rex1 in neuronal PC12 cells inhibits lamellipodia formation, membrane ruffling, spreading and migration (Yoshizawa et al., 2005); however, P-Rex1 plays no obvious role in neuronal morphology or migration during development (Donald et al., 2008). Single nucleotide polymorphisms (SNPs), copy number deletions and reduced mRNA levels of PREX1 are seen in children with autism spectrum disorders (J. Li et al., 2015). Evaluation of Prex1 knockout mice in behavioural models of autism revealed deficits in social recognition, reversal learning and fear extinction (J. Li et al., 2015). Recently, a deep learning approach that was used for analysing GWAS data from a large cohort of Taiwanese patients with severe depression, and this identified a SNP, rs4810894 adjacent to the PREX1 gene as a predictor of the responsiveness to antidepressant treatment (Lin et al., 2018). However, the functional relevance of the effects of this SNP on antidepressant treatment response is yet to be investigated.

Several studies have associated P-Rex1 with tumour growth and metastasis. P-Rex1 has a key role in cancer cell proliferation (Wong et al., 2016), and cooperates with platelet-derived grow factor receptor (PDGFR) to drive cancer cell migration (Campbell et al., 2013). P-Rex1 is overexpressed in several cancers via gene amplification (Dillon et al., 2015) or changes in epigenetic regulation (Barrio-Real et al., 2014; Wong et al., 2011). P-Rex1 mRNA is up-regulated in breast, prostate, thyroid, lymphoid, ovarian, adrenal, and kidney cancers

(Barrio-Real et al., 2014; Sosa et al., 2010), as well as in melanoma (Barrio-Real et al., 2014; Lindsay et al., 2011; Sosa et al., 2010). At the protein level, P-Rex1 overexpression has been observed in breast cancer, (Lindsay et al., 2011; Montero, Seoane, Ocana, & Pandiella, 2011; Sosa et al., 2010), prostate cancer (Qin et al., 2009), and melanoma (J. H. Wang et al., 2017). P-Rex1 signalling has been extensively studied in breast cancer, but there is still controversy in the literature over whether P-Rex1 contributes to mitogenic signalling in breast cancer cells (Barrio-Real et al., 2018; Dillon et al., 2015; Kazanietz, Barrio-Real, Casado-Medrano, Baker, & Lopez-Haber, 2018; H. J. Liu et al., 2016; Lopez-Haber, Barrio-Real, Casado-Medrano, & Kazanietz, 2016).

A few reports link P-Rex1 to metabolism. P-Rex1 was shown to mediate insulin signalling in several studies (Balamatsias et al., 2011; Ghalali, Wiklund, Zheng, Stenius, & Hogberg, 2014; E. K. Kim et al., 2012; Montero, Seoane, & Pandiella, 2013) and was show to be important for the insulin-stimulated upregulation of the glucose transporter GLUT4 into the plasma membrane of adipose cells (Balamatsias et al., 2011). Furthermore, P-Rex1 was shown to regulate the thermogenic potential of human brown adipose tissue (Xue et al., 2015). SNP analysis also suggested a potential linkage for P-Rex1 to the likelihood of obesity developing into type 2 diabetes (Lewis et al., 2010). However, there has been no investigation yet into the importance of P-Rex1 in metabolism *in vivo*. Therefore, another PhD student in our lab, Elpida Tsonou, has been investigating the roles of P-Rex1 in glucose homeostasis, and has discovered a role in glucose tolerance (unpublished data).

P-Rex1 has been shown to be required for pulmonary fibrosis, a late phase of pulmonary inflammation which can result in loss of lung function. Prex1 knockout mice exhibited reduced early leukocyte infiltration and development of fibrosis, in a bleomycin-induced model of pulmonary fibrosis which drastically increased survival (Liang et al., 2016).

In addition to neutrophils, P-Rex1 is also expressed in platelets (Qian et al., 2012b). Prex1 knockout mice show mild defects in haemostasis, and GPCR-dependent aggregation and dense granule secretion is partially impaired in Prex1-deficient platelets (Qian et al., 2012b). However, P-Rex1/Vav expression in platelets was found to be important for the platelet-dependent vascular adhesion and recruitment of neutrophils and eosinophils (Pan et al., 2015) (see section 1.5.2).

Finally, a recent study has shown that P-Rex1 protein is upregulated in the lung of asthma patients. P-Rex1 overexpression stimulated the proliferation of primary airway smooth muscle cells derived from patients with asthma, in response to stimulation with either PDGF or EGF, whereas downregulation of P-Rex1 in these cells had the opposite effect, suggesting that P-Rex1 might contribute to the development of airway hyper-responsiveness (AHR) in asthma. However, further studies are required to elucidate the exact role of P-Rex1 in this process (Y. Huang et al., 2019).

1.5 Rac-GTPases in neutrophils

Part of this introduction on Rac-GTPases and Rac-GEFs has been adapted from a recent review which I co-authored (Pantarelli & Welch, 2018).

Among Rac-GTPases, neutrophils express the ubiquitous isoform Rac1, the haematopoietic Rac2, and the widely expressed RhoG, but not the neuronal isoform Rac3 (Baker et al., 2016; Pantarelli & Welch, 2018). These GTPases are key regulators of neutrophil functions.

The Rac-dependent pathways that control actomyosin cytoskeletal dynamics (see section 1.3.2.1) are central to neutrophil adhesion and spreading, as well as to the formation of the leading edge during polarisation which provides force to push the plasma membrane forward to allow the cell to migrate (Johnsson et al., 2014; Ridley, 2015) (Figure 1.10). Indeed, the use of photoactivatable Rac has shown that localised activation of Rac at the leading edge is sufficient for inducing directional neutrophil migration in zebrafish (Yoo et al., 2010). As well as cell morphology, adhesion, polarisation and migration, Rac-GTPases also control other neutrophil responses that require cytoskeletal dynamics, such as phagocytosis and degranulation. Furthermore, as mentioned in section 1.1.3.1, active Rac2 is an integral part of the NADPH oxidase enzyme complex, and is thus directly involved in ROS production. In turn, ROS is required to make NETs, and both are crucial responses for killing pathogens (Van Avondt & Hartl, 2018).

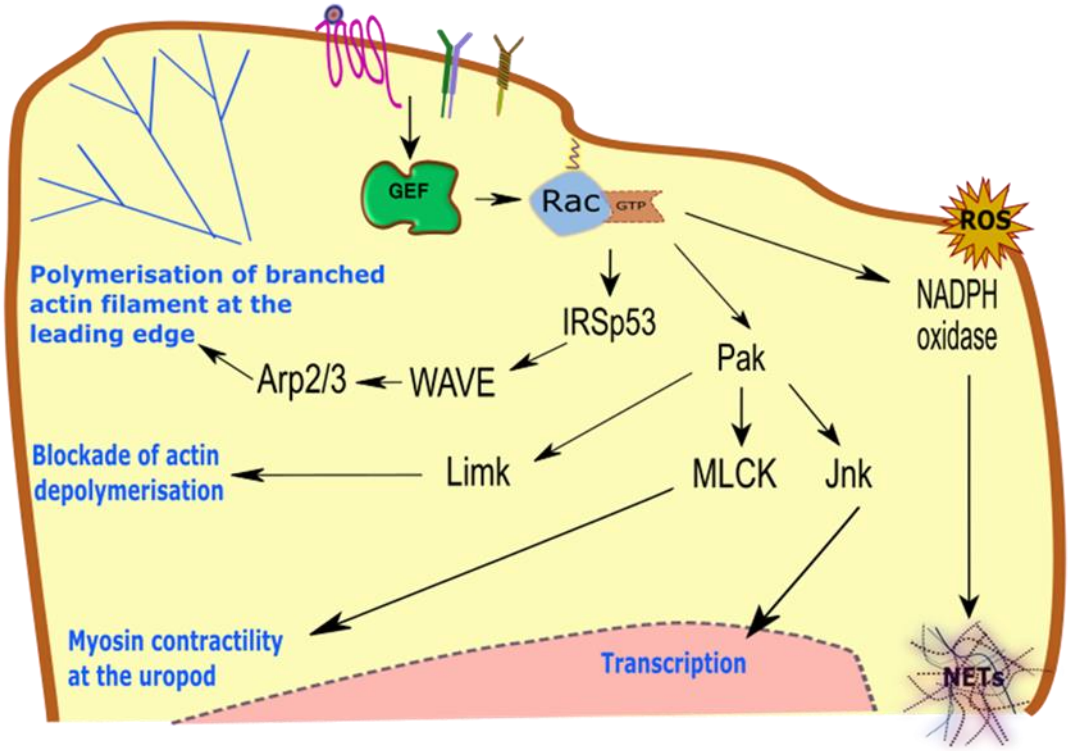

Figure 1.9: Rac-dependent neutrophil responses
One of the key molecular mechanisms underlying neutrophil responses is the small G protein Rac. Rac controls diverse processes, includings adhesion and spreading, migration, degranulation, phagocytosis and ROS formation, as well as contributing to gene regulation. The pathways depicted are thought to be important in all cell types, but not all have been specifically studied in neutrophils. Figure adapted from (Pantarelli & Welch, 2018).

Rac1 and/or Rac2 deficient mouse models have been used to study the role of Rac1 and Rac2 in neutrophil functions. Global Rac1 deficiency is embryonic lethal in mice, but drug-inducible conditional Rac1-deficiency in myeloid cells results in neutrophils with a migration defect (Gu et al., 2003). The cells can still move (Glogauer et al., 2003) but are unable to migrate directionally within a chemotactic gradient (Sun et al., 2004). *In vivo*, mice with conditional Rac1-deficiency, show impaired neutrophil recruitment during sterile peritonitis (Glogauer et al., 2003) and during acute fMLP-induced lung inflammation (Filippi, Szczur, Harris, & Berclaz, 2007). Furthermore, from work on macrophages, it is known that Rac1 is also necessary for FcR-mediated phagocytosis (Massol, Montcourrier, Guillemot, & Chavrier, 1998).

In contrast to Rac1, which controls cell spreading and directional migration, Rac2 is critical for neutrophil migration overall. Indeed, Rac2-deficient mice show reduced actin

polymerisation, L-selectin-dependent rolling and integrin-dependent spreading, and are unable to form stable leading edges and thus exhibit defects in neutrophil migration (Gu et al., 2003; Roberts et al., 1999; Troeger & Williams, 2013). Consequently, neutrophil recruitment is reduced in Rac2-deficient mice during sterile peritonitis and during immune-complex induced acute lung injury (Dooley et al., 2009). Interestingly, Rac2-deficient zebrafish larvae also show reduced neutrophil recruitment to cut wounds and poor immunity against *P. aeruginosa* infections (Keszei & Westerberg, 2014).

As mentioned above, in addition to their role in neutrophil migration and recruitment, Rac proteins also regulate other neutrophil responses. Isolated neutrophils from Rac2-deficient mice have a defect in superoxide production (C. Kim & Dinauer, 2001), and ROS production in Rac2-deficient cells can be restored by the reintroduction of wild-type Rac2 using retrovirus-mediated gene transfer (Filippi et al., 2004). Rac2-deficient murine neutrophils have reduced exocytosis of azurophil granules (Abdel-Latif et al., 2004; Gu et al., 2003). *In vivo*, they have reduced immunity to the pathogen *A. fumigatus* (Roberts et al., 1999).

While no Rac1 mutation is known to cause human immunodeficiency, a rare dominant-negative mutation in Rac2 (D57N) results in severe neutrophil dysfunction. This mutation causes an inability for neutrophils to be recruited to sites of infection and to clear infections, due to a marked deficiency in adhesion and chemotaxis, as well as an inability of neutrophils to kill ingested microbial targets, due to reduced ROS production and release of primary granules (Accetta et al., 2011; Ambruso et al., 2000; Williams et al., 2000).

Rac1 and Rac2 have non-redundant roles in neutrophil migration. Consequently, combined deficiency of Rac1 and Rac2 has more severe effects. It abolishes neutrophil recruitment to lungs infected with *E. coli* (Koh, Sun, Zhu, & Glogauer, 2005). It also delays recruitment into the synovial fluid of inflamed joints in an arthritis model triggered by *C. trachomatis* infection. This ameliorates the acute phase but causes more severe disease during the chronic phase (Zhang et al., 2005). Interestingly, reduced levels of Rac1 (and other Rho-GTPases and their regulators) were recently linked to the upregulation of microRNAs in human myelodysplastic syndrome, a condition characterised by a range of

functional neutrophil defects (Cao et al., 2017). However, further study is required to establish causal relationships and specificity.

Finally, the Rac-GTPase RhoG can signal upstream of Rac1 and Rac2, and might therefore be expected to have similar importance for neutrophil adhesion and migration. Indeed, RhoG does contribute to full polarisation of actin filaments at the leading edge of chemoattractant-stimulated neutrophils. However, unlike Rac1 and Rac2, RhoG is dispensable for the chemoattractant-stimulated actin polymerisation and migration of mouse neutrophils, as well as for neutrophil recruitment during sterile peritonitis, and seems therefore to play an unexpectedly minor role in neutrophil responses (Condliffe et al., 2006; Damoulakis et al., 2014).

1.5.1 Neutrophil Rac-GEFs

Several Rac-GEFs are known to have important roles in controlling neutrophil function (Figure 1.11). Among the 20 Dbl-family and 7 DOCK-family Rho-GEFs that are known to catalyse the activation of Rac, only a subset of these are known to be expressed in neutrophils. These include, P-Rex1 (Welch et al., 2002), Vav1, 2, and 3 (Gakidis et al., 2004), Pixα (Z. Li et al., 2003) and Tiam2 from the Dbl-family (Boespflug et al., 2014), as well as DOCK2 and DOCK5, which are from the DOCK family (Kunisaki, Nishikimi, et al., 2006).

These GEFs show preferences for activating different Rac isoforms, which are determined by the precise structure of their catalytic DHPH or DHR2 domains, for Dbl and DOCK-type Rac-GEFs, respectively. Some Rac-GEFs can also activate other types of Rho-GTPases. For example, Vav can activate RhoA as well as Rac (Bustelo, 2014). In addition to their catalytic domains, Rac-GEFs have varied multidomain structures that couple each GEF to specific upstream and effector proteins. Together, these mechanisms determine the cell responses controlled by Rac (Baker et al., 2016; Lawson & Ridley, 2018). Therefore, the activity of Rac-GEFs must be tightly regulated, through a combination of mechanisms, including phosphorylation, protein and lipid binding, unique to each type of GEF (Lawson & Ridley, 2018; Rossman et al., 2005).

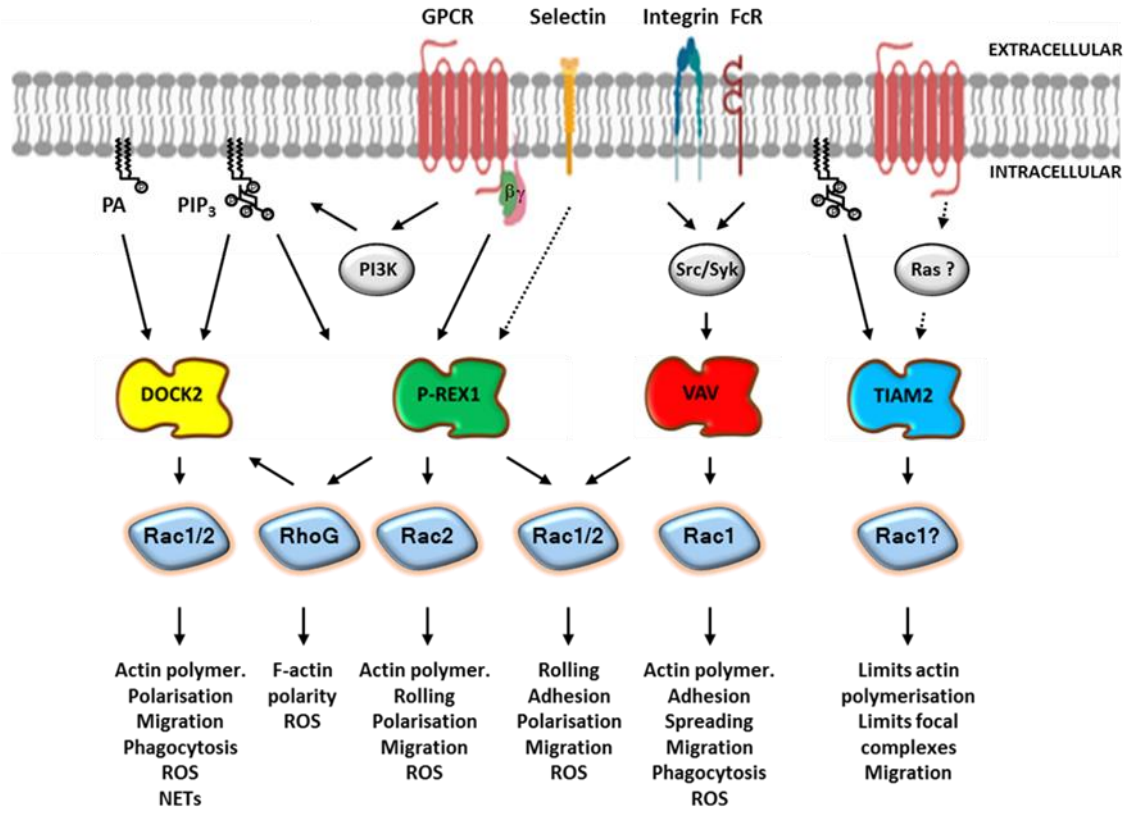

Figure 1.10: Signalling pathways of neutrophil Rac-GEFs
The Rac-GEF P-Rex1, which mediates signalling through GPCRs, E-selectin and TLR4 (not all shown here for simplicity), is activated by the lipid second messenger PIP_3 and by the Gβγ subunits of heterotrimeric G proteins. The Vav family Rac-GEFs, which are activated by tyrosine phosphorylation, are important in integrin and FcR signalling, but they also couple to TLR4 and GPCRs. It is currently unknown, which mechanisms control Tiam2 in neutrophils, except that this GEF controls chemoattractant induced responses. DOCK2 also signals upon GPCR stimulation. It is activated by RhoG and recruited to the plasma membrane by PIP_3 and phosphatidic acid (PA). The preferred Rac isoform for each Rac-GEF is shown here, but usually, the GEFs can activate both Rac1 and Rac2 to some extent. P-Rex1 can also activate RhoG and may thus signal in sequence with DOCK2 in some pathways. Figure adapted from (Pantarelli & Welch, 2018).

A central mechanism of neutrophil regulation is the lipid second messenger phosphatidylinositol-(3,4,5)-trisphosphate (PIP_3), which is produced by phosphoinositide 3-kinase (PI3K) within the cell membrane (McCormick, Chu, & Vermeren, 2019). Without PIP_3, neutrophils cannot generate stable polarity and migration (Hawkins & Stephens, 2015; Norton et al., 2016). PIP_3 localizes several Rac-GEFs, and other signalling proteins, to the plasma membrane and activates some directly, by binding to their PH domain. This enables the activation of Rac at the cell periphery which confers the firm adhesion and spreading of neutrophils. Polarized production of PIP_3 and activation of Rac induce the formation of a leading edge, neutrophil polarisation and migration (Johnsson et al., 2014). Importantly,

PIP_3-dependent regulation of neutrophil Rac-GEFs always occurs in conjunction with other signalling mediators that are unique to each GEF. One such example is P-Rex1, which is activated both by PIP_3 and by the Gβγ subunits of heterotrimeric G proteins, as described in section 1.5.1.1.

P-Rex1 is known to signal downstream of GPCRs, E-selectin and TLR4 in mouse neutrophils (Welch, 2015). Like P-Rex1, the Rac-GEF DOCK2 also signals in response to GPCR stimulation. However, in contrast to P-Rex1, DOCK2 is activated by the binding of active RhoG to its adaptor protein ELMO, and it is recruited to the plasma membrane by PIP_3 and phosphatidic acid (PA), a product of phospholipase D (PLD) or diacylglycerol (DAG) kinase activity (Damoulakis et al., 2014; Nishikimi et al., 2009) (see scheme in Figure 1.5). Interestingly, P-Rex1 can also activate RhoG and may thus signal in sequence with Dock2 in some pathways (Damoulakis et al., 2014). Upon GPCR stimulation, P-Rex1 can activate RhoG as well as Rac1 and Rac2. As active RhoG is an upstream regulator of DOCK2 (through Elmo), P-Rex1 might signal through RhoG to activate DOCK2. Vav family Rac-GEFs, instead, are activated by protein tyrosine kinases downstream of various types of receptors, including integrins, FcR, GPCRs and TLR4 (Bustelo, 2014). Tiam2 is another Rac-GEF that has been discovered relatively recently in neutrophils and little is currently known about its role in these cells (Boespflug et al., 2014). Tiam-family Rac-GEFs are generally directly activated by Ras and modulated by a variety of mechanisms, including phosphorylation, and they translocate to the plasma membrane upon binding PIP_3 (Boissier & Huynh-Do, 2014). In neutrophils, Tiam2 was shown to regulate chemoattratant-stimulated responses. However, the mechanisms of Tiam2 regulation in these cells remain to be elucidated.

1.5.1.1 P-Rex1

The description of P-Rex structure, mechanism of regulation, binding proteins and functions in other cell types than neutrophils was described in Section 1.4.1. The following section described the role of P-Rex1 in neutrophils.

The first study on P-Rex1 showed that knockdown of P-Rex1 in neutrophil-like NB4 cells provided the first evidence that P-Rex1 is important for myeloid cell function reducing fMLP-stimulated ROS production (Welch et al., 2002). Since then, most our current understanding of the role of P-Rex1 in neutrophils has been obtained through studies using

genetically modified mice. Prex1 knockout murine neutrophils have been shown to have reduced GPCR-dependent Rac2 and RhoG activity, whereas Rac1 activity was comparatively unchanged, thus demonstrating that P-Rex1 acts primarily on Rac2 and RhoG in neutrophils (Welch et al., 2005).

The chemotaxis of isolated Prex1 knockout neutrophils, as well as F-actin polymerisation and polarisation, are only partially reduced when compared to wild-type. They also have a migration defect, which comes from a reduction in cell speed (chemokinesis), whereas the directionality of migration (chemotaxis) is normal (Dong et al., 2005; Welch et al., 2005). However, *in vivo*, Prex1 knockout mice show a profound impairment in neutrophil and macrophage recruitment during sterile and septic inflammation (Welch et al., 2005). P-Rex1 mediates the E-selectin-dependent activation of the neutrophil integrin LFA-1 under flow conditions, thus controlling the slow rolling of neutrophils along the endothelial vessel wall, as well as the activation of the integrin Mac-1, to regulate neutrophil crawling along the vessel wall (J. M. Herter, Rossaint, Block, Welch, & Zarbock, 2013). Isolated Prex1 knockout neutrophils also show a substantial defect in GPCR-dependent ROS production when primed with lipopolysaccharide, whereas this defect is less pronounced in unprimed or TNFα-primed cells, suggesting that P-Rex1 controls neutrophil priming through TLR4 (Welch et al., 2005).

1.5.1.2 Vav

The Vav family consists of three members, Vav1, Vav2 and Vav3. They can activate all Rac isoforms, including RhoG, as well as Cdc42 *in vitro* and *in vivo*, although their cellular activity against Cdc42 is disputed and seems to be context dependent. Moreover, they can also activate RhoA *in vitro* but possibly not *in vivo* (Bartolome et al., 2006; Movilla, Dosil, Zheng, & Bustelo, 2001; Turner & Billadeau, 2002).

Vav-family GEFs have a molecular weight of approximately 100 kDa and are characterised by similar domain structures: the catalytical DH/PH domain tandem, a calponin homology CH domain, an acidic domain (AD), a zinc finger domain, a short proline-rich region and two SH3 domains flanking a single SH2 domain. The SH2 domain mediates recruitment of Vav to cytoplasmic or receptor-associated tyrosine kinases (Bustelo, 2000). Uniquely among Rho GEFs, the Vav family are largely controlled by tyrosine-phosphorylation

dependent relief of inhibitory intramolecular interactions. Their most important and highly conserved tyrosine residue, Tyrosine 174 in Vav1 (Tyr 173 in Vav3), are located in the SH2 domain and AD domain respectively (Bustelo, 2002). Non-phosphorylated Vav-proteins are inactive in a "closed" conformation mediated by intramolecular interactions between the CH-AD region and the catalytic DH-PH domain. Upon phosphorylation of the SH2 domain (Y174 in Vav1) by Src- and Syk- family kinases, these interactions are lost and the active catalytic site is released in order to initiate activation of Rac and of Rac-dependent responses (Aghazadeh, Lowry, Huang, & Rosen, 2000; Bustelo, 2014; Han et al., 1997).

Among Vav family GEFs, all three isoforms are expressed in white blood cells, and only Vav1 is haematopoietic cell specific (Turner & Billadeau, 2002). In neutrophils, Vav3 is expressed 30-fold more than that of Vav1, and 150-fold more than Vav2 (Gakidis et al., 2004).

Vav-family GEFs are best known for being activated downstream of RTKs, integrins, Fc receptors and cytokine receptors (e.g. TNFα and GM-CSF receptors). The SH2 domains mediates Vav recruitment to activated receptors, either by direct binding to RTKs or through intracellular protein tyrosine kinase signalling complexes which are formed upon receptor activation (Bustelo, 2000).

Vav Rac-GEFs are required for neutrophil adhesion and spreading upon GPCR stimulation and for complement or Fc receptor-induced phagocytosis and ROS formation (Gakidis et al., 2004; C. Kim, Marchal, Penninger, & Dinauer, 2003; Utomo, Cullere, Glogauer, Swat, & Mayadas, 2006). Mice lacking Vav1 and/or Vav3 or the entire Vav family have been used to study the functional roles of these GEFs in neutrophils (Swat & Fujikawa, 2005). However, deletion of either single Vav isoforms or combinations show only mild or no defects in migration, suggesting that, just like the P-Rex family, the Vav family alone is not enough for neutrophil migration. Specifically, Vav1-deficient neutrophils have an impairment in fMLP-stimulated actin polymerisation and chemotaxis (C. Kim et al., 2003). They also show reduced Mac-1-dependent crawling under flow conditions, both i*n vitro* and in MIP-2 inflamed cremaster muscle venules (Phillipson et al., 2009). However, neutrophils from Vav1/Vav3 deficient mice can adhere and chemotax towards fMLP, but show defects in either FcR- or integrin-dependent adhesion and spreading. This is not seen in cells lacking

either Vav isoform alone (Gakidis et al., 2004; Utomo et al., 2006). Furthermore, the firm adhesion of neutrophils to fMLP-inflamed cremaster muscle venules is reduced in Vav1/Vav3 deficient mice (Gakidis et al., 2004). Vav1/Vav2/Vav3 deficient neutrophils (Vav-null) show a substantial spreading defect (J. M. Herter et al., 2013). Yet surprisingly, neutrophil recruitment is largely normal during sterile peritonitis in Vav1 and Vav1/Vav3 deficient mice (Gakidis et al., 2004; C. Kim et al., 2003; Phillipson et al., 2009), upon immune-complex deposition in the skin or lung in Vav1/Vav3 deficient mice (Utomo et al., 2008), and during *S. aureus* infection of the lung in Vav-null mice (Graham et al., 2007). Despite this relatively normal neutrophil recruitment, Vav-null mice are less able to clear pulmonary infections of *P. aeruginosa* or *S. aureus* (Graham et al., 2007). This is likely due to a failure in bacterial killing rather than impaired recruitment of neutrophils to the site of inflammation, as Vav-null mice recruit similar numbers of neutrophils to the peritoneal cavity after thioglycollate challenge as control mice. In addition, these mice show impaired interstitial neutrophil migration during *L. monocytogenes* infection in the footpad, which suggests a prominent role of the Vav family in integrin-independent amoeboid neutrophil migration (Graham et al., 2009). Vav3-deficient neutrophils have defects in FcR-dependent phagocytosis and have reduced GPCR-dependent ROS formation, which is further exaggerated when cells lack both Vav1 and Vav3 (Utomo et al., 2006). Indeed, both Vav1 and Vav3 are essential in some (but not all) forms of complement-mediated phagocytosis, as well as Fcγ receptor-dependent phagocytosis and ROS production. Neutrophils missing the entire Vav family have partially impaired TLR- and GPCR-dependent ROS formation, whereas integrin-dependent ROS formation is completely lost. It is clear that the Vav family of GEFs are important for the regulation of Rac-dependent functions in neutrophils; however, there is a substantial level of redundancy between isoforms. Moreover, recent discoveries from our lab have shown a certain level of cooperation between P-Rex1 and Vav1 (see also Section 1.5.2).

1.5.1.3 PIX

One further Dbl-type GEF expressed in neutrophils is PIXα, which is known to activate both Rac and the related GTPase Cdc42 in other cell types. The predominant role of PIXα is in neutrophil chemotaxis, regulating directional sensing. However, this GEF was shown to activate Cdc42 rather than Rac during chemoattractant signalling (Z. Li et al., 2003). Another study suggested that PIXα can directly couple its associated GTPases within a complex

containing the kinase Pak1 and the Arf-GAP Git2, thus regulating the membrane localisation and activity of Rac1 under similar conditions (Mazaki et al., 2006). In general, the substrate specificity of PIXα (Rac vs Cdc42) depends on its dimerisation state, with the binding of Gβγ subunits turning the GEF monomeric and Cdc42-specific (Feng, Baird, & Cerione, 2004). Although this remains to be confirmed, the little literature available suggests that PIXα might activate Rac through Gβγ-independent neutrophil signalling pathways.

1.5.1.4 Tiam

The Tiam-family Rac-GEF Tiam2 was identified in neutrophils as a target of the transcription factor ATF3. When Tiam2 was knocked-down in mouse haematopoietic stem cells that were then differentiated in culture into neutrophil-like cells, these cells show an inhibition in chemotaxis, but increased fMLP-stimulated actin polymerisation and integrin clustering, which suggests that expression of this GEF may limit adhesion rather than promote it as other neutrophil Rac-GEFs do (Boespflug et al., 2014). However, the consequences of Tiam2 expression on other neutrophil responses and on recruitment *in vivo* remain to be investigated. Furthermore, the Tiam2 homologue Tiam1, which is widely expressed, including in some types of leukocytes, is currently under investigation in neutrophils by Dr Kirsti Hornigold in our lab, and found to regulate specifically adhesion-dependent neutrophil responses (unpublished data).

1.5.1.5 DOCK

DOCK2 and DOCK5 are the two known DOCK Rac-GEF family members expressed in neutrophils. Murine deficiency in these DOCK-type Rac-GEFs causes profound defects in neutrophil chemoattractant signalling, thus impairing actin polarisation, leading edge formation and migration speed, although these cells retain β2-integrin-mediated adhesion and directional sensing (Kunisaki, Nishikimi, et al., 2006; Nishikimi et al., 2009). Defects in GPCR-dependent ROS production were also reported in DOCK2 deficient neutrophils, although these could possibly be due to defects in the assembly of the NADPH oxidase complex because receptor-independent ROS production is also impaired (Kunisaki, Nishikimi, et al., 2006). Furthermore, DOCK5 deficiency alone has little effect on neutrophil function. However, the use of DOCK2/DOCK5 deficient neutrophils demonstrated that the combined deficiency exacerbates the migration impairments caused by DOCK2 deficiency (Kunisaki,

Tanaka, et al., 2006; Watanabe et al., 2014). The importance of these DOCK GEFs for neutrophil recruitment *in vivo* remains to be tested. Interestingly, a similar effect on migration as the mouse knockout was obtained when treating isolated neutrophils with CPYPP, a small-molecule inhibitor of these DOCK GEFs (Watanabe et al., 2014).

1.5.2 P-Rex1 and Vav1 cooperate in neutrophil responses

Neutrophils from mice deficient both in Prex1 and in the Vav-family Rac-GEF Vav1 have more profound defects in GPCR-dependent Rac activity, ROS formation, adhesion, and migration than cells that lack either the whole Prex or the whole Vav family (Lawson et al., 2011). This suggested that Prex1 and Vav1 can cooperate to generate robust levels of Rac activity in neutrophils (Figure 1.12). Furthermore, our lab showed recently that Prex1/Vav1 and Prex1/Vav3 deficient mice also have more profound impairments in neutrophil recruitment than mice lacking either GEF family, thus demonstrating *in vivo* synergy between these GEF families (Pan et al., 2015). In addition to this, intravital imaging revealed that this recruitment defect is caused by the loss of L-selectin and E-selectin-dependent neutrophil adhesion to the postcapillary endothelial microvasculature prior to extravasation. One of the most striking discoveries in this study was the requirement for P-Rex1, Vav1 and Vav3 to be expressed in platelets in order to mediate intravascular neutrophil adhesion and therefore recruitment in mice (Pan et al., 2015). Indeed, Prex1/Vav deficiency in platelets was sufficient to block neutrophil adhesion to the vessel wall. Prex1/Vav1 and Prex1/Vav3 deficient platelets had low surface levels of the selectin-ligand PSGL-1, and the mice showed a reduced occurrence of platelet-neutrophil adhesion in the circulation, which is prerequisite for leukocyte extravasation (Pan et al., 2015). Furthermore, platelets expressing of Prex1 and Vav were also important for the recruitment of other types of inflammatory cells. During allergic inflammation, the pulmonary recruitment of eosinophils, monocytes and lymphocytes was compromised by Prex1/Vav1 or Prex1/Vav3 deficient platelets, and airway inflammation was essentially abolished in Prex1/Vav1 and Prex1/Vav3 deficient mice, resulting in improved airway responsiveness (Pan et al., 2015).

Functions of P-Rex1 are less well-defined in macrophages and other types of leukocytes. Unlike in neutrophils, where Prex1 mainly mediates the activation of Rac2 and RhoG, and to a lesser extent Rac1, P-Rex1 is a major Rac1 regulator in macrophages (Z. L.

Wang, X. M. Dong, Z. Li, J. D. Smith, & D. Wu, 2008). Experiments with Prex1/Vav deficient animals have shown that these GEFs are also required for monocyte and macrophage recruitment (Pan et al., 2015).

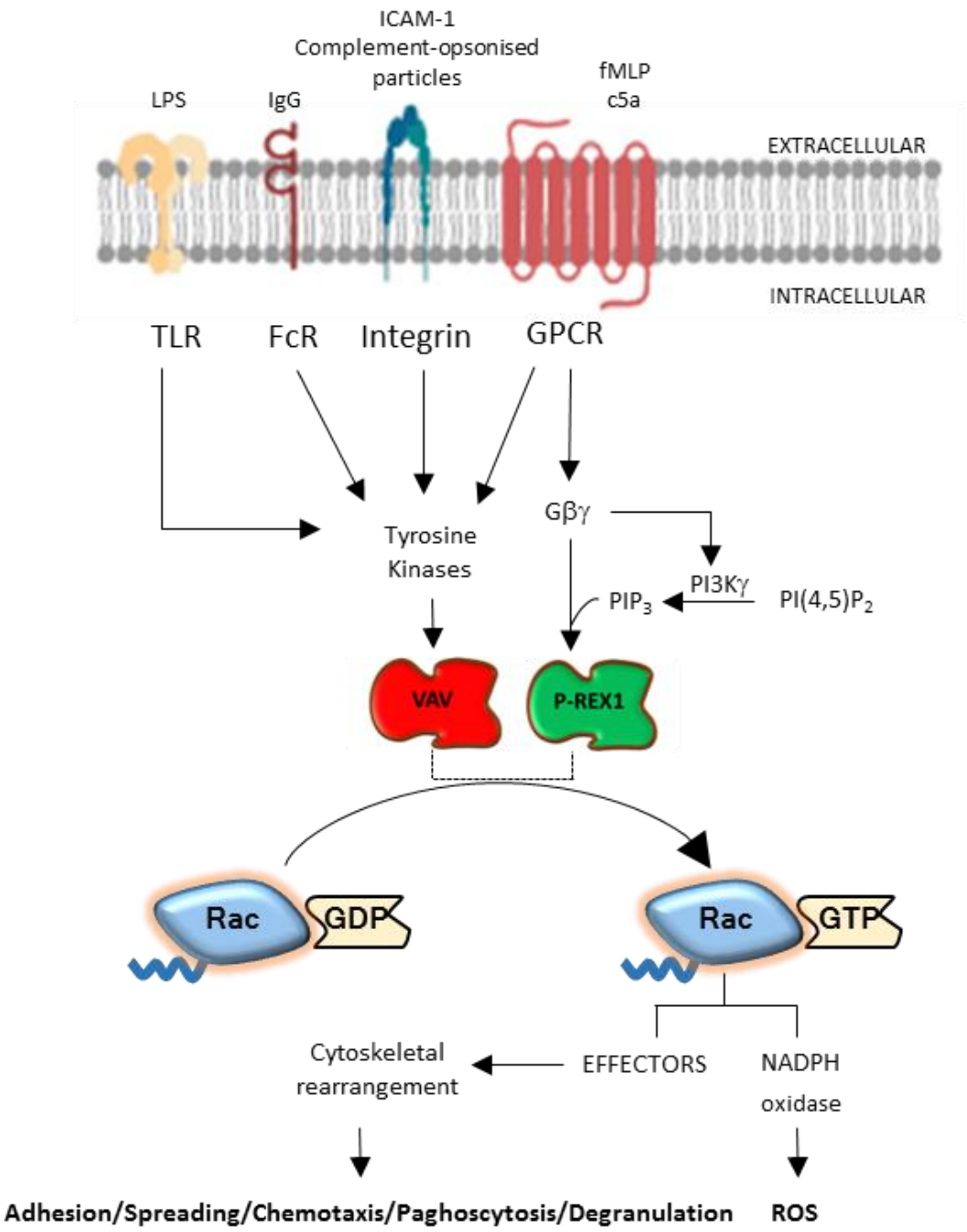

Figure 1.11: P-Rex and Vav family GEFs regulate Rac-dependent neutrophil functions
Proinflammatory signals activate various neutrophil receptors, including TLRs, FcRs, integrins and GPCRs. Vav family GEFs are activated downstream of these receptors via protein tyrosine kinase-dependent phosphorylation, whereas P-Rex1 is synergistically activated by the Gβγ subunits released upon GPCR engagement and by PIP_3, the lipid product of PI3Kγ and possibly other neutrophil class I PI3Ks. P-Rex1 and Vav catalyse the GTP-loading of Rac1 and Rac2, which in turn signal to a variety of downstream effectors leading to a range of responses that are essential for neutrophil function. Figure adapted from (Baker et al., 2016).

1.6 Norbin

Norbin, also known as neurochondrin or NCDN, is an essential, yet understudied, 79 kDa cytosolic adaptor protein. Norbin is a highly conserved protein among vertebrates (Mochizuki et al., 1999), without any catalytic activity or homology to other known proteins (Shinozaki, Maruyama, Kume, Kuzume, & Obata, 1997). The murine Norbin gene consists of 7 exons and spans about 10 kb on chromosome 4. The human Norbin protein is leucine rich (16% of leucine residues), consisting of 732 amino acids, with a molecular weight of 79 kDa. Structurally, it is predicted to consist entirely of armadillo repeats (Dr Simon Andrews, Babraham Institute Bioinformatics Facility, personal communication). A shorter splice variant has also been identified which lacks transcription from the first exon (Mochizuki-Sakisaka et al., 2004b; Mochizuki et al., 1999).

Norbin distribution was originally thought to be exclusively neuronal (Shinozaki et al., 1997), however, the protein has been also detected in chondrocytes, osteoblasts and osteocytes (Ishiduka et al., 1999), and lately our lab has shown its expression in macrophages and neutrophils (Pan et al., 2016). This supported a more general role for Norbin protein than previously expected. The expression of Norbin in neutrophils from the major focus of my study.

The protein is mostly cytosolic (Shinozaki, Kume, Kuzume, Obata, & Maruyama, 1999) and our knowledge of Norbin's functions is limited to the nervous system, where the protein is crucial. Norbin is abundant in neuronal tissue (Mochizuki et al., 1999), where it positively regulates neurite outgrowth and promotes synaptic plasticity (Shinozaki et al., 1999; Shinozaki et al., 1997). It was originally discovered in a screen for proteins that are upregulated in potassium channel blocker-induced long-term potentiation (LTP) in rat hippocampal slices (Shinozaki et al., 1997). Its expression induces neurite outgrowth (Shinozaki et al., 1997), whereas knockdown limits it (H. Wang et al., 2013). Two years later during an independent screen, Norbin was found capable of regulating the hydroxyapatite resorption activity of osteoclasts (Ishiduka et al., 1999).

Murine Norbin deficiency is early embryonic lethal (Mochizuki et al., 2003; H. Wang, Nong, Bazan, Greengard, & Flajolet, 2010), but targeted deletion in mouse neural stem cells revealed impairment in spatial learning and sensorimotor gating, causing epilepsy (Dateki et

al., 2005; H. Wang et al., 2009). Targeted deletion in postnatal forebrain impairs hippocampal plasticity, leading to schizophrenia-like behaviours (H. Wang et al., 2009), and deletion in cortical and hippocampal neurons disrupts adult neurogenesis and causes depression-like behaviours (H. Wang et al., 2015). These rodent phenotypes may be pertinent to humans, as Norbin levels are down-regulated in patients with epilepsy and dysregulated in schizophrenia (Matosin et al., 2015; Xu et al., 2017).

It has also been seen that Norbin is a neuronal target antigen in autoimmune cerebellar degeneration (Miske et al., 2017) and anti-Norbin autoantibodies might be associated with chorea minor (Rommel et al., 2017). Recently Norbin antibody has been identified as a possible new target of autoantibodies against neural cell-surface and intracellular antigens in patients with suspected autoimmune encephalitis, epilepsy or marked epileptiform activity in electroencephalography (Schumacher et al., 2019). Furthermore, clinical studies reported that Norbin antibody is associated with autoimmune ataxia (Weihua et al., 2019).

1.6.1 Norbin in GPCR signalling and trafficking

Mechanistically, Norbin binds directly to numerous GPCRs (33 GPCRs out of 45 tested in pull down studies with recombinant protein). Examples include GPCRs from GPCR superfamily A such as the melanin-concentrating hormone receptor-1 (MCHR1), and from GPCR superfamily C (mGluR1 and mGluR5). Norbin binds through its own C-terminus at the membrane-proximal part of the intracellular C-terminal tail of the GPCR (Francke et al., 2006; H. Wang et al., 2009; Ward, Jenkins, & Milligan, 2009). It can affect the constitutive (agonist-independent) trafficking of these GPCRs to and from the plasma membrane. Furthermore, Norbin can affect GPCR signalling, resulting in altered intracellular Ca^{2+} levels and Erk activity (Francke et al., 2006; H. Wang et al., 2009; Ward et al., 2009). For example, the interaction of Norbin with melanin concentrating hormone receptor-1 (MCHR1) was shown to inhibit the receptors' $G\alpha_{i/o}$ and $G\alpha_{q}$ dependent downstream signalling, but had no effect on the MCH-stimulation dependent internalisation of the receptor (Francke et al., 2006). In contrast, the co-expression of metabotropic glutamine receptor-5 (mGluR5) with Norbin had positive effects on the downstream signalling, transiently increasing intracellular calcium levels, as well as increasing the constitutive surface expression of the receptor on

the neuronal surface, controlling synaptic plasticity (H. Wang et al., 2009). Therefore, the regulation of GPCR surface expression and signalling by Norbin is context-dependent with regard to the GPCR it couples to. However, it is not possible to predict, from the primary structure of the GPCR, whether Norbin can bind to it, although it seems clear that Norbin only affects those GPCRs that it can bind to directly. Furthermore, it is not possible to predict the effect of Norbin binding on the trafficking and signalling of a GPCR, nor are the mechanisms known through which Norbin binding affects the trafficking and signalling of GPCRs. However, within a clinical context recent studies show that mGluR5 hypofunction is integral to glutaminergic dysregulation in schizophrenia and an altered protein-protein interaction of mGluR5 with Norbin suggests that protein-protein interactions in mGluR5-GluN complexes could play as potential targets for intervention in schizophrenia (Wang et al., 2018).

1.6.2 Interaction between P-Rex1 and Norbin

As mentioned in section 1.4 above, Rac-GEF activities are often regulated through complex formation between the GEF and other cellular proteins (Rossman et al., 2005). However, relatively few binding partners of P-Rex1 have been identified (Hornigold K, 2018; Welch, 2015) (see section 1.4.4). Therefore, our laboratory recently conducted a screen for more P-Rex1 binding proteins and this study identified Norbin as new binding partner of P-Rex1 in mouse brain (Pan et al., 2016).

This screen was initiated by former PhD student Mark Barber in the Welch lab (Dr Mark Barber, PhD Thesis, University of Cambridge, 2010). Possible candidates were coimmunoprecipitated with recombinant P-Rex1 from mouse brain cytosol fractions and identified by mass spectrometry. Norbin was identified in this process as a novel binding partner of P-Rex1. Afterwards, another previous PhD student (Dr Dingxin Pan, PhD Thesis, University of Cambridge, 2013) characterised the interaction between Norbin and P-Rex1 using a number of biochemical and cell-based assays and generated genetically modified mice deficient in Prex1 and Norbin, as described in Materials and Methods (see section 2.2).

In her study, Dr Pan used purified recombinant proteins to show that Norbin interacts directly with P-Rex1. Furthermore, mutagenesis experiments showed that Norbin interacts with P-Rex1 via the PH domain both *in vitro* and *in vivo*. Using a liposome-based Rac-GEF

activity assay, she showed that Norbin stimulates the Rac-GEF activity of P-Rex1 *in vitro*. However, the Norbin effect on P-Rex1 Rac-GEF activity was minor compared with Prex1 activation by PIP_3 or Gβγ (Hill et al., 2005; Welch et al., 2002), and it occurred additively with these stimuli, which suggested that Norbin might activate P-Rex1 by increasing the availability of P-Rex1 in the liposomes. Nonetheless, *in vivo*, using overexpression of both proteins in HEK293 cells, the stimulating effect of Norbin on P-Rex1 Rac1-GEF activity was quite robust upon stimulation of the cells with the GPCR ligand LPA. This suggested that the *in vitro* assay was not able to mimic the *in vivo* conditions completely. Importantly, Norbin and P-Rex1 promoted each other's plasma membrane localisation and together stimulated the formation of lamellipodia, membrane ruffling and cell spreading upon overexpression in endothelial PAE cells. The effect of Norbin on the membrane translocation of P-Rex1 was as large as that achieved by synergistic stimulation with PIP_3 and Gβγ. Therefore, Norbin is a major regulator of the subcellular localisation of P-Rex1. Altogether, from this study we concluded that Norbin is a positive regulator of P-Rex1 function that promotes P-Rex1 Rac1-GEF activity largely by increasing the membrane localisation of the GEF (Figure 1.13).

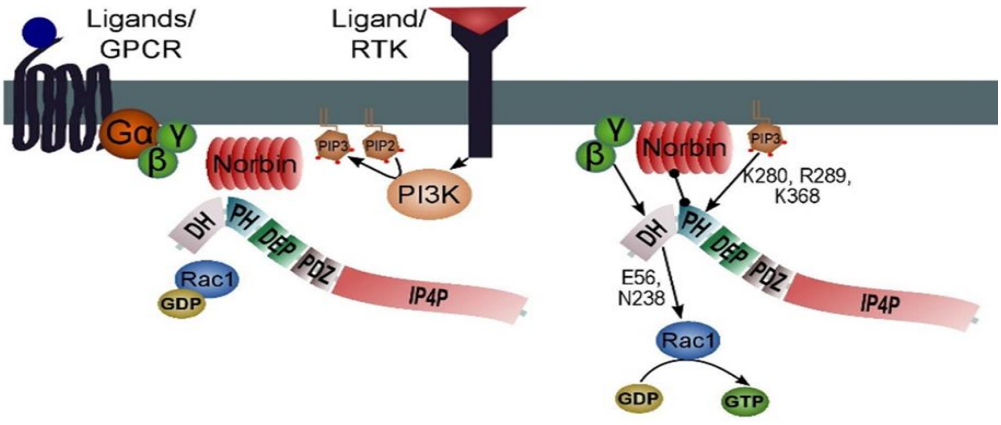

Figure 1.12: Schematic model of P-Rex1 regulation by Norbin
Norbin is a major regulator of the subcellular localisation of P-Rex1 (and vice versa). Norbin recruits P-Rex1 to the plasma membrane, bringing P-Rex1 into closer contact with its other activators (PIP_3 and Gβγ) and with its substrate Rac1. Thereby, Norbin facilitates the P-Rex1-mediated activation of Rac1 and Rac1-dependent remodelling of cytoskeletal structure to alter cell morphology. Figure adapted from (Hornigold K, 2018).

Chapter 2 - Hypothesis

The identification of P-Rex1 expression in neutrophils and the generation of Prex1 knockout mouse strains by our lab (Welch et al., 2005) have allowed an extensive investigation of this Rac-GEF in neutrophils. These studies showed that P-Rex1 is required for Rac2 activity, ROS production, actin polymerisation and migration speed in neutrophils, and for neutrophil recruitment to sites of inflammation (Pantarelli & Welch, 2018). Moreover, the lab has recently identified a direct interaction between P-Rex1 and the neuronal GPCR adaptor protein Norbin *in vitro* and showed that Norbin increases P-Rex1 function by promoting the membrane localisation of P-Rex1. Importantly, the study showed furthermore that Norbin is not only expressed in neurons but also expressed in neutrophils (Pan et al., 2016) (see section 1.6.2).

My PhD project builds on this previous research. The main aim of my PhD was to assess the role of Norbin in neutrophils and the importance of the Norbin/Prex1 interaction for these cells. From the previously published work (Pan et al., 2016), I expected that – if Norbin played any important role in neutrophils at all – it would probably act as a promoter of Prex1 function. Therefore, my hypothesis was that myeloid Norbin deficiency would reduce the Prex-dependent functions of neutrophils.

My study had three parts, which were chosen to evaluate my hypothesis and provide a comprehensive overview of the role of Norbin and the Norbin/Prex interaction in neutrophils. First, I used isolated neutrophils from mice with myeloid Norbin deficiency and mice with combined Norbin and Prex deficiency to investigate neutrophil responses. This included the investigation of adhesion and spreading, ROS formation, degranulation and bacterial killing (Chapter 4). The second part is a study of the signalling pathways and cell surface receptors of neutrophils from mice with myeloid Norbin deficiency and with combined Norbin/Prex deficiency (Chapter 5). The final part investigated mice with myeloid Norbin deficiency and with combined Norbin/Prex deficiency *in vivo*, testing neutrophil recruitment in a model of aseptic peritonitis and innate immunity in a model of pulmonary infection with *S. pneumoniae* (Chapter 6).

Chapter 3 - Materials and methods

3.1 Materials

All general laboratory reagents were purchased from Bio-Rad, Fisher Scientific, Invitrogen or Sigma-Aldrich, unless otherwise stated.

3.2 Mouse strains

All mouse strains used in this project were already available in the Welch lab. They are bred and housed in individually ventilated cages (IVC) at the Babraham Instiute's Biological Services Unit with 12 h lighting cycles with dusk and dawn settings, and with chow diet and water *ad libitum* in accordance with United Kingdom Home Office regulations. For infection with *S. pneumoniae*, animals were housed in isocages in a category II isolator facility. All mice in the facility are routinely tested for 64 pathogens, and no contamination has been found. Animal breeding and experiments were carried out with approval from the local ethics committee under the British Home Office Animal Scientific Procedures Act 1986.

All mouse strains are on C57BL/6 genetic background. $Prex^{-/-}$ mice were generated in the lab as previously described (Donald et al., 2008). $Prex1^{-/-}Prex2^{-/-}$ ($Prex^{-/-}$) and $Prex1^{+/+}Prex2^{+/+}$ ($Prex^{+/+}$) mice were originally mixed C57BL/6 and 129/OLA background but were backcrossed five times to C57BL/6 background. Since then, they were inter-crossed at least once every two years to minimise genetic drift. Dr Dingxin Pan, a former PhD student in the lab (PhD Thesis, University of Cambridge, 2013), generated a genetically modified mouse strain with a conditional Norbin deletion in mature myeloid cells by breeding a strain with a floxed Norbin allele ($Ncdn^{fl/fl}$) (Mochizuki-Sakisaka et al., 2004b), with a strain that expresses Cre recombinase under the regulation of the myeloid differentiation-specific mouse Lysozyme M promoter ($LysM^{Cre}$) on chromosome 10 (Clausen, Burkhardt, Reith, Renkawitz, & Forster, 1999). The resulting homozygous strain is here called $Ncdn^{-/-}$ for brevity. $Ncdn^{-/-}$ mice are born with the expected Mendelian frequency, appear healthy, are fertile, and have normal neutrophil development (see Chapter 4, Section 4.2). Efficient deletion of Norbin in the myeloid lineage was verified by western blotting (Appendix A, Supplementary Figure 1). In order to study the physiological role of the interaction between Norbin and Prex1 in myeloid cells, the $Ncdn^{-/-}$ strain was crossed to $Prex^{-/-}$ mice to generate a strain with myeloid-

specific Norbin and general Prex deficiency, called here Ncdn$^{-/-}$ Prex$^{-/-}$ for brevity. This corresponds effectively to a Norbin/Prex1 double deficiency in neutrophils, monocytes and macrophages, as Prex2 is not expressed in these cells. Ncdn$^{fl/fl}$, LysM^{Cre} and Prex$^{+/+}$ mice were used as control strains throughout. The panel of published and unpublished mouse strains used in this study is showed below (Figure 3.1).

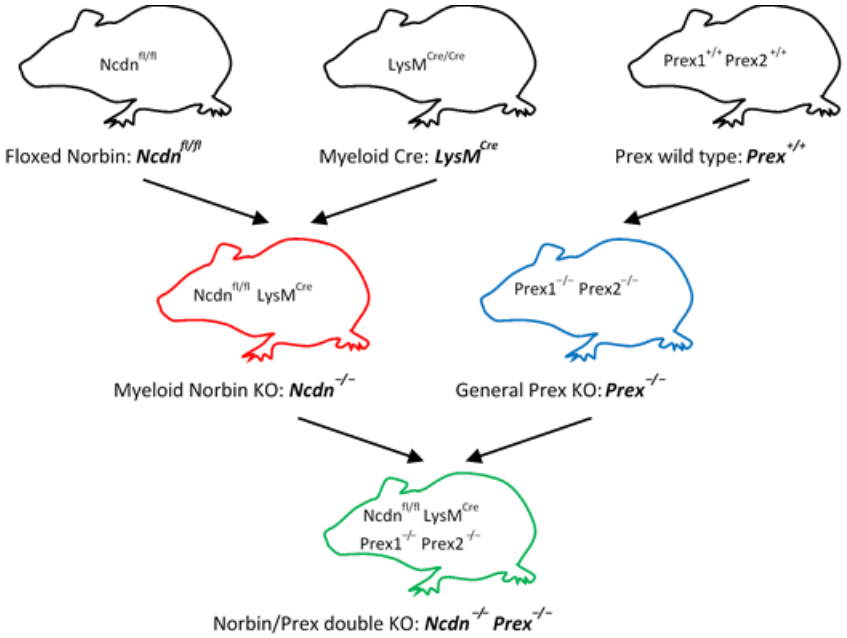

Figure 3.1: Diagram of mouse strains used in this study
Norbin and Prex deficient mouse strains used in this study. The strains are hereafter referred to as Ncdn$^{-/-}$, Prex$^{-/-}$ and Ncdn$^{-/-}$ Prex$^{-/-}$. Mice with KO of Norbin in the myeloid lineage (Ncdn$^{-/-}$, red) were generated by crossing Ncdn$^{fl/fl}$ with LysM^{Cre} mice (unpublished, generated by Dr Dingxin Pan, Welch Lab). Prex$^{-/-}$ (blue) are deficient of Prex1 and Prex2, and were described previously (Donald, Humby et al. 2008). Prex$^{-/-}$ mice were crossed to Ncdn$^{-/-}$ to generate Ncdn$^{-/-}$ Prex$^{-/-}$ that lack Norbin in the myeloid lineage and Prex1 and Prex2 throughout.

3.3 Molecular Biology Techniques

3.3.1 Purification of genomic DNA

Isolation of genomic DNA from tissue culture cells was performed using the Wizard Genomic DNA Purification Kit (Promega, A1120) according to the manufacturer's instructions. Briefly, cells were harvested using a 0.25% (w/v) Trypsin-0.53 mM EDTA solution, collected in a 1.5 mL micro-centrifuge tube and pelleted by a 10 s centrifuge at 16000 xg. The supernatant was removed, and the cell pellet was washed with PBS prior to being centrifuged again. PBS was removed, leaving behind the cell pellet with residual liquid to resuspend cells by vortexing. Cells were then lysed with the provided Nuclei Lysis Solution, treated with RNase Solution and incubated at 37^{o}C for 30 min. Afterwards, Protein Precipitation Solution was added and samples were kept on ice for 5 min prior to being centrifuged at 16000 *xg* for 4 min to pellet the proteins. DNA precipitation was performed by transferring the supernatant to a new tube containing isopropanol, centrifuging at 16000 *xg* for 1 min, washing the DNA pellet with 70% ethanol and air-drying it. The dry DNA pellet was then rehydrated with nuclease-free water at 65oC for 1 h.

To isolate genomic DNA from tissue biopsies, ear or tissue biopsies were collected in 1.5 mL micro-centrifuge tubes. Tissues were lysed with 500 µL of tissue lysis buffer (100 mM Tris-HCl, pH 8.5, 200 mM NaCl, 5 mM EDTA, 0,2% SDS) supplemented with 10 mg.mL^{-1} proteinase K in 10 mM Tris, pH 8.1, 1 mM EDTA, 50% glycerol. Samples were then incubated at 55^{o}C for 4 h, and DNA was precipitated by adding 350 µL of isopropanol, mixing by inversion and centrifuging at 12000 *xg* for 10 min. The supernatant was removed, and the DNA pellet was washed with 70% ethanol. Following this, samples were centrifuged again at 12000 *xg* for 5 min, the supernatant was removed, and the DNA pellet was left to air-dry. The dry DNA pellet was then rehydrated with 30 µL of TE buffer (10 mM Tris, pH 8.0, 1 mM EDTA) at 37^{o}C for 1 h.

3.3.2 Polymerase Chain Reaction (PCR)

PCR was performed according to the guidelines provided by the manufacturer of the Pfu DNA polymerase (Promega, M774A). Amplifications were carried out in 50 µl reaction volumes containing 100 ng template DNA, 5.5 µM forward and reverse primers (Sigma), 0.2

mM dNTPs (Bioline), 1 unit Pfu Polymerase in the manufacturer's supplied buffer and, when necessary, 5% DMSO. Reaction conditions for standard PCRs were: initial denaturing step at 95°C for 5 min, followed by 30 cycles of denaturing at 95°C for 30 s, re-annealing for 30 s at 60°C (or the optimal temperature for the primer pair as stated by the manufacturer; Sigma), extension at 74°C for 2 min/kb of DNA and completion with a final extension at 74°C for 5 min. The relevant DNA was isolated by agarose gel electrophoresis.

3.3.3 Mouse genotyping

Mouse genotyping of the $Ncdn^{fl/fl}$, $LysM^{Cre}$, $Ncdn^{-/-}$, $Prex^{+/+}$, $Prex^{-/-}$ $Prex^{+/+}$, $Prex^{-/-}$ and $Ncdn^{-/-}$ $Prex^{-/-}$ double knockout mouse strains was routinely performed in the lab by research assistant Laraine Crossland. Genomic DNA was isolated from mouse ear biopsies as described in section 3.3.1, and the genotyping was done by PCR following the protocol described in section 3.3.2. The sequences of the primers used are detailed in the table 3.1 below.

Table 3.1: List of primer pairs used for the genotyping of genetically modified mouse strains

Target	Forward primer	Reverse primer	PCR product size
Norbin Floxed allele	TCCTGCGCCTGGCAGTCAGC	TCCCCGAGCCCATGGATCGG	140 bp
Norbin Recombined allele	TCCTGCGCCTGGCAGTCAGC	ACAGACACGGGTCAAGTTCG	200 bp
CRE allele	TACCTGGCCTGGTCTGGACACAGTG	ATGGCTAATCGCCATCTTCCAGCAG	190 bp
EXON 1 allele	AGCTAAAGGCAGAAG GGAGAGACTCTGGAG	AGACAAATACCATGT CAGTCCAGGATCTTG	749 bp
Prex1 WT allele	GACCTGAGGTTTTT TTCTGGCCTCCGTGGC	GAAAGAGGCAGAAG CTGGGCACGCCTGGCC	1 kb
Prex1 KO allele	GGACCAGAGTTTGA CCCCTGAACCTGTGTG	CCAAATTAAGGGCC AGCTCATTCCTCCCAC	436 bp
Prex2 WT allele	GATGCACTTTCAAAA GGGCCTAGTCCTGCC	CCCACTGGTCTTGGT TAATGATGGGTGTCC	800 bp
Prex2 KO allele	TCACTGAAGCGGG AAGGGACTGGCTGC	GTTTCAGGTTCAGGG GGAGGTGTGGGAGG	800 bp

3.4 Protein Detection Techniques

3.4.1 SDS-PAGE

To separate proteins by size for coomassie staining or western-blotting, the BioRad Mini Protean II gel electrophoresis system was used to perform sodium dodecyl sulphate-polyacrylamide gel electrophoresis (SDS-PAGE). For some experiments, gels of 1.5 mm thickness were prepared. The resolving parts were cast first, followed by the stacking gels, using 2x buffer stocks. The amounts of acrylamide (37.5:1, 30% stock, BioRad) and water used for both the stacking and resolving gels and the final concentrations of the resolving gels are listed in Table 3.2. Otherwise precast gels for SDS-PAGE (4-15% Mini-PROTEAN, BioRad, 456-1086) were used.

Table 3.2: Resolving and stacking buffer recipe. The volume of Resolving and Stacking buffer, Bis-acrylamide,

Separating/Resolving gel		Stacking gel	
2x Separation Buffer (0.75 M Tris, 0.2% SDS, pH 8.8)	7.5 mL	2x Stacking Buffer (0.25 M Tris, 0.2% SDS, pH 6.8)	7.5 mL
30% Acrylamide 37.5:1	3 mL	30% Acrylamide 37.5:1	2.5 mL
Water	4.5 mL	Water	5 mL
10% APS	75 µL	Bromophenol Blue	35 µL
TEMED	15 µL	10% APS	75 µL
		TEMED	15 µL

Gels were polymerised with 0.1% Tetra-methyl-ethylenediamine (TEMED) (BioRad) and 0.05% ammonium persulphate (APS), from a freshly prepared 10% stock. Full Range (12-225 kDa) pre-stained molecular weight markers from GE Healthcare were used as standards. Electrophoresis was performed at 120 volts through the stacking gel and 180 volts through the resolving gel in 1x running buffer (10x running buffer stock: 0.25 M Tris, 1.92 M glycine, 1% SDS). SDS-PAGE sample buffer (Laemmli buffer, 4x: 0.4 M DTT, 160 mM Tris pH 6.8, 8% SDS, 50% glycerol, 0.012% bromophenol blue) was added to samples to a final 1.3x concentration (1.3x: 24 mM Tris pH 6.8, 21.6% glycerol, 6% β-mercaptoethanol, 1.3% SDS, 0.006% bromophenol blue), and samples were boiled for least 5 min prior to loading. Sometimes, samples were snap-frozen in liquid N_2 and stored at -80°C. They were

transported in liquid N_2 prior to reuse and were thawed by transferring from liquid N_2 into a boiling heat-block with boiling for at least 5 min. Samples were spun at 12,000 *xg* for 10 s to sediment condensation and were briefly vortexed to re-homogenise prior to loading onto the gel.

3.4.2 Transfer of proteins onto Polyvinylidene fluoride (PVDF) membrane

Following SDS-PAGE, proteins were transferred to PVDF membrane (Millipore) using a standard wet transfer protocol. Transfer buffer contained 24 mM Tris, 193 mM glycine and methanol (5% methanol for proteins between 120-200 kDa, or 10% methanol for proteins <100 kDa). Transfers were done using a mini trans-blot electrophoretic system (Bio-Rad), usually at 100 volts for 120 min, all with constant stirring and using cool packs.

3.4.3 Detection of proteins by western-blot

After transfer of proteins to PVDF, membranes were incubated for 1 h at room temperature in TBS-T (20 mM Tris pH 8, 150 mM NaCl, 0.05% Tween-20) plus 5% non-fat milk powder. Blots were then incubated overnight with primary antibody, at 4°C, in an appropriate blocking buffer (Table 3.3). Membranes were washed 5 × 10 min in TBS-T before incubating for 60 min with horseradish peroxidase (HRP) coupled goat anti-rabbit (Bio-Rad, 1:3000 in TBS-T/5% milk), or goat anti-mouse (Bio-Rad, 1:3000 in TBS-T) secondary antibodies, as appropriate. Blots were then washed a further 5 × 10 min in TBS-T. Proteins were detected by enhanced chemiluminescence (ECL) or ECL Prime (GE Healthcare) according to the manufacturer's instructions. Films were developed using an X-ray film processor (Xograph Imaging Systems).

3.4.4 Stripping and re-blotting of the membrane

If required, bound antibodies on western-blotting membranes were stripped off in stripping buffer (25 mM glycine, pH 2.0, 1% SDS) for 5 min at room temperature. Membranes were then washed in several changes of TBS-T before blocking and re-probing with a different primary antibody.

Table 3.3: Antibodies used for protein detection

Antibody target	Source	Dilution	Blocking Conditions
Norbin C1	Rabbit Dr Kie Mayuyama	1:1000	5% milk/TBS-T
Rac1	Mouse monoclonal Millipore (05-389)	1:3000	5% milk/TBS-T
Rac2	Goat monoclonal Millipore (07-604)	1:5000	5% milk/TBS-T
Phospho-p38 ^{MAPK} (Thr180/Thr182)	Rabbit polyclonal Cell Signalling (9211)	1:1000	5% milk/TBS-T
p38 ^{MAPK}	Rabbit polyclonal Cell Signalling (9212)	1:500	5% milk/TBS-T
Phospho-p44/42 MAPK (Thr202/Thr204)	Mouse polyclonal Cell Signalling (9106)	1:1000	5% milk/TBS-T
p44/42 MAPK	Rabbit polyclonal Cell Signalling (9102)	1:1000	5% milk/TBS-T
Phospho-SAPK/JNK (Thr183/Thr185)	Rabbit polyclonal Cell Signalling (9251)	1:200	5% BSA/TBS-T
SAPK/JNK	Rabbit polyclonal Cell Signalling (9252)	1:200	5% BSA/TBS-T
Phospho-AKT 308	Rabbit polyclonal Cell Signalling (9275)	1:200	5% BSA/TBS-T
Phospho-AKT 473	Rabbit polyclonal Cell Signalling (9271)	1:200	5% BSA/TBS-T
AKT	Rabbit polyclonal Cell Signalling (9272)	1:200	5% BSA/TBS-T

3.4.5 Coomassie-staining of proteins

To determine the presence of proteins and assess the quantity and purity of protein preparations, gels or western-blots were coomassie stained. Gels were incubated in the coomassie staining solution (0.1% Coomassie Brilliant Blue R-250, 50% methanol, 10% acetic acid) for 1 h, followed by several washes in gel de-staining solution (10% methanol, 7% acetic acid). Western-blots were stained with the same staining solution for 5 min, follow by several changes of blot de-staining solution (50% methanol, 7% acetic acid).

3.4.6 Densitometric Analysis of Western Blot X-Ray Films

X-ray films were scanned on a flatbed scanner (Epson V200 photos) and protein band intensities were analysed using Image-J software.

3.5 Neutrophil Purification

All experiments were performed with mature primary neutrophils isolated from the bone marrow of age- and sex-matched, young adult (8-14 week-old) mice. Neutrophils were prepared fresh each day. Endotoxin-free media was used throughout. The neutrophil purification was done at 4°C using two successive Percoll Plus density gradient centrifugations to ensure that the final preparation gave a pure and basal population of neutrophils.

Mouse bone marrow cells were flushed from femurs, tibias and pelvic bones with ice-cold Hank's Balanced Salt Solution (Sigma H6648), without Ca^{2+} or Mg^{2+}, and with 15 mM HEPES, pH 7.4 (RT), and 0.25% endotoxin-free and fatty acid-free (FAF) BSA (Sigma A8806), $HBSS^{--++}$, followed by trituration and filtering through a 40 µm cell strainer into a 50 mL polypropylene Falcon tube. A 12 mL layer of 58% Percoll Plus (GE Healthcare, 17544501) was carefully underlayed beneath the bone marrow cell suspension to create a step-gradient, and samples centrifuged at 1620 ×g, brake 0 (Beckman Coulter Allegra X-30R), for 30 min at 4°C. The cells in the lower 5 mL were collected, resuspended as previous, and the Percoll Plus gradient was repeated one more. Cells at the interphase (lymphocytes, monocytes and immature neutrophils) and the majority of the Percoll Plus were removed. The lower 5 mL (neutrophils and erythrocytes) were resuspended in ≥40 mL $HBSS^{--++}$. Cells were spun at 326 ×g, brake 7, for 10 min at 4°C and the supernatant discarded. Erythrocytes were lysed by resuspending cells in 3 mL of fresh Geye's solution (130 mM NH_4Cl, 5 mM KCl, 780 µM Na_2HPO_4, 176 µM KH_2PO_4, 5.5 mM glucose, 1 mM $MgCl_2$, 280 µM $MgSO_4$, 1.54 mM $CaCl_2$, 13.4 mM $NaHCO_3$) for 3 min at room temperature. Ice-cold $HBSS^{--++}$ was then added to a volume of ≥30 mL to dilute the Geye's solution and cells spun at 326 ×g, brake 7, for 10 min at 4°C. The supernatant was discarded and neutrophils resuspended in 10 mL Dulbecco's Phosphate Buffered Saline (DPBS, Thermo Scientific Fisher, 14040117) containing 0.1% glucose and 4 mM $NaHCO_3$ (DPBS++) per mouse used. Aliquots of 150 µL were taken for cell counting and for checking cell purity by haemocytometer and cytospins, respectively (Figure 3.2). Cells were then spun at 326 ×g, brake 7, for 10 min at 4°C and the supernatant discarded before the cells were resuspended in the final assay buffer at the appropriate concentration, as indicated for each assay.

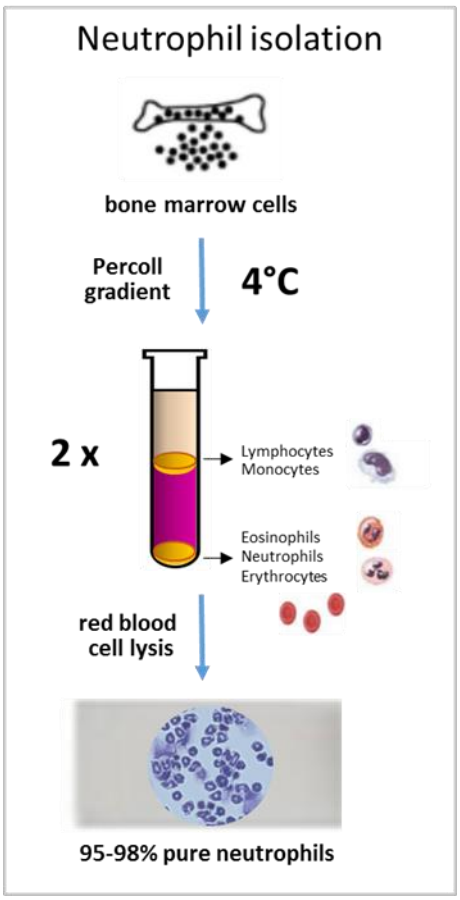

Figure 3.2: Schematic representation of the steps for neutrophil purification

3.5.1 Preparation of neutrophil lysates for Norbin western blot

To determine Norbin expression in isolated neutrophils, 1 x 10^7 cells.mL^{-1} were treated with the protease inhibitor diisopropyl fluorophosphate (DFP, 7 mM) (Sigma, D0879) for 10 min at room temperature, washed with endotoxin-free DPBS++, and boiling 4x SDS-PAGE sample buffer was added to a final concentration of 1.3x and samples boiled for 5 min. Due to the toxicity of DFP, the treatment was done under a chemical fume hood in the presence of another lab member, and DFP wash was disposed as recommended by the manufacturer. While the samples were boiling in sample buffer, the DNA was sheared by trituration through a 25G needle. Total cell lysates were separated by SDS-PAGE and western blotted with the appropriate antibody.

3.6 Neutrophil Responses

3.6.1 Adhesion, Spreading and Polarisation assays

Purified bone marrow derived neutrophils were resuspended at 2 × 10^6 cells.mL^{-1} in DPBS++. Cells were left unprimed on ice or were primed with 20 ng.mL^{-1} murine TNFα and 50 ng.mL^{-1} GM-CSF, for 45 min at 37°C, before 500 µL of cells were added to each well of a 24-well plate (Thermo Fisher, Nunc 142475) containing uncoated 13 mm glass cover slips and 500 µL of 2x fMLP stimulus in DPBS buffer or buffer alone. This resulted in 1 mL of 10^6 cells.mL^{-1} being stimulated with 1.5 µM fMLP. Cells were incubated for 10 or 25 min at 37°C, 5% CO_2, before being fixed for 15 min in 4% paraformaldehyde in DPBS, pH 7.4 at room temperature. Cells were washed twice in PBS and stained for the neutrophil specific marker Gr1 and for DNA (Ly6G & Ly6C) with a cocktail of FITC-Gr1 antibody (Table 3.4) and 20 mM Hoechst stain (Thermo Fisher, 62249), and Fc block (BD Biosciences, 553141) diluted 1:1,000 in PBS, for 30 min at room temperature. The coverslips were then washed three times in PBS and rinsed once in sterile H_2O before being mounted onto slides with ProLong Gold Antifade (Life Technologies, P36934).

For each coverslip, images were taken using a Nikon Eclipse Ti-E widefield system. The large image capture function was used to capture 27 images for each condition: three acquisitions of 9 adjacent fields of view each were taken at magnification 100X, placing the beam first at the centre and then to the right and left areas of the coverslip. The mean number of neutrophils was counted manually, and each cell was manually assigned to one of four different categories depending on its morphology (Table 3.5). The mean area of the neutrophils was calculated by drawing a mask around each cell (size: micron^2, 8000-infinity, pixel units) and establishing a threshold of saturation using Fiji X64 software. Finally, statistical analysis was performed using one-way Anova with Tukey's multiple comparison test using GraphPad software.

Table 3.4: Antibodies used for neutrophil markers

Antibody target	Fluorochrome	Clone/Source and Provider	Dilution and Application
Gr1	FITC	RB6-8C5 BD biosciences (553126)	1:400 (imaging) 1:800 (flow cytometry)
Ly6G	BV510	1A8 Biolegend (127633)	1:500 (flow cytometry)
Cd11b	AF647	M1/70 BD biosciences (557686)	1:1000 (flow cytometry)

Table 3.5: Categories of neutrophils depending on their different morphologies

Category	Example	Features
Spread Polar	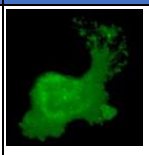	Spread cells with lamellipodia formation, membrane ruffling and clear front/back polarity
Spread Round	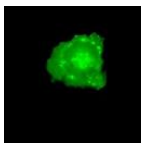	Spread cells without clear polarity
Unspread Polar	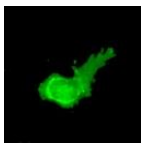	Evidence of lamellipodia and front/back polarity but no spreading
Unspread Round	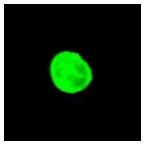	Uniform round shape, unspread

3.6.2 ROS production assays

Purified bone marrow-derived neutrophils were suspended at 1.5×10^6 cells.mL^{-1} in DPBS++ in the presence of 16 units.mL^{-1} horseradish peroxidase (HRP, Sigma, P8375) and 120 µM luminol (Sigma-Aldrich, 123072). ROS production was measured using a luminol-dependent

chemiluminescence assay. Luminol detects intracellular, as well as extracellular, superoxide production, as it is cell-permeable. Endogenous myeloperoxidase provides the peroxidase activity that is required for the intracellular production of light by luminol. The addition of HRP also allows the detection of extracellular ROS production. For experiments with unprimed neutrophils, cells were kept on ice after preparation, and were prewarmed for 5 min at 37°C prior to the assay. Alternatively, neutrophils were primed (or mock-primed) with 50x stocks of 250 $ng.mL^{-1}$ TNFα (R&D Systems, 410-MT-010) and 5 $\mu g.mL^{-1}$ GM-CSF (Petrotech, 315-03) for 45 min at 37°C or with 50 $\mu g.mL^{-1}$ *Escherichia coli* LPS (Sigma, L3024) (50x stock) for 90 min at 37°C prior to stimulation. Prewarmed 2.5x stocks of soluble agonists, 7.5 μM fMLP, 62.5 nM C5a (Sigma, C5788), or 1.25 μM Phorbol 12-myristate 13-acetate (PMA) or buffer-only mock stimuli, were then added to the cells and real time ROS production recorded at 37°C using a Berthold MicroLumat Plus luminometer (Berthold Technologies). The automatic injection port of the luminometer was used for the addition of fMLP and C5a as they elicit responses within seconds, whereas PMA was added manually. This resulted in final stimulus concentrations of 3 μM fMLP, 25 nM C5a and 500 nM of PMA. To illustrate the basal state of the cells obtained using the neutrophil preparation technique (described in section 2.4), Figure 3.3 shows that GPCR-stimulated ROS production was not observed unless the cells were primed beforehand to upregulate the receptors onto the cell surface.

For ROS assays with yeast particles, Zymosan A *S. cerevisae* particles (unlabelled, Thermo Fisher, Z2849) were washed twice and resuspended in DPBS++. The particulate Zymosan stimulus was then manually added to the cells at a concentration of $1.125 \times 10^6.mL^{-1}$ (equal to 3 yeast particles per neutrophil). For ROS assays with bacteria (*S. aureus* Wood 46), bacteria were washed in DPBS++ and opsonised by incubation in DPBS++ with 10% mouse serum for 15 min at 37°C, followed by resuspension in DPBS++. The bacterial stimulus was then added manually to cells that had been primed with 5 $ng.mL^{-1}$ murine TNFα and 100 $ng.mL^{-1}$ GM-CSF (final concentration) for 45 min at 37°C at a concentration of $1.875 \times 10^6.mL^{-1}$ (equal to 5 bacteria per neutrophil).

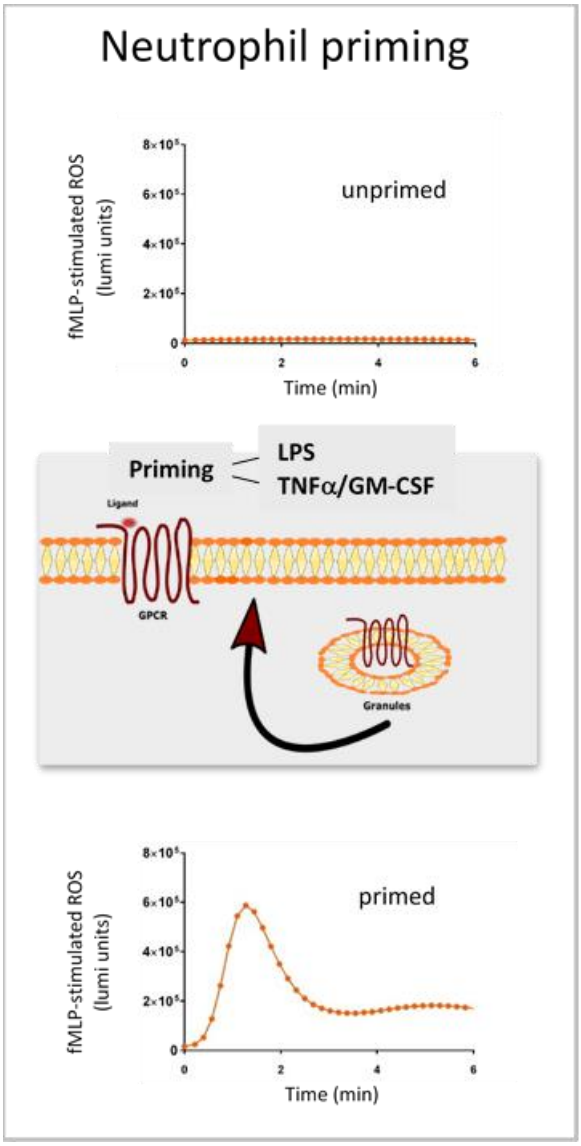

Figure 3.3: Neutrophil priming

Priming is a special mechanism for neutrophils to upregulate receptors that are stored on the secretory vesicles and granules onto the cell surface by degranulation (middle panel). Neutrophils were left unprimed on ice (top panel) or were primed with 5 ng.mL^{-1} TNFα and 100 ng.mL^{-1} GM-CSF (bottom panel) for 45 min at 37°C prior to stimulation with 3 μM fMLP and assessment of ROS production by luminometer. The data are representative from one of ≥10 experiments.

3.6.3 Bacterial killing assay *in vitro*

Staphylococcus aureus bacteria (*S. aureus* Wood 46) were stored at -80°C as glycerol stocks and subcultured in Luria Broth medium (LB) at 37°C to logarithmic growth from overnight cultures. Bacteria were washed in DPBS++ and opsonised by incubation in DPBS++ with 10% mouse serum for 15 min at 37°C, followed by washing in DPBS++. Opsonised bacteria were resuspended in DPBS++ with 10% mouse serum at 1 x 10^8.mL^{-1} or 5 x 10^7.mL^{-1}. Opsonised *S. aureus* cells (5 x 10^6.mL^{-1} or 2.5 x 10^6.mL^{-1}) were added to 5 x 10^6.mL^{-1} (final concentration) primed purified bone marrow derived neutrophils (2.5 x 10^7.mL^{-1} BMNs) for 15 min at 37°C, at ratio of either 1:1 bacteria or 2:1 bacteria per neutrophils when tested in the presence of increasing doses of the ROS inhibitor diphenyleneiodonium (DPI, 10 μM stock) (Sigma, D2926). After the indicated time, 50 μL aliquots were removed from each sample and added to 950 μL ice-cold LB containing 0.05% saponin. Samples in saponin were sonicated in a Misonix 3000 Probe Sonicator (output 1.5 for 10 s) to liberate intracellular bacteria and were returned to ice. Suspensions were serially diluted, plated onto LB-agar and incubated overnight at 37°C to enumerate surviving bacterial colonies. Parallel bacterial incubations were also run in the absence of neutrophils, and with or without DPI as controls.

3.6.4 Degranulation assay

The degranulation protocol was adapted from a protocol by Dr Sonja Vermeren, Centre for Inflammation Research, University of Edinburgh. Purified bone marrow derived neutrophils were resuspended at 5 × 10^6 cells.mL^{-1} in DPBS++. Cells were left unprimed on ice or were primed with 20 ng.mL^{-1} murine TNFα and 50 ng.mL^{-1} GM-CSF, for 45 min at 37°C, before 80 μL of cells were added to each well of a 96-well plate (Nunc). The plates had been previously blocked using 10% HI-FBS for 1 h at room temperature, and contained 20 μL of the indicated concentrations of fMLP in DPBS++ and/or cytochalasin B, or buffer alone. Cytochalasin B is an agent that prevents the polymerisation of F-actin, and as granule secretion is usually inhibited by the neutrophil cortical F-actin, cytochalasin B was added as a positive control to induce maximal gelatinase granule secretion. During stimulation with fMLP (or mock treatment), cells were incubated for 30 min at 37°C, 5% CO_2, followed by centrifugation at 300 ×g for 10 min at 4°C. Following this, 40 μL of the supernatant was removed, without disturbing the cells at the bottom of the well, and added to 20 μL 4x non-reducing SDS-PAGE

sample buffer (no β-mercaptoethanol or DTT) (Table 3.6). Samples were mixed without boiling, and 5 µL were loaded onto an SDS-PAGE gel incorporating gelatine (Table 3.7) and left to run for 20 min at 150 volts through the stacking and the resolving gels in 1x running buffer. Gels were equilibrated in 2.5% Triton X-100 for 30 min at room temperature to wash off the SDS. Gels were developed in developing buffer (Table 3.8) to allow the gelatinase to work by degrading the gelatine in the gel under gentle rocking overnight at room temperature. Gels were rinsed in dH_2O prior to coomassie staining, followed by several washes in gel de-staining solution (25% ethanol and 3% glycerol). Gels were scanned on a flatbed scanner (Epson V200 photo), and gelatinase activity intensities were analysed using Image-J software.

Table 3.6: 4X SDS loading buffer (non-reducing) (left)
Table 3.7: Developing buffer recipe (right)

4 X SDS loading buffer (non-reducing)	
Tris pH 6.8	160 mM
SDS	8%
Glycerol	50%
Bromophenol Blue	

Developing buffer	
NaCl	0.2 M
$CaCl_2$	5 mM
Tris-HCl pH 7.5	50 mM
Triton X-100	0.02 %

Table 3.8: Resolving and stacking buffer recipe. Bis-acrylamide, water, 10% APS and TEMED required for

Separating/Resolving gel		Stacking gel	
2x Separation Buffer (0.75 M Tris, 0.2% SDS, pH 8.8)	20 mL	2x Stacking Buffer (0.25 M Tris, 0.2% SDS, pH 6.8)	7.5 mL
30% Acrylamide 37.5:1	5.3 mL	30% Acrylamide 37.5:1	2.5 mL
Water	2.7 mL	Water	5 mL
1% gelatin B (need to be warmed up if turned gloopy)	2 mL		
10% APS	100 µL	10% APS	75 µL
TEMED	20 µL	TEMED	15 µL

3.7 Pak-CRIB Pull down of active Rac

In order to investigate the effect of Norbin deficiency and/or Prex1 deficiency on fMLP-stimulated Rac activity in primary bone marrow derived neutrophils, PAK-CRIB pull down assays were performed. This allows isolation of GTP-bound active Rac1 and Rac2 from total neutrophil lysates, compared to the total lysate controls, allowing the percentage of Rac that is in its active conformation to be calculated.

3.7.1 Production of GST-Pak-CRIB loaded beads

A GST-tagged version of the Cdc42/Rac-interactive binding domain of p21-activated kinase (GST-Pak-CRIB) was purified from transformed BL21 *E. coli* (Sander, ten Klooster, van Delft, van der Kammen, & Collard, 1999). The pellet from a 50 mL bacterial culture was resuspended in bacterial lysis buffer (20% sucrose, 10% glycerol, 50 mM Tris pH 8, 200 µM $Na_2S_2O_5$, 2 mM $MgCl_2$, 2 mM DTT, 100 µM PMSF, and 10 $\mu g.mL^{-1}$ each of leupeptin, pepstatin-A, aprotinin and antipain) at 4°C, followed by three rounds of sonication using a Misonix 3000 Probe Sonicator at 21 W for 15 s on ice. The cell lysate was ultracentrifuged at 118,000 ×g for 30 min, at 4°C, and the resultant supernatant incubated with prewashed glutathione sepharose 4B beads (GE Healthcare, 17075601) for 2 h with end-over-end rotation on ice. Beads were then washed three times in bacterial lysis buffer, followed by two washes in GST-FISH buffer (10% glycerol, 50 mM Tris pH 7.4, 100 mM NaCl, 1% NP-40, 2 mM $MgCl_2$). The GST-Pak-CRIB beads were stored in GST wash buffer (GST-FISH buffer plus 2 mM DTT, 100 µM PMSF, 10 $\mu g.mL^{-1}$ each of leupeptin, pepstatin A, aprotinin and antipain) at 4°C for up to one week. The quality and purity of GST-Pak-CRIB immobilised on glutathione sepharose beads was assessed by SDS-PAGE, followed by coomassie staining (Figure 3.4).

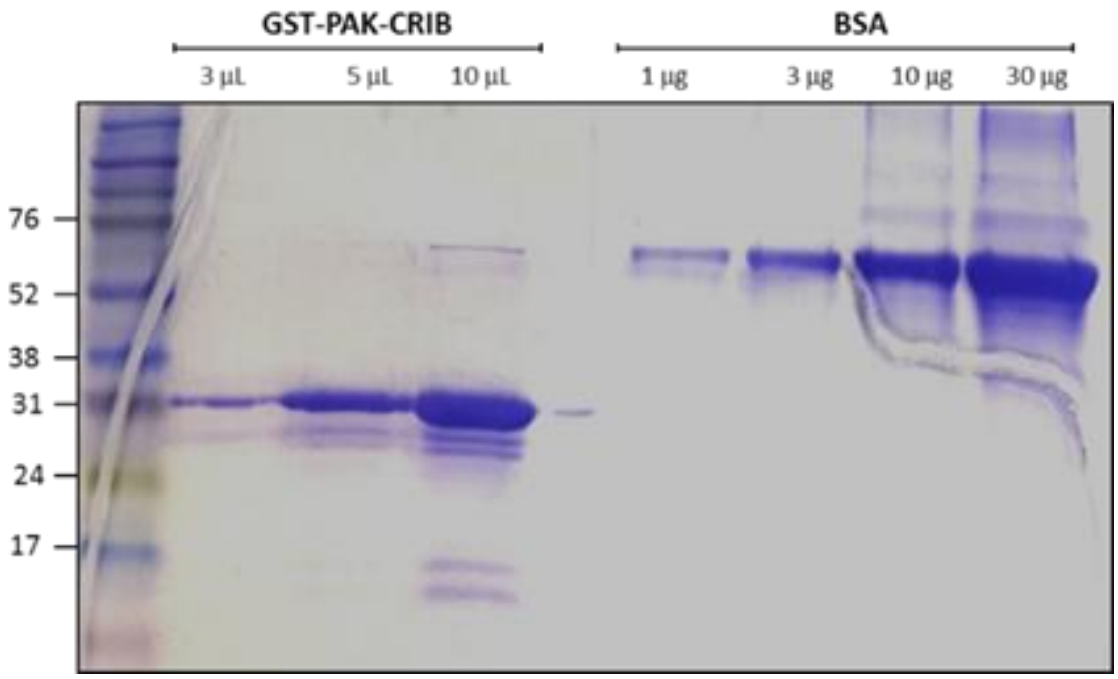

Figure 3.4: Coomassie-stained SDS-PAGE gel showing GST-PAK-CRIB production
After preparation of GST-PAK-CRIB coupled to glutathione sepharose beads, aliquots of the beads (volumes indicated) were boiled in SDS-PAGE buffer, separated on a 12% SDS-PAGE gel and the gel coomassie stained to evaluate the quality and purity of GST-PAK-CRIB production, compared to BSA standards of known quantity.

3.7.2 Rac activity assay

Purified bone marrow derived neutrophils were resuspended at 1×10^7 cells.mL^{-1} in DPBS++ and pre-warmed for 10 min at 37°C. Aliquots of 200 µL aliquots were then either stimulated between 0 and 15 s with 1, 3 or 10 µM fMLP (Sigma, F3506) or left unstimulated. The reaction was stopped by the addition of 1 mL of ice-cold lysis buffer (GST wash buffer, plus an extra 0.2% NP-40, to give a final concentration of 1% NP40) for 2 min. Samples were centrifuged at 12,000 *xg* for 3 min at 2°C, the supernatant transferred into fresh precooled tubes, and 2% of the supernatant removed as a total lysate control. The remaining sample was incubated with 10 µL of GST-Pak-CRIB beads, rotating end-over-end for 15 min on ice. The beads were then washed 5 times in GST-wash buffer, each time spinning at 18,000 *xg* for 30 s at 2°C. Finally, 40 µL of boiling SDS-PAGE sample buffer was added to samples to a final 1.3x concentration, and samples were boiled for least 5 min prior to loading. Total lysate samples were diluted in 4× SDS-PAGE buffer to a final 1.3x concentration. Samples were then snap-frozen in liquid N_2 and stored at -80°C prior to analysis. GTP-Rac and total

Rac were then quantified by running the samples on 13.5% SDS-PAGE and Western Blotting with Rac1 antibody (Millipore, 05-389, 1:3000) or Rac2 antibody (Millipore, 07-604, 1:5000) in Tris Buffered Saline (TBS), 0.05% Tween-20, 5% non-fat powdered milk. This was followed by five washes in TBS-T (1x TBS, 0.05% Tween-20) for a total of 1 h before addition of the secondary antibody (goat anti-mouse IgG-Horseradish Peroxidase [HRP] conjugate, BioRad, 1:3000; or goat anti-rabbit IgG Horseradish Peroxidase [HRP] conjugate, BioRad, 1:3000, as appropriate) in blocking buffer. The incubation was carried out for 1 h and followed by a further five washes in TBS-T for a total of 1 h. Proteins were detected by enhanced chemiluminescence (ECL) or ECL Prime (GE Healthcare) according to the manufacturer's instructions. Films were developed using an X-ray film processor (Xograph Imaging Systems). Blots were scanned and GTP-Rac and total Rac levels were quantified using ImageJ software.

3.8 Analysis of GPCR signalling pathways: Erk, p38^{Mapk}, Jnk, Akt

Purified bone marrow derived neutrophils were resuspended at 1×10^7 cells.mL^{-1} in HBSS^{--++}. Cells were primed with 20 ng.mL^{-1} murine TNFα and 40 ng.mL^{-1} GM-CSF, for 45 min at 37°C, prior to stimulation for 10, 45 or 180 s with 0.3 or 1 μM fMLP (Sigma) in DPBS++, or mock treatment with DPBS++ alone. The reaction was stopped by the addition of excess ice-cold DPBS++ for 2 min. Samples were centrifuged at 12,000 *xg*for 30 s at 2°C. Cell pellets were lysed with 9 volumes of ice-cold RIPA buffer (30 mM Hepes pH 7.4, 150 mM NaCl, 1% Nonidet P-40, 0.5% deoxycholate, 0.1% SDS, 5 mM EGTA, 4 mM EDTA), supplemented with 1 mM DTT, 1 mM PMSF, protease inhibitors (1 μg.mL^{-1} leupeptin, 1 μg.mL^{-1} pepstatin A, 1 μg.mL^{-1} aprotinin, 1 μg.mL^{-1} antipain) and phosphatase inhibitors (50 mM NaF, 10 mM β-Glycerophosphate, 10 mM $Na_2P_2O_7$ and 1.5 mM Na_3VO_4) for 5 min on ice with frequent vigorous vortexing. Cell lysates were centrifuged at 12,000 *xg* for 30 s at 2°C to sediment debris. SDS-PAGE sample buffer was added to the supernatant to a final 1.3x concentration, and samples were boiled for least 5 min prior to loading. Western blotting was performed to probe levels of total and active, phosphorylated protein for p38, Erk, Jnk and Akt (see Table 3.3 for antibody catalogue numbers, dilutions and conditions for incubation).

3.9 Analysis of endogenous receptor levels on the neutrophil plasma membrane

Mouse bone marrow cells were flushed from femurs, tibias and pelvic bones with ice-cold $HBSS^{--++}$, passed through 40 µm filters, and counted using a haemocytometer. Cells were pelleted at 326 × g, brake 7, for 10 min at 4°C and resuspended in ice-cold DPBS++ at 4×10^7 cells.mL^{-1}, before being subjected to one of the following conditions: some were kept on ice throughout, to maintain basal levels of the receptors at the cell surface and minimise any receptor trafficking. Alternatively, cells were incubated for 30-45 min at 37°C to allow constitutive receptor trafficking to occur, or they were primed with 20 ng.mL^{-1} murine TNFα and 40 ng.mL^{-1} GM-CSF, for 45 min at 37°C, in order to induce maximal upregulation of receptors to the plasma membrane. In some instances, cells were also stimulated for 10 or 30 min with 100 nM recombinant C5a (Sigma, C5788) in order to elicit agonist-induced receptor internalisation. Cells were then centrifuged at 10,000 ×g, brake 9, for 30 s at 4°C, resuspended in an ice-cold staining cocktail with antibodies for GPCRs (Table 3.9) and neutrophil markers, FITC-Gr1 or BV510-Ly6G and AF647-Cd11b (Table 3.4) and containing Fc block (BD Biosciences, 553141) diluted 1:1,000 in DPBS++, followed by incubation for 20 min on ice for staining. Stained cells were spun at 10,000 ×g, brake 9, for 30 s and pellets resuspended in 1 mL of ice-cold $HBSS^{--++}$ with 1 mM EDTA and kept on ice until the analysis. Flow cytometry of cells was performed using a BD Biosciences LSR-Fortessa or BD Biosciences Fortessa A flow cytometer and data analysis was performed using FlowJo single-cell analysis software. Neutrophils were identified by Gr1 or by Ly6G and CD11b staining, and GPCR surface expression levels were measured as the mean intensity of the PE signal from the PE-GPCR antibody. Figure 3.5 illustrates the differences in CD11b (Mac-1) staining that was obtained after using each of the different neutrophil priming and mock priming techniques. This show that the neutrophils left on ice had low levels of the integrin on their surface, suggesting that they were truly basal cells. It suggested furthermore that mock priming (incubation at 37°C) upregulated integrin to the neutrophil surface to some extent, whereas priming with TNFα and GM-CSF upregulated it maximally to the neutrophil surface, as expected.

Table 3.9: Antibodies used for GPCR detection

Antibody target	Fluorochrome	Clone/Source and Provider	Dilution and Application
CXCR1	PE	U45-632 BD Pharmigen (566383)	1:60
CXCR2	PE	SA0044G4 BioLegend (149303)	1:60
CXCR4	PE	2B11 Invitrogen (12-9991-81)	1:60
C5a-R	20/70 PE	Rat mAb Abcam (53434)	1:60

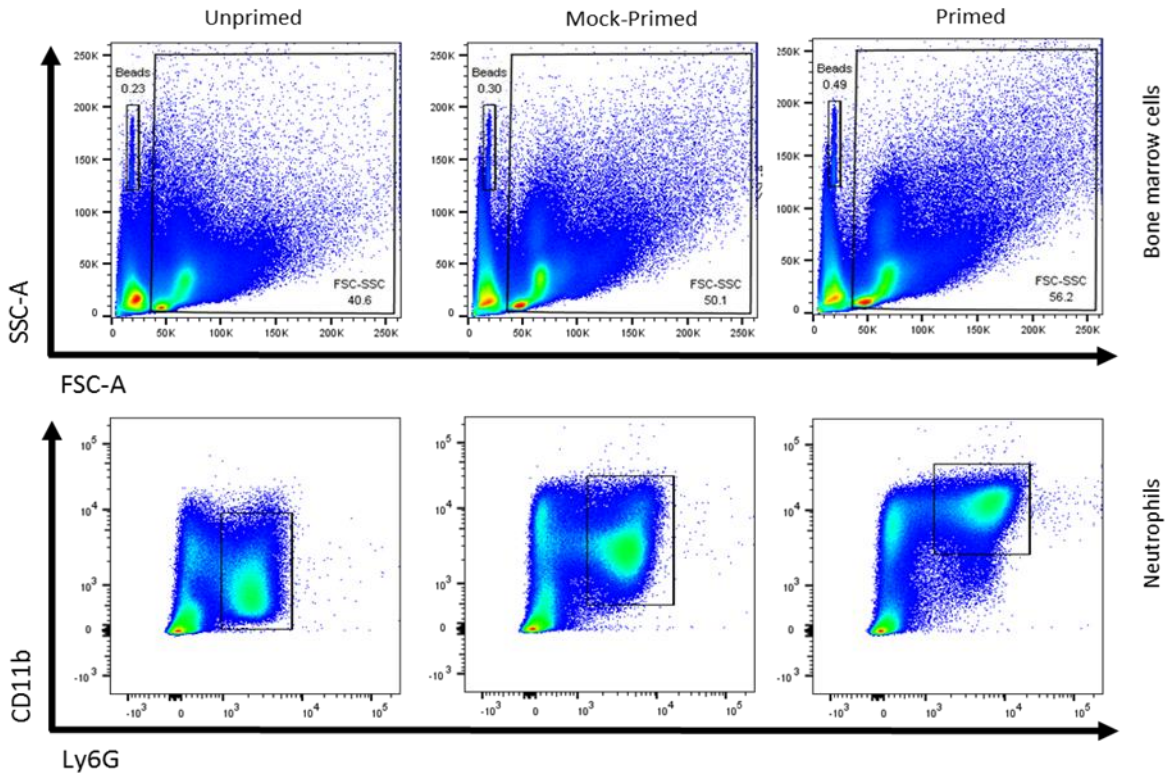

Figure 3.5: Priming of neutrophils upregulates CD11b to the surface
Bone marrow cells from Ncdn$^{fl/fl}$ mice were either left on ice, unprimed (left panel), mock primed for 45 min at 37°C (middle panel) or primed with 20 ng.mL^{-1} murine TNFα and 40 ng.mL^{-1} GM-CSF, for 45 min at 37°C (right panel), before staining with Ly6G and CD11b antibodies on ice. Flow cytometric analysis for testing forward and side scatter (top panel). Neutrophils were identified by Ly6G staining and the extent of priming was assessed by the amount of CD11b (Mac-1 integrin) on the neutrophil surface. The data are representative of ≥6 experiments.

3.10 *In vivo* models

To test the role of Norbin in neutrophil recruitment to sites of inflammation and infections, and to investigate the antibacterial immunity of Norbin and Norbin/Prex1 deficient mice *in vivo*, I used two different inflammatory animal models: (i) thioglycollate (TGC)-induced sterile peritonitis; (ii) *Streptococcus pneumoniae* induced pulmonary infection which was done either with or without prior neutrophil depletion.

3.10.1 Peritoneal neutrophil recruitment assay (TGC-induced aseptic peritonitis)

Mice of the specified genotypes were subjected to 0.25 mL intraperitoneal injections of sterile H_2O (mock) or 3% thioglycollate (Sigma, T9032) that had been preprepared in sterile H_2O and autoclaved prior to injection (test). At 3 h after the injections, mice were culled by CO_2 asphyxiation and pithing, and were subjected to peritoneal lavages. Lavages involved the injection of 8 mL DPBS/5 mM EDTA into the peritoneum and aspirating the liquid back into the syringe to collect recruited cells. A second injection of 8 mL PBS/5 mM EDTA was then performed followed by an incision in the peritoneal wall to collect any remaining liquid, which was pooled with the previous lavage. Collected cells were pelleted at 10,000 *xg* for 30 s at room temperature, and most of each sample was resuspended in a staining cocktail of antibodies for neutrophil markers FITC-Gr1 and AF647-Cd11b (Table 3.4) with Fc block (BD Biosciences, 553141) diluted 1:1,000 in DPBS++. Cells were incubated in the staining cocktail for 20 min on ice in the dark and then washed in DPBS/5 mM EDTA before being resuspended in DPBS/5 mM EDTA/1 $\mu g.mL^{-1}$ DAPI for flow cytometric analysis. An addition of 5.0-5.9 µm Spherotech beads (Spherotech, ACBP-50-10) was made to each sample, giving a final concentration of 1.25×10^5 $particles.mL^{-1}$, to enable the quantification of the number of cells per given volume by flow cytometry using a BD Biosciences LSRII flow cytometer. Neutrophils were detected as cells with high levels of Gr1 and Cd11b staining. Analysis of the flow data was done using FlowJo single-cell analysis software, and the number of cells recorded corrected to the volume initially recovered during the peritoneal lavage, to account for any cells lost in the process.

In parallel, the remaining cells were counted using a haemocytometer, taking a mean of at least 4 counts per sample. Other aliquots of the cells were cytospun onto microscope

slides at 300 *xg* for 3 min at room temperature and stained with Kwick-Diff staining (Thermo Scientific Shandon, 9990700). Cytospin slides were assessed by light microscopy to determine the percentage of neutrophils present, using their characteristic nuclear shape to identify neutrophils (see Section 6.2, Figure 6.1A). At least 200 cells from 3 different fields of view were counted per slide. The number of neutrophils that had migrated to the inflamed peritoneum upon TGC challenge was calculated based on the total cell count and differential cell count. Both methods, flow cytometry and cytospin, which I used in parallel throughout, gave similar results.

3.10.2 Streptococcus pneumoniae model

Inoculum preparation

Streptococcus pneumoniae (TIGR4, serotype 4) was grown to mid-log phase (OD_{500} = 0.5-0.7) in Todd-Hewitt broth (Oxoid) supplemented with 0.5% yeast extract (Oxoid) at 37°C, 5% CO_2. The bacteria were collected by centrifugation, and resuspended at OD_{500} = 1.0 PBS/20% glycerol (Sigma-Aldrich) prior to snap-freezing in liquid N_2 and storage at -80°C. Stocks were assessed for viable CFU counts and homogeneity by plating out serial dilutions of three frozen samples on blood agar plates (LB agar, supplemented with 5% defibrinated horse blood (Oxoid) after incubation for 24 h at 37°C, 5% CO_2. *S. pneumoniae* colonies were confirmed by the presence of an α-haemolytic zone and sensitivity to optochin (Millipore, 74042). Virulent stocks were maintained by performing an *in vivo* passage every 6-12 months (A. K. Stark et al., 2018).

Intranasal infection

In a category 2 laboratory, frozen stocks of *S. pneumoniae* were thawed on ice, and washed twice by centrifugation in HBSS (Sigma-Aldrich, 6648), before being resuspended at 4 x 10^7 $CFU.mL^{-1}$ in HBSS. The suspension was kept on ice at all times, and used for infection within 2 h of thawing (no loss of viability was observed under these conditions). In the category 2 unit of the small animal facility, light anaesthesia was induced in one mouse at the time, by inhalation of 3% isoflurane and maintained with 2 % isoflurane. Anaesthetised mice (males aged 8-12 weeks) were made to inhale 2 x 10^6 CFU *S. pneumoniae* in 50µL sterile HBSS through both nostrils. Mock-treated animals received the same volume of sterile DPBS. Animals were observed closely to confirm inhalation of the dose and full recovery from

anaesthesia. Once the animal was fully recovered, the next mouse was treated. In most experiments, generally, the infection dose was confirmed by plating out serial dilutions of the inoculum on blood agar plates, as described above.

Pulmonary lavages

At the specified times following infection, mice were euthanized by CO_2 inhalation, followed by severing of the femoral artery. Broncho-alveolar lavage (BAL) was performed by making a small incision in the trachea using sharp forceps, inserting a venflon device (1.1 x 32 mm, BD 391452) and lavaging manually by slow injection and subsequent aspiration of 1 mL of DPBS. The BAL was stored on ice until further use.

Homogenisation of perfused lung

Lungs were perfused with 10 mL DPBS through the right ventricle using a 10 mL syringe. The lungs were removed surgically using aseptic technique and placed in a GentleMACS C Tube (Miltenyi Biotec, 130093237) containing 2 mL DPBS. Lungs were homogenized using the mouse lung dissociation enzyme kit from Miltenyi (130095927) according to the manufacturer's instructions, and placed into a GentleMACS tissue homogeniser (on setting 2.1 Lung) for 40 s for tissue dissociation. The lung homogenate was incubated for 45 min at 37°C. The digestion was stopped by placing the tubes on ice, and the homogenate was transferred to 15 mL tubes (BD Falcon, 1130502) and washed by centrifugation at 500 *xg* for 5 min at 4°C in 10 mL cold DPBS. The pellet was resuspended in 3 mL 37.5% isotonic Percoll (GE Healthcare) in DPBS at room temperature and centrifuged at 650 *xg* for 20 min with low acceleration and no brake. The supernatant including tissue debris was removed, and the cell pellet was washed and resuspended in cold DPBS. Single-cell suspensions were processed for flow cytometry as described below.

Leukocyte recruitment into the lung (lavages and tissue)

The pulmonary recruitment of leukocytes following infection with *S. pneumoniae* was analysed in aliquots of the BAL and the perfused lung homogenate by flow cytometry. Cells were incubated in antibody staining cocktail (detailed in Table 3.10) for 40 min on ice in the dark and then washed in sterile DPBS before being resuspended in Fixation Buffer (Biolegend, 420801) for flow cytometric analysis. An addition of 5.0-5.9 µm Spherotech

beads (Spherotech, ACBP-50-10) was made to each sample, giving a final concentration of 1.25×10^5 particles.mL^{-1}, to enable quantification of the cells. The flow cytometric analysis was done using a BD Biosciences Fortessa A flow cytometer. Neutrophils were detected as cells with high levels of Ly6G and CD11b staining (Cotter & Muruve, 2006). Macrophages and inflammatory monocytes were identified as cells with high levels of CD11b and CD11bhi Ly6Chi staining. The gating strategy for the cell population obtained from the lung homogenisation is shown in Figure 3.6. Analysis of flow data was done using FlowJo single-cell analysis software and the number of cells recorded, corrected for the volume initially recovered from the BAL lavage.

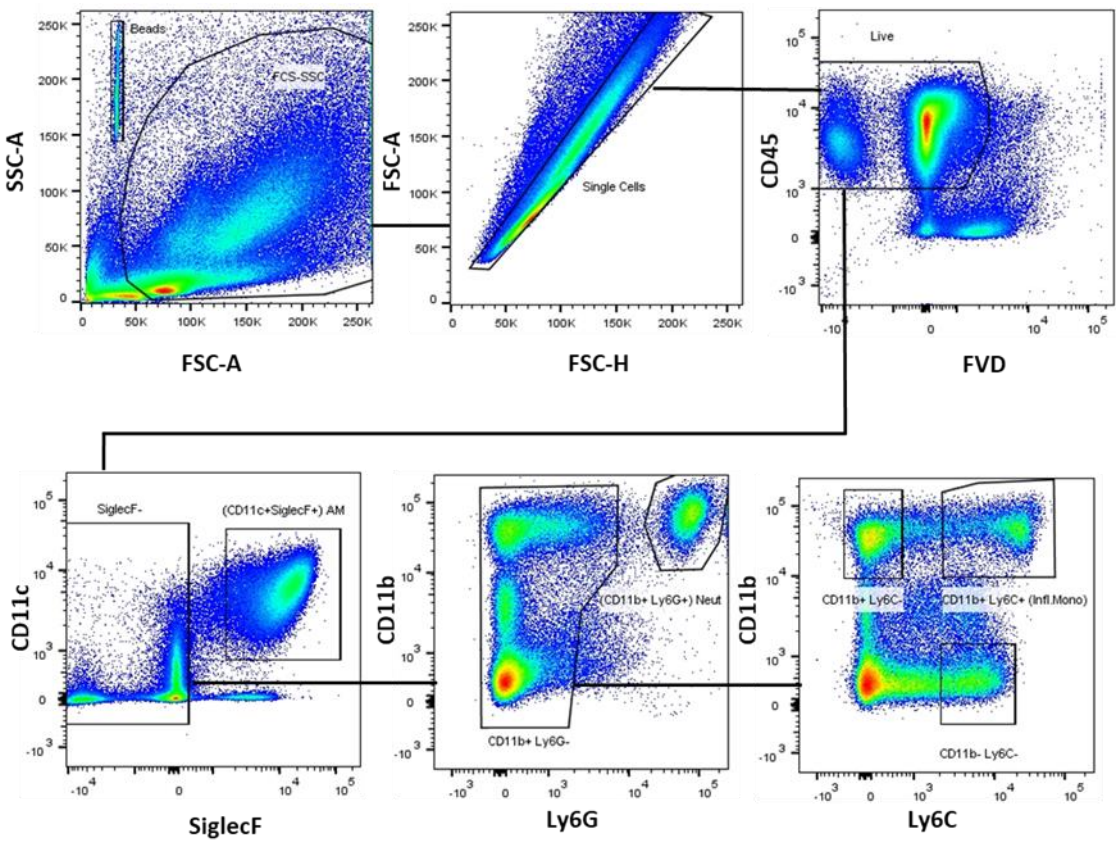

Figure 3.6: Gating strategy for lung myeloid populations 18h post *S. pneumoniae* infection
Flow cytometry plots show the separation of myeloid single-cell suspensions from whole lungs. FSC-A and SSC-A indicate forward and side scatter, respectively. Live cells were gated based on viability dye (FVD) and CD45 expression. Representative plots demonstrate the expression of CD11c+ and SiglecF+ cells (Alveolar Macrophages); the expression of CD11b+ and Ly6G+ (Neutrophils); and the expression of CD11b+ and Ly6C+ (Inflammatory Monocytes).

Table 3.10: Antibodies used for leukocytes recruitment detection in *S. Pneumoniae* model

Laser	Fluorochrome	Antibody target	Clone/Source and Provider	Dilution and Application
488 nm 530/30	FITC	CD24	M1/69 Biolegend (101805)	1:400
405 nm 450/50	BV421	Ly6C	AL-21 BD Biosciences (562727)	1:500
405 nm 525/50	BV510	Ly6G	1A8 Biolegend (127633)	1:500
405 nm 780/60	BV785	CD11c	N418 Biolegend (117335)	1:500
561 nm 585/15	PE	SiglecF	E50-2440 BD Biosciences (552126)	1:500
640 nm 670/14	AF647	CD11b	M1/70 BD biosciences (557686)	1:1000
640 nm 780/60	eF780	Fixable Viability Die (FVD)	eBiosciences (65086514)	1:5000
355 nm 379/28	BUV395	CD45	30-F11 BD Biosciences (564279)	1:300

Bacterial counts in pulmonary lavages and lung tissue

In parallel, 200 µL aliquots of the lung homogenate and BAL were subjected to bacterial counts, by preparing serial dilutions in DPBS and plating on blood agar plates. Plates were incubated for 24 h at 37°C and bacterial colonies counted. The bacterial load within the lungs and the BAL was determined from plates of appropriate colony density (≈20-200 colonies/plate), using the following formula:

CFU (Colony forming units) = colony count × dilution factor

3.10.3 Neutrophil depletion in the *Streptococcus pneumoniae* model

To achieve robust neutrophil depletion, mice were injected intraperitoneally with two doses of 1A8 monoclonal anti-Ly6G antibody (BioXCell, BE0075-1) at 25 $mg.kg^{-1}$ in 200 µL PBS at 24 h and 0 h prior to infection, followed by intranasal challenge with *S. pneumoniae*, or mock treatment (Table 3.11), as described above. Neutrophil-depleted animals were compared with animals that had been mock-treated with the equivalent dose of isotype control IgG (monoclonal 2A3 anti-trinitrophenol, BioXCell, BE0089). Prior to injections of Ly6G or isotype control antibodies, a 50 µL tail blood sample was taken for the enumeration of peripheral blood neutrophil counts. Tail blood samples were collected into microvette capillary tubes covered with EDTA, to prevent blood clotting. Blood samples were spun at 600 *×g*, for 6 min at room temperature, and the supernatant discarded. Erythrocytes were lysed by resuspending the cells in 500 µL of fresh Geye's A solution (130 mM NH_4Cl, 5 mM KCl, 780 µM Na_2HPO_4, 176 µM KH_2PO_4, 5.5 mM glucose) for 5 min at RT. DPBS was then added to a volume of ≥1.5 mL to dilute the Geye's solution and cells spun at 300 ×g, 6 min at RT. The supernatant was discarded and the pellet resuspended in a staining cocktail with antibodies for neutrophil markers (Table 3.10). An addition of 5.0-5.9 µm Spherotech beads was made to each sample, giving a final concentration of 1.25×10^5 $particles.mL^{-1}$, to enable the quantification of the by flow cytometry using a BD Biosciences Fortessa A flow cytometer. Neutrophils were detected as cells with high levels of CD24 and CD11b staining, with CD24 antibody being used instead of Ly6G, as the 1A8 depleting antibody targets the Ly6G epitope. Analysis of flow data was done using FlowJo single-cell analysis software and the number of cells recorded corrected for the number of beads acquired.

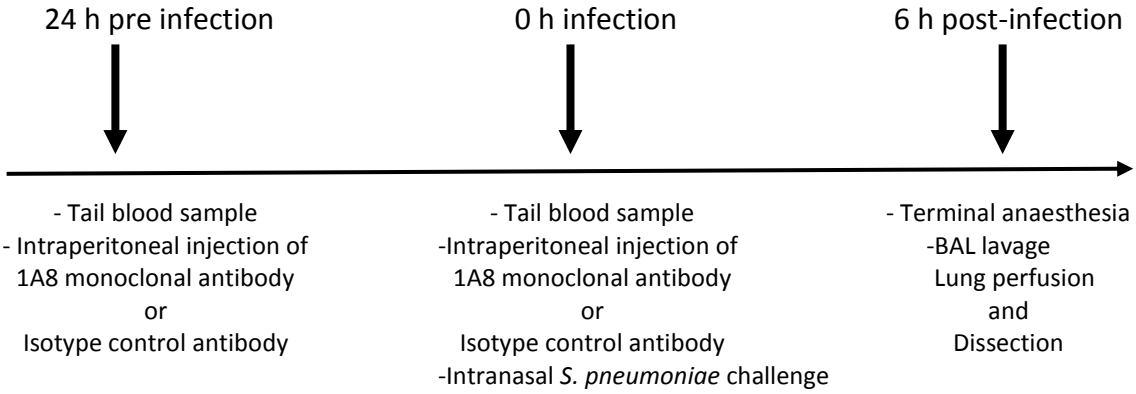

Table 3.10: Schematic diagram of the neutrophil depletion time points in the *S. pneumoniae* model

3.11 Experimental design and statistical analysis

Wherever feasible, mice from the same sex and matched age where used. The setting for sample sizes was based on previous knowledge in the laboratory, from the literature or from pilot studies. Simple comparisons between single independent measurements from two groups were made using two-tailed unpaired Student's t-tests or Mann-Whitney U-tests as appropriate. Depending on experimental design, single or repeated measures one-way analysis of variance (ANOVA), two-way ANOVA, or three-way ANOVA were used to test for effects of interventions. The threshold for statistical significance was set at $P<0.05$. P-values reported are from t-tests, or from multiplicity-adjusted Dunnett's or Holm-Sidak's post-hoc adjustments, as appropriate. Where hypothesis testing was non-significant, the p values have not been explicitly noted. Prior to statistical analysis, data were tested for normality of distribution, in order to determine if parametric or non-parametric analysises were appropriate. Where appropriate, data were log-transformed or square root-transformed prior to statistical analysis to adjust for variance between groups. Statistical outliers were identified using Tukey's test and where removed from the datasets. Effect sizes and variances are reported throughout the text as group means ± standard error with the relevant P-values from group comparisons. Data are graphed and reported as the means ± standard error of raw, log-transformed, normalised or individual data points, as appropriate. Group sizes (n) are listed in Figure legends. The software packages Excel 2016 (Microsoft Office) and Prism 8.0 (GraphPad) were used for tabulation, statistical analysis and graphing.

Chapter 4 - Myeloid Norbin deficiency increases the responses of isolated neutrophils

4.1 Introduction: Expression of Norbin in neutrophils and generation of mice with myeloid Norbin-deficiency

As described in section 1.6.2 of Chapter 1, our lab recently discovered that the GPCR-adaptor protein Norbin is a direct binding partner of P-Rex1 (Pan et al., 2016). Norbin activates P-Rex1 Rac GEF activity both *in vitro* and *in vivo* and promotes the membrane localisation of the GEF. Co-expression of Prex1 and Norbin in PAE cells induces Rac-dependent actomyosin cytoskeletal dynamics, causing the cells to assume the characteristic morphology of active Rac, namely lamellipodia and membrane ruffling (Pan et al., 2016). As Pan et al investigated the consequences of the Norbin/Prex1 interaction for cell functions largely by using overexpression systems, we decided to assess the biological consequences of this interaction at the endogenous level. A tissue distribution analysis carried on by Dr Dingxin Pan, a former PhD student in the laboratory, showed that Norbin is expressed in myeloid cells, including neutrophils (Supplement Figure 1A) which was surprising given that Norbin was expected to be selectively neuronal (Pan et al., 2016). These findings, together with the well-known role of P-Rex1 in neutrophil responses (Welch et al., 2005) opened the opportunity to study endogenous Norbin and P-Rex1 in neutrophils, using Norbin and/or Prex deficient mice. Neutrophils are terminally differentiated and short-lived cells, in which protein expression levels are difficult to manipulate other than by genetic methods. In addition, neutrophil-like cell lines are not a suitable alternative, because they represent immature stages of neutrophil development and therefore insufficiently recapitulate normal neutrophil biology. Hence, we often use genetically modified mice to study the functions of proteins in neutrophils *in vitro* and *in vivo*. In order to study the functional role of endogenous Norbin in primary neutrophils, Dr Pan generated a mouse strain with a deletion of Norbin specifically in the myeloid linage, namely neutrophils, monocytes and macrophages. This strain $Ncdn^{-/-}$ (unpublished) was derived by crossing $Ncdn^{fl/fl}$ mice (Mochizuki-Sakisaka et al., 2004a) with the myeloid lineage Cre strain LysM-Cre (Clausen et al., 1999). In addition, the Norbin-deficient mice were crossed with a strain that carries a general Prex1 and Prex2 deficiency ($Prex^{-/-}$) (Welch et al., 2005) to generate the $Ncdn^{-/-}$ $Prex^{-/-}$ strain with combined Norbin and Prex deficiency (unpublished; see Figure 3.1 for a schematic diagram of the breeding

strategy). Moreover, she showed by western blotting that the 79 kDa band of Norbin was successfully deleted in the $Ncdn^{-/-}$ mice both in resident peritoneal leukocytes (which are 90% macrophages) and in septic peritonitis leukocytes (50% neutrophils and 40% peritoneal macrophages under these conditions) (Supplement Figure 1B, unpublished).

4.2 Norbin is efficiently deleted in neutrophils from mice with myeloid Norbin deficiency

Many experiments presented in this thesis were performed with isolated bone marrow-derived neutrophils. Therefore it was important to demonstrate that Norbin was efficiently deleted from isolated neutrophils in the $Ncdn^{-/-}$ strain. For this aim, I freshly purified mature neutrophils from the bone marrow of $Ncdn^{fl/fl}$, $LysM^{Cre}$ and $Ncdn^{-/-}$ mice using double $Percoll^{+}$ density gradient and, assessed their purity by cytospin and DiffKwik staining, which confirmed >90% purity. The cells were then pretreated with the potent serine protease inhibitor di-isopropyl fluorophosphate (DFP) and total cell lysates prepared. These cell lysates were subjected to western blotting with Norbin C1 antibody, and equal protein loading was assessed by coomassie staining. The WBs of $Ncdn^{fl/fl}$ and $LysM^{Cre}$ cells showed a 79 kDa band, the size expected for Norbin, and this was efficiently deleted in the $Ncdn^{-/-}$ neutrophils (Figure 4.1). The efficiency of the deletion was 93% and 90%, compared to $Ncdn^{fl/fl}$ and $LysM^{Cre}$, respectively, as assessed by densitometric analysis using ImageJ, and taking into account that the the purity of the neutrophil preparations was 98%. Furthermore, the normal morphology of the cells, as assessed by cytospin, and the number of mature neutrophils recovered from the bone marrow suggested that neutrophil development is normal in mice with myeloid Norbin deficiency (Figure 4.2A and B). In order to determine the proportion of neutrophils in the control and Norbin deficient mice, blood samples were lysed and stained for viable cells, CD45, Ly6G and CD11b. Following analysis, both strains were seen to contain 20% neutrophils amongst their white blood cells (Figure 4.2C), as expected (Cotter, Norman, Hellewell, & Ridger, 2001; O'Connell & E Brown, 2015). Finally, the expression of the neutrophil markers was comparable between control and Norbin-deficient bone marrow-derived neutrophils (Figure 4.2D).

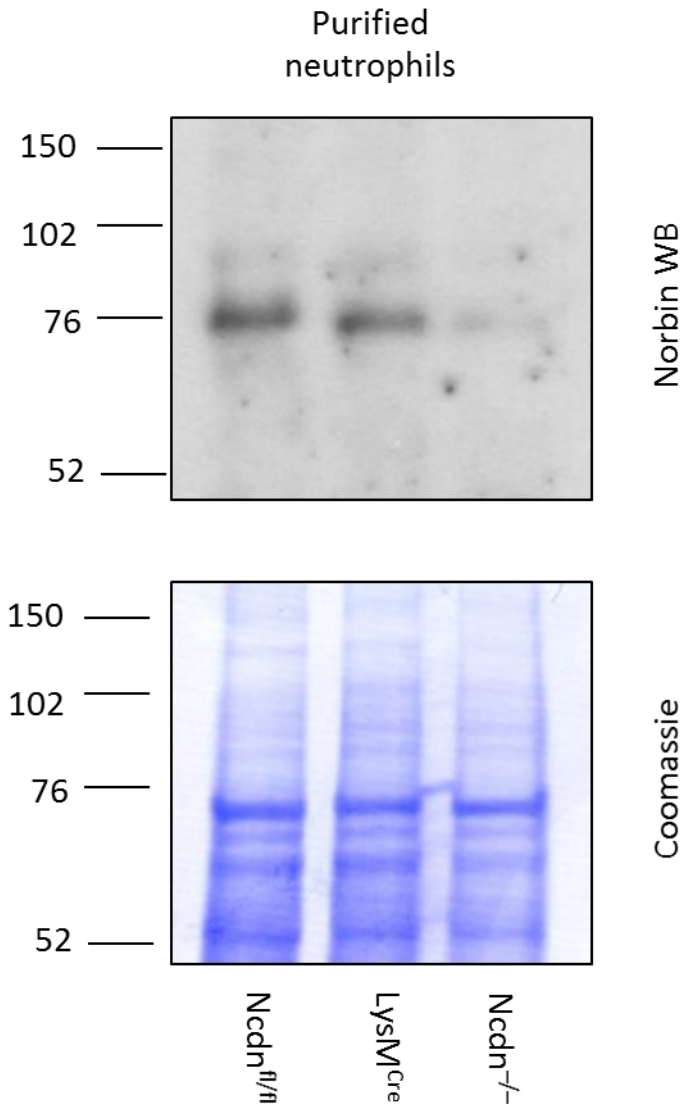

Figure 4.1: Norbin is deleted in Ncdn$^{-/-}$ mouse neutrophils
Norbin western blot of total lysates (5% v/v) of isolated diisopropyl fluorophosphate-treated bone marrow derived-neutrophils from Ncdn$^{fl/fl}$ (floxed Norbin), LysM^{Cre} (myeloid Cre) and Ncdn$^{-/-}$ (myeloid Norbin KO) mice. The representative WB from one experiment of Ncdn$^{fl/fl}$, LysM^{Cre} lysates showed a 79 kDa band that was efficiently deleted in Ncdn$^{-/-}$ lysates.

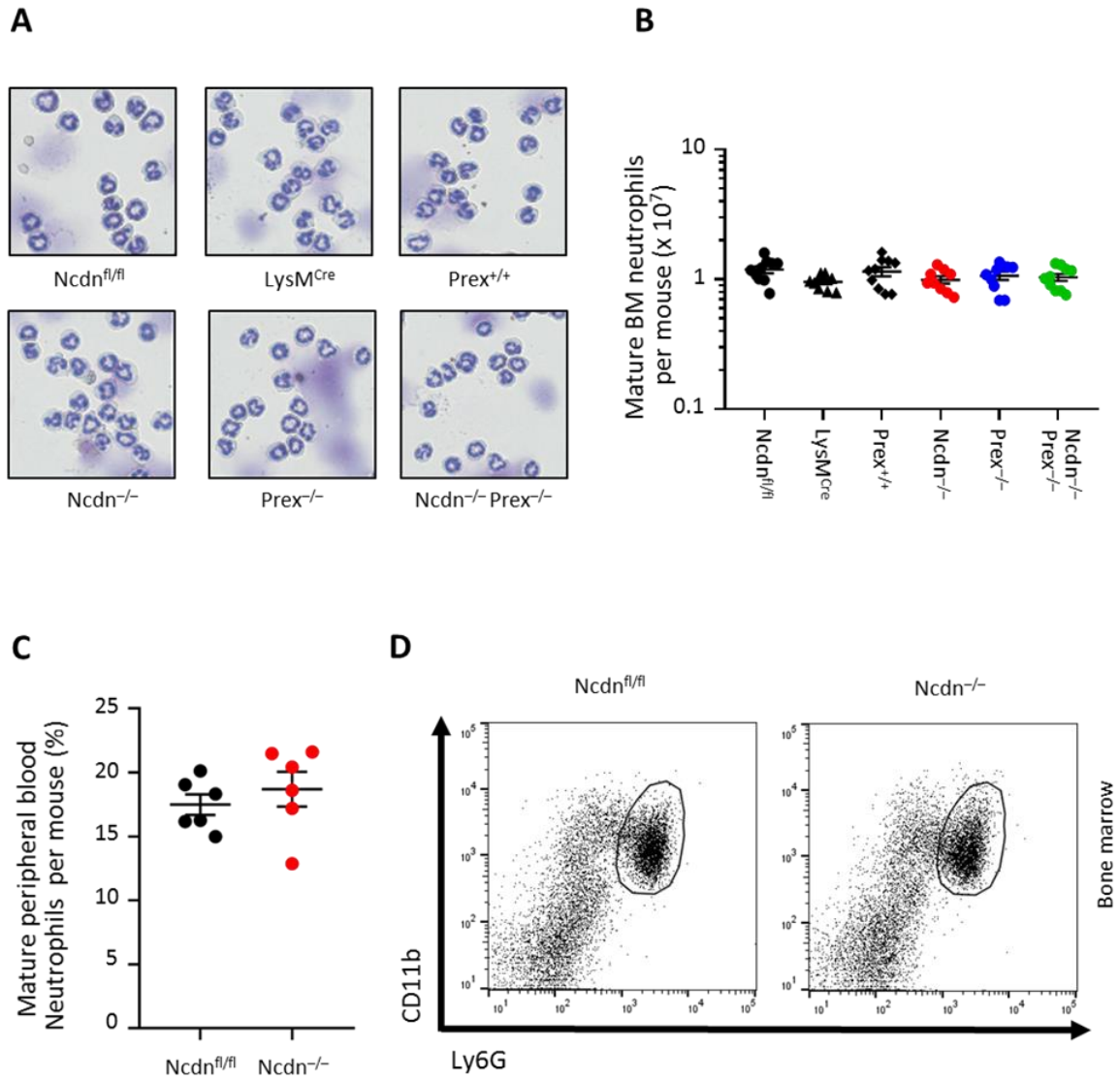

Figure 4.2: Neutrophil development is normal in mice with myeloid Norbin deficiency

(A) Representative DiffKwik-stained cytospin slides of mature neutrophils freshly isolated from the bone marrow of Ncdn$^{fl/fl}$, LysM^{Cre}, Prex$^{+/+}$, Ncdn$^{-/-}$, Prex$^{-/-}$ and Ncdn$^{-/-}$Prex$^{-/-}$ mice using double Percoll^{+} density gradient. (B) Quantification of mature neutrophils from the bone marrow isolated as in A shows that neutrophil numbers are normal in mice with myeloid Norbin deficiency. (C) Flow cytometry analysis of peripheral blood shows that neutrophil numbers assessed by Ly6G and Cd11b staining are normal in mice with myeloid Norbin deficiency. (D) Bone marrow neutrophils were labelled with Ly6G and CD11b markers and analysed by flow cytometry. Representative dot plots are shown with neutrophil numbers quantified as the percentage of total leukocytes. The expression of neutrophil markers is normal in mice with myeloid Norbin deficiency.

4.3 Norbin deficiency increases neutrophil adhesion and spreading but it does not affect polarisation

As described in section 1.4.5 of chapter 1, Prex1 deficiency causes a mild impairment in neutrophil adhesion and actin polymerisation (Lawson et al., 2011; Welch et al., 2005). Moreover, we observed that Norbin affects P-Rex1 dependent actin cytoskeletal structure and cell morphology in endothelial cells (Pan et al., 2016). Therefore, I assessed the ability of purified bone marrow derived $Ncdn^{-/-}$ and $Ncdn^{-/-}$ $Prex^{-/-}$ neutrophils to adhere, spread and polarise on glass cover slips, compared to neutrophils from sex- and age-matched $Prex^{-/-}$ and $Ncdn^{fl/fl}$ mice. Neutrophils were either primed with 20 $ng.mL^{-1}$ TNFα and 50 $ng.mL^{-1}$ GM-CSF or left unprimed and then left to adhere to coverslips for 10 min either in the presence of 1.5 µM fMLP in DPBS, or in DPBS alone, before fixing with paraformaldehyde. Fixed neutrophils were stained for the neutrophil-specific marker Gr1 (Ly6C & Ly6G) with a FITC-tagged antibody, as well as for DNA with Hoechst stain. This allowed the identification of neutrophils by their Gr1 staining and their characteristic horseshoe-shaped nuclear staining.

Imaging was performed using a Nikon Eclipse Ti-E widefield immunofluorescence microscope. To assess adhesion, the number of neutrophils per field of view was counted manually and expressed as the mean number of cells per mm^2. Under basal conditions (unprimed and unstimulated) 547 $Ncdn^{fl/fl}$ neutrophils adhered per mm^2 within 10 min (Figure 4.4A), whereas Prex deficiency caused a small decrease in adhesion to 440 cells per mm^2, as expected from previous work (Lawson et al., 2011; Welch et al., 2005). However, there was a striking increase in the adhesion of $Ncdn^{-/-}$ neutrophils to 1000 cells per mm^2. Surprisingly, this result showed that Norbin has the opposite effect on neutrophil adhesion compared to Prex1. Furthermore, this increase was sustained in the $Ncdn^{-/-}$ $Prex^{-/-}$ cells, where 806 cells adhered per mm^2. These differences in adhesion between $Ncdn^{-/-}$ and $Prex^{-/-}$ and between $Ncdn^{-/-}$ and $Ncdn^{-/-}$ $Prex^{-/-}$ cells were statistically significant. Hence, Norbin deficiency trumped the effects of Prex1 deficiency on neutrophil adhesion under these conditions. Similar results were obtained upon fMLP stimulation, except that the slight reduction in adhesion observed in $Prex^{-/-}$ cells was rescued by this treatment (641 cells per mm^2 adhered), as expected from previous work (Lawson et al., 2011). Similar to the basal condition, the increase in the adhesion of $Ncdn^{-/-}$ neutrophils, was highly significant compared to $Ncdn^{fl/fl}$ under these fMLP-stimulated conditions.

Next, primed conditions were tested, where neutrophils were pre-treated with TNFα and GM-CSF prior to the assay in order to upregulate receptors to the cell surface. Under these primed conditions, neutrophils from the $Prex^{-/-}$ strain no longer showed a defect in adhesion. However, the increase in adhesion of unprimed $Ncdn^{-/-}$ and $Ncdn^{-/-}$ $Prex^{-/-}$ was also observed in primed cells, and additional stimulation with fMLP increased the number of adherent $Ncdn^{-/-}$ $Prex^{-/-}$ neutrophils even further. Therefore, Norbin deficiency causes increased neutrophil adhesion under all conditions tested, and this effect was independent of Prex1 as it was preserved in the absence of the GEF.

To test whether Norbin and the Norbin/Prex1 interaction play a role in regulating neutrophil spreading, I measured the surface area of the cells analysed above using ImageJ analysis of a cell-mask (Figure 4.4B). Unprimed and unstimulated $Ncdn^{fl/fl}$ neutrophils had an average surface area of 127 μm^2 without and of 159 μm^2 with fMLP stimulation. Prex1 deficiency caused a small decrease in cell spreading, although this did not quite reach statistical significance under this condition. In contrast, $Ncdn^{-/-}$ neutrophils had a significantly larger surface average area of 150 μm^2 without and 176 μm^2 with fMLP stimulation. TNFα/GM-CSF priming increased the surface area of $Ncdn^{fl/fl}$ neutrophils, as expected (this is assumed to be due to the up-regulation of integrins during priming), to 144 μm^2 without and 154 μm^2 with fMLP stimulation. However, the area of $Ncdn^{-/-}$ neutrophils was larger again, 164 μm^2 and 176 μm^2, respectively. This difference between $Ncdn^{fl/fl}$ and $Ncdn^{-/-}$ neutrophils reached statistical significance under basal, primed and fMLP stimulated conditions. In contrast, Prex-deficiency significantly reduced neutrophil spreading both upon fMLP stimulation and upon priming. Therefore, in contrast to Prex1 deficiency, Norbin deficiency increases neutrophil spreading under all conditions tested. Furthermore, the spreading of $Ncdn^{-/-}$ $Prex^{-/-}$ cells was at least as much as that of $Ncdn^{fl/fl}$ cells under all conditions, showing that the additional Prex1 deficiency cold not override the increase in neutrophil spreading that was caused by the Norbin deficiency.

Adhering neutrophils adopt different morphologies between priming and stimulation conditions. To assess the effects of Norbin deficiency on these morphologies, I proceeded by assigning each cell to one of four different categories, depending on morphology. The categories were (I) unspread/round (yellow), (II) unspread/polar (purple), (III) spread/round

(green), and (IV) spread/polar (blue). Under basal conditions, most cells were unspread/round, whereas fMLP stimulation mostly increased the proportion of polarised cells and TNFα/GM-CSF priming the proportion of spread cells (Figure 4.4C). In $Ncdn^{-/-}$ neutrophils, the proportion of polarised cells was not greatly affected, neither under basal conditions, nor upon fMLP stimulations or upon priming. Hence, overall Norbin deficiency increased the ability of neutrophils to adhere and spread, but does not affect their ability to polarise.

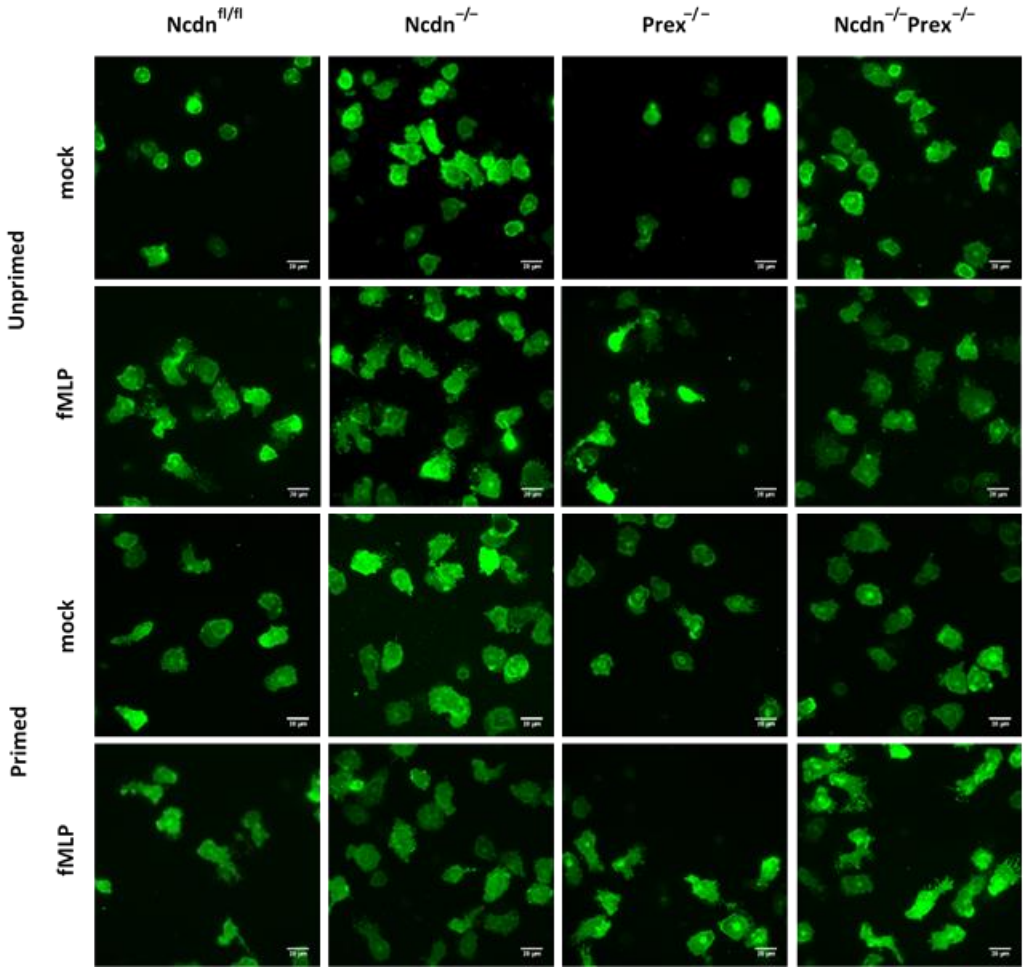

Figure 4.3: Representative fluorescence microscopy images of Gr1 stained adhering neutrophils isolated from $Ncdn^{fl/fl}$, $Ncdn^{-/-}$, $Prex^{-/-}$ and $Ncdn^{-/-}$ $Prex^{-/-}$ mice

Neutrophils isolated from mice of the indicated genotypes were primed with 50 $ng.mL^{-1}$ murine TNFα and 20 $ng.mL^{-1}$ GM-CSF, for 45 min at 37°C, or left on ice (unprimed). Cells were plated onto glass coverslips and stimulated with 1.5 µM fMLP or mocked treated with buffer for 10 min. Cells were fixed with PFA and stained with FITC-Gr1 antibody and Hoechst (Gr1 staining is shown here). Images are one representative field of view from 3 sets of 9 adjacent images taken across the width of each coverslip. Duplicate coverslips were assessed for each condition. Images shown are from one experiment representative of 3 independent experiments. Quantification is shown in Figure 4.4.

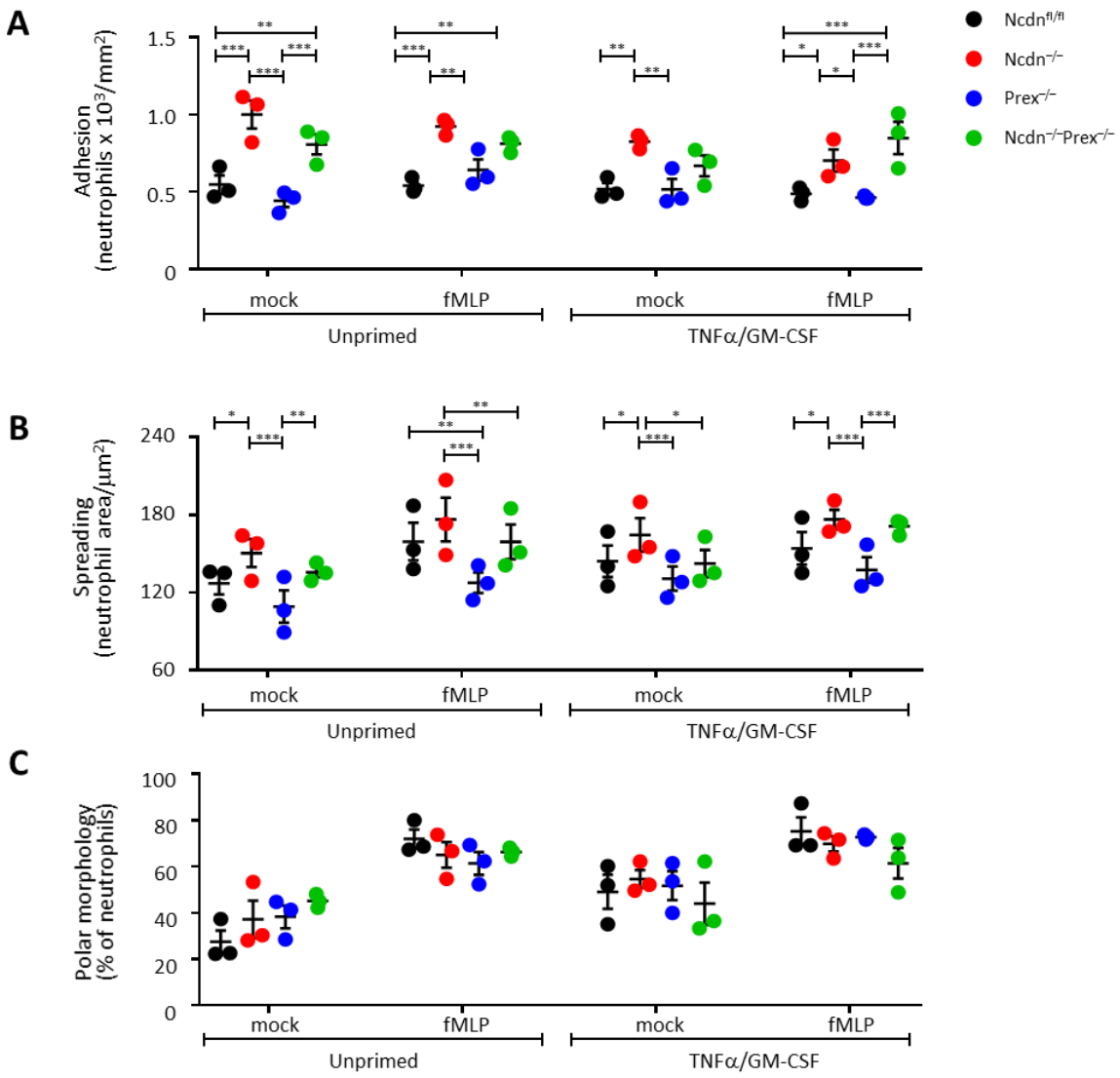

Figure 4.4: Norbin-deficient neutrophils show increased adhesion and spreading but normal polarisation
Neutrophils isolated from mice of the indicated genotypes were primed with 50 ng.mL^{-1} murine TNFα and 20 ng.mL^{-1} GM-CSF, for 45 min at 37°C, or left on-ice (unprimed). Cells were plated onto glass coverslips and stimulated with 1.5 µM fMLP or mocked treated with buffer for 10 min. Neutrophils were fixed with PFA and stained with FITC-Gr1 antobody and Hoechst. Images from 3 sets of 9 adjacent fields of view from across the width of each coverslip were analysed. Duplicate coverslips were assessed for each condition. Representative images are shown in Figure 4.3. (A) Adhesion of neutrophils, calculated as mean number of cells per mm^2. (B) Spreading of neutrophils, determined by assigning a mask using ImageJ and calculating the surface area of the mask. (C) Polarisation of neutrophils, assessed by assigning each cell to one of four morphology categories, as indicated in table 3.6 in section 3.6.1. Polar/unspread and polar/spread cells are scored in this quantification as % of total. Data (A-C) are mean ± SEM of 3 independent experiments. All conditions were assessed in parallel. The statistical significance was assessed using two-way Anova with Holm-Sidak's multiple comparisons test.

4.4 Norbin deficiency increases GPCR-dependent and fungal-particles dependent of ROS production

ROS formation by the neutrophil NADPH oxidase is a Rac-dependent response (Nguyen, Green, & Mecsas, 2017). One way of eliciting the ROS response in isolated neutrophils is by priming with inflammatory agents such as TNFα/GM-CSF or lipopolysaccharide (LPS) to upregulate surface receptors and NADPH oxidase components to the cell membrane, followed by stimulation of GPCRs such as the fMLP or the C5a receptors. I assessed the ability of isolated primed neutrophils from the different genotypes to produce ROS upon stimulation either through the fMLP or the C5a receptor.

First, I studied TNFα/GM-CSF-primed neutrophils stimulated with 3 μM fMLP. Under these conditions, ROS production was rapid, finishing within a minute, as expected (Figure 4.5A). Furthermore, as expected from our previous studies, Prex1 deficiency caused a defect in ROS production (Damoulakis et al., 2014; Lawson et al., 2011; Welch et al., 2005). In contrast, $Ncdn^{-/-}$ neutrophils showed the opposite effect, as ROS production was increased compared to $Ncdn^{fl/fl}$ (Figure 4.5A).

Quantification of this ROS production showed that the differences between $Ncdn^{-/-}$ and $Prex^{-/-}$ and between $Ncdn^{-/-}$ and $Ncdn^{-/-}$ $Prex^{-/-}$ were statistically highly significant (Figure 4.5B). Therefore, endogenous Norbin limits ROS production when expressed. As previously seen for adhesion and spreading, again Norbin deficiency had the opposite effect on this response compared to Prex deficiency. Furthermore, in $Ncdn^{-/-}$ $Prex^{-/-}$ cells, ROS production was decreased to a similar level as in $Prex^{-/-}$ cells. Thus, unlike for adhesion and spreading, the requirement for Prex1 in TNFα/GM-CSF-primed and fMLP-stimulated ROS production could not be overridden by the Norbin deficiency.

Next, I tested if this effect was specific to fMLP receptor-dependent ROS production. Neutrophils were primed with TNFα/GM-CSF as before, and then stimulated with 25 nM C5a (Figure 4.5C). I obtained similar results as with the fMLP stimulation, which shows that Norbin limits GPCR-dependent ROS production more generally. Moreover, these responses again required Prex1, whether Norbin was expressed or not.

Next, I tested ROS production in neutrophils primed through a different pathway, using LPS, which signals through the TLR4. LPS-primed, fMLP-stimulated ROS production was reduced in Prex-deficient neutrophils (Figure 4.5D), as expected from previous work (Damoulakis et al., 2014; Lawson et al., 2011; Welch et al., 2005). However, as seen with cytokine priming, Norbin deficiency increased ROS production. This increase in ROS production was highly significant compared to the $Ncdn^{fl/fl}$ and $Prex^{-/-}$ cells. Therefore, Norbin expression limits GPCR-dependent ROS production, regardless of the priming pathways used. However, in $Ncdn^{-/-}$ $Prex^{-/-}$ cells, ROS production was just as high as in $Ncdn^{-/-}$ cells, which shows that Norbin could override the requirement for Prex in this response. This is in contrast to the cytokine-primed response, where Prex was required. Therefore, there is a difference in the functional roles of Norbin and Prex between the two priming pathways examined, Norbin expression limiting ROS production whether Prex is required or not, and Prex being required in Norbin-deficient cells primed with TNFα and GM-CSF but not in cells primed with LPS.

ROS production plays a key role in neutrophil-dependent host defence against bacterial and fungal pathogens. Therefore, next I examined the importance of Norbin and Prex in ROS production elicited by zymosan yeast particles, which engage Fc, complement and pattern recognition receptors. $Ncdn^{-/-}$ neutrophils showed a statistically significant increase in zymosan-induced ROS production compared to $Ncdn^{fl/fl}$ (Figure 4.6B), whereas the response in $Ncdn^{-/-}$ $Prex^{-/-}$ cells was similar to $Prex^{-/-}$ cells. Hence, similar to GPCR-dependent ROS formation, Norbin expression limits the ROS response to fungal particles, and furthermore, this response required Prex1 whether Norbin is expressed or not.

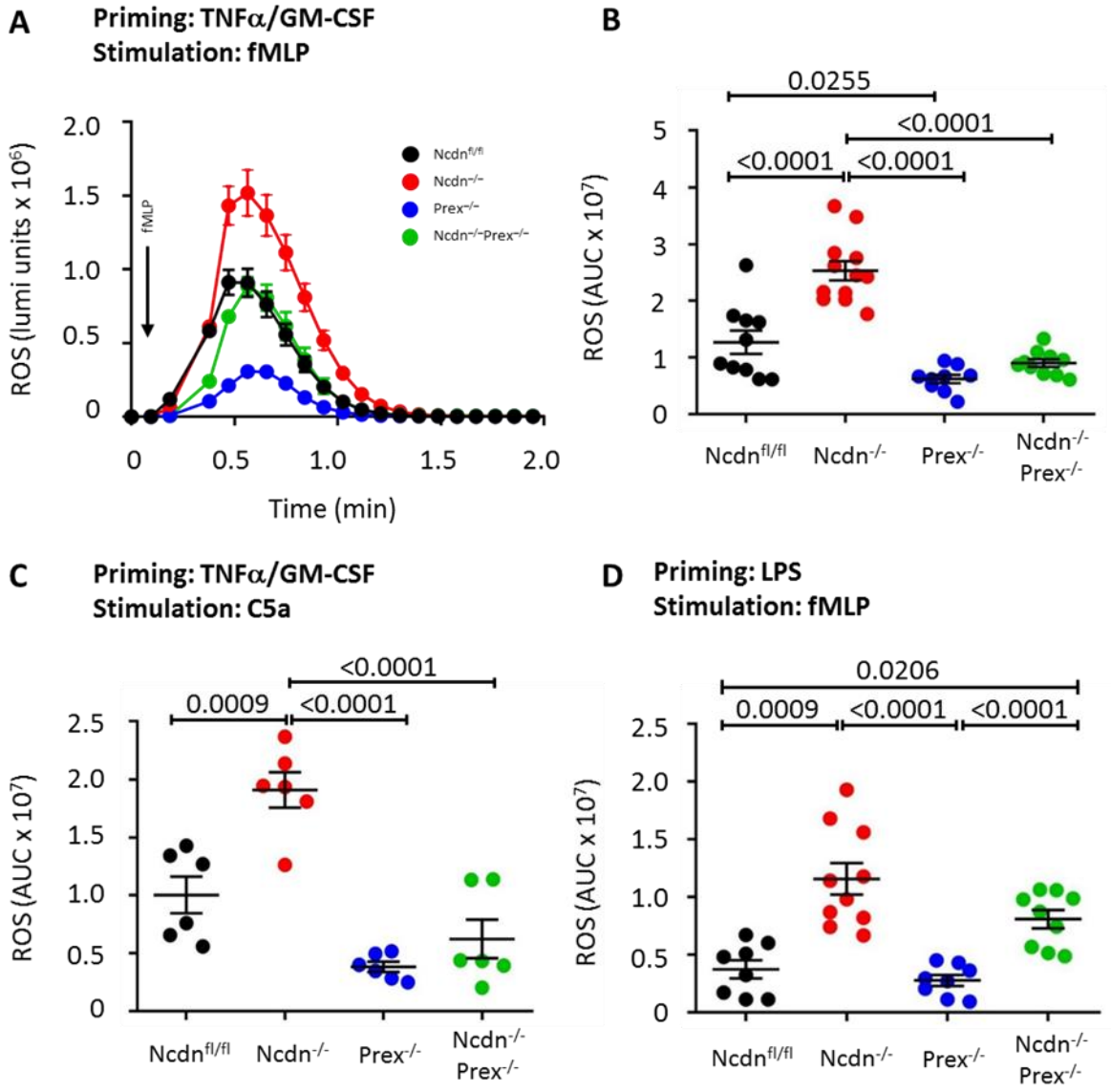

Figure 4.5: **Norbin-deficient neutrophils show increased ROS production**
Neutrophils were purified from Ncdn$^{fl/fl}$ (black), Ncdn$^{-/-}$ (red), Prex$^{-/-}$ (blue) and Ncdn$^{-/-}$ Prex$^{-/-}$ (green) mice and primed with the indicated agent prior to stimulation with fMLP or C5a. ROS assays were carried out in the presence of 120 µM luminol and 16 units.mL^{-1} HRP, and chemiluminescence was assessed in real time by luminometer over 2 min to measure intracellular and extracellular ROS production. (A) Representative traces of ROS production in neutrophils primed with 5 ng.mL^{-1} TNFα and 100 ng.mL^{-1} GM-CSF for 45 min at 37°C prior to stimulation with 3 µM fMLP. (B) Quantification of the area under the curve (AUC) of ROS assays such as the one shown in (A). (C) AUC of ROS production in neutrophils primed with 5 ng.mL^{-1} TNFα and 100 ng.mL^{-1} GM-CSF for 45 min at 37°C prior to stimulation with 25 nM C5a. (D) AUC of ROS production in neutrophils primed with 500 nM.mL^{-1} LPS for 90 min at 37°C prior to stimulation with 3 µM fMLP. (B-D) Each dot is the mean from one experiment of the AUC integrated over two minutes. Data are mean ± SEM of the indicated number of independent experiments. Statistical significance was assessed using one-way Anova with Tukey's multiple comparisons test. Mock-stimulated ROS production was negligible and is not shown here, for clarity.

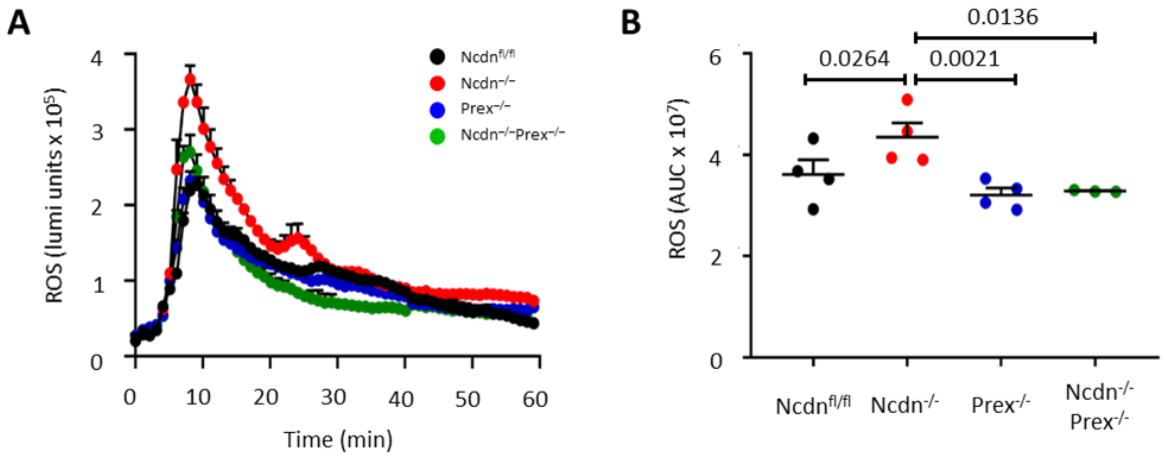

Figure 4.6: **Zymosan-induced ROS production is increased in Norbin-deficient neutrophils**
Neutrophils were purified from Ncdn$^{fl/fl}$ (black), Ncdn$^{-/-}$ (red), Prex$^{-/-}$ (blue) and Ncdn$^{-/-}$ Prex$^{-/-}$ (green) mice and incubated with zymosan at a ratio of 3:1 particles per neutrophil at 37°C in the presence of 120 µM luminol and 16 units.mL^{-1} HRP. Chemiluminescence was measured by luminometer over 60 min. (A) Representative traces of ROS production by Ncdn$^{fl/fl}$ (black), Ncdn$^{-/-}$ (red), Prex$^{-/-}$ (blue) and Ncdn$^{-/-}$ Prex$^{-/-}$ (green) neutrophils. (B) Quantification of ROS production (AUC) in response to zymosan. Each dot is the mean of one experiment. Data are mean ± SEM of 3-4 of independent experiments. Statistical significance was assessed using one-way Anova with Tukey's multiple comparisons test.

4.4.1 Norbin does not affect receptor-independent (PMA-stimulated) ROS production

Receptor-independent ROS production in neutrophils can be stimulated by PMA, a direct activator of protein kinase C (PKC). This response is often used to test if the NADPH oxidase complex is functional. PMA-stimulated ROS production was normal in cells of all genotypes tested (Figure 4.7A and B). This indicates that the integrity of the NADPH oxidase complex was not compromised by Prex or Norbin deficiency, and importantly suggests furthermore that the increased ROS production observed in Ncdn$^{-/-}$ neutrophils stimulated with fMLP, C5a or zymosan was not just not due to an overall increased amount of NADPH oxidase activity. Hence, Norbin deficiency affects the upstream signalling pathways rather than the NADPH oxidase itself.

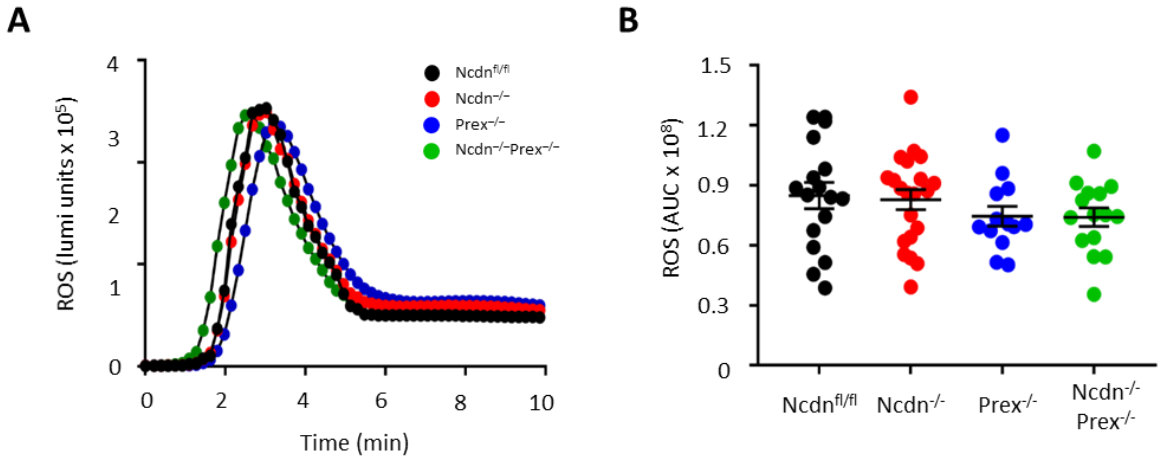

Figure 4.7: **PMA-dependent ROS production is normal in Norbin-deficient neutrophils**
(A) Representative traces of ROS production in Ncdn$^{fl/fl}$ (black), Ncdn$^{-/-}$ (red), Prex$^{-/-}$ (blue) and Ncdn$^{-/-}$ Prex$^{-/-}$ (green) neutrophils stimulated with 500 nM PMA. (B) AUC of PMA-stimulated ROS production over 10 minutes. Each dot is the mean of one experiment. Data are mean ± SEM of 10 independent experiments.

4.5 Norbin-deficiency increases the capacity of isolated neutrophils to kill bacteria by ROS production

ROS production by NADPH oxidase activity is a major response that enables neutrophils to kill bacteria. Thus, next I examined the ability of isolated neutrophils from $Ncdn^{fl/fl}$, $LysM^{Cre}$, $Ncdn^{-/-}$ and $Ncdn^{-/-}$ $Prex^{-/-}$ mice to kill *S. aureus*. Isolated neutrophils were primed with 10 $\mu g.mL^{-1}$ TNFα, 20 $\mu g.mL^{-1}$ GM-CSF for 45 min and then incubated for 15 min at 37°C with mouse serum opsonised *S. aureus* at a ratio of 1 bacterium per neutrophil with mixing every 5 minutes. Samples were added to an excess of ice-cold LB 0.05% saponin and sonicated to liberate ingested bacteria. Surviving bacteria were enumerated by plating on LB agar overnight and subsequent counting of colonies. For this experiment, neutrophils from two different control strains, the $Ncdn^{fl/fl}$ mouse and the $LysM^{Cre}$ mouse, were compared to the $Ncdn^{-/-}$ and the $Ncdn^{-/-}$ $Prex^{-/-}$ deficient cells. In this assay, Norbin deficiency significantly enhanced the ability of neutrophils to kill *S. aureus*, as around twice as many bacteria were killed in $Ncdn^{-/-}$ samples compared to $Ncdn^{fl/fl}$ and $LysM^{Cre}$ control cells. Furthermore, this role of Norbin was independent of Prex1 because, a similar increase was seen in $Ncdn^{-/-}$ $Prex^{-/-}$ neutrophils (Figure 4.8A).

To test whether the increased ability of $Ncdn^{-/-}$ neutrophils to kill *S. aureus* was due to the increased ROS production, I performed the bacterial killing assay in the presence of a titration curve with the ROS inhibitor diphenyleneiodonium (DPI). Isolated neutrophils from $Ncdn^{fl/fl}$ and $Ncdn^{-/-}$ mice were incubated with mouse serum-opsonised *S. aureus* for 15 min at 37°C at a ratio of 2:1, with a serial dilution of DPI. With increasing doses of DPI, the $Ncdn^{-/-}$ neutrophils gradually lost their advantage over $Ncdn^{fl/fl}$ cells in killing *S. aureus*, and at higher doses, both genotypes were equally sensitive to DPI (Figure 4.8B). Therefore, the increased ROS production observed in $Ncdn^{-/-}$ neutrophils gave rise to the increased ability of these cells to kill bacteria.

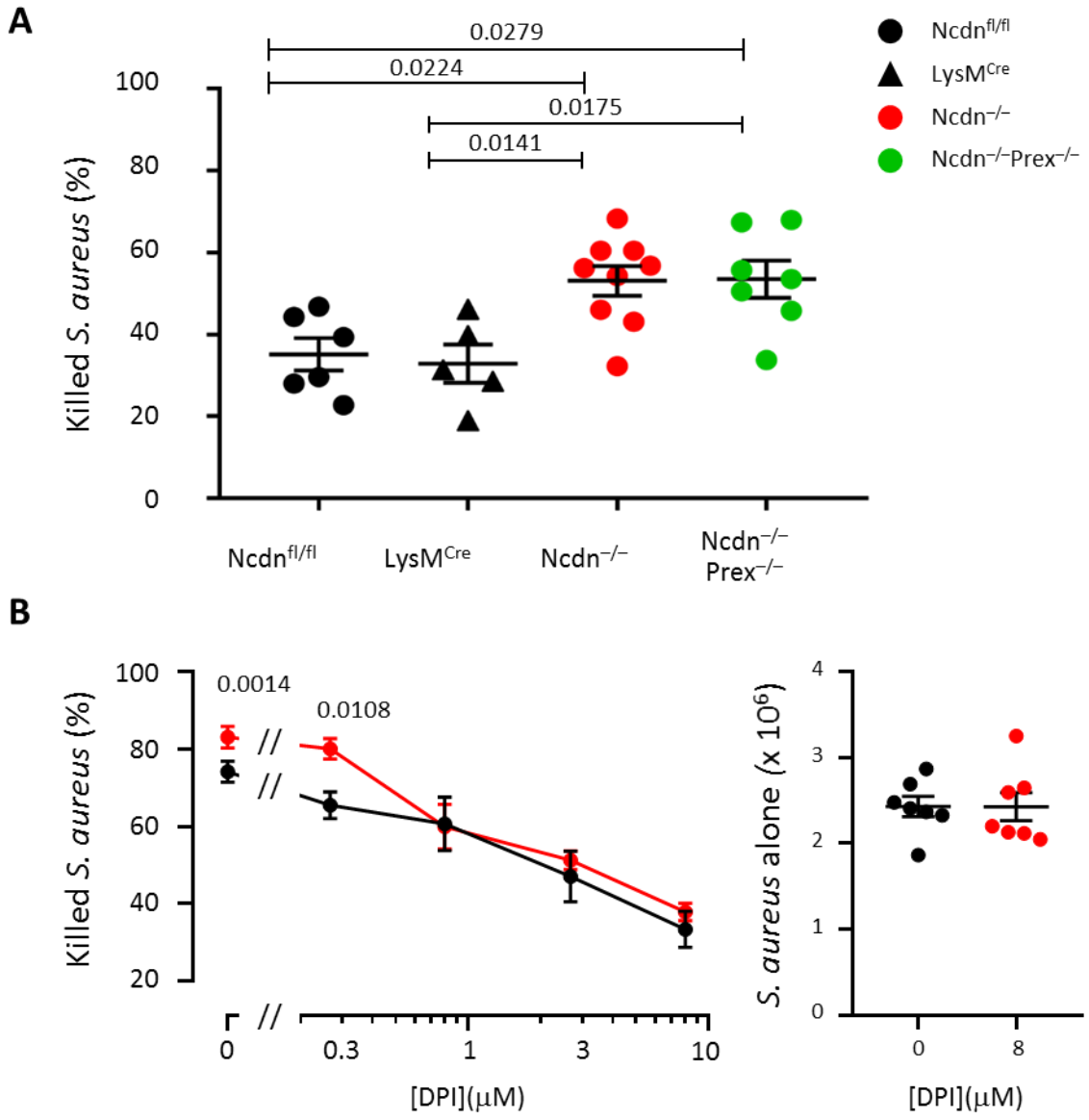

Figure 4.8: Norbin-deficient neutrophils have an increased capacity to kill bacteria, in a ROS-dependent manner

Neutrophils isolated from mice of the indicated genotypes were primed with 50 ng.mL^{-1} murine TNFα and 20 ng.mL^{-1} GM-CSF, for 45 min at 37°C prior incubation with mouse serum-opsonised *S. aureus* at a ratio of (A) 1:1 (B) or 1:2 (bacteria to neutrophils for 15 min), in (B) with the indicated concentrations of the ROS inhibitor diphenyleneiodonium (DPI). After the incubation, samples were added to an excess of ice-cold LB 0.05% saponin and sonicated to liberate ingested bacteria. Surviving bacteria were enumerated by plating on LB agar overnight and counting of CFUs. Each dot in (A)and (B, right hand panel) is the mean of an experiment performed in duplicate. Data are mean ± SEM of 5-9 independent experiments. Statistical significance was assessed using (A) one-way Anova with Tukey's multiple comparison test or (B) two-way ANOVA with Sidak's multiple comparisons test.

4.6 Norbin-deficiency causes constitutive secretion of gelatinase granules

Neutrophils store many of their cell surface receptors internally, on the membrane of various populations of secretory granules, in order to avoid full-blown activation of these cells while they are circulating in the blood stream. These cell surface receptors are upregulated onto the plasma membrane upon priming, by degranulation. One of the neutrophil granule subsets that is most easily mobilised are gelatinase granules, which are characterised by gelatinase (MMP9) that is released into the extracellular space upon degranulation. The increased ability of Norbin-deficient neutrophils to adhere and produce ROS, suggested that some cell surface receptors conferring these responses may be upregulated in $Ncdn^{-/-}$ cells due to increased degranulation. Therefore, I next analysed the effect of Norbin deficiency on neutrophil degranulation by measuring gelatinase activity released into the supernatant of neutrophils stimulated with increasing concentrations of fMLP with or without cytochalasin B. Priming with 20 $ng.mL^{-1}$ TNFα and 50 $ng.mL^{-1}$ GM-CSF was used to induce maximal gelatinase granule secretion. Indeed, basal $Ncdn^{-/-}$ neutrophils showed a statistically significant increase in gelatinase activity in the supernatant compared to $Ncdn^{fl/fl}$ cells, suggesting a constitutively increased level of degranulation caused by the Norbin deficiency (Figure 4.9B). This constitutive degranulation was overcome by increasing dose of fMLP, priming with TNFα and GM-CSF and cytochalasin B treatment, as stimulated neutrophils from $Ncdn^{fl/fl}$ and $Ncdn^{-/-}$ mice released similar amounts of gelatinase activity under those conditions (Figure 4.9A). Hence, overall the gelatinase content of $Ncdn^{-/-}$ neutrophils was normal. Therefore, Norbin-deficient neutrophils showed constitutive secretion of gelatinase, which could in part explain the increased responsiveness of Norbin-deficient neutrophils to various receptor stimuli.

In summary, $Ncdn^{-/-}$ neutrophils showed increased adhesion, spreading, ROS production, ROS-dependent bacterial killing and some constitutive degranulation. These findings showed that Norbin expression suppressed neutrophil responses, contrary to our initial expectations. Hence, myeloid Norbin is an important regulator of neutrophil responses. Furthermore, only some the effects of Norbin were Prex1-dependent.

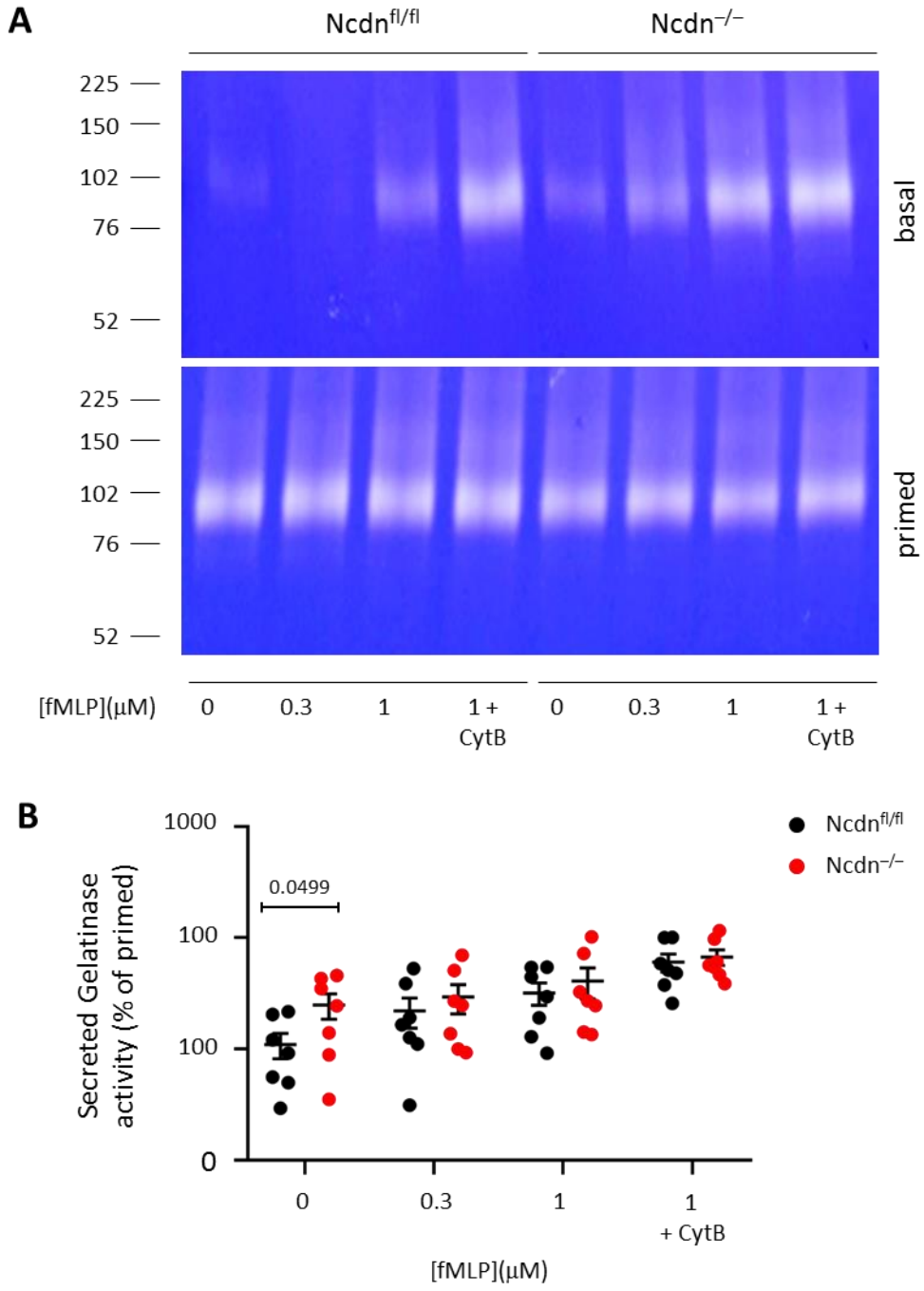

Figure 4.9: Norbin deficiency causes constitutive neutrophil degranulation

(A) Representative coomassie-stained gelatine gels, showing gelatinase activity released from $Ncdn^{-/-}$ and $Ncdn^{fl/fl}$ neutrophils. Neutrophils were either primed with 20 $ng.mL^{-1}$ TNFα and 50 $ng.mL^{-1}$ GM-CSF to induce maximal gelatinase granule secretion or left unprimed on ice prior to stimulation with increasing concentrations of fMLP and 10 µM cytochalasin B, as indicated. (B) Quantification of gelatinase activity in unprimed cells, expressed as % of the primed response. Each dot is the mean of one experiment. Data are mean ± SEM of 7 independent experiments (in 1 experiment, 0.5 µM fMLP was used instead of 0.3 µM). Statistical significance was assessed using two-way Anova with Sidak's multiple comparisons test.

Chapter 5 - Myeloid Norbin deficiency increases GPCR-dependent signalling and GPCR trafficking in neutrophils

5.1 Introduction: Signalling and trafficking roles of Norbin

Antibacterial and antifungal neutrophil responses require signalling through Rac and Rac-GEFs. For example, these proteins control neutrophil adhesion, ROS production and degranulation (Pantarelli & Welch, 2018). P-Rex1 is one of the Rac-GEFs that generates Rac activity and Rac-dependent neutrophil responses, especially those elicited by GPCR signalling.

Norbin has never been described in myeloid cells prior to our initial study on the Prex1/Norbin interaction (Pan et al., 2016). However, there is some literature on the role of Norbin in signalling, from studies on recombinant Norbin protein, on deletion of endogenous Norbin in neurons, and on overexpression of Norbin in other cell types. Together, these studies suggest possible mechanisms through which Norbin might regulate neutrophil responses. Recombinant Norbin binds directly to numerous GPCRs *in vitro* (33 out of the 45 tested to date), at the membrane-proximal part of their intracellular C-terminal tail (Francke et al., 2006; H. Wang et al., 2009; Ward et al., 2009). Overexpression or deletion of Norbin can affect the constitutive trafficking of GPCRs to the plasma membrane, and/or the downstream signalling pathways of GPCRs. For example, deletion of Norbin alters the steady-state cell surface level of the GPCR mGluR5 in primary cortical neurons cells without affecting total mGluR5 levels (Wang, Westin et al. 2009). Norbin expression can either up- or downregulate Ca^{2+} signalling upon stimulation of the GPCRs MCHR1 and mGluR5 (Francke, Ward et al. 2006, Wang, Westin et al. 2009, Ward, Jenkins et al. 2009), and it can enhance mGluR5-induced ERK1/2 phosphorylation (Francke, Ward et al. 2006, Wang, Westin et al. 2009). In general, however, it is unknown how Norbin binding affects the trafficking and signalling of these GPCRs.

In our recent paper (Pan et al., 2016), we showed that recombinant Norbin binds P-Rex1 and stimulates its Rac-GEF activity directly. Overexpression of Norbin in HEK293 cells promoted P-Rex1 activity upon stimulation of LPAR-family GPCRs with LPA. Co-expression of both Norbin and P-Rex1 in endothelial cells induced robust membrane translocation of both proteins and elicited Rac-mediated cell morphologies (Pan et al., 2016). From this study, we

concluded that Norbin promotes P-Rex1 function largely by bringing this Rac-GEF into proximity of its activators, PIP_3 and $G\beta\gamma$, and of its substrate Rac, thus facilitating Rac-dependent cell responses.

Based on this literature, I decided to perform the following assays in order to characterise the underlying molecular mechanism through which Norbin might affect neutrophil responses: (i) testing of the effects of Norbin deficiency on GPCR-dependent Rac activity, as well as other GPCR signalling pathways in neutrophils; (ii) evaluation of the effects of Norbin deficiency on GPCR trafficking in neutrophils.

5.2 GPCR-dependent activation of Rac is increased in Norbin-deficient neutrophils

First, I tested Rac activity. I used PAK-CRIB pull down assay to isolate active Rac1 and Rac2 from total lysates (TL) of isolated $Ncdn^{fl/fl}$ and $Ncdn^{-/-}$ neutrophils after stimulation with increasing doses of fMLP for 10 seconds. This assay is based on the ability of GTP-loaded, but not the GDP-loaded, forms of Rac1 and Rac2 to bind to the CRIB domain of the kinase PAK with high affinitiy. As expected, Rac1 and Rac2 activity increased with increasing doses of fMLP in the $Ncdn^{fl/fl}$ control cells. Surprisingly, the fMLP-stimulated activity of both Rac1 and Rac2 was higher in $Ncdn^{-/-}$ cells compared to $Ncdn^{fl/fl}$ control cells at all concentrations of fMLP tested, whereas basal Rac activity in mock-stimulated cells was near the detection limit and no higher in the Norbin-deficient cells than in controls (Figure 5.1A).

Quantification of the Rac1 and Rac2 activities by densitometric analysis of WBs from 3-7 independent experiments showed that active Rac1 made up 0.17±0.08% of the total Rac1 in buffer-treated $Ncdn^{fl/fl}$ control cells and 0.9±0.29% in fMLP-stimulated cells. No significant difference was seen between $LysM^{Cre}$ and $Ncdn^{fl/fl}$ cells. Similarly, in buffer-treated $Ncdn^{-/-}$ cells Rac1 activity was no different to the control cells. However, fMLP stimulation increased Rac1 activity in $Ncdn^{-/-}$ cells to 1.85±0.81% of the total, a two-fold increase compared to $Ncdn^{fl/fl}$ (Figure 5.1B). Quantification of Rac2 activity showed a similar pattern. 0.03% of Rac2 was active in buffer-treated $Ncdn^{fl/fl}$ cells and 0.41% upon fMLP stimulation. Again, $LysM^{Cre}$ cells and buffer-treated $Ncdn^{-/-}$ cells were no different to

controls, but fMLP stimulation of $Ncdn^{-/-}$ cells increased active Rac2 to 1.08±0.32% of the total, a 2.5-fold increase compared to $Ncdn^{fl/fl}$ (Figure 5.1C). (Note that Figure 5.1 shows normalised data, for clearer graphical representation, but quantification and statistical analysis were done on raw data).

Therefore, Norbin-deficiency increases the GPCR-dependent activation of Rac1 and Rac2.

In addition, fMLP-stimulated Rac1 activity in $Ncdn^{-/-}$ $Prex^{-/-}$ neutrophils (1.16±0.34% of total) was similar to the level in $Ncdn^{-/-}$ cells, which showed that Prex1 is not required for the effects of Norbin-deficiency on Rac1 activity (Figure 5.1B). In contrast, fMLP-stimulated Rac2 activity was not significantly increased in $Ncdn^{-/-}$ $Prex^{-/-}$ neutrophils compared to controls, which revealed that the GPCR-mediated activation of Rac2 depends on Prex1 even when Norbin is deleted (Figure 5.1C). These results are in accordance with the literature showing that Prex1 has a substrate preference for Rac2 over Rac1 (Welch et al., 2005).

Hence, Norbin expression limits the GPCR-mediated activation of Rac1 and Rac2 in neutrophils, and the deletion of Norbin is sufficient to relieve this suppression. Furthermore, Norbin-deficiency does not overcome the requirement for P-Rex1 in activating Rac2 upon GPCR stimulation.

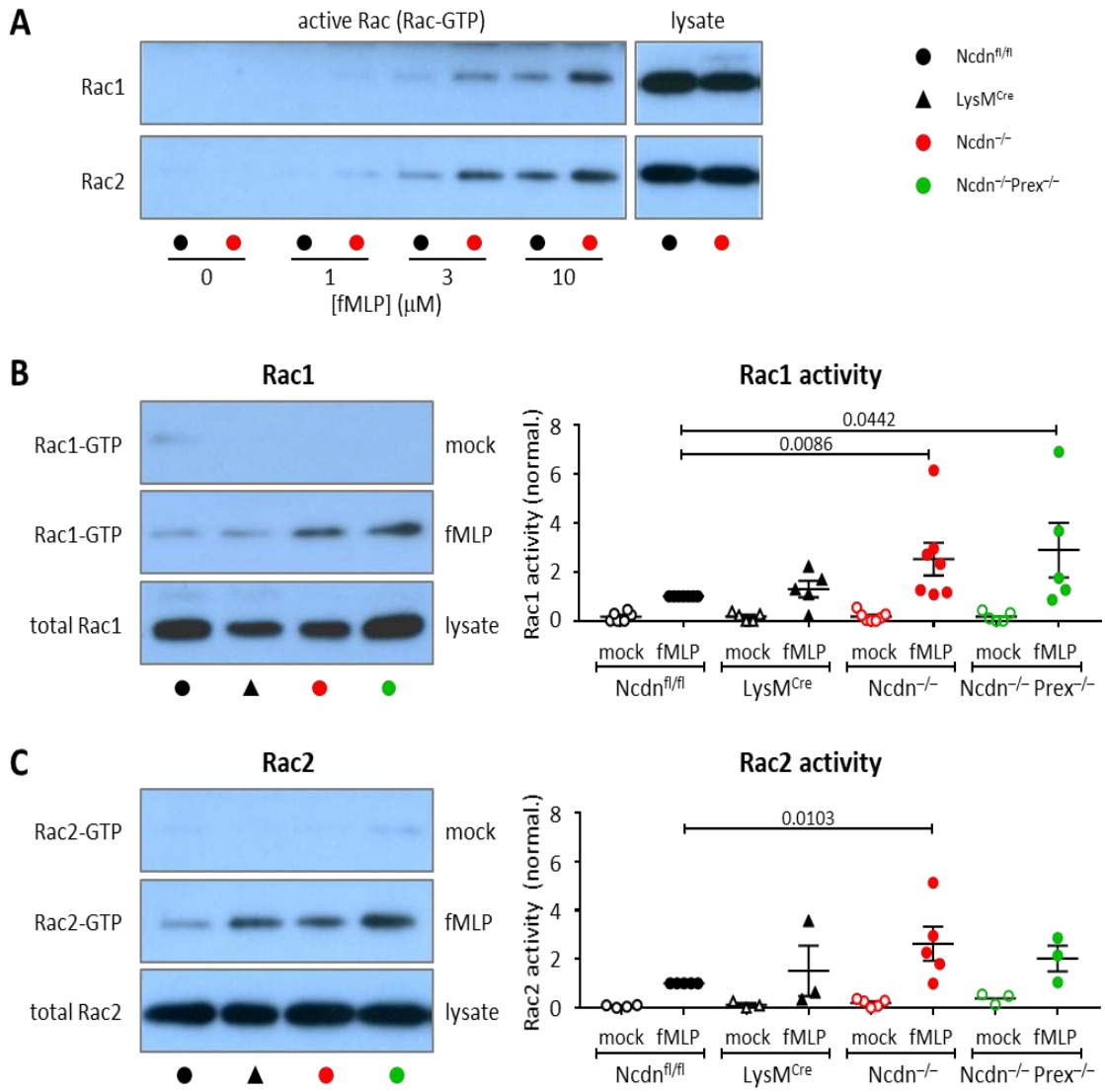

Figure 5.1: Norbin-deficient neutrophils have increased Rac activity upon fMLP stimulation
(A) Unprimed Ncdn$^{fl/fl}$ (black) and Ncdn$^{-/-}$ (red) neutrophils were prewarmed to 37°C for 3 min and then stimulated with increasing concentrations of fMLP, as indicated, for 10 s, lysed and subjected to PAK-CRIB assay to measure Rac1 and Rac2 activation as described in Materials and Methods. The levels of active (GTP-loaded) Rac1 and Rac2 were determined by WB. 2% of the total lysate was blotted as a control for total Rac1 and Rac2 levels and blots were processed in parallel to allow a direct comparison. Representative WB from one experiment representative of 3 independent experiments are shown. (B and C, left-hand panels) Representative WBs for (A) Rac1 and (B) Rac2 activity in unprimed Ncdn$^{fl/fl}$, LysM^{Cre}, Ncdn$^{-/-}$ and Ncdn$^{-/-}$ Prex$^{-/-}$ neutrophils mock stimulated (top panel) or stimulated with 10 μM fMLP (middle panel) and subjected to PAK-CRIB assay compared to 2% of total lysate control (bottom panel). (B and C, right-hand panels) Quantification of Rac1 and Rac2 activity by densitometric analysis of WBs such as those shown on the left panel. (B-C) Rac1 and Rac2 activities were calculated as a percentage of the total lysate control and are expressed as normalised to the fMLP-stimulated Ncdn$^{fl/fl}$ condition. Each dot is the mean of one experiment. Data are mean ± SEM of the indicated number of independent experiments. Statistical significance was assessed on the log-transformed raw data (non-normalised) using two-way Anova with Dunnett's multiple comparisons test.

5.3 Norbin deficiency increases GPCR-dependent Erk activity

To analyse other GPCR-dependent signalling pathways, I measured the fMLP-stimulated activation of Erk, $p38^{Mapk}$, Jnk and Akt in TNFα/GM-CSF-primed isolated neutrophils from $Ncdn^{fl/fl}$ and $Ncdn^{-/-}$ mice. Cells were mock-stimulated or stimulated with different doses of fMLP (0.3 μM or 1 μM) for 10, 45 or 180 seconds. Activity of the signalling pathways was assessed in total neutrophil lysates by western blotting for the activated phosphorylated form of proteins and the total protein (Figure 5.2A). The western blots showed that fMLP stimulation induced an activation of all these pathways, with a distinct peak of activity at 1 μM fMLP and 45 seconds. Quantification by densitometric analysis showed that, fMLP-stimulated phospho-Erk levels were 2-fold higher in $Ncdn^{-/-}$ neutrophils compared to $Ncdn^{fl/fl}$ cells under this conditions (Figure 5.2B). In contrast, no significant difference was seen between $Ncdn^{fl/fl}$ and $Ncdn^{-/-}$ cells in the other GPCR signalling pathways ($p38^{Mapk}$, Jnk and Akt) under any of the conditions tested (Figure 5.2B). In summary, Norbin deficiency increases fMLP-stimulated Erk activity, which shows that Norbin limits this pathway when it is expressed. However, Norbin did not obviously affect other GPCR signalling pathways under the conditions tested, which suggests a degree of pathway specificity.

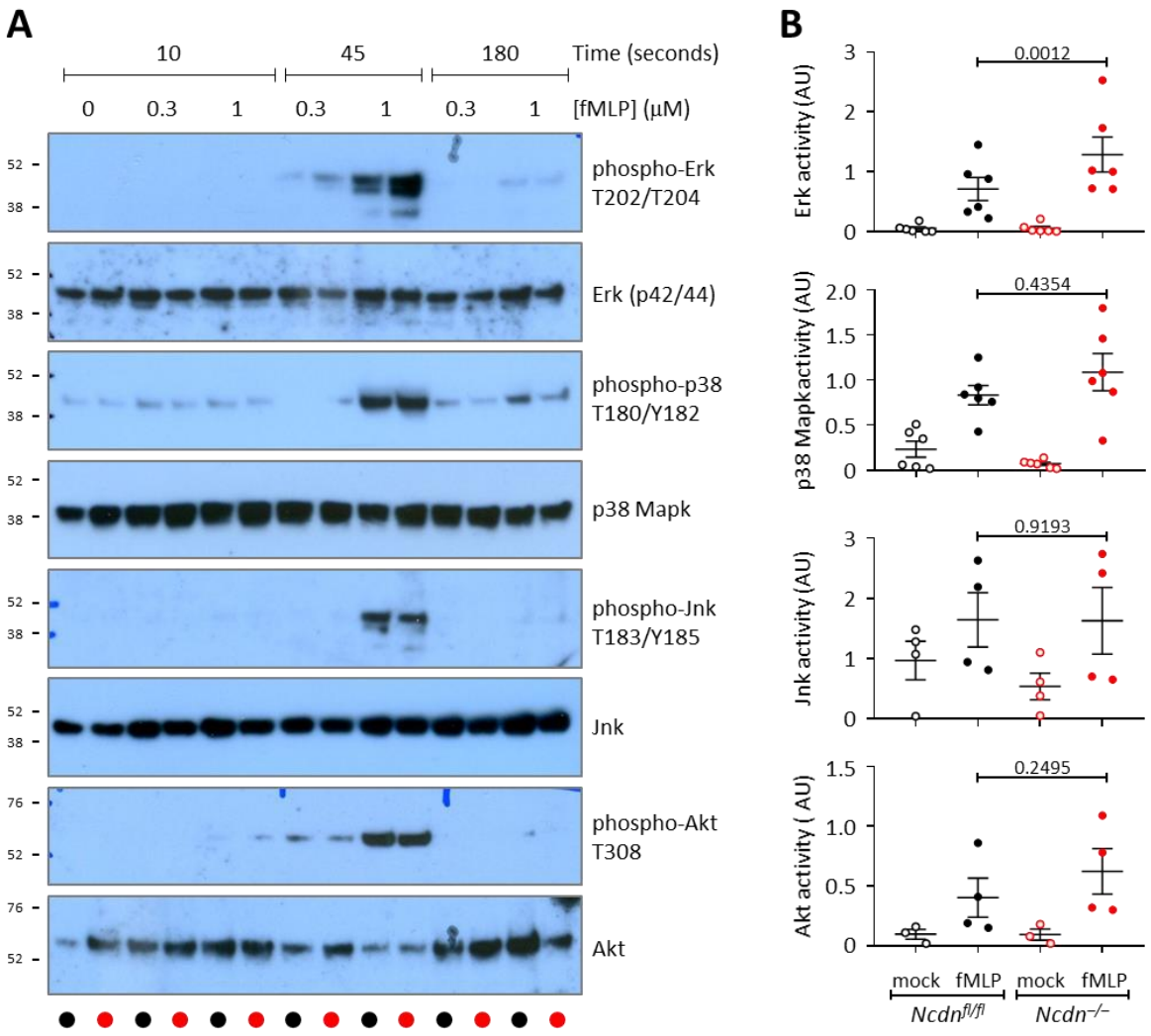

Figure 5.2: Norbin-deficient neutrophils have increased fMLP-stimulated Erk activity, whereas several others GPCR signalling pathways seem unaffected

(A) Representative WBs showing the phospho-protein levels and total protein levels of indicated signalling proteins in total lysates of isolated bone marrow neutrophils from $Ncdn^{fl/fl}$ and $Ncdn^{-/-}$ mice. Neutrophils were primed for 45 min at 37°C with 20 $ng.mL^{-1}$ TNFα and 50 $ng.mL^{-1}$ GM-CSF prior to stimulation with the concentrations of fMLP and the time points indicated. (B) Quantification of the activities of the indicated signalling proteins by densitometric analysis of WBs such as those shown on the left. Quantitated are the mock-stimulated conditions and the stimulation with 1 µM fMLP at 45 s. Activity was calculated by dividing the band intensities of phospho-proteins by the total protein controls. Each dot is the mean of one experiment. Data are mean ± SEM of 3-6 independent experiments as indicated. Statistical significance was assessed using two-way Anova with Sidak's multiple comparisons test.

5.4 Norbin-deficiency increases the cell surface levels of several GPCRs

As introduced in section 5.1, Norbin is known to regulate the steady-state surface levels of GPCRs. Furthermore, preliminary data from Dr Martin Baker, a former PhD student in the laboratory, demonstrated that P-Rex1 also controls GPCR trafficking. He showed that Prex1 deficiency affects the level of the endogenous GPCR C5aR1 on the surface of neutrophils upon stimulation with the chemoattractant ligand C5a. He also showed that overexpression of Prex1 in HEK293 cells blocks the internalisation of the GPCR S1PR1 induced by stimulation with the agonist S1P (unpublished). These data prompted me to investigate if Norbin modulates GPCR trafficking in neutrophils, and whether this function would be Prex1 dependent.

To assess the effects of Prex1 and/or Norbin deletion on the levels of GPCRs on the neutrophil surface, I used antibodies against the endogenous neutrophil GPCRs C5aR1, CXCR1, CXCR2 and CXCR4, to detect their cell surface levels by flow cytometry. These experiments were done in crude bone-marrow cells instead of purified neutrophils in order to preserve receptor levels on the cell surface as much as possible by minimising preparation time and handling. The cells were subjected to various different conditions: either they were kept on ice throughout, to maintain basal levels of the receptors at the cell surface and prevent any receptor trafficking. Alternatively, they were incubated for 30-45 min to allow constitutive receptor trafficking to occur, or they were primed in order to induce maximal upregulation of receptors to the plasma membrane. In some instances, cells were also stimulated with receptor ligand, in order to elicit agonist-induced receptor internalisation.

First, I tested C5aR1, the receptor for C5a, because this was one of the stimuli that had induced increased ROS production in $Ncdn^{-/-}$ cells in my previous experiments. Bone-marrow cells from $Ncdn^{fl/fl}$ and $Ncdn^{-/-}$ mice were stimulated with 100 nM C5a for 10 and 30 min, or were mock-stimulated for 30 min at 37°C. Cells were then stained with PE-C5aR1 antibody and with antibodies for neutrophil markers, FITC-Gr1 or BV510-Ly6G and AF647-Cd11b, followed by analysis through flow cytometry (see Table 3.5 of antibodies in Materials and Methods for conditions). Neutrophils were identified by their characteristic forward and

side scatter as well as by these markers, whilst the mean signal of PE-C5aR1 was used as a measure of the surface expression of the endogenous GPCR.

I found that, under mock-stimulated conditions, GPCR C5aR1 surface levels were 1.56-fold higher in $Ncdn^{-/-}$ cells compared to $Ncdn^{fl/fl}$ cells, which shows that, under conditions which allow some level of constitutive receptor trafficking, Norbin-deficient neutrophils have more C5aR1 on their surface than control cells. In contrast, the agonist-induced internalization of C5aR1 in response to C5a stimulation was normal in $Ncdn^{-/-}$ cells, in accordance with the literature on the role of Norbin in constitutive GPCR trafficking but not in ligand-induced trafficking (Figure 5.3A). To corroborate this further, TNFα/GM-CSF-primed neutrophils induced a five-fold increase in C5aR1 surface levels in $Ncdn^{fl/fl}$ cells compared to basal condition (cells on ice, no trafficking), but in $Ncdn^{-/-}$ neutrophils this was even higher, by a further 1.33-fold compared to $Ncdn^{fl/fl}$ cells. In contrast, under basal condition that allow no trafficking, receptor surface levels were normal (Figure 5.3B). Moreover, comparison of mock-stimulated cells from four genotypes revealed that, despite the expected increase in C5aR1 surface levels in $Ncdn^{-/-}$ compared to $Ncdn^{fl/fl}$ cells (1.48-fold), the level of C5aR1 was normal in $Prex^{-/-}$ and $Ncdn^{-/-}$ $Prex^{-/-}$ neutrophils, which showed that the upregulation of this GPCR to the cell surface of Norbin-deficient cells was dependent on the expression of Prex1 (Figure 5.3C).

In summary, Norbin-deficiency leads to an upregulation of the GPCR C5aR1 on the neutrophil surface under conditions that allow constitutive receptor trafficking, in a Prex1-dependent manner, but it does not obviously affect agonist-induced receptor internalisation. The increased surface level of C5aR1 could explain, at least in part, why C5a-stimualted ROS production is increased in Norbin-deficient neutrophils.

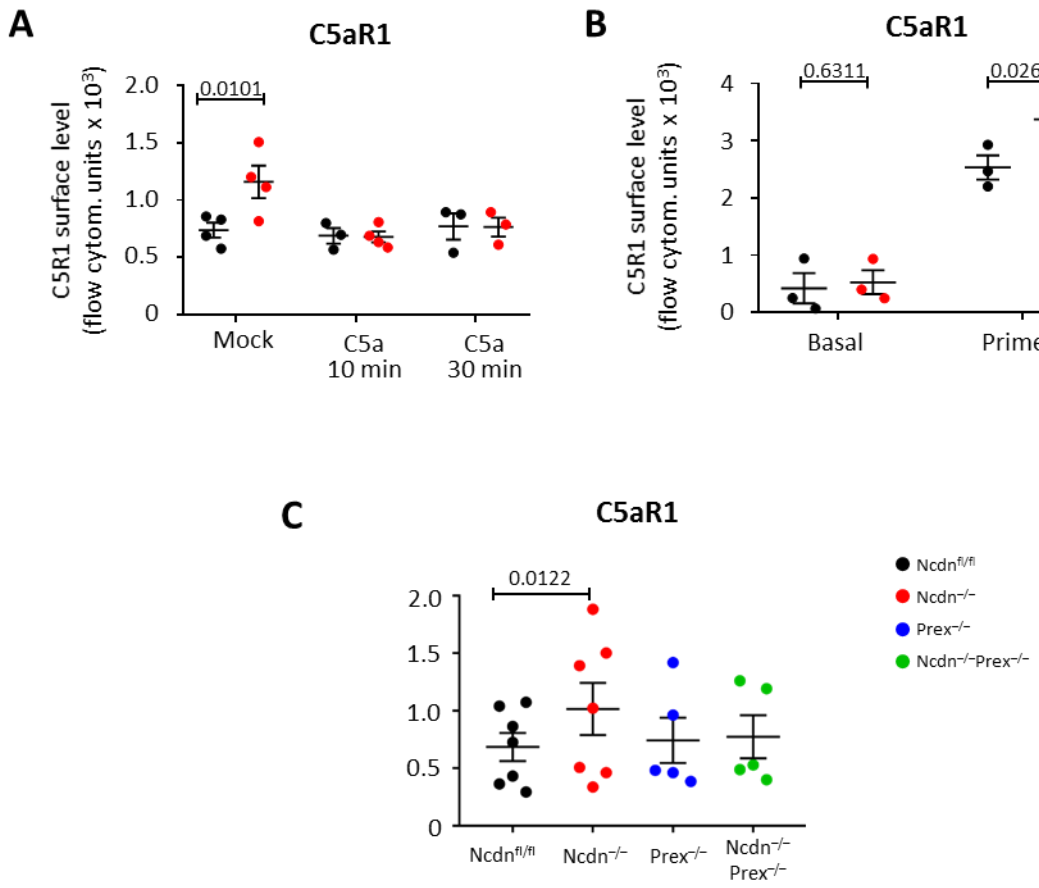

Figure 5.3: Norbin-deficient neutrophils have increased cell surface levels of the GPCR C5aR1 under conditions that allow constitutive GPCR trafficking

(A) Bone marrow cells from Ncdn$^{fl/fl}$ and Ncdn$^{-/-}$ mice were incubated for 30 min at 37°C in the absence (mock) or presence of 100 nM C5a, or C5a was added for the last 10 min of this incubation, as indicated, before the cells were transferred onto ice and stained to investigate the levels of C5aR1 on the neutrophil surface by flow cytometry. (B) Bone marrow cells from Ncdn$^{fl/fl}$ and Ncdn$^{-/-}$ mice were primed with 20 ng.mL^{-1} murine TNFα and 40 ng.mL^{-1} GM-CSF for 45 min at 37°C, or were left on ice (basal) before being transferred onto ice and stained to investigate the levels of C5aR1 on the neutrophil surface by flow cytometry. (C) Bone marrow cells from Ncdn$^{fl/fl}$, Ncdn$^{-/-}$, Prex$^{-/-}$ and Ncdn$^{-/-}$ Prex$^{-/-}$ mice were incubated for 30-45 min at 37°C, before being transferred onto ice and stained to investigate the levels of C5aR1 on the neutrophil surface by flow cytometry. Neutrophils were detected by their scatter characteristics and FITC-Gr1 (Ly6C and LY6G) or BV510-Ly6G and AF647-Cd11b antibody staining, whilst C5aR1 surface levels were detected by PE-C5aR1 antibody. All conditions were assessed in parallel. Each dot is the mean of one experiment. Data are mean ± SEM of the indicated number of independent experiments. Statistical significance in (A) and (B) was assessed using two-way Anova with Sidak's multiple comparison test and (C) by one-way Anova with Tukey's multiple comparisons test.

The literature shows that primary sequence cannot predict which GPCRs Norbin can bind and which not (H. Wang et al., 2015; H. Wang et al., 2009). Therefore, to get a picture of how wide-ranging the effects of Norbin-deficiency are on surface levels of other GPCRs in addition to C5aR1, we decided to use a candidate approach, choosing a selection of other important neutrophil GPCRs for which antibodies were commercially available. I found antibodies against CXCR1, CXCR2 and CXCR4 which were able to detect endogenous GPCR levels by flow cytometry. Again, crude bone-marrow cells were used in order to preserve receptor levels on the cell surface as much as possible, and cells were either left on ice (basal) or primed with TNFα/GM-CSF for 30 min at 37°C. Cells were then stained with the GPCR antibodies and neutrophil markers, followed by analysis through flow cytometry. The neutrophils were identified by their characteristic forward and side scatter and by their mean signal of PE-CXCR1, PE-CXCR2 or PE-CXCR4 was used as a measure of surface expression of the endogenous GPCRs.

From these experiments, I saw that the surface levels of CXCR4 (the receptor for SDF-1α) were higher in $Ncdn^{-/-}$ compared to $Ncdn^{fl/fl}$ cells under both basal and primed conditions (Figure 5.4A). Hence, as seen with C5aR1, Norbin-deficiency led to increased levels of this GPCR on the neutrophil surface. However, unlike C5aR1, the upregulation of CXCR4 occurred even under conditions that minimised receptor trafficking, which suggested that either CXCR4 is stored on a more readily mobilised type of vesicle than C5aR1, or the total cellular levels of CXCR4 could be elevated in $Ncdn^{-/-}$ cells. Unlike either C5aR1 or CXCR4, the surface levels of CXCR1 and CXCR2 were unaffected by the Norbin deficiency (Figure 5.4B and C), which is in accordance with the literature that showed these GPCRs to be constitutively localised on the plasma membrane instead of granules, or alternatively they may not be affected because Norbin cannot physically interact with these particular GPCRs.

The reduction of CXCR2 of the neutrophil surface upon priming was expected, as this GPCR is known to be shed rapidly from the neutrophil surface upon stimulation with TNFα, by proteolysis cleavage (Asagoe, Yamamoto, Takahashi, Suzuki, et al., 1998). Both basal and shed levels of CXCR2 were normal in $Ncdn^{-/-}$ cells (Figure 5.4C). Based on these results, we

can conclude that the effects of Norbin deficiency on receptor trafficking show some degree of specificity for certain types of GPCRs.

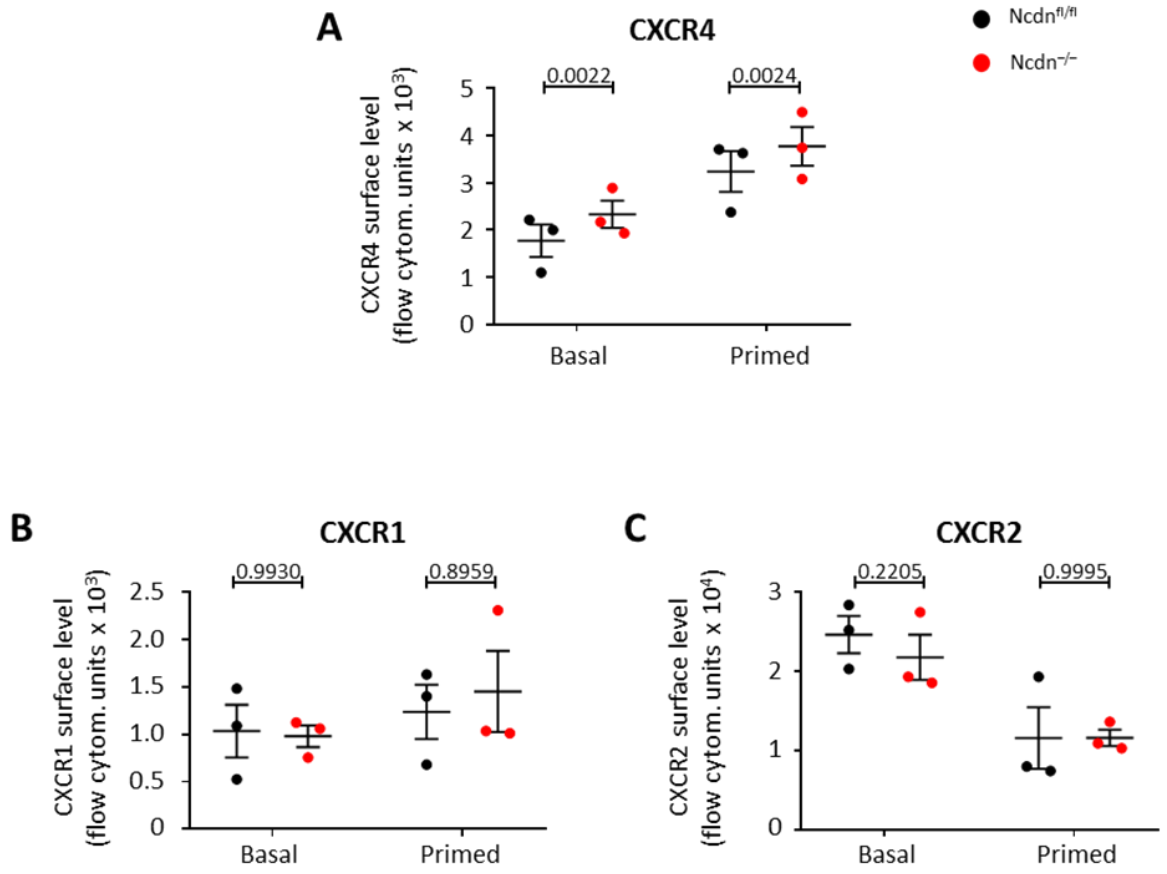

Figure 5.4: Norbin-deficient neutrophils have constitutively increased surface levels of the GPCR CXCR4 and normal surface levels of CXCR1 and CXCR2

Bone marrow cells from $Ncdn^{fl/fl}$ and $Ncdn^{-/-}$ mice were primed with 20 $ng.mL^{-1}$ murine TNFα and 40 $ng.mL^{-1}$ GM-CSF for 30 min at 37°C, or left on ice (basal), before being transferred onto ice and stained to investigate the levels of the GPCRs on the neutrophil surface by flow cytometry. Neutrophils were detected by their scatter characteristics and FITC-Gr1 (Ly6C and Ly6G) antibody staining, whilst GPCR surface levels were detected by (A) PE-CXCR4, (B) PE-CXCR1 or (C) PE-CXCR2 antibodies. All conditions were assessed in parallel. Each dot is the mean of one experiment. Data are mean ± SEM of 3 independent experiments. Statistical significance was assessed using two-way Anova with Sidak's multiple comparisons test.

In order to test whether Norbin can affect any other type of neutrophil surface protein, in addition to GPCRs, I tested the surface of Mac-1 integrin, one of the major neutrophil β2-integrins (Figure 5.5). Mac-1 surface levels were normal both under basal and primed conditions. Furthermore, Dr Dingxin Pan, who generated the Norbin-deficient mouse

strains, tested the surface levels of the neutrophil selectin L-selectin and of the selectin-ligand PSGL1, as well as of the other major neutrophil β2-integrin LFA-1 (unpublished data). Again, the levels of these proteins on the surface of Ncdn$^{-/-}$ neutrophils were normal, both under basal and primed conditions (Appendix A, Supplementary Figure 2).

To summarise, Norbin-deficiency leads to an upregulation of some but not all GPCRs onto the neutrophil surface, and it does not affect the surface levels of several other major types of neutrophil receptors and adhesion molecules.

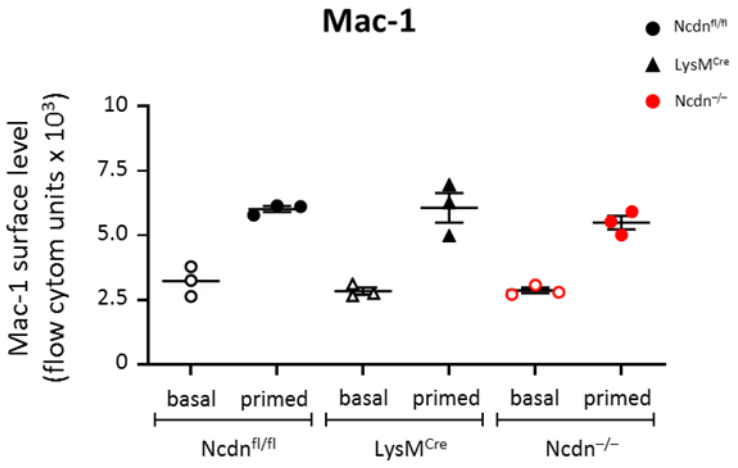

Figure 5.5: Norbin-deficient neutrophils have normal cell surface levels of Mac-1 integrin
Bone marrow cells from Ncdn$^{fl/fl}$, LysM^{Cre} and Ncdn$^{-/-}$ mice were primed with 20 ng.mL^{-1} murine TNFα and 40 ng.mL^{-1} GM-CSF for 45 min at 37°C, or left on ice (basal), before being transferred onto ice and stained to investigate the level of Mac-1 integrin on the neutrophil surface by flow cytometry. Neutrophils were detected by their scatter characteristics and BV510-Ly6G and AF647-Cd11b (Mac-1) antibody staining. All conditions were assessed in parallel. Data are mean ± SEM of 3 independent experiments. Statistical significance was assessed using two-way Anova with Sidak's multiple comparisons test.

Chapter 6 - Myeloid Norbin-deficiency increases immunity

6.1 Introduction: Neutrophils and macrophages in *in vivo* early inflammation models

Based on the results described in Chapters 4 and 5, I decided to test the functional role of myeloid Norbin *in vivo*, regarding both the recruitment of leukocytes to sites of inflammation and antibacterial immunity. For this aim, I used two different animal models of inflammation: (i) thioglycollate (TGC)-induced sterile peritonitis and (ii) *Streptococcus pneumoniae*-induced pulmonary infection.

The TGC-induced sterile peritonitis model is a well-established model for studying neutrophil recruitment to sites of inflammation (Baron & Proctor, 1982; Call et al., 2001; Leijh, Vanzwet, Terkuile, & Vanfurth, 1984; Y. M. Li, Baviello, Vlassara, & Mitsuhashi, 1997; Melnicoff, Horan, & Morahan, 1989). The peritoneal cavity of healthy mice contains resident macrophages (around 90% of leukocytes present), B1 lymphocytes (around 5-10%) and some basophils and mast cells. Mice respond to i.p. challenge with the irritant TGC by initially recruiting neutrophils, and then other types of inflammatory cells, into the inflamed peritoneal cavity. This recruitment starts immediately after challenge, with circulating neutrophils emigrating out of the blood stream into the inflamed peritoneum within the hour and peaking at 3 h (Pan et al., 2015), followed by mobilisation of a storage pool of mature neutrophils out of the bone marrow compartment (depending on the dose of TGC used), and then the maturation and mobilisation of bone marrow neutrophil precursors, which reach the peritoneal cavity later that day (Remick et al., 2001). Other leukocytes types are recruited more slowly. The recruitment of monocytes into the inflamed-peritoneal cavity usually occurs from 12 h onwards for several days (Cook, Braine, & Hamilton, 2003; Mooney et al., 2010), and these cells differentiate into macrophages at the site of inflammation, remaining present around 5-7 days after challenge, when lymphocytes become recruited. Overall, aseptic peritonitis is resolved within one week, although lymphocytes can remain in the peritoneal cavity until two weeks after challenge (Cook et al., 2003).

I chose quite a low dose of TGC (i.p. administration of 0.25 mL of 3% TGC) (Pan et al., 2015) compared to many other studies. Furthermore, I sacrificed the mice 3 h after TGC challenge, at the peak of early neutrophil recruitment (Pan et al., 2015), before culling the

mice and performing peritoneal lavages. These conditions were sufficient to elicit neutrophil recruitment while mice showed no more than mild clinical signs. Peritoneal lavage cells were counted by haemocytometer and identified by both cytostaining and flow cytometry.

The second model was a bacterial infection, which allowed me to evaluate innate immunity as well as leukocyte recruitment. As the Babraham Institute is interested in host defence during ageing, I chose a model of bacterial pneumonia, as this type of infection is particularly relevant in ageing. There are several approaches for establishing bacterial pneumonia in mice, and I chose intranasal (i.n.) infection with *Streptococcus pneumoniae*.

S. pneumoniae (pneumococcus) is a gram-positive category II pathogen that is the leading cause of community-acquired pneumonia, particularly harmful in young children, the elderly and immunocompromised adults, resulting in high morbidity and mortality in both developing and industrialized countries. Around 4 million people die worldwide each year from *S. pneumoniae* infections (Dockrell, Whyte, & Mitchell, 2012).

In healthy individuals, *S. pneumoniae* is a common inhabitant of the upper respiratory tract where it persists as a commensal bacterium usually for a period of weeks or months, generally without any adverse consequences (Bogaert, De Groot, & Hermans, 2004). Both in humans and in mice, the course of infection with *S. pneumoniae* commences with asymptomatic colonisation of the nasopharynx, which (despite the absence of symptoms) has an immunising effect (Gillespie & Balakrishnan, 2000; Richards, Ferreira, Miyaji, Andrew, & Kadioglu, 2010). Lower respiratory tract infection is presumed to occur upon microaspiration of *S. pneumoniae* from the nasopharynx, and can persist in the lower airway mucosa when resident alveolar macrophages fail to clear the bacteria through ineffective phagocytosis. These alveolar macrophages, as well as lung epithelial cells, release pro-inflammatory cytokines into the lung tissue and airways to attract first neutrophils (within a few hours) and later on other types of leukocytes (Bergeron et al., 1998; Gillespie & Balakrishnan, 2000). At high doses of *S. pneumoniae*, influx of neutrophils was reported to increase further even after 24 hours (Fillion et al., 2001). Neutrophil recruitment to the *S. pneumoniae* infected lung depends on the integrins Mac-1 and $\alpha_4\beta_1$ (Kadioglu et al., 2011).

If the infection remains uncontrolled at this stage, the bacteria multiply rapidly in the alveoli followed by an increase in monocyte and lymphocyte recruitment, which peaks 3 days after the inoculation. Then, the bacteria can also invade the blood stream, causing septicaemia. If bacterial infection is not sufficiently controlled during this final stage (72-96 hours), due to an immune-suppression or immuno-deficiency, further bacterial multiplication occurs, leading to massive tissue damage and high mortality (Gillespie, Mcwhinney, & Kibbler, 1991; Braun, Novak, Gao, Murray, & Shenep, 1999; Cauwels, Wan, Leismann, & Tuomanen, 1997; Gillespie & Balakrishnan, 2000).

There is some controversy in the literature as to how important neutrophils are for clearing pulmonary *S. pneumoniae* infections. During infection with low doses (10^4) of *S. pneumoniae*, no recruitment of neutrophils was seen, and alveolar macrophages alone were able to clear the infection, as shown by experimental macrophage depletion (Dockrell et al., 2003). However, further studies clearly showed that neutrophils are important for accelerating the clearance of *S. pneumoniae* (Dockrell et al., 2012). Neutrophil depletion in neonate vs adult mice showed furthermore that neonates are more dependent on neutrophils than adults for clearing *S. pneumoniae* from lungs (Garvy & Harmsen, 1996). Moreover, neutrophils were shown to secrete TRAIL (TNF-related apoptosis-inducing ligand) during pulmonary infection with *S. pneumoniae*, and this neutrophil-derived TRAIL promoted macrophage death through the apoptotic rather than the necrotic route, thus limiting overwhelming lung inflammation, while at the same time improving bacterial clearance and survival of the mice (Steinwede et al., 2012). The drawback of neutrophil recruitment to the *S. pneumoniae* infected lung is that the activated neutrophils also mediate much of the tissue damage associated with this infection (Dockrell et al., 2012). Taken together, it seems clear that neutrophils are important for the early response to pulmonary infection with *S. pneumoniae*, except perhaps under conditions of very low bacterial titres and with some dependence on the age of the subject.

I chose a medium-titre dose of *S. pneumoniae* (i.n. administration of 2 x 10^6 CFU bacteria per mouse in a volume of 50 μL), which would result in around 50% of wild type mice dying after 4 days if the disease were allowed to progress to that stage (A. K. Stark et al., 2018). In the early phase of the infection this dose has been reported to induce a

moderate pneumonia characterised by a mild neutrophilic alveolitis peaking by 24 h (Taut et al., 2008). In order to optimise conditions, I also performed a time course of neutrophil recruitment, and based on these data I studied the effects of Norbin deficiency at two different time points. Finally, to address the controversy in the literature about the importance of neutrophils in clearing *S. pneumoniae*, I also tested this directly as part of my study, by depleting neutrophils prior to the infection.

To summarise, in this chapter, I will describe the effects of murine Norbin deficiency and Norbin/Prex deficiency on neutrophil recruitment during (TGC)-induced sterile peritonitis and during pulmonary challenge with *S. pneumoniae*, as well as defining the ability of these mice to clear pulmonary *S. pneumoniae* infections, and the neutrophil-dependence of this response.

6.2 Norbin-deficiency does not affect neutrophil recruitment during aseptic peritonitis

We know from previous work in the laboratory that Prex-deficiency reduces the recruitment of neutrophils to the peritoneum during TGC-induced aseptic peritonitis (Welch et al., 2005). Here, I tested the functional role of Norbin in neutrophil recruitment during TGC-induced aseptic peritonitis, by comparing $Ncdn^{fl/fl}$, $LysM^{Cre}$ and $Ncdn^{-/-}$ mice using the conditions described in the introduction to this chapter (i.p. administration of 0.25 mL of 3% TGC, culls and lavages after 3 h). In order to assess the effect of combined Norbin- and Prex-deficiency, compared to Prex-deficiency alone, I also tested $Prex^{+/+}$, $Prex^{-/-}$ and $Ncdn^{-/-}$ $Prex^{-/-}$ mice under the same conditions.

In each experiment, mock-treated and TGC-treated mice from the different mouse strains were compared in parallel. I tested fewer mock-stimulated than TGC-stimulated mice, to reduce mouse numbers as much as possible, and as previous projects in the laboratory had shown that very few neutrophils are present in the peritoneum of control mice under the very clean conditions of the Babraham animal facility (individual ventilated cage (IVC) housing and all husbandry performed in air-filtered change stations). I analysed all experiments both by cytospin microscopy and by flow cytometry, again because previous

work in the laboratory had shown slight variations between the results obtained by these methods. The cytospin results are presented here first.

As expected, mock-treated control animals from all strains had very few neutrophils in their peritoneum, fewer than 10^4 cells per animal. Most (around 90-95%) of the total peritoneal lavage leukocytes under these conditions (around 10^6 per mouse) were resident peritoneal macrophages, and the rest were mostly B1 lymphocytes (Figures 6.1A and 6.2A, left-hand panels). In contrast, at 3 h after TGC challenge there was substantial recruitment of neutrophils into the peritoneum (Figures 6.1A and 6.2A, right-hand panels). This was clearly visible both in the cytospins (Figure 6.1A) and in the flow cytometry plots (Figure 6.2A), where there was an evident increase in the number of Gr1 (Ly6C & Ly6G) high, Mac-1 high cells (neutrophils) between control and TGC-injected mice.

Cytospin analysis showed that neutrophil recruitment into the peritoneum of the different control mouse strains 3 hours after TGC challenge was similar, where 0.69±0.10 x 10^6, 0.96 ± 0.21 x 10^6 and 0.81 ± 0.11 x 10^6 neutrophils were recruited in $Ncdn^{fl/fl}$, $LysM^{Cre}$ and $Prex^{+/+}$ control animals, respectively. In contrast, 1.15 x 10^6 neutrophils were recruited into the peritoneum of $Ncdn^{-/-}$ mice, suggesting that Norbin deficiency might cause a mild increase in the recruitment of neutrophils to the peritoneum (Figure 6.1B, left-hand panel). However, this increase reached statistical significance only compared to the $Ncdn^{fl/fl}$ control strain but not the $LysM^{Cre}$ control strain. Hence, overall Norbin-deficiency had no significant effect on neutrophil recruitment, judging by cytospin analysis.

As discussed above, a previous study from our lab had shown that TGC-induced neutrophil recruitment to the inflamed peritoneum is reduced by 50% in $Prex1^{-/-}$ mice (Welch et al., 2005). I obtained similar results here with $Prex^{-/-}$ animals. As shown in Figure 6.1B (right-hand panel), 0.35 ± 0.12 x 10^6 $Prex^{-/-}$ neutrophils were recruited into the peritoneum of $Prex^{-/-}$ animals in response to TGC, a significant reduction compared to 0.91 x 10^6 in the $Prex^{+/+}$ control mice. Furthermore, in the $Ncdn^{-/-}$ $Prex^{-/-}$ double deficient mice, only an average of 0.26 ± 0.07 x 10^6 neutrophils were recruited into the peritoneum under the same conditions. This means the double-deficient mice have as little neutrophil recruitment as the $Prex^{-/-}$ mice, and less than the $Ncdn^{-/-}$ mice, which implies that Prex1 is required for neutrophil recruitment regardless of whether Norbin is expressed or not.

Comparison of the neutrophil counts with total leukocyte counts in the peritoneal lavages showed that neutrophil recruitment largely accounted for the increase in total leukocyte numbers observed in the TGC-inflamed peritoneum, showing an increase from the 1×10^6 residential cells in mock-treated mice to 2×10^6 total leukocytes in TGC-treated mice across the various genotypes, except in the $Prex^{-/-}$ and $Ncdn^{-/-}$ $Prex^{-/-}$ strains which had low neutrophil recruitment. Because of the low number of mock-treated control mice used, I could not perform a statistical analysis of the TGC-induced increase in total leukocyte numbers. However, overall these total leukocyte numbers suggested that, after 3 h of TGC challenge, neutrophils were the predominant cell type recruited during this early inflammatory response, as expected (Figure 6.1B and C).

To summarise the results obtained by cytospin analysis, Norbin deficiency does not significantly affect neutrophil recruitment during TGC-induced aseptic peritonitis, and Prex1 is required for TGC-induced neutrophil recruitment irrespectively of Norbin expression.

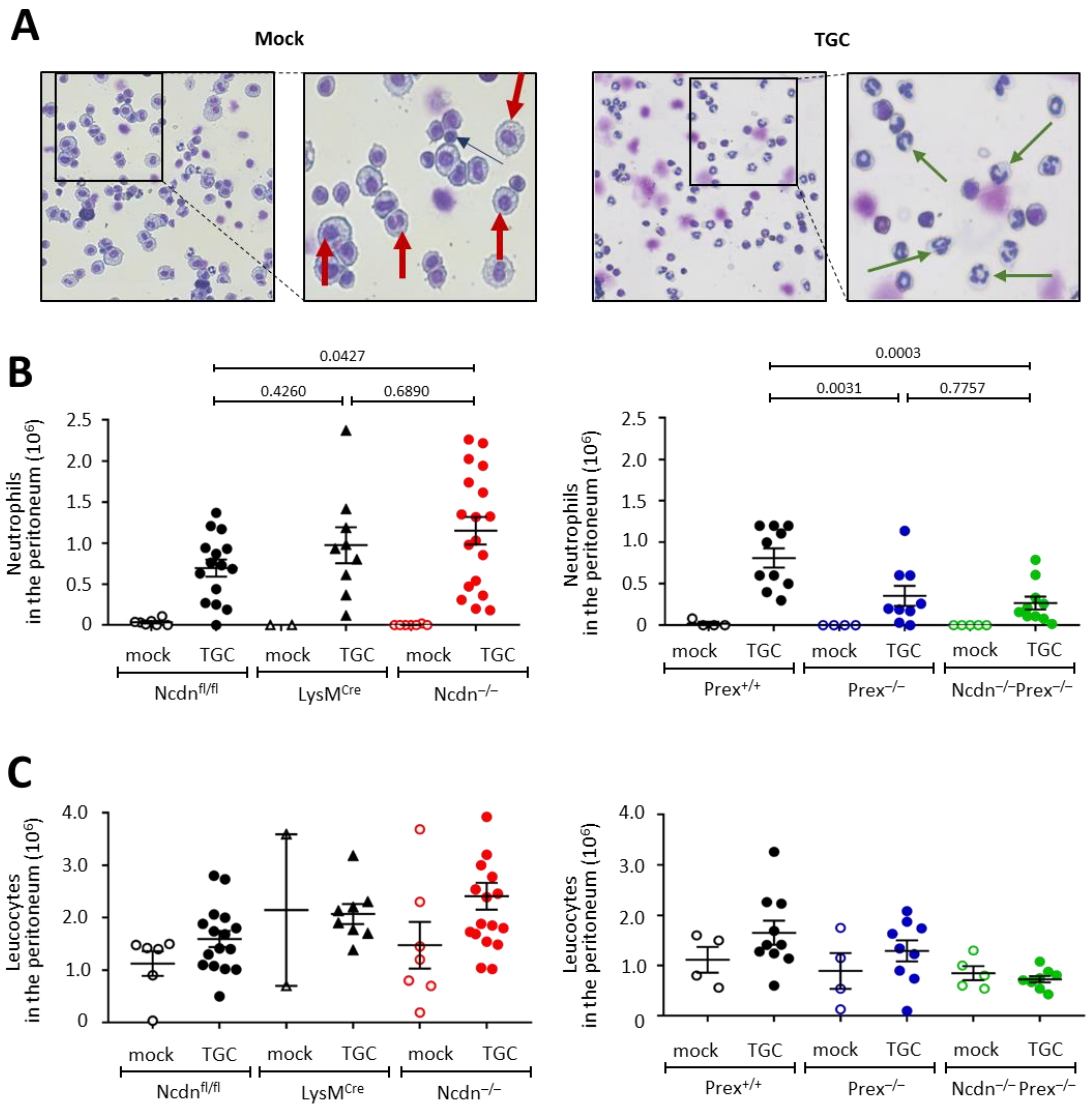

Figure 6.1: Norbin deficiency does not affect neutrophil recruitment during TGC-induced sterile peritonitis
Mice of the indicated genotypes were challenged by intraperitoneal injection of 0.25 mL 3% thioglycollate (TGC) in water or were mock-treated with water. Mice were culled by CO_2 asphyxiation 3 h after the injection. Peritoneal lavages were performed and the number of neutrophils recruited to the peritoneum assessed by haemocytometer and cytospin microscopy. (A) Representative cytospin images of peritoneal neutrophil recruitment from mock-treated (left-hand panel) and TGC-injected (right-hand panel) $Ncdn^{fl/fl}$ neutrophils. Peritoneal lavage cells were cytospun and then fixed and stained with Kwick-Diff reagent. The red arrows point to resident peritoneal macrophages, the blue arrow to a resident lymphocyte and the green arrows to neutrophils, identified by their characteristic nuclear morphology. (B) Quantification of the total number of neutrophils recruited into the peritoneum, and (C) the total number of leukocytes in the peritoneum, as assessed by cell counting and cytospin analysis. Each dot represents one mouse. Data are mean ± SEM of 2-7 mock-treated mice and 8-18 thioglycollate-injected mice per genotype, pooled from 7 independent experiments. Statistical significance was assessed using two-way Anova with Tukey's multiple comparisons test.

In parallel to the cytospin analysis, the same experiments were also analysed by flow cytometry (Figure 6.2). Quantification of the Gr1/Mac-1 high cells showed again that $Ncdn^{-/-}$ mice had increased neutrophil recruitment in response to TGC-challenge compared to the $Ncdn^{fl/fl}$ mice but not compared to the $LysM^{Cre}$ mice (Figure 6.2B left-hand panel). Also, Prex deficiency was again seen to significantly decrease TGC-induced neutrophil recruitment, and Norbin deficiency could not override this requirement for Prex1 in the ($Ncdn^{-/-}$ $Prex^{-/-}$) double KO mice (Figure 6.2B, right-hand panel). Compared to the cytospin analysis, fewer neutrophils were identified in the peritoneal lavages by flow cytometry, although the differences between genotypes were similar. The lower neutrophil numbers seen by flow cytometry can be explained by the flow cytometric analysis taking only single cells into account, whereas microscopy analyses allowed for identification of cells that were adherent to others. Indeed, we observed by cytospin that neutrophils were often recovered in groups, particularly upon TGC-challenge, presumably because the inflammation stimulated cell-cell adhesion. As a consequence of this apparently lower level of neutrophil recruitment detected by flow cytometry, the increase in total leukocytes that had been observed by cytospin analysis was not obvious by flow cytrometric analysis.

Taken together, however, both methods of analysis gave essentially the same results, namely that Norbin deficiency does not significantly affect neutrophil recruitment during aseptic peritonitis, and that Prex1 is required regardless of whether Norbin is expressed or not. The apparent small increase in neutrophil recruitment in Norbin-deficient mice was only seen in comparison to the $Ncdn^{fl/fl}$ control strain but not compared to $LysM^{Cre}$, and the variability between individual mice was large enough to suggest that these control strains were not significantly different from each other.

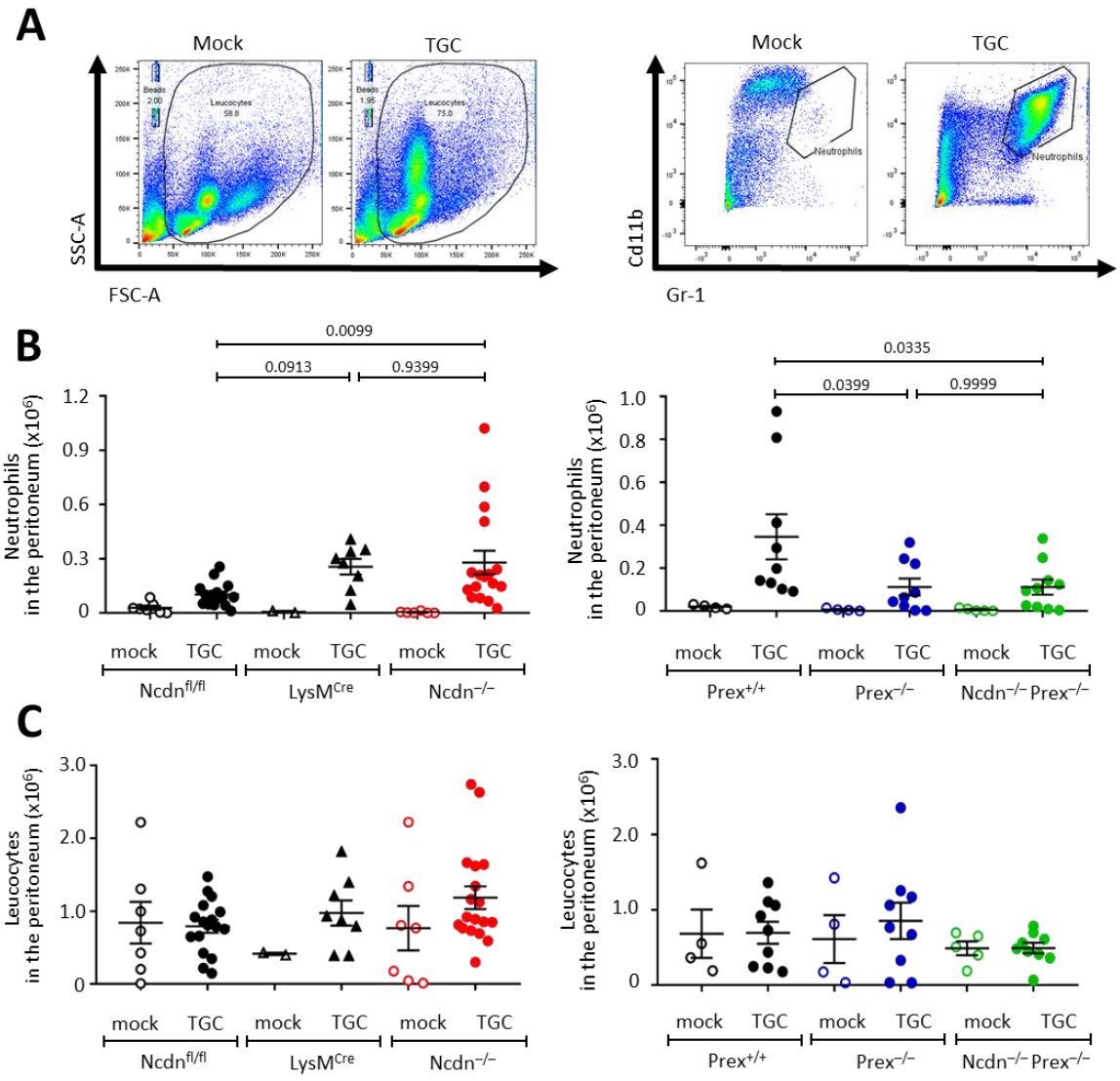

Figure 6.2: **Norbin-deficiency does not affect neutrophil recruitment to the TGC-inflamed peritoneum**
The same peritoneal lavage samples of TGC-treated and mock-treated mice in Figure 6.1 were analysed in parallel by flow cytometry. (A) Representative gating of total leukocytes in forward (FSC) and side scatter (SSC) plots and identification of neutrophils by FITC-Gr1 (Ly6C & L6G) high and AF647-Mac-1 (Cd11b) high staining is shown for mock-treated and TGC-injected Ndnc$^{fl/fl}$ mice, as indicated. Spherotech beads were used as a counting reference. (B) Number of neutrophils recruited to the peritoneum, identified by Gr1 (Ly6c & Ly6G) high and Mac-1 high staining. (C) Total number of leukocytes in the peritoneum, identified by FSC and SSC signals compared to the Spherotech bead standard. Each dot represents one mouse. Data are mean ± SEM of 2-7 mock-treated mice and 8-18 TGC-injected mice per genotype, up to 3 mice per genotype per day, pooled from 7 independent experiments. Statistical significance was assessed using two-way Anova with Tukey's multiple comparisons test.

6.3 Characterisation of pulmonary infection with *S. pneumoniae*

I initially learnt the model of *S. pneumoniae*-induced acute lung inflammation from Dr Anne-Katrien Stark (Okkenhaug lab, Laboratory of Lymphocyte Signalling and Development, Babraham Institute) who used it to study the role of lymphocytes in the late stage of this infection (A. K. Stark et al., 2018). Dr Stark also provided me throughout this study with bacterial stocks (TIGR4, serotype 4) that were kept virulent by *in vivo* passage at least once a year and were characterised for their haemolytic ability by growth on blood agar. I began by performing pilot experiments with $Ncdn^{fl/fl}$ control mice to adapt the conditions for the purpose of my study of the early, neutrophil-dependent stage of this infection model.

To assess the dynamics of *S. pneumoniae*-induced neutrophil recruitment and the survival of bacterial colony-forming units (CFUs) in the infected lung *in vivo*, I carried out a time course study in $Ndnc^{fl/fl}$ mice. Mice were inoculated with a 50 μL inoculum containing 2 x 10^6 *S. pneumoniae* CFU under light general anaesthesia, or were mock-treated with buffer only, and were then culled for analysis after various time points from 3 h up to 24 h. Broncho-alveolar lavage (BAL) was performed, followed by perfusion of the lung with DPBS and excision and homogenisation of the perfused lung. Both BAL and lung homogenates were analysed for the presence of leukocytes and for the survival of bacteria.

The BAL recovers cells from the alveolar airspace. In mock-infected mice, these lavage cells are largely resident alveolar macrophages and a few lung epithelial cells. In *S. pneumoniae* infected mice, the lavage additionally contains leukocytes that extravasated from the alveolar vasculature through the interstitium and alveolar epithelium into the airspace. In contrast, the perfused lung homogenate contains leukocytes that are sufficiently firmly adhered (either within the vasculature, in the interstitium or on the surface of the lung epithelium) not to have been flushed away by the perfusion.

To best describe the optimisation of the infection model, I present here the collated data from all experiments and time points performed with $Ncdn^{fl/fl}$ control mice, instead of showing data from individual pilot experiments. Mock-treated animals (stippled lines) had 5.6 x 10^1 neutrophils and 5.20 x 10^3 macrophages in the BAL, and they had 1.72 x 10^3 neutrophils and 4.21 x 10^4 monocytes/macrophages in the perfused lung (Figure 6.3A and

B). Hence, there were very few tissue resident neutrophils in the steady state, as previously reported (Kreisel et al., 2010). The number of neutrophils in the BAL increased to 1.49 x 10^3 at 18 h (Figure 6.3A), likely because the i.n. mock treatment caused a low level of inflammation, whereas neutrophil numbers in the lung homogenate of mock-infected mice remained constant throughout the time course (Figure 6.3B).

In mice infected with *S. pneumoniae*, neutrophil numbers were markedly increased even at the earliest time point tested, 3 h after inoculation, when 4-5 x more neutrophils (green line) were present in both BAL (2.06 x 10^2 cells) and lung homogenate (8.73 x 10^3 cells) compared to mock-treated animals (Figure 6.3A and B). At the 6 h time point after infection, the number of the neutrophils recruited increased sharply to 4.14 x 10^3 in the BAL and 5.81 x 10^4 in the lung homogenate. It peaked at 18 h, with 7.74 x 10^4 neutrophils in the BAL and 1.92 x 10^6 in the lung, and remained constantly high until the final time point tested at 24 h (4.75 x 10^4 neutrophils in the BAL and 2.08 x 10^6 in the lung) (Figure 6.3A and B). Hence, these conditions of *S. pneumoniae* infection caused a rapid recruitment of neutrophils that was 52 times higher in the BAL and 330 times higher in the lung homogenate compared to mock-treated animals.

In contrast to this acute neutrophil recruitment, the number of monocytes/macrophages (Cd11c+, Cd11b+, Ly6C+ cells) in BAL and lung homogenate remained much more even throughout these experiments. A constant number (5-9 x 10^3) of macrophages (purple stippled line) was present in the BAL of mock-infected mice, although a modest increase became evident only 24 h after the infection (1.59 x 10^4 cells, purple line (Figure 6.3A and B). Further flow cytometric analysis identified these resident leukocytes as alveolar macrophages, as expected (data not shown). Similarly, in the perfused lung homogenate of mock-treated mice, there was also a fairly constant number of macrophages (5-8 x 10^4) throughout the time course. In contrast, increased numbers of monocytes/macrophages were seen in the lung homogenate of *S. pneumoniae* infected mice from 6 h after the infection (4.17 x 10^5 cells) onwards, and this increased further to 1.25 x 10^6 the end of the time course (Figure 6.3A and B). Further flow cytometric analysis identified these newly infiltrated cells as inflammatory monocytes (Figure 6.3C).

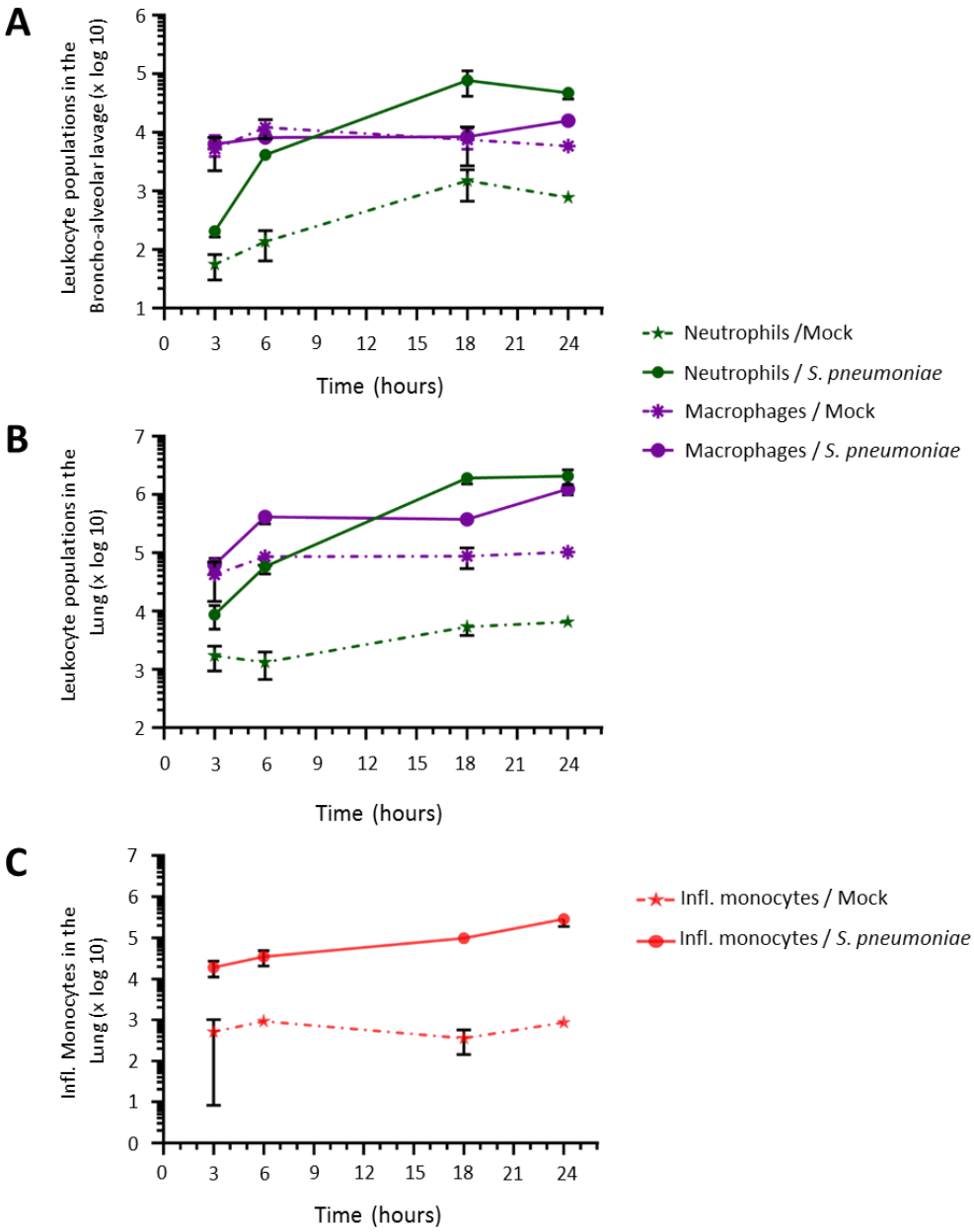

Figure 6.3: **Time course of neutrophil and monocyte recruitment in Ncdn$^{fl/fl}$ control mice in the pulmonary *S. pneumoniae* infection model**

Ncdn$^{fl/fl}$ mice were given an intranasal administration of 2 x 10^6 CFU *S. pneumoniae* in 50 µL sterile HBSS (solid lines) or were mock-treated with the same volume of buffer (stippled lines). Mice were culled by CO_2 asphyxiation at 3, 6, 18 and 24 h after the infection and the numbers of neutrophils (green lines), monocytes/macrophages (purple lines) and inflammatory monocytes (red lines) in BAL (A) and lung homogenate (B) assessed by flow cytometry. (A) Number of neutrophils (Ly6G^{hi}, Cd11b^{hi} cells) and monocytes/macrophages (Cd11b^{+}, Cd11c^{+}, Ly6C^{+} cells) recovered in the BAL. (B) Number of neutrophils (Ly6G^{hi}, Cd11b^{hi} cells) and monocytes/macrophages (Cd11b^{+}, Cd11c^{+}, Ly6C^{+} cells) recovered in the lung homogenate. (C) Number of inflammatory monocytes (CD11b^{hi}, Ly6C^{hi} cells) recovered in the lung homogenate. Data are mean ± SEM of 1-2 mock-treated and 2-3 *S. pneumoniae*-infected mice per time point and experiment, pooled from 4 individual experiments performed at the 3 h, 6 h and 18 h time points, and of 1 mock-treated and 6 *S. pneumoniae*-infected mice from 1 experiment performed at the 24 h time point.

In contrast to this presence of inflammatory monocytes in the lung homogenate, inflammatory monocytes ($CD11b^+$ $Ly6C^+$ cells) (J. Yang, Zhang, Yu, Yang, & Wang, 2014), as well as eosinophils (Siglec-F^+, $CD11C^-$ cells) (Stevens, Taeg, Pujanauski, Hao, & Braciale, 2007) remained essentially absent from the BAL over the duration of the experiment (data not shown), as expected from other studies (Fillion et al., 2001). Therefore, it seems likely that the inflammatory monocytes in the lung homogenate were recruited into this tissue in response to the infection but had not yet transmigrated through the epithelium within the time-frame of these experiments.

Overall, under the conditions tested, significant recruitment of neutrophils was seen both in the BAL and lung homogenate, whereas significant recruitment of monocytic cells was only observed in the lung homogenate, as expected (Figure 6.3). Furthermore, the numbers of cells recovered from the BAL were significantly lower than those in the lung homogenate throughout the different treatments, time points and cell types, also as expected.

In parallel to neutrophil recruitment, I measured bacterial survival as colony forming units (CFUs), both in the BAL and in the perfused lung homogenate (Figure 6.4) of the same *S. pneumoniae*-infected and mock-treated $Ncdn^{fl/fl}$ control mice as shown in Figure 6.3.

Mock-treated animals (stippled line) had 1.0-8.25 x 10^1 CFU of *S. pneumoniae* in the BAL and 1.0-9.66 x 10^1 CFU in the perfused lung, as identified by the haemolytic action of bacterial colonies on blood agar plates. Furthermore, the CFU in the BAL and lung homogenate of mock-infected mice remained constantly low throughout the time course. Hence, there was a negligible titre of *S. pneumoniae* both in the BAL and in the lung homogenate of control animals, as expected. This is testament to the high standard of cleanliness in our biological support unit. To maintain these low background titres and avoid cross-contamination, I adopted the practice of housing mock-treated and *S. pneumoniae*-infected mice in separate isocages throughout the experiments.

In mice infected with 2 x 10^6 *S. pneumoniae* (solid line), bacterial numbers remained markedly elevated in the BAL at the two earliest time point tested, 3 h and 6 h after inoculation. In the BAL, 1.16 x 10^5 CFU and 7.67 x 10^5 CFU were recovered at the 3 h and 6 h time points, respectively. The apparent increase in bacterial CFU between the 3 h and 6 h

time points could either reflect bacterial growth within the airspace, or be a result of variability between mice or technical issues. In any event, less than 40% of bacterial CFU were recovered at the 6 h time point compared to the titre used for infection. In contrast, the bacterial titre in the BAL had declined sharply at the 18 h time point to 3.26 x 10^2 CFU and dropped even further at the final 24 h time point, to 4.5 x 10^1 CFU, almost back to control levels. Hence, the largest impact on antibacterial immunity within the airspace was seen between the 6 h and 18 h time points.

In the lung homogenate, 1.12 x 10^4 CFU and 3.81 x 10^5 CFU were recovered at the 3 h and 6 h time points after infection, respectively, and unlike in the BAL, numbers remained roughly at that level (5.39 x 10^4 CFU) at 18 h, before falling at the final 24 h time point tested to 3.14 x 10^2 CFU. Hence, bacteria are cleared from the airspace more rapidly than from the perfused lung tissue, presumably because bacteria survived in hard-to reach niches within the lung tissue. Overall, between the BAL and lung homogenate, 6 h and 18 h were the most interesting time points regarding the clearance of *S. pneumoniae* infections.

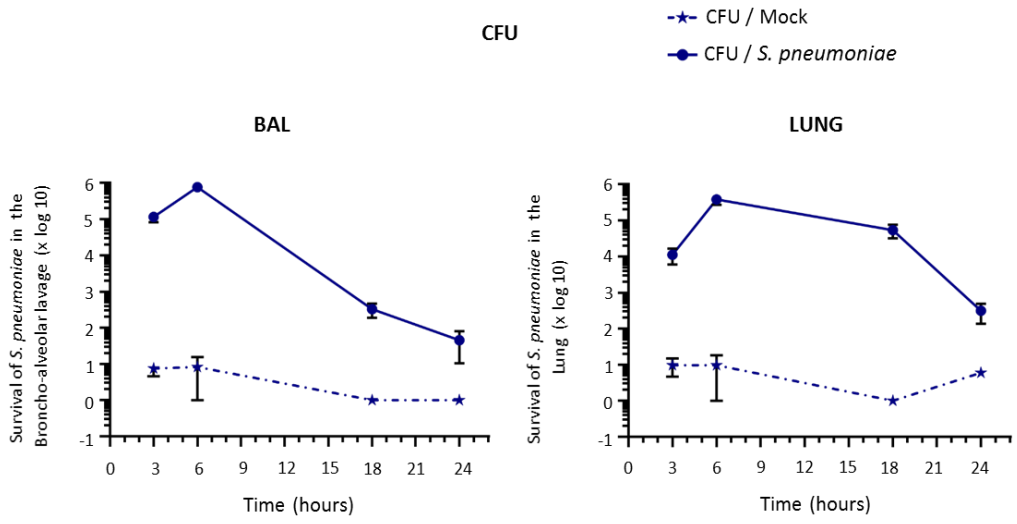

Figure 6.4: Time course of bacterial survival in Ncdn$^{fl/fl}$ control mice in the *S. pneumoniae* pulmonary infection model

Serial dilutions of the same BAL (left hand panel) and perfused lung homogenate (right hand panel) samples from Ncdn$^{fl/fl}$ mice infected with 2 x 10^6 CFU *S. pneumoniae* or mock-treated mice as in Figure 6.3. were analysed for bacterial survival as colony forming units (CFU) on blood agar plates. Data are mean ± SEM of 1-2 mock-treated and 2-3 *S. pneumoniae*-infected mice per time point and experiment, pooled from 4 individual experiments performed at the 3h, 6 h and 18 h time points, and of 1 mock-treated and 6 *S. pneumoniae*-infected mice from 1 experiment performed at the 24 h time point.

Based on my optimisation assays, and taking into account both neutrophil recruitment and bacterial clearance, I chose the 6 h time point for subsequent experiments as a condition where substantial but not maximal neutrophil recruitment was seen, and the 18 h time point as a condition where neutrophil recruitment was maximal and where these neutrophils (or alveolar macrophages) in the airspace had ample time to clear bacteria.

6.4 Norbin deficiency increases the immunity of mice to pulmonary *S. pneumoniae* infection without affecting neutrophil recruitment

In Chapter 4, I showed that *in vitro* Norbin-deficient neutrophils have elevated ROS production and degranulation, and an increased ability to kill *S.aureus*. These findings opened the hypothesis that Norbin deficient neutrophils might also have an increased capacity for killing pathogens *in vivo*.

To learn whether Norbin-deficiency has an impact on antibacterial immunity *in vivo*, $Ncdn^{fl/fl}$, $LysM^{Cre}$ and $Ncdn^{-/-}$ were tested in parallel in the pulmonary *S. pneumoniae* infection model at the 6 h and 18 h time points. To assess the effect of Prex deficiency and of combined Prex/Norbin deficiency, $Prex^{+/+}$, $Prex^{-/-}$ and $Ncdn^{-/-}$ $Prex^{-/-}$ mice were also tested in the same model at the 18 h time point.

As described in Figures 6.3 and 6.4, the mice were infected i.n. with 2 x 10^6 CFU *S. pneumoniae* or were mock-infected, culled after 6 h or 18 h, the bronchioles lavaged, lungs perfused, dissected and homogenised, and both the BAL and perfused lung homogenate were assessed for the survival of bacteria as CFU on blood agar, and for the numbers of the different leukocyte populations by flow cytometry.

Firstly, animals from the two control strains, $Ncdn^{fl/fl}$ and $LysM^{Cre}$, were compared to $Ncdn^{-/-}$ mice at the 6 h time point. As expected from the pilot experiments, mock-treated animals from all strains had no bacterial CFU in the BAL (Figure 6.5A, left-hand panel) or in the perfused lung homogenate (Figure 6.5A right hand panel). In mice infected with *S. pneumoniae*, bacterial numbers recovered in the BAL were markedly high in the $Ncdn^{fl/fl}$ and

LysM^{Cre} mice, with 6.74 x 10^5 and 8.82 x 10^5 bacteria remaining, respectively, at the 6 h time point, similar to the findings in the pilot experiments. In contrast, only 5.64 x 10^4 bacterial CFU were left in the BAL of Ncdn$^{-/-}$ mice under the same conditions, a 12-fold and 16-fold decrease compared to Ncdn$^{fl/fl}$ and LysM^{Cre} mice ($p=0.0003$ and $p<0.0001$), respectively (Figure 6.5A left-hand panel). Therefore, Norbin deficiency increases the ability of mice to kill *S. pneumoniae* in the airspace during pulmonary infection by more than 10-fold.

Similarly, in the perfused lung homogenates of the infected mice, bacterial numbers were high in Ncdn$^{fl/fl}$ and the LysM^{Cre} mice, with 3.33 x 10^5 and 1.07 x 10^6 bacteria present in the lung at the 6 h time point, whereas only 4.46 x 10^4 bacteria were left in the lung homogenate of Ncdn$^{-/-}$ mice (Figure 6.5.A right-hand panel). Therefore, Norbin-deficient mice had a 7.5-fold increased capacity to kill bacteria in lung tissue compared to Ncdn$^{fl/fl}$ and 24-fold increase compared to LysM^{Cre} mice ($p=0.1252$ and $p=0.0006$, respectively). Therefore, Ncdn$^{-/-}$ mice were able to clear bacteria more efficiently than the two control strains both from the airspace and the perfused lung tissue.

With regards to the cell populations, mock-treated control animals from the Ncdn$^{fl/fl}$, LysM^{Cre} and Ncdn$^{-/-}$ strains had very few neutrophils in the BAL, ranging between 2.2 x 10^1 - 1.71 x 10^2 neutrophils, or 4.96 x 10^3 – 1.63 x 10^4 neutrophils in the perfused lung. Hence, there were very few tissue resident neutrophils in the steady state, as expected from the pilot experiments. In addition and again, as expected, *S. pneumoniae* infection caused a marked increase in neutrophil numbers both in the BAL and perfused lung homogenate. Neutrophil numbers in the BAL of infected Ncdn$^{fl/fl}$, LysM^{Cre} and Ncdn$^{-/-}$ mice, ranged between 3.69 x 10^3 and 1.05 x 10^4. In the perfused lung, neutrophil numbers were 4.30 x 10^5 in Ncdn$^{fl/fl}$, 2.36 x 10^5 in LysM^{Cre} and 3.68 x 10^5 in Ncdn$^{-/-}$. However, there was no significant difference in neutrophil recruitment between Ncdn$^{-/-}$ mice and Ncdn$^{fl/fl}$ and LysM^{Cre} controls during pulmonary infection with *S. pneumoniae*.

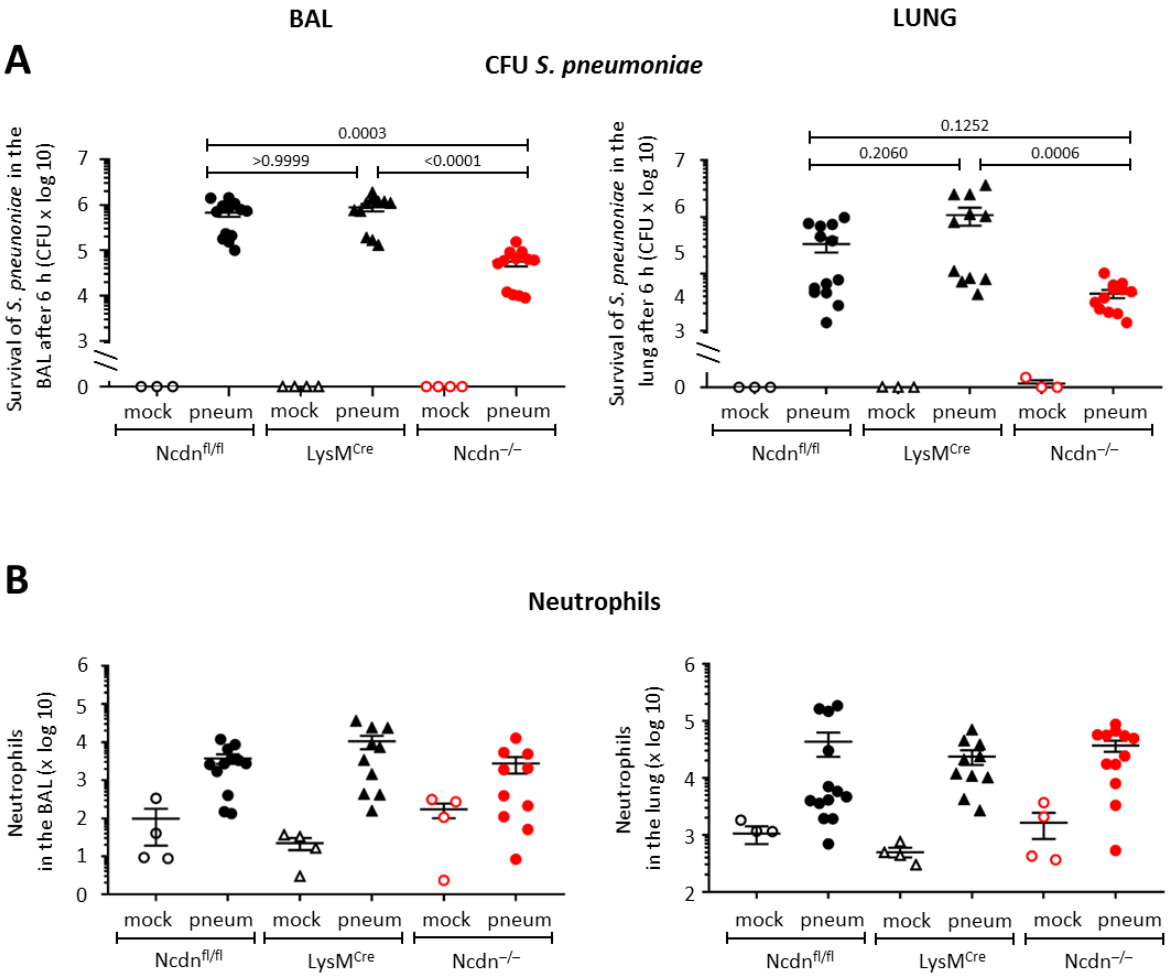

Figure 6.5: Norbin deficiency increases the immunity of mice to pulmonary *S. pneumoniae* infection
Mice of the indicated genotypes were given an intranasal administration of 2 x 10^6 CFU *S. pneumoniae* in 50 µL sterile HBSS or were mock-treated with the same volume of buffer. Mice were culled by CO_2 asphyxiation at 6 h after the infection and (A) serial dilutions of BAL (left hand panel) and perfused lung homogenate (right hand panel) were analysed for bacterial survival as CFU on blood agar plates. In parallel the (B) number of neutrophils (Ly6G^{hi}, Cd11b^{hi} cells) of BAL (left hand panel) and perfused lung homogenate (right hand panel) were assessed by flow cytometry. Each dot represents one mouse. Data are mean ± SEM of 3-4 mock-treated mice and 10-13 *S. pneumoniae*-infected mice per genotype, pooled from 4 independent experiments. Statistical significance was assessed using Kruskal-Wallis analysis with Dunn's multiple comparisons test.

In mock-treated control animals from all strains, the numbers of monocytes/ macrophages were around 10^4 - 10^5cells both in the BAL and in the lung homogenate (Figure 6.6A, left-hand panel). In the BAL of infected mice, the same range of monocyte/macrophage numbers (10^4 - 10^5cells) was observed, and further flow cytometric analysis showed that these cells were mostly alveolar macrophages (Figure 6.6B, left-hand panel), whereas no inflammatory monocytes were present in the BAL, as expected (Figure 6.6C, left-hand panel). In contrast, in the perfused lung homogenate, a significant population of inflammatory monocytes (10^4 cells) was recruited in response to the *S. pneumoniae* infection, to a similar level in all strains, and contributing to around half of the monocytes and macrophages present in this tissue, compared to the tissue of mock-infected control animals which only contained around 10^2 - 10^3 inflammatory monocytes. There appeared to be a modest significant difference in both alveolar macrophage numbers and inflammatory monocyte numbers between $Ncdn^{fl/fl}$ and $Ncdn^{-/-}$ strains, with reduced numbers in the $Ncdn^{-/-}$ strain, resulting in an overall significant difference also in total monocyte/macrophage numbers (Figure 6.6). However, there was a slight difference in monocyte and macrophage recruitment between the two different control strains, and these cell populations in the $LysM^{Cre}$ strain were similar to those of $Ncdn^{-/-}$ mice. Therefore, we can conclude that Norbin deficiency did not affect monocyte and macrophage numbers during pulmonary infection with *S. pneumoniae*.

Taken together, the data model show that Norbin deficiency increases the ability of mice to clear pulmonary *S. pneumoniae* infection 10-fold, without affecting the recruitment of neutrophils or monocytes, or the numbers of resident macrophages. This increase in innate immunity in the absence of altered neutrophil recruitment suggests either that Norbin-deficient neutrophils can kill bacteria more efficiently *in vivo*, or that neutrophils are not the cause of this increased immunity. The increased antibacterial immunity of isolated Norbin-deficient neutrophils (see Chapter 4) would support the first possibility. However, I also investigated the second possibility (see section 6.6 below).

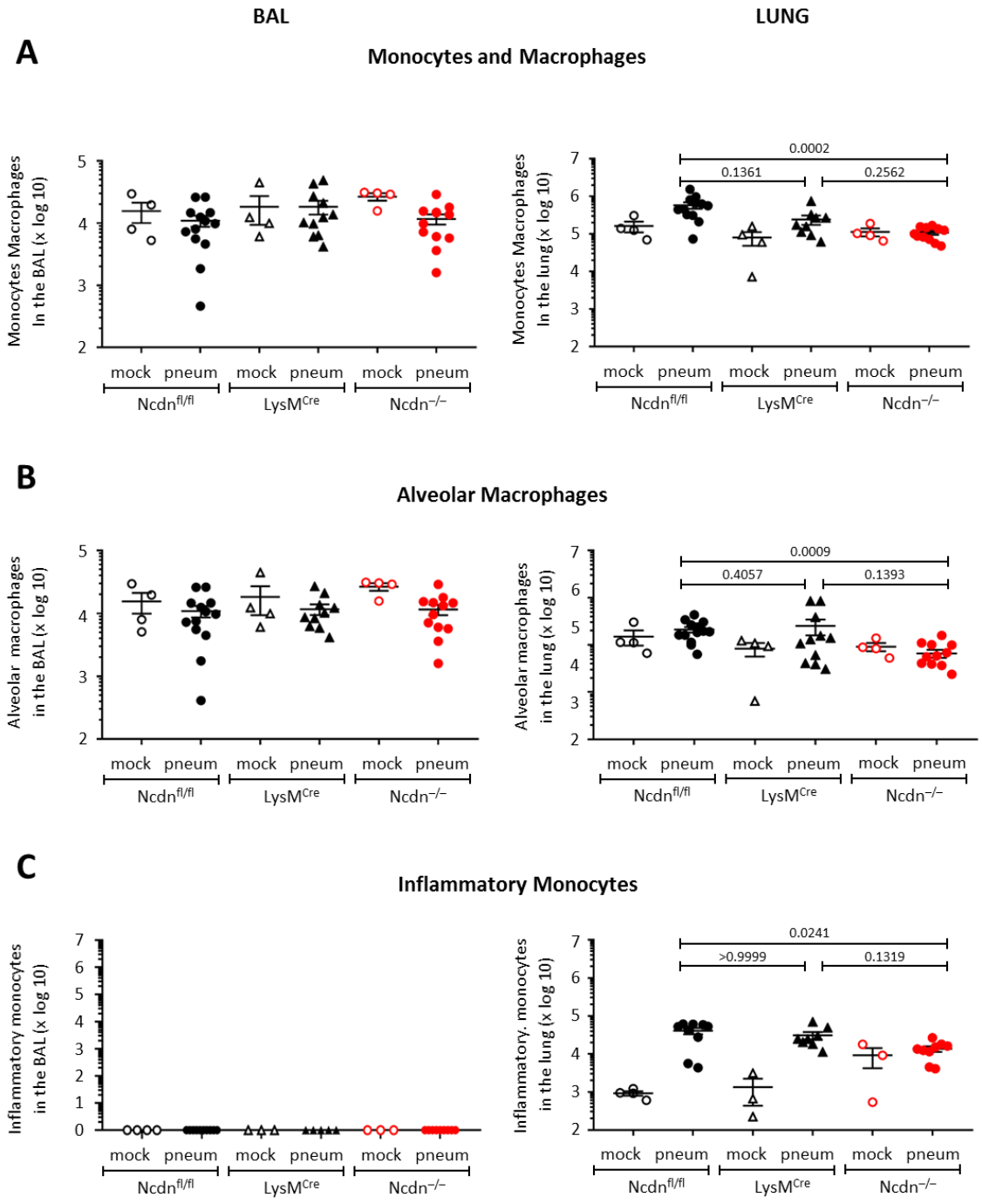

Figure 6.6: Norbin-deficiency does not affect neutrophil and monocyte recruitment during pulmonary infection with *S. pneumoniae*

The same bronchoalveolar lavage and lung homogenates samples of *S. pneumoniae*-infected and mock-infected mice in Figure 6.5 were analysed in parallel by flow cytometry for the (A) number of monocytes and macrophages ($Cd11b^+$, $Cd11c^+$, $Ly6C^+$ cells), (B) number of alveolar macrophages ($CD11c^+$, $SiglecF^+$ cells) and (C) number of inflammatory monocytes ($CD11b^{hi}$, $Ly6C^{hi}$ cells) recovered in the BAL (left-hand panels) and in the perfused lung homogenate (right-hand panel) from mice of the indicated genotypes and infected with 2×10^6 CFU *S. pneumoniae* or mock-treated mice, as assessed by flow cytometry. Data are mean ± SEM of 3-4 mock-treated mice and 10-13 *S. pneumoniae*-infected mice per genotype, pooled from 4 independent experiments. Statistical significance was assessed using Kruskal-Wallis analysis with Dunn's multiple comparisons test.

To examine whether the improved immunity of Norbin-deficient mice to *S. pneumoniae* infection would persist overtime, I also tested the later time point of 18 h. As expected from the pilot experiments, the control strains $Ncdn^{fl/fl}$ and $LysM^{Cre}$ had cleared most of the bacteria from the airspace at that point, as only $1.34 \times 10^3 – 1.03 \times 10^3$ bacterial CFU were recovered from the BAL at that point (Figure 6.7A, left-hand panel), 100-fold fewer compared to the 10^5 bacteria counted at the 6 h time point (Figure 6.5A). Compared to these control mice, the $Ncdn^{-/-}$ strain cleared the bacteria to a similar level, having only 1.13×10^3 bacterial CFU left in their BAL after 18 h (Figure 6.7A, left-hand panel). Hence, Norbin deficieny accelerated the clearance of bacteria from the airspace, but a low level of bacterial load remained in all strains after 18 h.

In contrast to the BAL, and as expected from the pilot experiments, in the perfused lung homogenates of *S. pneumoniae* infected mice, bacterial numbers were still high at the 18 h time point in the $Ncdn^{fl/fl}$ and the $LysM^{Cre}$ control mice, with 5.39×10^4 and 4.76×10^4 bacteria being recovered from this tissue, whereas only 1.35×10^4 bacteria were left under these conditions in $Ncdn^{-/-}$ strain (Figure 6.7A, right-hand panel). Therefore, Norbin-deficient mice still had a 4-fold increased capacity to kill bacteria compared to $Ncdn^{fl/fl}$ under these conditions, and a 3.5-fold increase compared to $LysM^{Cre}$ mice. There was a significant difference in CFU numbers between $LysM^{Cre}$ and $Ncdn^{-/-}$ strains ($p=0.0180$) at this later time point, although the difference between $Ncdn^{fl/fl}$ and $Ncdn^{-/-}$ did not quite reach significance ($p=0.1153$), likely due to the low "n" numbers used in $Ncdn^{fl/fl}$ mice. Therefore, Norbin deficient-mice cleared bacteria from the BAL and from the lung faster than the two control strains at an early time point (Figure 6.5A), and the increased immunity of $Ncdn^{-/-}$ mice also persisted in the lung tissue at this later time point.

With regards to the leukocyte populations, mock-treated control animals from all strains had few neutrophils in BAL and lung at the 18 h time-point, ranging between $7.58 \times 10^2 – 3.56 \times 10^3$ in the BAL and $2.36 \times 10^3 – 1.48 \times 10^4$ in the lung, as expected from the pilot experiments (Figure 6.7B). In *S. pneumoniae* infected $Ncdn^{fl/fl}$ and $LysM^{Cre}$ control mice, neutrophil numbers in the BAL were 7.58×10^3 - 6.89×10^3, respectively, and 1.42×10^6 - 7.65×10^5 in the lung. This neutrophil recruitment into the BAL was a little lower than expected from the pilot experiments, whereas neutrophil numbers in the perfused lung were as expected. Nevertheless, $Ncdn^{-/-}$ infected mice had 7.14×10^3 neutrophil in their BAL

and 5.25 x 10^5 in their lungs under these conditions, and therefore showed no detectable difference in neutrophil recruitment compared to the control strains (Figure 6.7B). This means that, also at this time point, neutrophil numbers in the airways or lung tissue were normal and could not account for the increased antibacterial immunity of Norbin-deficient mice.

Similarly, the numbers of monocytes/macrophages in mock-treated and *S. pneumoniae* infected $Ncdn^{fl/fl}$ and $LysM^{Cre}$ control mice was also as expected, both in the BAL fluid and in the lung homogenate, and again no effect of Norbin-deficiency was seen on these monocyte/macrophage numbers (Figure 6.7C).

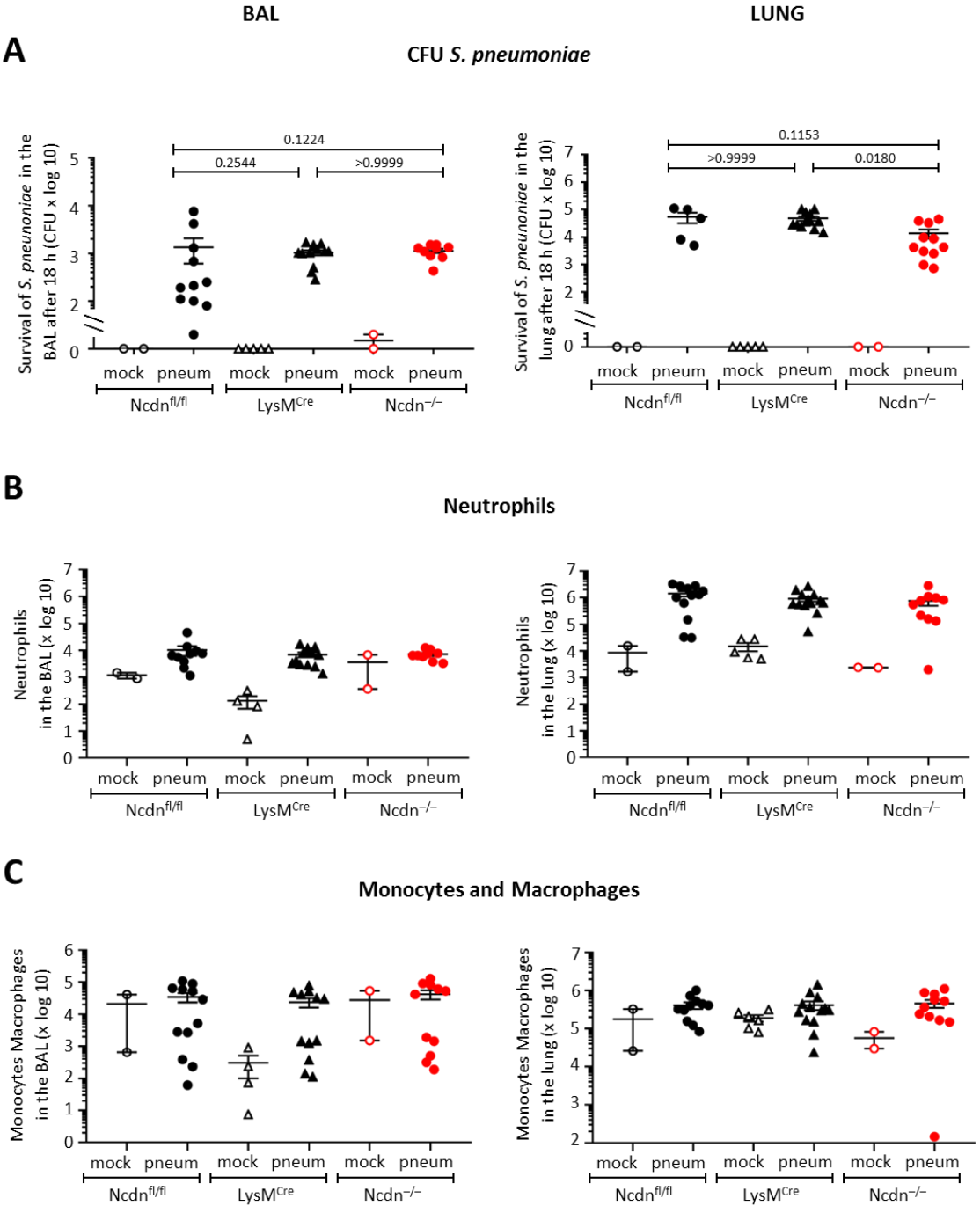

Figure 6.7: Norbin deficiency maintained the immunity of mice to pulmonary S. pneumoniae infection at a later time point

Mice of the indicated genotypes were given an intranasal administration of 2 x 10^6 CFU *S. pneumoniae* in 50 µL sterile HBSS or were mock-treated with the same volume of buffer. Mice were culled by CO_2 asphyxiation at 18 h after the infection and (A) serial dilutions of BAL (left hand panel) and perfused lung homogenate (right hand panel) were analysed for bacterial survival as CFU on blood agar plates. In parallel the (B) number of neutrophils (Ly6G^{hi}, Cd11b^{hi} cells) and (C) number of monocytes and macrophages (Cd11b^{+}, Cd11c^{+}, Ly6C^{+} cells) from BAL (left hand panel) and perfused lung homogenate (right hand panel) were assessed by flow cytometry. Each dot represents one mouse. Data are mean ± SEM of 2-4 mock-treated mice and 7-12 *S. pneumoniae*-infected mice per genotype, pooled from 4 independent experiments. Statistical significance was assessed using Kruskal-Wallis analysis with Dunn's multiple comparisons test.

6.5 Norbin-deficiency provides antibacterial immunity during pulmonary infection with *S. pneumoniae* even in immun-deficient ($Prex^{-/-}$) mice

In order to investigate the effects of Prex-deficiency and combined Norbin/Prex deficiency on antibacterial immunity, the same study of *S. pneumoniae* infection was carried out at the 6 h and 18 h time point in $Prex^{+/+}$, $Prex^{-/-}$ and $Ncdn^{-/-}$ $Prex^{-/-}$ mice. The panel of data from $Prex^{+/+}$, $Prex^{-/-}$ and $Ncdn^{-/-}$ $Prex^{-/-}$ mice treated with *S. pneumoniae* for 6 h are shown in Figure 6.8. As both time points show similar trends, in the next paragraph only the 18h time point is decribed in detail.

In mock-treated animals from all strains, no bacterial CFU were recovered from the BAL (Figure 6.9A left-hand panel) and only very few from the lung (Figure 6.9A, right-hand panel), as expected. In $Prex^{+/+}$ control mice infected with 2 x 10^6 *S. pneumoniae*, the CFU of surviving bacteria in the BAL after 18 h were 2.66 x 10^3, similar to what was seen with the other ($Ncdn^{fl/fl}$ and $LysM^{Cre}$) control strains (Figure 6.7). In contrast, $Prex^{-/-}$ mice still had 6.28 x 10^4 bacterial CFU in their BAL under the same conditions, 24-fold more than the $Prex^{+/+}$ controls, meaning that $Prex^{-/-}$ mice are immune-deficient, which was not unexpected but had never been shown before (Figure 6.9A, left-hand panel). Importantly, in contrast to $Prex^{-/-}$ mice, $Ncdn^{-/-}$ $Prex^{-/-}$ double-deficient mice only had 3.53 x 10^3 CFU in their BAL, 18-fold fewer than the immune-deficient $Prex^{-/-}$ mice and the almost same as the $Prex^{+/+}$ control mice. Therefore, the deletion of Norbin in $Ncdn^{-/-}$ $Prex^{-/-}$ mice was sufficient to overcome the immuno-deficiency caused by the absence of Prex, effectively restoring immunity. A similar trend, but lacking statistical significance because of larger variability between $Prex^{-/-}$ mice, was observed also in the perfused lung homogenate at 18 h (Figure 6.9A, right-hand panel).

Moreover, no detectable differences were seen either in neutrophil recruitment (Figure 6.9B) or in the numbers of monocytes/macrophages (Figure 6.9C) in the BAL and the perfused lung homogenate between $Prex^{+/+}$ and $Prex^{-/-}$. This demonstrates that P-Rex1 is not required for neutrophil recruitment into the infected lung, unlike in aseptic peritonitis. This was perhaps unsurprising, as different GEFs are required for recruitment to different organs, and our laboratory has shown previously that P-Rex1 and Vav family Rac-GEFs cooperate in neutrophil recruitment to the inflamed lung (Pan et al., 2015). However, in the

BAL, Ncdn$^{-/-}$ Prex$^{-/-}$ mice had a small, but significant decrease in the number of neutrophils compared to the Prex$^{+/+}$ and Prex$^{-/-}$ mice (Figure 6.9B).

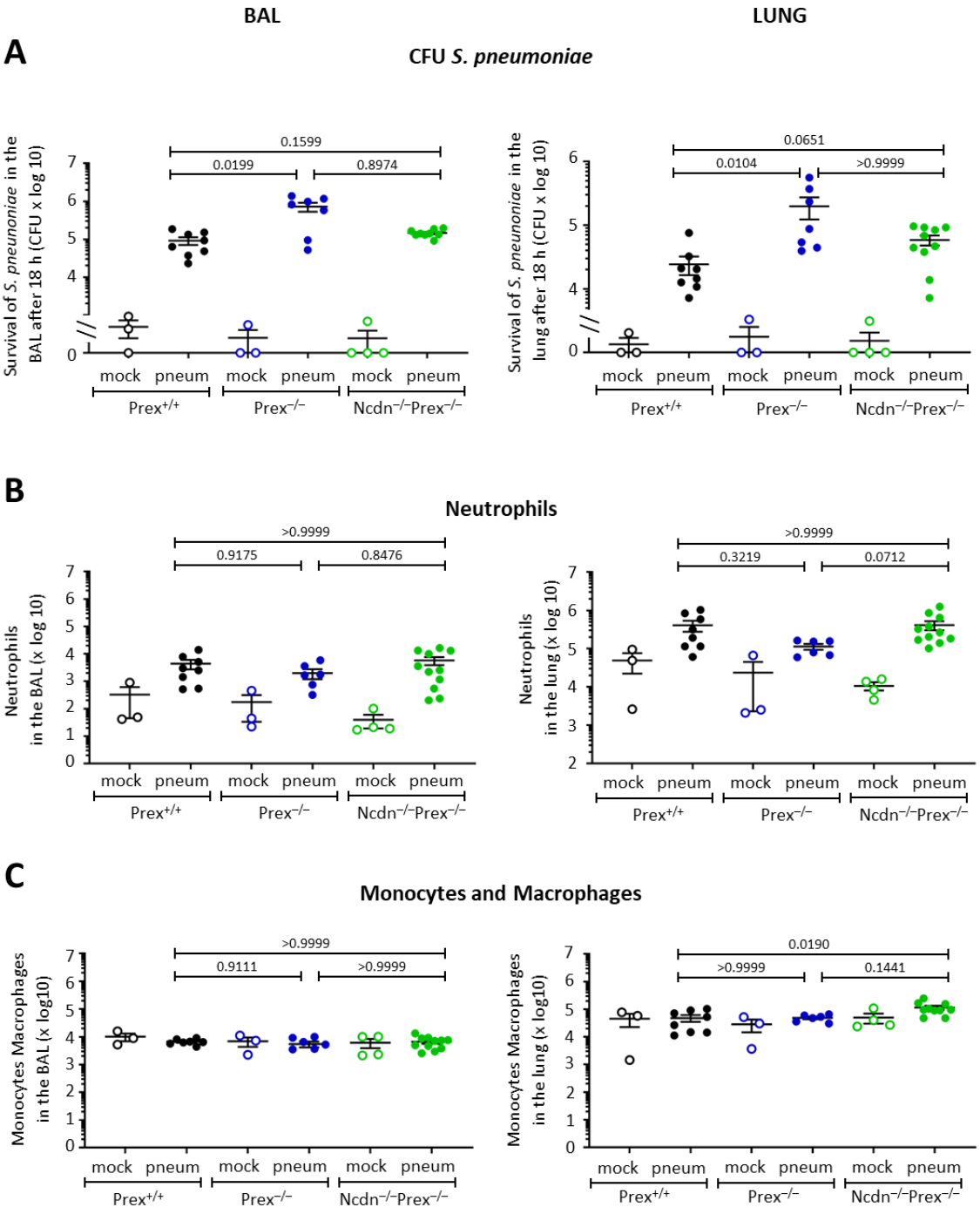

Figure 6.8: Norbin-deficiency provides antibacterial immunity during pulmonary infection with *S. pneumoniae*, even in immune-deficient (Prex$^{-/-}$) mice at 6 h after infection.

Mice of the indicated genotypes were given an intranasal administration of 2 x 10^6 CFU *S. pneumoniae* in 50 µL sterile HBSS or were mock-treated with the same volume of buffer. Mice were culled by CO_2 asphyxiation at 6 h after the infection and (A) serial dilutions of BAL (left hand panel) and perfused lung homogenate (right hand panel) were analysed for bacterial survival as CFU on blood agar plates. In parallel the (B) number of neutrophils (Ly6G^{hi}, Cd11b^{hi} cells) and (C) number of monocytes and macrophages (Cd11b^{+}, Cd11c^{+}, Ly6C^{+} cells) from BAL (left hand panel) and perfused lung homogenate (right hand panel) were assessed by flow cytometry. Each dot represents one mouse. Data are mean ± SEM of 3-4 mock-treated mice and 12-18 *S. pneumoniae*-infected mice per genotype, pooled from 5 independent experiments. Statistical significance was assessed using Kruskal-Wallis analysis with Dunn's multiple comparisons test.

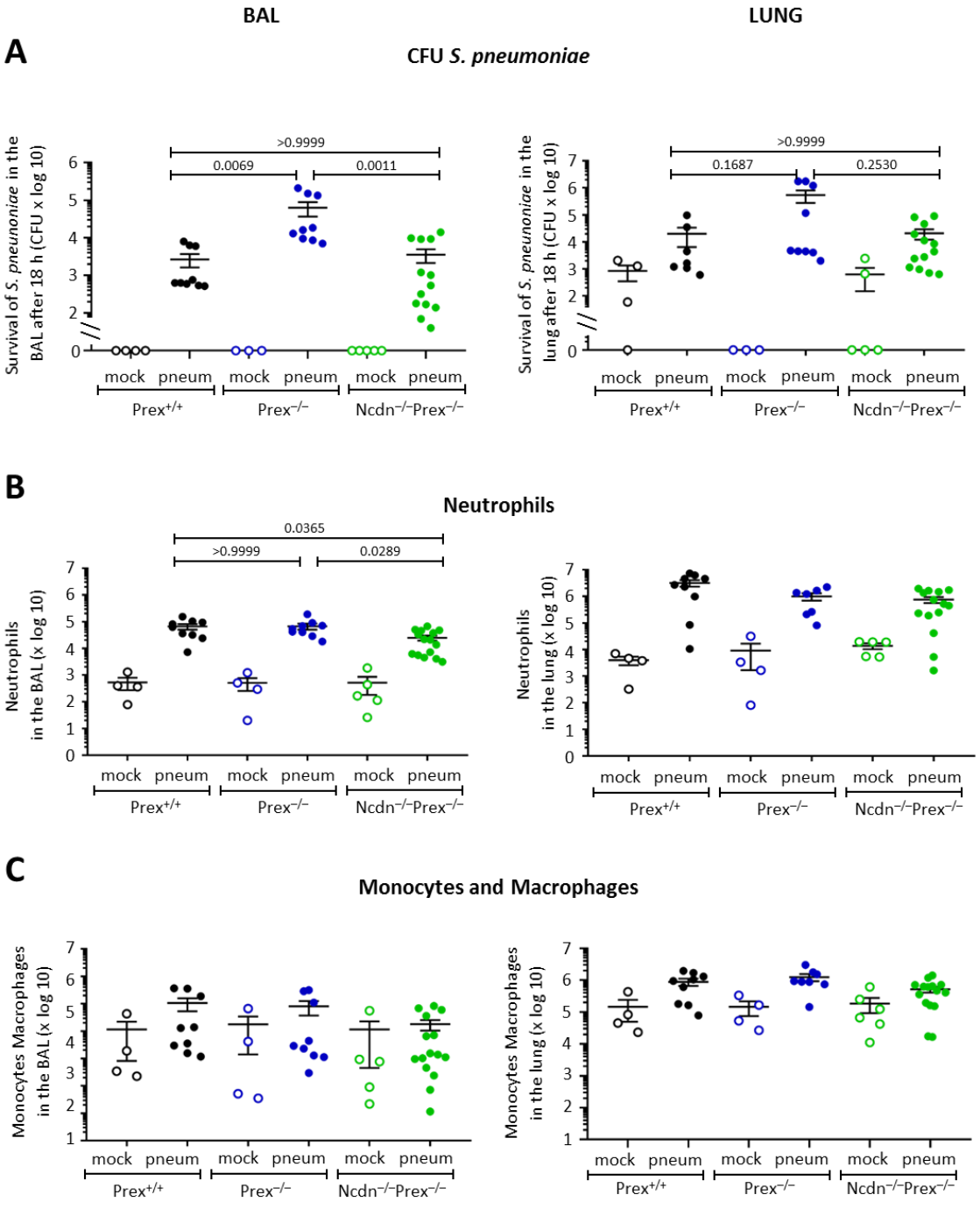

Figure 6.9: Norbin-deficiency provides antibacterial immunity during pulmonary infection with *S. pneumoniae*, even in immune-deficient (Prex$^{-/-}$) mice at 18h

Mice of the indicated genotypes were given an intranasal administration of 2 x 10^6 CFU *S. pneumoniae* in 50 µL sterile HBSS or were mock-treated with the same volume of buffer. Mice were culled by CO_2 asphyxiation at 18 h after the infection and (A) serial dilutions of BAL (left hand panel) and perfused lung homogenate (right hand panel) were analysed for bacterial survival as CFU on blood agar plates. In parallel the (B) number of neutrophils (Ly6G^{hi}, Cd11b^{hi} cells) and (C) number of monocytes and macrophages (Cd11b^{+}, Cd11c^{+}, Ly6C^{+} cells) from BAL (left hand panel) and perfused lung homogenate (right hand panel) were assessed by flow cytometry. Each dot represents one mouse. Data are mean ± SEM of 3-4 mock-treated mice and 12-18 *S. pneumoniae*-infected mice per genotype, pooled from 5 independent experiments. Statistical significance was assessed using Kruskal-Wallis analysis with Dunn's multiple comparisons test.

In conclusion, expression of Norbin in myeloid cells suppresses the antibacterial immune function of these mice *in vivo*. Deletion of Norbin relieves this suppression, thus increasing the capacity of myeloid cells to kill bacteria, without affecting the recruitment of these myeloid cells to the site of infection. Finally, deletion of myeloid Norbin is sufficient to overcome the immune-deficiency caused by Prex-deficiency.

6.6 The increased immunity to *S. pneumoniae* infection in myeloid Norbin deficiency derives from neutrophils

The fact that neutrophil recruitment was normal during pulmonary infections despite the increased clearance of bacteria in Norbin-deficient mice (Figure 6.4) suggested two possibilities: (i) that the bactericidal capacity of neutrophils is increased, which my experiments in Chapter 4 have shown to be the case, or (ii) that this immune protection might be derived from other cell types. The latter possibility was pertinent in light of the controversy in the literature as to the importance of neutrophils in this infection, as detailed in the introduction to this chapter. Indeed, macrophage depletion assays have shown that resident alveolar macrophages are required for the resolution of *S. pneumoniae* infections and the importance of neutrophils was shown to depend on the titre of the inoculum and on the age of the animal (Dockrell et al., 2003; Herbold et al., 2010). To evaluate whether the increased immunity of Norbin-deficient mice stems from neutrophils, I therefore performed antibody-mediated neutrophil depletion prior to infecting the mice with *S. pneumoniae*.

To deplete neutrophils, $Ncdn^{-/-}$ and $Ncdn^{fl/fl}$ mice were given i.p. monoclonal anti-Ly6G antibody 1A8 (25 $mg.kg^{-1}$) (Bruhn, Dekitani, Nielsen, Pantapalangkoor, & Spellberg, 2016), whereas control animals received the equivalent amount of isotype control antibody at -24 h and 0 h prior to infection with 2 x 10^6 CFU of *S. pneumoniae*. The 1A8 clone is selective for the Ly6G epitope and does not deplete Ly6C+ inflammatory monocytes, unlike the Gr1 monoclonal antibody that had been widely used for neutrophil depletion in earlier studies (Daley et al., 2008).

To confirm neutrophil depletion, 50 μL tail blood samples were taken from $Ncdn^{fl/fl}$ and $Ncdn^{-/-}$ mice before dosing with isotype control IgG or 1A8 antibody, at time 0 h, 24 h

after the first administration of the antibodies. Isotype control IgG-treated $Ncdn^{fl/fl}$ and $Ncdn^{-/-}$ mice had 4.82 x 10^3 and 3.65 x 10^3 neutrophils in 50 μL of peripheral blood, respectively (Figure 6.10A), very close to the expected 10^6 neutropils.mL^{-1}. In contrast, $Ncdn^{fl/fl}$ and $Ncdn^{-/-}$ mice treated with 1A8 monoclonal antibody only had 1.50 x 10^3 and 0.63 x 10^3 neutrophils, respectively, in 50 μL peripheral blood, a decrease of 70% and 83%, respectively. Hence, 1A8 monoclonal antibody-treated animals from both strains showed a significant depletion of neutrophils from their systemic circulation after only a single dose of antibody treatment (Figure 6.10A).

After establishing that neutrophil depletion was efficient, I proceeded to infect $Ncdn^{fl/fl}$ and $Ncdn^{-/-}$ mice treated with either isotype control or 1A8 antibody at time 24 h and 0 h with 50 μL of 2 x 10^6 *S. pneumoniae*, or mice were mock infected with buffer only. After 6 h, the mice were culled, bronchioles lavaged, and the survival of bacteria in the BAL assessed as CFU on blood agar, as well as leukocyte numbers by flow cytometry.

As expected, mock- infected animals from both the $Ncdn^{fl/fl}$ and $Ncdn^{-/-}$ strains had very few neutrophils in their BAL, regardless of whether they had been injected with isotype control or 1A8 antibody. Isotype control IgG-treated $Ncdn^{fl/fl}$ and $Ncdn^{-/-}$ mice had 8.8 x 10^1 and 2.5 x 10^2 neutrophils in the BAL and 1A8 monoclonal Ly6G-treated animals 2.4 x 10^2 and 6.2 x 10^1 neutrophils, respectively (Figure 6.10B). In addition, isotype control IgG-treated and *S. pneumoniae*-infected $Ncdn^{fl/fl}$ and $Ncdn^{-/-}$ mice showed the marked recruitment of neutrophils into the airspace that was expected for this 6 h time point (Figure 6.10B), with no difference between the genotypes (5.48 x 10^3 and 3.78 x 10^3 neutrophils, respectively). In contrast, 1A8 antibody-treated and *S. pneumoniae*-infected $Ncdn^{fl/fl}$ and $Ncdn^{-/-}$ mice, recruited far fewer neutrophils into the BAL, again with no difference between the genotypes, (6.34 x 10^2 and 4.55 x 10^2 neutrophils, respectively) (Figure 6.10B). This is a level of depletion of neutrophils in the BAL of *S. pneumoniae*-infected mice equivalent to 89% in $Ncdn^{fl/fl}$ mice and 88% in $Ncdn^{-/-}$ mice compared to the isotype-treated control mice.

In contrast to this efficient depletion of neutrophils, the number of monocytes/macrophages recovered in the BAL remained unaltered by either the isotype control or 1A8 antibody treatment, both in mock-infected and *S. pneumoniae*-infected $Ncdn^{fl/fl}$ and $Ncdn^{-/-}$ mice (Figure 6.10C).

Under these conditions, which efficiently depleted neutrophils without altering monocyte/macrophage numbers, I then proceeded to analyse whether neutrophil depletion affects the increased antibacterial immunity observed in $Ncdn^{-/-}$ mice. First, no bacterial CFU were found in the BAL of mock-infected animals from the $Ncdn^{fl/fl}$ and $Ncdn^{-/-}$ mice strains after 6 h, regardless of whether they mice had received isotype control IgG or 1A8 antibody, as expected (Figure 6.10D). In contrast, isotype control IgG-treated $Ncdn^{fl/fl}$ animals infected with 2 x 10^6 *S. pneumoniae* had a substantial number of bacteria left in the BAL after 6 h (1.02 x 10^4) (Figure 6.10D), although somewhat less than expected from previous experiments without any antibody pre-treatment. Importantly, isotype control IgG-treated $Ncdn^{-/-}$ mice infected with *S. pneumoniae* had far fewer bacteria (1.5 x 10^3) left in the BAL under the same conditions (Figure 6.10D). Hence, as expected from experiments performed without prior isotype control antibody treatment, 7-fold more bacteria were killed in $Ncdn^{-/-}$ mice compared to $Ncdn^{fl/fl}$ mice (p=0.0074), confirming again that Norbin deficiency substantially increases antibacterial immunity. Interestingly, 1A8 antibody-treated $Ncdn^{fl/fl}$ animals infected with *S. pneumoniae* had 6.73 x 10^3 bacteria left in their BAL, only insignificantly (34%, p=0.9992) fewer than their isotype control-treated counterparts, and significantly (4.5 times) more than in isotype control-treated $Ncdn^{-/-}$ mice (p=0.0089) (Figure 6.10D). Thus, my data suggest that in otherwise healthy adult control mice, neutrophils are not essential for the early clearance of *S. pneumoniae* bacteria, at least not at the titre and timing used here. This is in agreement with some of the literature which claims that alveolar macrophages play a more central role than neutrophils in clearing this type of bacteria under similar conditions.

However, very surprising results were obtained in the 1A8 antibody-treated $Ncdn^{-/-}$ mice infected with *S. pneumoniae*, which had 7.81 x 10^3 CFU left in their BAL, similar to the 1A8-antibody treated $Ncdn^{fl/fl}$ mice (6.73 x 10^3) meaning that neutrophil depletion had removed any advantage that Norbin-deficient mice had in killing bacteria, compared to $Ncdn^{fl/fl}$ control mice. Neutrophil depletion made their immunity 5 times worse than that of their isotype control-treated counterparts (p=0.0076) and indistinguishable from that of *S. pneumoniae*–infected $Ncdn^{fl/fl}$ mice (p=0.9995) (Figure 6.10D).

Therefore, unlike in control mice, neutrophils were important for the clearance of *S. pneumoniae* in $Ncdn^{-/-}$ mice. The results show that Norbin-deficiency has afforded a more

important role to neutrophils in clearing of *S. pneumoniae* infection than these cells have under normal circumstances. Considering that neutrophil recruitment is unaffected in Ncdn$^{-/-}$ mice, this suggests that the increased antibacterial responses of Ncdn$^{-/-}$ neutrophils that I demonstrated in Chapter 4 are the root cause of the increased importance of neutrophils in clearing this type of infection.

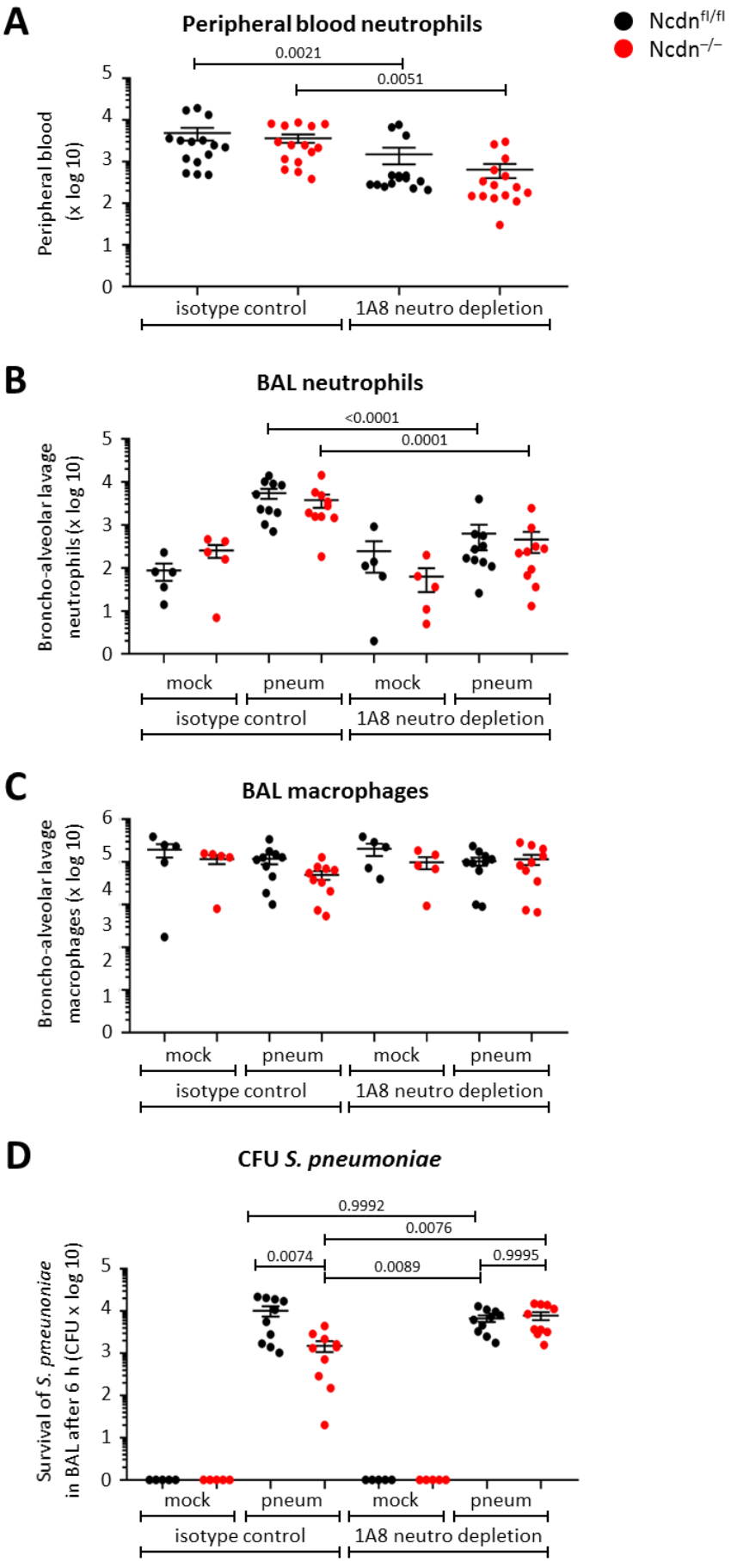
A
Peripheral blood neutrophils
Ncdn^fl/fl
Ncdn^−/−
0.0021
0.0051
Peripheral blood (x log 10)
isotype control
1A8 neutro depletion
B
BAL neutrophils
<0.0001
0.0001
Broncho-alveolar lavage neutrophils (x log 10)
mock
pneum
mock
pneum
isotype control
1A8 neutro depletion
C
BAL macrophages
Broncho-alveolar lavage macrophages (x log 10)
mock
pneum
mock
pneum
isotype control
1A8 neutro depletion
D
CFU S. pneumoniae
0.9992
0.0076
0.0074
0.0089
0.9995
Survival of S. pneumoniae in BAL after 6 h (CFU x log 10)
mock
pneum
mock
pneum
isotype control
1A8 neutro depletion

Figure 6.10: The increased immunity to *S. pneumoniae* infection in myeloid Norbin deficiency derives from neutrophils

(A) Effect of 1A8 monoclonal Ly6G antibody treatment on blood neutrophil counts from $Ncdn^{-/-}$ and $Ncdn^{fl/fl}$ mice. Mice were administered either with isotype control IgG or 1A8 monoclonal Ly6G antibody at 24 h and 0 h, and tail blood samples were taken at 0 h before intranasal administration of DPBS or 2 x 10^6 *S. pneumoniae*. Blood neutrophil counts were quantified by labelling cells for CD24 and CD11b and analysis by flow cytometry. (B-C) Mice treated either with isotype control IgG or 1A8 monoclonal Ly6G antibody were given an intranasal administration of 2 x 10^6 CFU *S. pneumoniae* in 50 µL sterile HBSS, or mock-treated with buffer as a control. Mice were culled and BAL performed 6 h after the infection. (B) Total number of neutrophils recruited to the lung was identified by staining of CD24 and Mac-1. (C) Total number of macrophages recruited to the lung was identified by staining of Mac-1. (D) BAL were subjected to bacterial counts, by plating serial dilutions on blood agar plates. The bacterial load was determined from blood agar plates with 20-200 colonies per plate. Each dot represents one mouse. Data are mean ± SEM of 5 mock-infected mice and 10 *S. pneumoniae*-infected mice per genotype, up to 3 mice per genotype per day pooled from 5 independent experiments. Statistical significance was assessed using two-way Anova with Tukey's multiple comparisons test.

Chapter 7 – Discussion

The main findings of my PhD are that the GPCR adaptor and P-Rex1 interacting protein Norbin has important functional roles in neutrophils and in neutrophil-mediated antibacterial immunity. In essence, myeloid Norbin is an immune-suppressor. Norbin deficiency makes neutrophils more important for the clearance of pneumococcal infection in the lung by increasing their capacity for killing bacteria. Briefly isolated Norbin-deficient neutrophils showed increased adhesion and spreading, as well as increased ROS production, constitutive degranulation and an increased capacity to kill *S. aureus* in a ROS dependent manner. Norbin deficiency raised the cell surface levels of some GPCRs as well as increasing GPCR-dependent Ras/Erk and Rac signalling. Norbin deficiency provided immunity against pulmonary infection with *S. pneumoniae* in a neutrophil-dependent manner and was sufficient to restore the impairment in immunity caused by Prex-deficiency, without affecting neutrophil recruitment. Only some of these functions of myeloid Norbin required P-Rex1 (Figure 7.1).

History and rationale of this study

My study built on previous work in our lab, which had identified Norbin as a direct binding partner and regulator of the Rac-GEF P-Rex1 (Pan et al., 2016). The main conclusion from this initial study was that Norbin is a major regulator of P-Rex1 plasma membrane localisation, bringing P-Rex1 into close contact with its substrate Rac and its activators PIP_3 and G$\beta\gamma$, and thereby increasing signalling through the P-Rex1/Rac pathway to induce changes in cell morphology. Furthermore, the study also showed that Norbin is expressed not just in neurons, as was previously thought, but also in myeloid cells (neutrophils and macrophages) (Pan et al., 2016). This previous study had largely been done using recombinant proteins and overexpression in cell lines. The aim of my project was to assess the role of Norbin, and the interdependency of Norbin and P-Rex1, in a physiologically relevant biological system, and as P-Rex1 is a well-known regulator of neutrophil responses, we decided to study this in primary mouse neutrophils. My objectives were to assess the signalling pathways, antimicrobial responses and tissue recruitment of Norbin and Norbin/Prex1-deficient neutrophils, through an integrated *in vitro* and *in vivo* analysis.

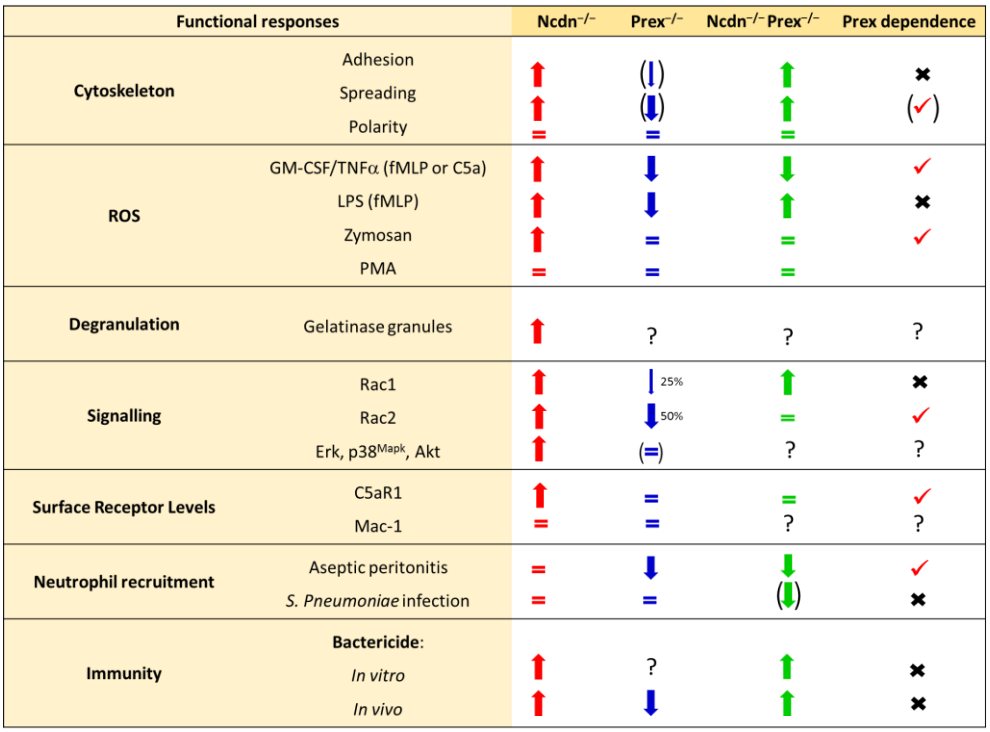

Figure 7.1: Summary of Norbin and Prex functions in neutrophil
Up and down direction of arrows denote increased and decreased responses, respectively.
Thickness of arrows denote the magnitude of responses
= symbol denotes normal response compared to controls.
Symbol in brackets denote effect under specific experimental conditions.
? symbol denotes experiments to be done.
Rac, Erk, $p38^{Mapk}$ and Akt activity data and Mac-1 surface levels for Prex1-deficient mice were taken from (Welch et al., 2005) and (Lawson et al., 2011).

Dr Dingxin Pan, the former PhD student in the laboratory who conducted the original Norbin study, also generated the $Ncdn^{-/-}$ mouse strain with Norbin deletion in the myeloid linage and the $Ncdn^{-/-}$ $Prex^{-/-}$ strain with combined Norbin and Prex deficiency, prior to leaving the laboratory. She also showed that Norbin expression was successfully deleted in the $Ncdn^{-/-}$ mice, in their resident peritoneal macrophages and in neutrophils recruited to the peritoneum during LPS-induced peritonitis. I began my study by confirming that Norbin was also efficiently deleted from isolated mature bone-marrow derived $Ncdn^{-/-}$ neutrophils, and I used a combination of cell counting, flow cytometry and cytospin analysis to show that neutrophil development was normal in $Ncdn^{-/-}$ and $Ncdn^{-/-}$ $Prex^{-/-}$ mice.

The antibacterial and antifungal innate immune functions of neutrophils require signalling through the small GTPase Rac and the Rac-GEFs that activate Rac. These proteins

control neutrophil adhesion and migration, as well as neutrophil effector responses essential for immunity, such as the production of reactive oxygen species (ROS) and the release of proteases by degranulation (Pantarelli & Welch, 2018). P-Rex1, which was discovered in our lab (Welch et al., 2002) is one such Rac-GEF that regulates actin polymerisation, adhesion, migration speed and ROS production in neutrophils, as well as neutrophil recruitment to sites of inflammation (Pantarelli & Welch, 2018; Welch et al., 2005). From our initial study on the Norbin/Prex1 interaction (Pan et al., 2016), we expected that - if Norbin had any discernible role in mouse neutrophils at all – it was likely to act largely through Prex1, and that Norbin-deficiency would exacerbate the impairment in neutrophil responses that the lab had previously described for Prex1-deficient mice (Welch, 2015). Hence, I began by characterising neutrophil responses that are known to require Prex1.

Role of Norbin in neutrophil adhesion, spreading and polarity

First, I assessed the ability of Norbin-, Prex1- and Norbin/Prex1-deficient bone marrow-derived isolated neutrophils to adhere, spread and polarise on glass, using immunofluorescence microscopy. These experiments revealed that the deletion of Norbin promotes neutrophil adhesion and spreading, both in unprimed and TNFα/GM-CSF-primed cells, and both with and without stimulation with fMLP, without affecting neutrophil polarity. This was in contrast to Prex1 deficiency, which caused a trend to reduced neutrophil adhesion in basal cells, as expected from previous work (Lawson et al., 2011), and significantly reduced neutrophil spreading under several conditions.

The increased adhesion and spreading in Norbin-deficient neutrophils was my first completely unexpected finding, as it suggested that Norbin may have a largely opposite role to Prex in neutrophils, instead of promoting Prex function, as was expected (Pan et al., 2016). Interestingly, Prex was not required for the increased adhesion caused by Norbin deficiency, as Norbin/Prex-double deficient cells also adhered more, but the Rac-GEF was required for the Norbin-deficiency dependent increase in neutrophil spreading. The reason for this discrepancy in Prex dependency is unclear, but it likely derives from the different roles of Rac1 and Rac2 in neutrophil adhesion and spreading. For example, Rac2 deficiency reduces whereas Rac1-deficiency increases the spreading of neutrophil-like cells derived from haematopoietic stem cells (Gu et al., 2003). Prex1 has a substrate preference for Rac2

over Rac1 in neutrophils (Welch et al., 2005), so perhaps the loss of Prex1-dependent Rac2 activity limits the spreading of Norbin/Prex-deficient cells. Along the same lines, Rac1 was shown to be more important for neutrophil adhesion than Rac2, although both GTPases contribute (Gu et al., 2003), and it is perhaps for this reason that Prex expression was less important for Norbin deficiency-induced neutrophil adhesion. Overall, it seems that Norbin, when expressed, limits neutrophil adhesion and spreading, likely by suppressing Rac1 and Rac2 activity, rather than being primarily a regulator of Prex1 that promotes Rac activity.

It would be interesting to investigate the effects of Norbin and Norbin/Prex1 on neutrophil adhesion and spreading further under shear-flow conditions, as previous work had shown that Prex1 plays a much more important role in neutrophil adhesion under flow conditions that mimic the shear stress in postcapillary venules, by controlling the affinity state of the neutrophil β2-integrins LFA-1 and Mac-1 (J. M. Herter et al., 2013). To pursue the relevance to integrins, a summer student in the laboratory whom I co-supervised, Anna Mandel, performed adhesion assays with Norbin and Norbin/Prex-deficient neutrophils on various surfaces, and found a larger increase in the adhesion of Norbin/Prex-deficient cells plated on the integrin ligands poly-RGD and ICAM-1, compared to cells on glass. This suggested that Norbin deficiency might increase the activity of β2-integrins on the neutrophil surface. Indeed, she conducted further experiments using blocking antibodies against CD11a (LFA-1), CD11b (Mac-1) and CD54 (ICAM-1) which abrogated the increased adhesion of Norbin/Prex1-deficient neutrophils, showing that it was indeed dependent on these integrins. Detailed titration curves of such blocking antibodies should enable us to reveal if the Norbin/Prex1-deficient cells are more sensitive to integrin inhibition than control neutrophils.

Finally, neutrophil polarisation, just like adhesion and spreading, is also a Rac-dependent response (Pantarelli & Welch, 2018), but unlike these processes it remained unaffected both by the Prex deficiency (as expected) and by the Norbin deficiency. This suggests that Norbin does not govern indiscriminately all Rac-dependent responses in neutrophils.

Role of Norbin in ROS production

Next, I tested ROS production, starting with GPCR-dependent ROS in primed cells, using stimulation of either the C5a receptor or the fMLP receptor. Even more clearly than in adhesion and spreading, Norbin and Prex showed opposite effects on the ROS response, with Norbin-deficiency increasing and Prex-deficiency decreasing it, both upon stimulation with fMLP or with C5a, and regardless of the priming pathway used. These results showed that Prex is required for GPCR-dependent ROS production whereas Norbin expression limits it. Interestingly, when both Prex and Norbin were knocked-out, GPCR-dependent ROS production was reduced in neutrophils primed through the TNFα/GM-CSF cytokine pathways, to the same level as in Prex-deficient cells, whereas it was elevated in cells primed through the LPS pathway, to the level seen in Norbin-deficient cells. Hence, Norbin deficiency-induced LPS-primed ROS production is independent of Prex, whereas Norbin deficiency-induced TNFα/GM-CSF-primed ROS production requires Prex. Therefore, among the signalling pathways upstream of ROS production that are limited by Norbin expression, some require Prex and some do not.

Previous work showed that priming of the ROS response through both the TNFα/GM-CSF cytokine pathways and the LPS/TLR4 pathway involves Prex1, but the requirement for Prex1 was much more pronounced in the LPS/TLR4 pathway (Damoulakis et al., 2014; Lawson et al., 2011; Welch et al., 2005). Therefore, the lack of effect of Prex-deficiency in LPS-primed Ncdn$^{-/-}$ Prex$^{-/-}$ cells compared to Ncdn$^{-/-}$ cells was surprising and suggested that another GEF or regulator of Rac might compensate for the loss of Prex1 in this response. Different types of Rac-GEFs in neutrophils couple to different upstream regulators, and thus contribute to distinct downstream responses. For example, Vav1 and P-Rex1 can both signal downstream of the fMLP receptor, but they are regulated in different ways. P-Rex1 is mainly activated by PIP_3 and G$\beta\gamma$, whereas Vav1 is mainly activated by tyrosine phosphorylation. We imagine that, within the same receptor pathway, there is redundancy to make sure there is always sufficient Rac activity available in the cells. A previous study from our lab showed that Prex1 and Vav1 can cooperate in the LPS priming of ROS production (Lawson et al., 2011). I have therefore begun to investigate the possibility of Vav1 being regulated by Norbin (see discussion on Rac activity below).

In addition to soluble agonists, I also tested ROS production in response to bacteria (ongoing) and to fungal particles (zymosan). As with the soluble stimuli, I observed that ROS production was significantly increased in Ncdn$^{-/-}$ neutrophils upon stimulation with zymosan. Furthermore, this Norbin deficiency-induced ROS production was also again dependent on Prex1, as it was abrogated in Ncdn$^{-/-}$ Prex$^{-/-}$ cells, to the level seen in Prex$^{-/-}$ neutrophils. My preliminary experiments with *S. aureus* bacteria show the same pattern. Bacteria and fungi activate a wide range of receptors, including pattern recognition receptors and receptors that recognise opsonisation, such as FcRs and integrins. This suggests that Norbin-deficiency might not only affect GPCR-coupled neutrophil signalling pathways, but also signalling through other types of receptors, although it may be difficult to evaluate the extent to which bacteria and zymosan stimulate ROS production via GPCRs. Most inhibitors of GPCR signalling only affect one or a subset of GPCRs. However, a small molecule, BIM-46187, has been described as a pan-GPCR inhibitor that prevents the interaction of GPCRs with all classes of heterotrimeric G protein (Ayoub et al., 2009), although it does seem to affect Gα_q preferentially (Schmitz et al., 2014). Use of this compound in adhesion assays and in particle-stimulated ROS assays might help evaluate to what extent Norbin regulates these responses through GPCR signalling.

One possible explanation for why more ROS was produced in Ncdn$^{-/-}$ neutrophils than in control cells could have been that the NADPH oxidase complex which produces ROS is hyperactive. However, firstly there was no constitutive ROS production in Norbin-deficient cells in the absence of a stimulus, precluding the possibility that the NADPH oxidase is constitutively active. Secondly, to test if there might simply be more NADPH oxidase complex in Ncdn$^{-/-}$ neutrophils, I treated the cells with PMA, an artificial activator of PKC that stimulates the oxidase complex in a receptor-independent way. These data showed normal ROS production in neutrophils from all strains, meaning that there is a normal amount of NADPH oxidase complex in Ncdn$^{-/-}$ neutrophils. Therefore, Norbin deficiency affects the upstream signalling pathways of ROS formation rather than the integrity, amount or constitutive activity of the NADPH oxidase complex itself.

Role of Norbin in bacterial killing by isolated neutrophils

The elevated ROS production in Norbin-deficient neutrophils suggested that these cells may have an increased capacity for killing pathogens. I tested this by incubating purified neutrophils with serum-opsonised *S. aureus* bacteria and by counting of the bacterial CFU that survived after 15 min. Indeed, more *S. aureus* were killed by Norbin-deficient neutrophils compared to control neutrophils. These experiments defined Norbin as a suppressor of neutrophil-mediated bacterial killing *in vitro*. Furthermore, Prex was not required for Norbin deficiency-induced bacterial killing, because when both Norbin and Prex were deleted, the same number of bacteria were killed as with Norbin-deficiency alone.

Neutrophils use ROS production to kill bacteria, as exemplified by the inability of neutrophils from chronic granulomatous disease (CGD) patients who have inactivating mutations in one of the catalytic NADPH oxidase subunits to kill bacteria, which leads to recurrent infections (Roos, 2016). Therefore, I investigated next whether the increased bacterial killing by $Ncdn^{-/-}$ neutrophils was due to their increased ROS production. Using a titration curve of DPI, an inhibitor of ROS production, in the bacterial killing assay, I saw that the increased killing of *S. aureus* in Norbin-deficient neutrophils was indeed ROS-dependent, because at DPI concentrations of 1 μM or higher, these cells had no more advantage over $Ncdn^{fl/fl}$ control cells in killing *S. aureus*.

In this study, I only explored the ability of Norbin-deficient neutrophils to kill *S. aureus*, a gram-positive aerobic organism, *in vitro*. It would be interesting to also assess the ability of $Ncdn^{-/-}$ neutrophils to kill other types of gram-positive bacteria (e.g. *S. pneumoniae*) and gram-negative bacteria (e.g. *E. coli*), as well as fungal pathogens such as *Candida albicans* and *Aspergillus fumigatus*. Gram-positive bacteria have a relatively porous cell wall, whereas gram-negative bacteria have two lipid bilayers and middle layer of peptidoglycan which provides a permeability barrier, and yeast have an even more impermeable cell wall (Vatansever et al., 2013). Hence, it is conceivable that the increased ROS production in $Ncdn^{-/-}$ neutrophils only protects from a subset of bacterial and fungal pathogens. For example, *in vivo* studies have shown that neutrophils kill *S. pneumoniae* in as ROS-independent (but degranulation-dependent) manner (see discussion of *in vivo* results below).

It would also be interesting to test the intra- vs extra-cellular killing of bacteria by performing the killing assay at longer time-points that allow phagocytosis of the bacteria and then comparing the level of bacterial killing the presence and absence of antibiotics such as gentamycin that cannot penetrate into the neutrophil. Neutrophils produce ROS both intra- and extracellularly, and ROS assays can distinguish between these. For example, HRP can be omitted from our assay in order to measure only intracellular ROS produced by the NADPH oxidase and endogenous myeloperoxidase. Furthermore, ROS is required for the production of NETs, which is an important mechanism for killing extracedllular bacteria, and we could evaluate NET formation as is briefly described below.

Role of Norbin in degranulation

In addition to ROS production, neutrophils kill pathogens via degranulation. For example, patients with CGD usually only suffer from infections with certain types of bacteria and fungi, because the lytic enzymes contained in granules are still able to kill many pathogens. In support of this notion, mice deficient in the neutrophil granule serine proteases elastase and/or cathepsin G have a reduced ability to clear fungal infections (Tkalcevic et al., 2000). Thus, I tested the mobilisation of neutrophil gelatinase granules through degranulation, by measuring the activity of gelatinase released into the extracellular milieu.

I observed that Norbin-deficiency causes some degree of constitutive degranulation of gelatinase granules in cells that are incubated at 37°C under condition that allow constitutive receptor trafficking. In contrast, stimulation of the cells with fMLP and cytochalasin B and/or priming of the cells with TNFα/GM-CSF induced similar levels of gelatinase activity release in $Ncdn^{-/-}$ and $Ncdn^{fl/fl}$ control cells, which showed that $Ncdn^{-/-}$ neutrophils did not simply contain more gelatinase. This constitutive degranulation may explain the increased ability of Norbin-deficient neutrophils to adhere and produce ROS, as many receptors that mediate these responses are stored on the surface of neutrophil granules and become upregulated on the neutrophil surface upon fusion of the granule membrane with the plasma membrane (see discussion on GPCR surface levels below).

Neutrophil adhesion and ROS production, the other responses that were increased in Norbin-deficient cells, are absolutely dependent on Rac, whereas the role of Rac in neutrophil degranulation is thought to be restricted to only one subset of granules. Rac2 was

reported to be critical for azurophil (primary) granule exocytosis, but dispensable for the degranulation of lactoferrin-containing (secondary and gelatinase) granules (Abdel-Latif et al., 2004). This has always been puzzling, as the degranulation of all granule types requires re-arrangements of the actin cytoskeleton. In view of that report, it therefore seemed likely that the increased gelatinase secretion in Ncdn$^{-/-}$ neutrophils might be a Rac-independent response. To test this directly, Dr Kirsti Hornigold in the laboratory tested the secretion of gelatinase activity by isolated neutrophils from control and Rac2-deficient mice, using the same conditions I used in my assays with Norbin-deficient cells, and she obtained clear proof that Rac2 is indeed required for the degranulation of gelatinase granules (unpublished data). We believe that, as azurophil granules are the population which is hardest to mobilise, perhaps Abdul-Latif et al used conditions which were too blunt to reveal a role for Rac in the degranulation of other granule types. It would be interesting to repeat our experiments with Ncdn$^{-/-}$ neutrophil degranulation also for secondary and azurophil granules. In summary, however, all neutrophil responses tested so far were affected by Norbin and were also Rac-dependent neutrophil responses. In addition to the neutrophil responses that I have tested to date in Ncdn$^{-/-}$ and Ncdn$^{-/-}$ Prex$^{-/-}$ neutrophils, there are other important effector responses that I have not tested, due to time-constraints, including cytokine production, migration/chemotaxis, NET formation and apoptosis. I have started optimising a phagocytosis assay either with adhering cells or cells in suspension, however further optimisation work needs to be done before any conclusions can be drawn.

Role of Norbin in neutrophil GPCR signalling

To link the increased adhesion, spreading, ROS production, degranulation and bacterial killing in Norbin-deficient neutrophils to possible underlying molecular mechanisms, I evaluated the effects of Norbin deficiency on neutrophil signalling and cell surface receptors. First, I tested Rac activity, as P-Rex1 activates Rac, Norbin regulates P-Rex1, and so far all Norbin-mediated neutrophil responses are also Rac-dependent.

Our previous studies showed that Prex1-deficient isolated neutrophils have a defect in fMLP-stimulated Rac activation, mostly affecting the Rac-homologues Rac2 and RhoG, but also Rac1 (Damoulakis et al., 2014; Lawson et al., 2011; Welch et al., 2005). Surprisingly, Norbin again showed the opposite effect to Prex1: there was more fMLP-stimulated Rac1

and Rac2 activity in Ncdn$^{-/-}$ neutrophils compared to control cells at all concentrations of fMLP tested. In contrast, basal Rac1 and Rac2 activities, in the absence of fMLP stimulation, were nearly undetectable in cells from both strains. In addition, I saw a similarly significant increase in Rac1 activity, but not in Rac2 activity, when both Norbin and Prex were deleted, which means that Prex is not required for the increase in Rac1 activity caused by Norbin deficiency. In contrast, GPCR-mediated activation of Rac2 was low in Ncdn$^{-/-}$ Prex$^{-/-}$ cells, meaning that Rac2 activity was dependent on Prex even when Norbin was deleted (although there appeared to be a non-significant tendency for increased Rac2 activity also in Ncdn$^{-/-}$ Prex$^{-/-}$ cells). These results are in accordance with the literature showing that Prex1 has a substrate preference for Rac2 over Rac1 (Welch et al., 2005).

In summary, Norbin expression limits GPCR-stimulated Rac1 and Rac2 activity in neutrophils, and the deletion of Norbin is sufficient to relieve this suppression. Furthermore, Norbin-deficiency does not overcome the requirement for Prex1 in activating Rac2 upon GPCR stimulation. It is worth discussing that basal Rac activity in Norbin deficient cells was normal. Therefore, Norbin expression only limited Rac activity upon GPCR stimulation but did not lead to constitutive Rac activity, meaning that Norbin-deficiency poises the system to receptor activation but does not cause intrinsically active neutrophils (see also the section on cell surface receptors below).

The Rac activity experiments up to now were done in unprimed cells that were prewarmed to 37°C for 3 min prior to the addition of fMLP, conditions where GPCR levels on the cell surface are likely to be limiting. Thus, it would also be interesting to study the effects of Norbin deficiency on Rac activity in the context of various priming pathways and in response to other agonists that stimulate Rac activity. In addition, it would be interesting to test the effects of Norbin-deficiency on the activity of the more distantly related Rac-family member RhoG, which is also a substrate of Prex1.

The laboratory has previously shown that Norbin does not affect Rac activity directly, neither *in vitro* nor when overexpressed in HEK293 cells in the absence of P-Rex1 (Pan et al., 2016). Therefore, as Norbin-deficiency affects Rac1 activity in Ncdn$^{-/-}$ Prex$^{-/-}$ neutrophils, other Rac-GEFs or regulators of Rac, in addition to Prex1, must couple to Norbin in these cells, and Norbin must limit their ability to activate Rac. This led me to speculate that one of

the GEFs which compensates for the loss of Prex in Norbin/Prex-deficient neutrophils might be Vav1. Vav1-deficient neutrophils have a similar phenotype to Prex1-deficient neutrophils regarding GPCR-dependent responses, but unlike Prex1, Vav-GEFs have a substrate preference for Rac1 over Rac2 (Lawson, Donald, Anderson, Patton, & Welch, 2011). In contrast, Dock-deficient neutrophils have impaired ROS production even upon stimulation with PMA, which is not the case in $Ncdn^{-/-}$ and $Ncdn^{-/-}$ $Prex^{-/-}$ neutrophils. Furthermore, ongoing work in our lab showed that Tiam1-deficient neutrophils have defects only when cells are adherent, which is again not the case here. Hence, Vav1 seemed the most likely candidate, and I therefore conducted preliminary experiments using western blots to test for the activating phosphorylation of Vav1 on Tyr173, which indicated that fMLP-stimulated Vav1 activity is indeed elevated in $Ncdn^{-/-}$ neutrophils compared to $Ncdn^{fl/fl}$ neutrophils. Further experiments are currently ongoing, but if these results can be confirmed, they imply that Norbin limits neutrophil Rac1 activity by blocking Vav1.

In addition to Rac, I also tested other GPCR signalling pathways in $Ncdn^{-/-}$ and $Ncdn^{fl/fl}$ neutrophils, namely the activation of Erk, $p38^{Mapk}$, Jnk and Akt in response to fMLP stimulation. All of these pathways were maximally activated after stimulation with 1 μM fMLP for 45 seconds. Importantly, I observed that Erk activity was significantly increased in Norbin-deficient neutrophils under these conditions compared to $Ncdn^{fl/fl}$ control cells, whereas the other pathways seemed unaffected under all conditions tested. Therefore, there is a degree of pathway specificity in Norbin-dependent regulation of GPCR signalling in neutrophils, some pathways being blocked by Norbin expression (Rac and Erk) and some not (Akt, $p38^{Mapk}$ and Jnk), at least under the conditions tested. It was surprising which pathways were affected by the Norbin deficiency and which were not, because $p38^{Mapk}$ and Jnk are downstream targets of Rac, and therefore one could have expected for these pathways to be increased in a similar manner to Rac activity. However, I measured Rac activity under somewhat different conditions, so this remains to be investigated further. The fact that Norbin deficiency increased Erk activity, and considering that Erk is activated by MEK downstream of Ras, suggests that Norbin might regulate Ras as well as Rac. I have started testing this possibility by performing Raf-RBD pull down assays for Ras activity. However, preliminary analysis would suggest that Norbin may not regulate Ras, which would imply that other signalling pathways upstream of Erk may be involved.

Increased GPCR-dependent activation of Erk had been described previously upon co-expression of Norbin in HEK293 cells together with mGluR5 (H. Wang et al., 2009), but not upon co-expression with histamine-receptor 1 or melanin-concentrating hormone receptor 1 (Ward et al., 2009), although all of these GPCRs interact with Norbin; therefore the reason why Erk signalling is regulated by Norbin downstream of one, but not the other receptors is unknown. Also, the mechanism of Norbin-dependent regulation of Erk activity has never been elucidated. In contrast to the study by Wang et al, who saw increased Erk signalling upon overexpression of Norbin, I saw increased Erk activity upon deletion of Norbin. Therefore, the signalling pathways from Norbin to Erk seem to depend on the GPCR and the cell line, and remain to be elucidated. As indicated above, I am planning to test the effects of Norbin-deficiency on Ras, which is an upstream key regulator of Erk. In addition to the pathways I have already tested, one could also test Ca^{2+} signalling, as Norbin is known to regulate GPCR-dependent intracellular Ca^{2+} transients upon overexpression in HEK293 cells (Francke et al., 2006; H. Wang et al., 2009; Ward et al., 2009). One could load Norbin-deficient and control neutrophils with Fluo-4 prior to stimulation with fMLP to monitor Ca^{2+} fluxes by imaging, and use titration curves of the Ca^{2+} inhibitor BAPTA-AM to determine differences in sensitivity between genotypes.

In would be interesting to investigate whether the elevated GPCR-stimulated Rac and Erk activities in Norbin-deficient neutrophils are required for the increased cell responses of Norbin-deficient cells. One could use titration curves with Rac inhibitors such as NSC23766 and EHT1864, and with Erk inhibitors such as SCH772984 and BVD-523, during fMLP-stimulated ROS assays in Norbin-deficient and control neutrophils. ROS assays would provide a sufficiently sensitive read-out for this purpose. Rac inhibitors have limited specificity but should be adequate for reporting differences in sensitivity between the genotypes.

Role of Norbin in neutrophil GPCR trafficking

The literature has shown that Norbin can regulate the steady-state surface levels of GPCRs. For example, co-expression of metabotropic glutamine receptor-5 (mGluR5) with Norbin in neuronal N2a cells led to constitutively increased levels of the receptor on the neuronal surface, whereas downregulation of Norbin in primary cortical neurons reduced mGluR5 levels on the cell surface. The same paper also showed less mGluR5 on the cell surface in

primary cortical neurons of mice with conditional deletion of Norbin in the forebrain (H. Wang et al., 2009). Similarly, co-expression of Norbin with melanin-concentrating hormone receptor-1 (MCHR1) in HEK293 cells was shown to inhibit $G\alpha_{i/o}$ and $G\alpha_q$ dependent Ca^{2+} signalling, but increased the steady-state cell surface levels of the receptor, without affecting the MCH stimulation-dependent internalisation of the receptor (Francke et al., 2006), although a more recent paper by the same laboratory reported normal levels of the MCHR1 in HEK293 with inducible overexpression of Norbin (Ward et al., 2009). The mechanisms through which Norbin regulates this steady-state surface expression of GPCRs has not yet been elucidated.

In addition, as described above, I saw constitutive degranulation in Norbin-deficient neutrophils. This is relevant because several types of neutrophil GPCRs, including the fMLP receptor FPR1 and the C5a receptor C5aR1, are stored on the membrane of granules and upregulated onto the neutrophil surface when granules fuse with the plasma membrane (Monari et al., 2002; Rorvig et al., 2013; Sengelov, 1995). In view of this literature, combined with the increased GPCR signalling that I found in Norbin-deficient neutrophils, I decided to investigate the levels of GPCRs on the neutrophil surface under several different conditions. I compared cells that were either kept ice-cold throughout to prevent receptor trafficking, or were mock-primed or primed at 37°C, conditions which allow degranulation as well as normal receptor trafficking by endo- and exocytosis to occur.

Indeed, I found an increase of the GPCR C5R1 at the cell surface in the $Ncdn^{-/-}$ cells that had been mock-primed or primed with TNFα and GM-CSF, but not in cells that were kept on ice. These results showed that, under conditions where receptor trafficking can occur, Norbin expression limits the cell surface levels of this GPCR. This increased surface level of C5aR1 could explain, in part, why GPCR signalling was increased in Norbin-deficient cells. In contrast to this Norbin-dependent steady-state transport of the C5aR1 to/from the plasma membrane, the agonist-induced internalisation of the receptor in response to neutrophil stimulation with C5a was unaffected by the Norbin deficiency. It is also interesting that priming of neutrophils with TNFα and GM-CSF increased the level of C5aR1 both in $Ncdn^{-/-}$ and $Ncdn^{fl/fl}$ cells further, so that primed $Ncdn^{-/-}$ neutrophils had the highest surface levels of C5aR1. This result suggests that the constitutive degranulation of gelatinase

granules observed in Ncdn$^{-/-}$ neutrophils cannot be the only mechanism underlying the increased GPCR level on the neutrophil surface, because priming overcame the Norbin deficiency-dependent increase in degranulation. Therefore, it seems likely that, once GPCRs are delivered onto the neutrophil surface, Norbin expression promotes their re-internalisation, and that this step is blocked by the Norbin deficiency.

Relevant to my findings, Dr Martin Baker, a former PhD student in the laboratory, demonstrated that Prex1 also controls GPCR trafficking (Martin Baker, PhD Thesis University of Cambridge, 2015, unpublished data). He showed that Prex1 deficiency reduces the level of C5aR1 on the surface of neutrophils, but only upon stimulation with C5a. Inversely, he showed that overexpression of Prex1 in HEK293 cells blocks the internalisation of the GPCR S1PR1 upon stimulation with the agonist S1P, by regulating the agonist-stimulated phosphorylation of the GPCR. Therefore, although it might appear that Prex1 and Norbin have opposing roles in GPCR trafficking, this is not actually the case, because Norbin controls constitutive GPCR trafficking whereas Prex1 regulates the agonist-induced internalisation of GPCRs. Interestingly, however, I found that the upregulation of C5aR1 in mock-primed Norbin-deficient neutrophils was Prex1 dependent, because cell surface levels of the receptor were normal in Ncdn$^{-/-}$ Prex$^{-/-}$ cells. We showed previously that P-Rex1 is dispensable for the secretion of azurophil granules (Welch et al., 2005). However, it is unknown if P-Rex1 is involved the degranulation of gelatinase and/or specific granules. If so, then Norbin/ Prex deficiency would reduce both the delivery of GPCRs to the neutrophil surface by degranulation (Norbin- and Prex-dependent) and the constitutive re-internalisation of GPCRs (Norbin-dependent). Degranulation assays with Prex-deficient, and Norbin/Prex-deficient cells could test this hypothesis.

According to the literature, primary sequence cannot predict which GPCRs Norbin can bind and which not. Therefore, to further investigate which types of neutrophil receptors are controlled by Norbin, we used a candidate approach, looking at CXCR1, CXCR2 and CXCR4 surface levels, as these are important neutrophil GPCRs, in addition to C5aR1, and as antibodies are available that are able to detect these endogenous GPCRs by flow cytometry.

In these experiments, I found an increase of CXCR4 on the cell surface in Ncdn$^{-/-}$ cells that had been kept either basal (on ice) or primed with TNFα and GM-CSF. Hence, as previously seen with C5aR1, Norbin-deficiency led to increased levels of this GPCR on the neutrophil surface. Nevertheless, unlike with C5aR1, the upregulation of CXCR4 occurred even under conditions that minimised receptor trafficking, which suggested that either CXCR4 is stored on a more readily mobilised type of vesicles than C5aR1, or the total cellular levels of CXCR4 might be elevated in Ncdn$^{-/-}$ cells. I am planning to verify the latter hypothesis by blotting total lysates from Ncdn$^{-/-}$ neutrophils with CXCR4 antibody.

Unlike either C5aR1 or CXCR4, the surface levels of CXCR1 and CXCR2 were unaffected by the Norbin deficiency. This was perhaps unsurprising, because these two GPCRs are known not to be stored on granules, but to be constitutively localised on the plasma membrane (Murphy, 1997). In consequence, CXCR1 was not upregulated during neutrophil priming, and CXCR2 surface levels in fact dropped dramatically in response to priming, as expected, because this receptor is shed by proteolysis under inflammatory conditions (Asagoe, Yamamoto, Takahashi, Suzuki, et al., 1998). Furthermore, these particular GPCRs may also not be affected by the Noribin deficiency because Norbin cannot physically interact with them. This remains to be investigated.

Finally, in order to assess whether the role of Norbin in receptor trafficking is restricted to GPCRs or also seen with other classes of receptors, I tested Mac-1 levels on the neutrophil surface. Both in basal Ncdn$^{-/-}$ cells (on ice) and in cells primed with TNFα and GM-CSF, Mac-1 surface levels were normal. These data are complemented by further data from Dr Pan, who observed that Norbin-deficient neutrophils had normal surface levels of several other types of receptors and adhesion molecules, including L-selectin, PSGL-1, and the β2-integrin LFA-1, both in the basal and primed state. The finding that Mac-1 levels, in particular, were normal was surprising, considering that Mac-1 is stored on overlapping granule subtypes to C5aR1. This suggests again that the delivery of GPCRs to the neutrophil surface by degranulation is only one of the roles of Norbin in trafficking. The other is to specifically regulate the re-internalisation of GPCRs that it can directly interact with, and this step would not apply to integrins. The finding that both LFA-1 and Mac-1 surface levels were normal was also surprising considering the increase of neutrophil adhesion observed in

Norbin-deficient cells *in vitro*. However, this does not exclude the possibility that Norbin deficiency might increase the activity of β2-integrins on the neutrophil surface, as discussed above in the section on blocking antibodies. Overall, based on these results on neutrophil receptor levels, we can conclude that the effects of Norbin deficiency on receptor trafficking

Surface Receptor Levels	Conditions	Ncdn$^{-/-}$
C5aR1	Basal Mock-Primed Primed Ligand-stimulated	= ↑ ↑ =
CXCR4	Basal Primed	↑ ↑
CXCR1	Basal Primed	= =
CXCR2	Basal Primed	= =
Adhesion Molecules (L-selectin, PSGL-1, LFA-1, Mac-1)	Basal Primed	= =

Figure 7.2: Summary of surface receptor levels in Ncdn$^{-/-}$ deficient neutrophils

show some degree of specificity for certain types of GPCRs (Figure 7.2).

It seems likely that other neutrophil GPCRs could be affected by Norbin, in addition to the ones I already investigated. To test this, one could identify other GPCRs controlled by Norbin in an unbiased manner using biotinylation of neutrophil surface proteins, isolation of these biotinylated proteins from lysates of Norbin-deficient and control neutrophils using streptavidin, and identification by mass spectrometry. The literature shows that Norbin only affects the trafficking of those GPCRs that it can bind to directly, suggesting a direct mechanism (Francke et al., 2006; H. Wang et al., 2009). Moreover, from the literature and my data combined, it appears that Norbin can both up- or downregulate the cell surface levels of GPCRs. Therefore, to assess how Norbin controls GPCR levels on the neutrophil surface (delivery, retention or internalisation), one could biotinylate proteins on the surface of Norbin-deficient and control neutrophils using pulse-chase labelling, combined with cell fractionation (Clemmensen, Udby, & Borregaard, 2014) into plasma membrane, endosome and granule fractions, and analysis of the fractions by western blotting and mass spectrometry.

Role of Norbin in neutrophil recruitment

As discussed so far, I discovered that Norbin-deficiency increases antibacterial responses of isolated neutrophils, and that its effects on neutrophil responses might be explained by altered GPCR surface levels and by increased Rac/Erk pathway activities. To explore the functional role of myeloid Norbin and the Norbin/P-Rex1 interaction *in vivo*, I studied the recruitment of leukocytes to sites of inflammation, and I tested antibacterial immunity. For this aim, I used two different inflammation animal models, thioglycollate (TGC)-induced sterile peritonitis and *S. pneumoniae*-induced pulmonary infection.

I compared in parallel, mock-treated and TGC-treated mice from different mouse strains and analysed all experiments both by cytospin microscopy and by flow cytometry. Taken together, both methods revealed a neutrophil recruitment defect during aseptic peritonitis when Prex1 was deleted, as expected (Welch et al., 2005). In contrast, Norbin deficiency seemed to increase neutrophil recruitment slightly, but this reached statistical significance only compared to the $Ncdn^{fl/fl}$ control strain but not the $LysM^{Cre}$ control strain. As there was a slight but not significant difference in neutrophil recruitment between the two different control strains, and as neutrophil numbers in the $LysM^{Cre}$ strain were similar to that of $Ncdn^{-/-}$ mice, we concluded that myeloid Norbin deficiency overall did not alter neutrophil recruitment. Interestingly, $Ncdn^{-/-}$ $Prex^{-/-}$ mice had as little neutrophil recruitment as $Prex^{-/-}$ mice, and less than $Ncdn^{-/-}$ mice, which implied that Prex1 is required for neutrophil recruitment *in vivo* regardless of whether Norbin is expressed or not.

TGC-induced peritonitis is a model of sterile inflammation. As there was no effect of Norbin deficiency on neutrophil recruitment in this model, it is difficult to speculate whether Norbin has a role in sterile inflammatory conditions. One could test the levels of inflammatory cytokines in this model to investigate further, or test Norbin-deficient mice in other models of sterile inflammation. If the presence of Norbin suppresses these types of inflammation as it suppresses anti-bacterial immunity, one would assume that inflammation is increased when Norbin is deleted, potentially causing auto-immunity like phenotypes.

The absence of any significant effect on neutrophil recruitment observed in Norbin deficient mice during sterile peritonitis is inconsistent with the constitutive increase in adhesion I observed in isolated Norbin-deficient neutrophils. As there were increased

surface level of GPCRs in Norbin-deficient neutrophils, we could have expected more integrin to be activated by GPCR signalling, with consequently increased neutrophil adhesion and more neutrophils adhering to the blood vessel wall and able to migrate to the site of inflammation. It is possible that more $Ncdn^{-/-}$ cells adhered on the vessel side, prior to transmigrating, or that they are adhered more firmly on the peritoneal wall and could therefore not be lavaged out. This could be addressed by histological analysis of the peritoneal wall vasculature. However, the data in the lung homogenate of *S. pneumoniae* infected mice (see below) would argue against that option, as they suggested normal neutrophil numbers in the whole perfused lung tissue.

Role of Norbin in *S. pneumoniae* infection

To investigate the capacity of Norbin-deficient mice to kill bacteria *in vivo*, and to further investigate neutrophil recruitment, I adapted a protocol of *S. pneumoniae*-induced acute lung inflammation from our Lymphocyte Signalling programme. My time course study revealed that neutrophils appeared in the lung as early at 3 h after inoculation with *S. pneumoniae*. The number of the neutrophils recruited in response to bacterial infection peaked at the 18 h time point and remained high at 24 h. In contrast to this acute neutrophil recruitment, the number of monocytes/macrophages in the BAL remained even throughout the time course. Moreover, as expected from other studies (Fillion et al., 2001), inflammatory monocytes and eosinophils remained essentially absent in the BAL over the duration of the experiment. However, increased numbers of monocytes/macrophages were seen in the lung homogenate of *S. pneumoniae* infected mice from 6 h after the infection onwards, and increased more at the end of the time course. Flow cytometric analysis identified these newly infiltrated cells as inflammatory monocytes. Regarding bacterial survival, colony forming units (CFUs) were still markedly elevated at the two earliest time point tested, 3 h and 6 h after inoculation, both in the BAL and lung homogenate whereas the bacterial titre in the BAL declined sharply at the 18 h time point and dropped even further at the final 24 h time point, almost back to control levels. In contrast, in the lung homogenate, bacterial numbers remained high at 18 h, before falling at the 24 h time point. Hence, bacteria were cleared from the airspace more rapidly than from the perfused lung tissue, presumably because they could survive in hard to reach niches within the lung tissue.

Compared to the titre of bacteria used for infection (2 x 10^6 CFU/mouse), even at the earliest time points tested (3 h and 6 h), less than 40% of bacterial CFU were recovered from the BAL. Therefore, either the lavages were inefficient, and only a subset of live bacteria were lavaged out of the airspace, or bacteria had already been killed at these early time points. The latter seems likely, considering that neutrophil recruitment was already significant after 3 h. To test the efficacy of lavages, one could infect the mice and then lavage them after a much shorter time, long enough for bacteria to disperse in the airspace but not to be killed. I chose 6 h and 18 h time point for subsequent experiments because this time window was the most interesting regarding the clearance of *S. pneumoniae* and the presence of leukocytes.

To our surprise, the results showed that Norbin deficiency improved immunity against pulmonary infection with *S. pneumoniae*. Indeed, at the 6 h time point, Norbin-deficient mice had a 12-16 fold increased capacity to kill bacteria compared to the two control strains, and at the 18 h time point, they still had a 3.5-4 fold increased capacity to kill bacteria in the perfused lung homogenate. Hence, Norbin-deficient mice were able to clear bacteria from the airspace faster than the two control strains, and this increased immunity of $Ncdn^{-/-}$ mice persisted at later time points. Therefore, $Ncdn^{-/-}$ mice were able to clear bacteria more efficiently than the two control strains both from the airspace and from perfused lung tissue.

Both At the 18 h time point, when most mouse strains were able to clear the infection from the airspace, $Prex^{-/-}$ mice still had a significant level of live bacteria in their BAL, a 24-fold increase compared to $Prex^{+/+}$ controls, showing that they were immune-deficient, which was not unexpected but had never been demonstrated before *in vivo*. Interestingly, $Ncdn^{-/-}$ $Prex^{-/-}$ mice had almost the same level of immunity as $Prex^{+/+}$ control mice, with 18-fold fewer live bacteria surviving in their BAL than in the immune-deficient $Prex^{-/-}$ mice, showing that that the additional deletion of Norbin could overcome this immune-deficiency.

In parallel, I was interested to understand whether Norbin deficiency protects from bacterial infection through increased neutrophil recruitment. Although neutrophil recruitment was normal in Norbin-deficient mice in the aseptic peritonitis, this had to also

be assessed in the pneumonia model, as neutrophil recruitment to different organs is controlled by different adhesion molecules and adhesion signalling pathways (Baker et al., 2016). However, $Ncdn^{-/-}$ infected mice showed no detectable difference in neutrophil recruitment upon infection with *S. pneumoniae* compared to $Ncdn^{fl/fl}$ and $LysM^{Cre}$ control mice. Therefore, just like in the aseptic peritonitis, Norbin was dispensable for neutrophil recruitment into the infected lung. Likewise, a lack of defect in neutrophil recruitment was seen also between $Prex^{+/+}$ and $Prex^{-/-}$ mice. This demonstrates that P-Rex1 is not required for neutrophil recruitment into the infected lung, unlike in aseptic peritonitis. This was perhaps unsurprising, as different GEFs are required for recruitment to different organs, and our laboratory has shown previously that P-Rex1 and Vav family Rac-GEFs cooperate in neutrophil recruitment to the inflamed lung (Pan et al., 2015). Interestingly, $Ncdn^{-/-}$ $Prex^{-/-}$ mice had a small, but significant decrease in the number of neutrophils in the BAL compared to the $Prex^{+/+}$ and $Prex^{-/-}$ mice, suggesting that combined Norbin/Prex-deficiency might cause a slight decrease in recruitment. However, the $Prex^{+/+}$ control strain showed slightly more recruitment than the $Ncdn^{fl/fl}$ and $LysM^{Cre}$ control strains in parallel experiments. Hence, this result should be interpreted with caution, and more experimental evidence would be required to investigate thie potential decrease in neutrophil recruitment of $Ncdn^{-/-}$ $Prex^{-/-}$ mice. Overall, therefore, neutrophil recruitment was normal in $Ncdn^{-/-}$ and $Ncdn^{-/-}$ $Prex^{-/-}$ mice, meaning that the improved immunity of these mice did not result from increased neutrophil recruitment. In addition, there was no effect of Norbin deficiency on the numbers of monocytes or resident macrophages in the infected lung under any of the conditions tested.

Taken together, the pulmonary *S. pneumoniae* infection model showed that Norbin deficiency increases the ability of mice to clear bacterial infection around 10-fold, without affecting the recruitment of neutrophils or monocytes, or the numbers of resident macrophages.

Role of Norbin in neutrophil-mediated bacterial killing *in vivo*

The fact that neutrophil recruitment was normal during pulmonary infection despite the increased clearance of bacteria in Norbin-deficient mice suggested that, either neutrophils killed bacteria more efficiently, or the immune-protective phenotype derived from other cell

types. As mentioned in the introduction to Chapter 6, the literature is controversial as to how important neutrophils are in this particular type of infection. Indeed, macrophage depletion assays have shown that resident alveolar macrophages are required for the resolution of *S. pneumoniae* infections (Dockrell et al., 2003; Herbold et al., 2010), and that the importance of neutrophils depends on the titre of the inoculum and on the age of the animal (Dockrell et al., 2003; Garvy & Harmsen, 1996). To evaluate whether the increased immunity of Norbin-deficient mice resulted from neutrophils, I performed antibody-mediated neutrophil depletion prior to infecting the mice with *S. pneumoniae*.

Acute treatment with 1A8-antibody was efficient in depleting neutrophils, achieving a level of depletion of around 85%, both in $Ncdn^{fl/fl}$ and $Ncdn^{-/-}$ mice, and both in the peripheral blood and in the BAL upon *S. pneumoniae* infection, without altering the numbers of alveolar macrophages. However, this level of neutrophil depletion did not affect the ability of $Ncdn^{fl/fl}$ control mice to kill bacteria during *S. pneumoniae* infection. This result confirmed the current consensus that neutrophils are not essential in this infection, at least in immune-competent adult mice, and that macrophages play a more central role in clearing *S. pneumoniae*. Surprisingly, however, when neutrophils were depleted in $Ncdn^{-/-}$ mice, these mice lost completely the 10-fold advantage they had in killing the pathogen compared to $Ncdn^{fl/fl}$ controls. Therefore, this result showed that neutrophils in $Ncdn^{-/-}$ mice have a more important role in clearing *S. pneumoniae* than they have under normal circumstances.

The increased immunity of Norbin and Norbin/Prex1-deficient mice, in the absence of increased neutrophil recruitment, together with the increased responses of isolated Norbin- and Norbin/Prex1-deficient neutrophils, suggest that the immune-protection is afforded by enhanced neutrophil function *in vivo*. To examine this, one could test ROS production, degranulation (elastase release), and NET formation in the lungs of Norbin-deficient and control mice infected with *S. pneumoniae*. It would be also interesting to measure the levels of inflammatory cytokines and chemokines (TNFα, IL6, KC) during *S. pneumoniae* infections in BAL and plasma by ELISA, to determine if myeloid Norbin deficiency increases these systemically, although this seems unlikely, as neutrophil recruitment into the lung was normal.

The literature shows that ROS production by the NADPH oxidase is not required for the killing of *S. pneumoniae in vivo*, and that killing is rather dependent on the secretion of the neutrophil serine proteases cathepsin G and elastase (Hahn et al., 2011; Standish & Weiser, 2009). For example, mice with a deletion of the catalytic gp91^{phox} subunit of the NADHP oxidase show no defect in the killing of *S. pneumoniae* (Marriott et al., 2008). In that study, the loss of ROS was shown to increase neutrophil recruitment, which was most likely a consequence of reduced neutrophil apoptosis, and therefore longer survival of neutrophils in the lung in the absence of ROS production. This resulted in increased cytokine production, MPO release and survival of the mice in pneumococcal pneumonia (Marriott et al., 2008). In order to test whether the increased ability of Norbin-deficient mice to kill *S. pneumoniae* derives from their increased ROS production, it may be possible to treat them with ROS inhibitors *in vivo*, or perhaps to cross them with gp91$^{phox-/-}$ mice. In any event, I did also observe constitutive degranulation of gelatinase granules in Norbin-deficient mice, and it is possible that other granules subtypes are also affected. Measurement of MPO and elastase release in addition to inhibition of ROS would address the relative importance of these two responses. In addition, it would be interesting to measure the occurrence of NETs and the level of neutrophil apoptosis in the infected lung of Norbin-deficient mice.

As Norbin is expressed in macrophages as well as neutrophils, and as it is also deleted by the LysM-directed Cre recombinase in our Ncdn$^{-/-}$ mice, it would also be interesting to investigate if macrophages and monocytes contribute to the increased resolution of *S. pneumoniae* infection in these mice, together with neutrophils. In order to address this, one could deplete macrophages using clodronate liposomes (Weisser, van Rooijen, & Sly, 2012), prior to *S. pneumoniae* infection, in a similar manner to the neutrophil depletion experiments I performed. If Norbin was also important in macrophages, one could also investigate its role in macrophages *in vitro*. Macrophage precursors can be isolated from mouse bone marrow, differentiated *in vitro*, and assayed for principal responses such as phagocytosis of apoptotic neutrophils, ROS production and bacterial killing.

Final conclusion and future directions

The results of my PhD project demonstrated for the first time that neutrophils from Norbin-deficient mice have increased adhesion, spreading, ROS production, degranulation and

bactericidal capacity *in vitro*, that Norbin-deficient mice have a 10-fold better antibacterial immunity against pneumococcal infection than control mice, and that this increased immunity derives from neutrophils. Hence, Norbin is an important regulator of neutrophil functions and acts as an immune suppressor. Furthermore, Norbin/Prex-deficient mice showed that only a subset of Norbin-dependent neutrophil responses require Prex1. Norbin is more important for neutrophil function than we had anticipated, and overall has a stronger impact than Prex. We hypothesise that Norbin regulates neutrophil responses by a combination of two major mechanisms, the control of GPCR trafficking and the control of GPCR signalling through Rac and Erk (Figure 7.3). These mechanisms will need to be explored by future work as outlined here above.

Seeing how important myeloid Norbin is for antibacterial innate immunity, it seems possible that deregulation of myeloid Norbin may play a causal role in human immune-deficiencies or inflammatory disease. It would be very interesting to investigate this possibility in the future, by assessing Norbin expression levels during inflammatory disease and infection both in mouse and human. Using mouse models of inflammation (for example aseptic peritonitis and *S. pneumoniae*-induced lung infection), one could isolate neutrophils and monocytes from the inflamed tissues and western blot lysates for Norbin levels. Similarly, Norbin levels could be investigated in sputum or blood samples of human patients with inflammatory or infectious diseases of the lung, such as ARDS and COPD. To further evaluate Norbin expression in human inflammatory and immune diseases, a bioinformatic analysis of disease databases could be performed. If such investigations find that Norbin is indeed deregulated in human inflammatory or immune-conditions, then the Norbin pathway could become interesting for pharmaceutical and biotechnology companies, who might benefit from our project in the future. By characterising a novel pathway that could be a therapeutic target in inflammatory and immune disorders, we would inform their strategies for developing anti-inflammatory drugs or drugs that improve the immune response. Moreover, the molecular mechanisms controlled by myeloid Norbin are unlikely to be disease-specific, so their exploitation could have wider applications. Finally, it seems unfeasible to inhibit Norbin directly, as it is an intracellular adaptor protein that works through protein/protein interaction. However, it seems feasible to exploit the effects of Norbin on cell surface GPCR levels. If specific GPCRs could be identified in diseases with

deregulation of Norbin, then drugs could be developed against these GPCRs. Half of the world's pharmaceuticals are directed against GPCRs, so this seems a worthwhile future avenue.

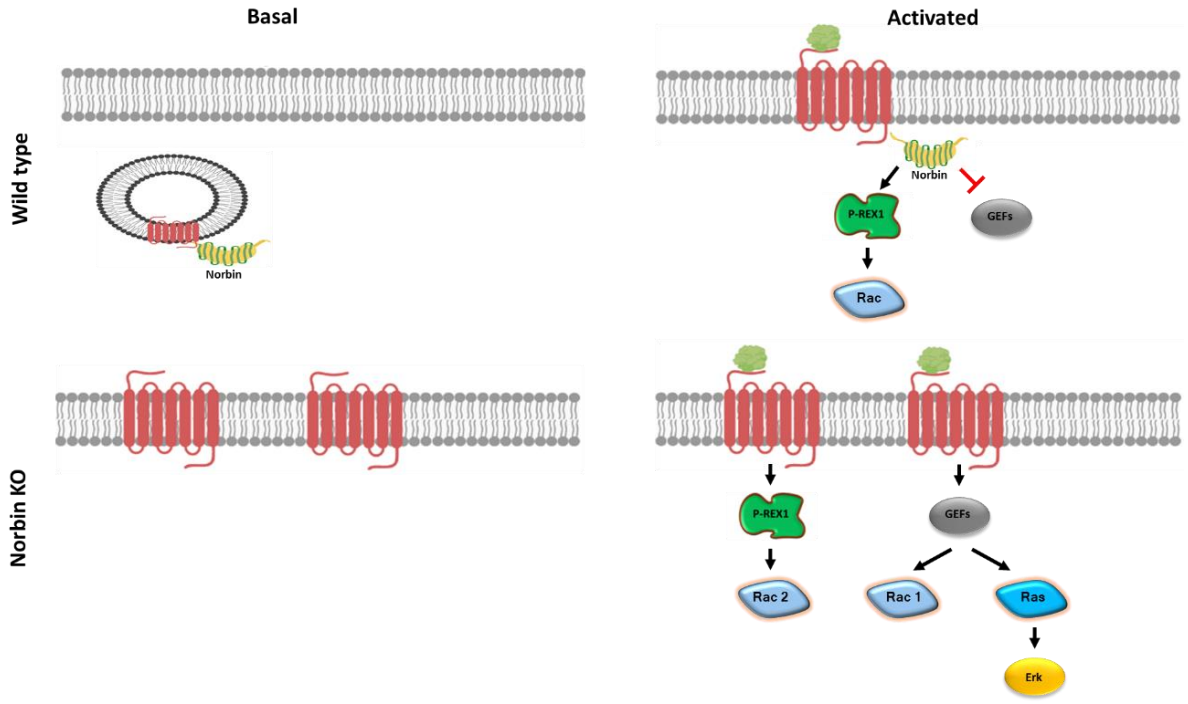

Figure 7.3: Working model
In control neutrophils, GPCRs are stored on the membrane of granules. Secretion of these granules upon neutrophil activation upregulates the GPCRs to the neutrophil plasma membrane. When GPCRs become activated, Norbin permits signalling through Prex1 to Rac2, but it blocks GPCR signalling through other GEFs. To which extent Norbin affects Prex1 activity or Prex1 localisation in neutrophils remains to be tested. Norbin-deficient neutrophils show constitutive degranulation and upregulation of GPCRs on the neutrophil surface. In addition, Norbin-deficiency likely results in GPCRs being selectively retained at the cell surface, as the surface levels of other receptor types (e.g. Mac-1) are normal. The increased GPCR surface levels allow for more GPCR signalling. In the absence of Norbin, Prex1 can still activate Rac2 in response to the stimulation of GPCRs, but the block on other GEFs is removed, so Rac1 is more active. Preliminary data suggest that one of the GEFs inhibited by Norbin is Vav1. Erk is also more active in Norbin-deficient cells, suggesting that the Norbin may regulate Ras-GEFs and Ras activity as well as the Rac pathway, which also remains to be explored.

Chapter 8 - Bibliography

Abdel-Latif, D., Steward, M., Macdonald, D. L., Francis, G. A., Dinauer, M. C., & Lacy, P. (2004). Rac2 is critical for neutrophil primary granule exocytosis. *Blood, 104*(3), 832-839.

Abram, C. L., & Lowell, C. A. (2009). The ins and outs of leukocyte integrin signaling. *Annual Review Immnulogy, 27*, 339-362.

Abtin, A., Jain, R., Mitchell, A. J., Roediger, B., Brzoska, A. J., Tikoo, S., . . . Weninger, W. (2014). Perivascular macrophages mediate neutrophil recruitment during bacterial skin infection. *Nature Immunology, 15*(1), 45-53.

Accetta, D., Syverson, G., Bonacci, B., Reddy, S., Bengtson, C., Surfus, J., . . . Verbsky, J. (2011). Human phagocyte defect caused by a Rac2 mutation detected by means of neonatal screening for T-cell lymphopenia. *Journal of Allergy and Clinical Immunology, 127*(2), 535-538.

Aghazadeh, B., Lowry, W. E., Huang, X. Y., & Rosen, M. K. (2000). Structural basis for relief of autoinhibition of the Dbl homology domain of proto-oncogene Vav by tyrosine phosphorylation. *Cell, 102*(5), 625-633.

Ahuja, S. K., Lee, J. C., & Murphy, P. M. (1996). CXC chemokines bind to unique sets of selectivity determinants that can function independently and are broadly distributed on multiple domains of human interleukin-8 receptor B - Determinants of high affinity binding and receptor activitation are distinct. *Journal of Biological Chemistry, 271*(1), 225-232.

Ambruso, D. R., Knall, C., Abell, A. N., Panepinto, J., Kurkchubasche, A., Thurman, G., . . . Roos, D. (2000). Human neutrophil immunodeficiency syndrome is associated with an inhibitory Rac2 mutation. *Proceedings of the National Academy of Sciences of the United States of America, 97*(9), 4654-4659.

Amulic, B., Cazalet, C., Hayes, G. L., Metzler, K. D., & Zychlinsky, A. (2012). Neutrophil function: from mechanisms to disease. *Annual Review Immnulogy, 30*, 459-489.

Anderson, K. E., Chessa, T. A. M., Davidson, K., Henderson, R. B., Walker, S., Tolmachova, T., . . . Hawkins, P. T. (2010). PtdIns3P and Rac direct the assembly of the NADPH oxidase on a novel, pre-phagosomal compartment during FcR-mediated phagocytosis in primary mouse neutrophils. *Blood, 116*(23), 4978-4989.

Anderson, L. R., Owens, T. W., & Naylor, M. J. (2014). Structural and mechanical functions of integrins. *Biophysical Reviews, 6*(2), 203-213.

Anton, P. A., Targan, S. R., & Shanahan, F. (1989). Increased Neutrophil Receptors for and Response to the Proinflammatory Bacterial Peptide Formyl-Methionyl-Leucyl-Phenylalanine in Crohns-Disease. *Gastroenterology, 97*(1), 20-28.

Asagoe, K., Yamamoto, K., Takahashi, A., Suzuka, K., Maeda, A., Nohgawa, M., . . . Sasada, M. (1998). Down-regulation of CXCR2 expression on human polymorphonuclear leukocytes by TNF-alpha. *Journal of Immunology, 160*(9), 4518-4525.

Asagoe, K., Yamamoto, K., Takahashi, A., Suzuki, K., Maeda, A., Nohgawa, M., . . . Sasada, M. (1998). Down-regulation of CXCR2 expression on human polymorphonuclear leukocytes by TNF-alpha. *The Journal of Immunology, 160*(9), 4518-4525.

Aslan, J. E., Spencer, A. M., Loren, C. P., Pang, J., Welch, H. C., Greenberg, D. L., & McCarty, O. J. (2011). Characterization of the Rac guanine nucleotide exchange factor P-Rex1 in platelets. *Journal of molecular signaling, 6*, 11.

Ayoub, M. A., Damian, M., Gespach, C., Ferrandis, E., Lavergne, O., De Wever, O., . . . Prevost, G. P. (2009). Inhibition of Heterotrimeric G Protein Signaling by a Small Molecule Acting on G alpha Subunit. *Journal of Biological Chemistry, 284*(42), 29136-29145.

Babior, B. M., Lambeth, J. D., & Nauseef, W. (2002). The neutrophil NADPH oxidase. *Archives of Biochemistry and Biophysics, 397*(2), 342-344.

Bachelerie, F., Ben-Baruch, A., Burkhardt, A. M., Combadiere, C., Farber, J. M., Graham, G. J., . . . Zlotnik, A. (2014). International Union of Pharmacology. LXXXIX. Update on the Extended Family of Chemokine Receptors and Introducing a New Nomenclature for Atypical Chemokine Receptors. *Pharmacological Reviews, 66*(1), 1-79.

Baker, M. J., Pan, D., & Welch, H. C. (2016). Small GTPases and their guanine-nucleotide exchange factors and GTPase-activating proteins in neutrophil recruitment. *Current Opinion in Hematology, 23*(1), 44-54.

Balamatsias, D., Kong, A. M., Waters, J. E., Sriratana, A., Gurung, R., Bailey, C. G., . . . Mitchell, C. A. (2011). Identification of P-Rex1 as a Novel Rac1-Guanine Nucleotide Exchange Factor (GEF) That Promotes Actin Remodeling and GLUT4 Protein Trafficking in Adipocytes. *Journal of Biological Chemistry, 286*(50), 43229-43240.

Barber, M. A., Donald, S., Thelen, S., Anderson, K. E., Thelen, M., & Welch, H. C. (2007). Membrane translocation of P-Rex1 is mediated by G protein betagamma subunits and phosphoinositide 3-kinase. *The Journal of Biological Chemistry, 282*(41), 29967-29976.

Barlic, J., Khandaker, M. H., Mahon, E., Andrews, J., DeVries, M. E., Mitchell, G. B., . . . Kelvin, D. J. (1999). beta-Arrestins regulate interleukin-8-induced CXCR1 internalization. *Journal of Biological Chemistry, 274*(23), 16287-16294.

Baron, E. J., & Proctor, R. A. (1982). Elicitation of Peritoneal Polymorphonuclear Neutrophils from Mice. *Journal of Immunological Methods, 49*(3), 305-313.

Barrio-Real, L., Benedetti, L. G., Engel, N., Tu, Y. P., Cho, S., Sukumar, S., & Kazanietz, M. G. (2014). Subtype-specific overexpression of the Rac-GEF P-REX1 in breast cancer is associated with promoter hypomethylation. *Breast Cancer Research, 16*(5).

Barrio-Real, L., Lopez-Haber, C., Casado-Medrano, V., Goglia, A. G., Toettcher, J. E., Caloca, M. J., & Kazanietz, M. G. (2018). P-Rex1 is dispensable for Erk activation and mitogenesis in breast cancer. *Oncotarget, 9*(47), 28612-28624.

Bartolome, R. A., Molina-Ortiz, I., Samaniego, R., Sanchez-Mateos, P., Bustelo, X. R., & Teixido, J. (2006). Activation of Vav/Rho GTPase signaling by CXCL12 controls

membrane-type matrix metalloproteinase-dependent melanoma cell invasion. *Cancer Res, 66*(1), 248-258.

Basu, S., Hodgson, G., Katz, M., & Dunn, A. R. (2002). Evaluation of role of G-CSF in the production, survival, and release of neutrophils from bone marrow into circulation. *Blood, 100*(3), 854-861.

Bekkering, S. (2013). Another look at the life of a neutrophil, *World Journal Hematology* 2(2): 44-58.

Benarafa, C., & Simon, H. U. (2017). Role of granule proteases in the life and death of neutrophils. *Biochem Biophys Res Commun, 482*(3), 473-481.

Bergeron, Y., Ouellet, N., Deslauriers, A. M., Simard, M., Olivier, M., & Bergeron, M. G. (1998). Cytokine kinetics and other host factors in response to pneumococcal pulmonary infection in mice. *Infection and Immunity, 66*(3), 912-922.

Bock, D., Martin, U., Gartner, S., Rheinheimer, C., Raffetseder, U., Arseniev, L., . . . Klos, A. (1997). The C terminus of the human C5a receptor (CD88) is required for normal ligand-dependent receptor internalization. *European Journal of Immunology, 27*(6), 1522-1529.

Boespflug, N. D., Kumar, S., McAlees, J. W., Phelan, J. D., Grimes, H. L., Hoebe, K., . . . Karp, C. L. (2014). ATF3 is a novel regulator of mouse neutrophil migration. *Blood, 123*(13), 2084-2093.

Bogaert, D., De Groot, R., & Hermans, P. W. (2004). Streptococcus pneumoniae colonisation: the key to pneumococcal disease. *Lancet Infect Dis, 4*(3), 144-154.

Boissier, P., & Huynh-Do, U. (2014). The guanine nucleotide exchange factor Tiam1: A Janus-faced molecule in cellular signaling. *Cell Signal, 26*(3), 483-491.

Borregaard, N. (2010). Neutrophils, from marrow to microbes. *Immunity, 33*(5), 657-670.

Boulay, F., Mery, L., Tardif, M., Brouchon, L., & Vignais, P. (1991). Expression Cloning of a Receptor for C5a Anaphylatoxin on Differentiated Hl-60 Cells. *Biochemistry, 30*(12), 2993-2999.

Boulay, F., Tardif, M., Brouchon, L., & Vignais, P. (1990). Synthesis and Use of a Novel N-Formyl Peptide Derivative to Isolate a Human N-Formyl Peptide Receptor Cdna. *Biochem Biophys Res Commun, 168*(3), 1103-1109.

Bratton, D. L., & Henson, P. M. (2011). Neutrophil clearance: when the party is over, clean-up begins. *Trends Immunol, 32*(8), 350-357.

Braun, J. S., Novak, R., Gao, G., Murray, P. J., & Shenep, J. L. (1999). Pneumolysin, a protein toxin of Streptococcus pneumoniae, induces nitric oxide production from macrophages. *Infection and Immunity, 67*(8), 3750-3756.

Brinkmann, V., Reichard, U., Goosmann, C., Fauler, B., Uhlemann, Y., Weiss, D. S., . . . Zychlinsky, A. (2004). Neutrophil extracellular traps kill bacteria. *Science, 303*(5663), 1532-1535.

Bruhn, K. W., Dekitani, K., Nielsen, T. B., Pantapalangkoor, P., & Spellberg, B. (2016). Ly6G-mediated depletion of neutrophils is dependent on macrophages. *Results Immunol, 6*, 5-7.

Buchanan, J. T., Simpson, A. J., Aziz, R. K., Liu, G. Y., Kristian, S. A., Kotb, M., . . . Nizet, V. (2006). DNase expression allows the pathogen group A Streptococcus to escape killing in neutrophil extracellular traps. *Current Biology, 16*(4), 396-400.

Burridge, K., & Wennerberg, K. (2004). Rho and Rac take center stage. *Cell, 116*(2), 167-179.

Bustelo, X. R. (2000). Regulatory and signaling properties of the Vav family. *Molecular and Cellular Biology, 20*(5), 1461-1477.

Bustelo, X. R. (2002). Regulation of Vav proteins by intramolecular events. *Front Biosci, 7*, d24-30.

Bustelo, X. R. (2014). Vav family exchange factors: an integrated regulatory and functional view. *Small GTPases, 5*(2), 9.

Calebiro, D., & Godbole, A. (2018). Internalization of G-protein-coupled receptors: Implication in receptor function, physiology and diseases. *Best Practice & Research Clinical Endocrinology & Metabolism, 32*(2), 83-91.

Call, D. R., Nemzek, J. A., Ebong, S. J., Bolgos, G. L., Newcomb, D. E., & Remick, D. G. (2001). Ratio of local to systemic chemokine concentrations regulates neutrophil recruitment. *American Journal of Pathology, 158*(2), 715-721.

Campbell, A. D., Lawn, S., McGarry, L. C., Welch, H. C., Ozanne, B. W., & Norman, J. C. (2013). P-Rex1 Cooperates with PDGFR beta to Drive Cellular Migration in 3D Microenvironments. *PLoS One, 8*(1).

Cao, M. W., Shikama, Y., Kimura, H., Noji, H., Ikeda, K., Ono, T., . . . Kimura, J. (2017). Mechanisms of Impaired Neutrophil Migration by MicroRNAs in Myelodysplastic Syndromes. *Journal of Immunology, 198*(5), 1887-1899.

Carman, C. V., Sage, P. T., Sciuto, T. E., de la Fuente, M. A., Geha, R. S., Ochs, H. D., . . . Springer, T. A. (2007). Transcellular diapedesis is initiated by invasive podosomes. *Immunity, 26*(6), 784-797.

Carman, C. V., & Springer, T. A. (2004). A transmigratory cup in leukocyte diapedesis both through individual vascular endothelial cells and between them. *The Journal of Cell Biology, 167*(2), 377-388.

Carretero-Ortega, J., Walsh, C. T., Hernandez-Garcia, R., Reyes-Cruz, G., Brown, J. H., & Vazquez-Prado, J. (2010). Phosphatidylinositol 3,4,5-triphosphate-dependent Rac exchanger 1 (P-Rex-1), a guanine nucleotide exchange factor for Rac, mediates angiogenic responses to stromal cell-derived factor-1/chemokine stromal cell derived factor-1 (SDF-1/CXCL-12) linked to Rac activation, endothelial cell migration, and in vitro angiogenesis. *Mol Pharmacol, 77*(3), 435-442.

Cash, J. N., Davis, E. M., & Tesmer, J. J. G. (2016). Structural and Biochemical Characterization of the Catalytic Core of the Metastatic Factor P-Rex1 and Its Regulation by PtdIns(3,4,5)P-3. *Structure, 24*(5), 730-740.

Cauwels, A., Wan, E., Leismann, M., & Tuomanen, E. (1997). Coexistence of CD14-dependent and independent pathways for stimulation of human monocytes by gram-positive bacteria. *Infection and Immunity, 65*(8), 3255-3260.

Chavez-Vargas, L., Adame-Garcia, S. R., Cervantes-Villagrana, R. D., Castillo-Kauil, A., Bruystens, J. G., Fukuhara, S., . . . Vazquez-Prado, J. (2016). Protein kinase A (PKA) Type I interacts with P-Rex1, a Rac guanine nucleotide exchange factor: Effect on PKA localization and P-Rex1 signaling. *Journal of Biological Chemistry*.

Chen, H. H. D., Young, K. H., & Jones, P. G. (2001). Identification of RGS 9 interacting proteins. *Faseb Journal, 15*(4), A579-A579.

Chimini, G., & Chavrier, P. (2000). Function of Rho family proteins in actin dynamics during phagocytosis and engulfment. *Nature Cell Biology, 2*(10), E191-E196.

Christopher, M. J., & Link, D. C. (2007). Regulation of neutrophil homeostasis. *Current Opinion in Hematology, 14*(1), 3-8.

Chuntharapai, A., & Kim, K. J. (1995). Regulation of the Expression of Il-8 Receptor a/B by Il-8 - Possible Functions of Each Receptor. *Journal of Immunology, 155*(5), 2587-2594.

Chuntharapai, A., Lee, J., Hebert, C. A., & Kim, K. J. (1994). Monoclonal-Antibodies Detect Different Distribution Patterns of Il-8 Receptor-a and Il-8 Receptor-B on Human Peripheral-Blood Leukocytes. *Journal of Immunology, 153*(12), 5682-5688.

Claing, A., Chen, W., Miller, W. E., Vitale, N., Moss, J., Premont, R. T., & Lefkowitz, R. J. (2001). beta-Arrestin-mediated ADP-ribosylation factor 6 activation and beta 2-adrenergic receptor endocytosis. *Journal of Biological Chemistry, 276*(45), 42509-42513.

Clausen, B. E., Burkhardt, C., Reith, W., Renkawitz, R., & Forster, I. (1999). Conditional gene targeting in macrophages and granulocytes using LysMcre mice. *Transgenic Res, 8*(4), 265-277.

Clemmensen, S. N., Udby, L., & Borregaard, N. (2014). Subcellular fractionation of human neutrophils and analysis of subcellular markers. *Methods Molecular Biology, 1124*, 53-76.

Condliffe, A. M., Chilvers, E. R., Haslett, C., & Dransfield, I. (1996). Priming differentially regulates neutrophil adhesion molecule expression/function. *Immunology, 89*(1), 105-111.

Condliffe, A. M., Webb, L. M. C., Ferguson, G. J., Davidson, K., Turner, M., Vigorito, E., . . . Hawkins, P. T. (2006). RhoG regulates the neutrophil NADPH oxidase. *Journal of Immunology, 176*(9), 5314-5320.

Cook, A. D., Braine, E. L., & Hamilton, J. A. (2003). The phenotype of inflammatory macrophages is stimulus dependent: Implications for the nature of the inflammatory response. *Journal of Immunology, 171*(9), 4816-4823.

Cotter, M. J., & Muruve, D. A. (2006). Isolation of neutrophils from mouse liver: A novel method to study effector leukocytes during inflammation. *Journal of Immunological Methods, 312*(1-2), 68-78.

Cotter, M. J., Norman, K. E., Hellewell, P. G., & Ridger, V. C. (2001). A novel method for isolation of neutrophils from murine blood using negative immunomagnetic separation. *Am J Pathol, 159*(2), 473-481.

Cowburn, A. S., Condliffe, A. M., Farahi, N., Summers, C., & Chilvers, E. R. (2008). Advances in neutrophil biology - Clinical implications. *Chest, 134*(3), 606-612.

Cowland, J. B., & Borregaard, N. (1999). The individual regulation of granule protein mRNA levels during neutrophil maturation explains the heterogeneity of neutrophil granules. *Journal Leukocyte Biology, 66*(6), 989-995.

Cross, A. R., & Segal, A. W. (2004). The NADPH oxidase of professional phagocytes--prototype of the NOX electron transport chain systems. *Biochim Biophys Acta, 1657*(1), 1-22.

Cua, D. J., & Tato, C. M. (2010). Innate IL-17-producing cells: the sentinels of the immune system. *Nature Reviews Immunology, 10*(7), 479-489.

Czermak, B. J., Sarma, V., Pierson, C. L., Warner, R. L., Huber-Lang, M., Bless, N. M., . . . Ward, P. A. (1999). Protective effects of C5a blockade in sepsis. *Nat Med, 5*(7), 788-792.

Damoulakis, G., Gambardella, L., Rossman, K. L., Lawson, C. D., Anderson, K. E., Fukui, Y., . . . Hawkins, P. T. (2014). P-Rex1 directly activates RhoG to regulate GPCR-driven Rac signalling and actin polarity in neutrophils. *Journal of Cell Science, 127*(Pt 11), 2589-2600.

Dancey, J. T., Deubelbeiss, K. A., Harker, L. A., & Finch, C. A. (1976). Neutrophil Kinetics in Man. *Journal of Clinical Investigation, 58*(3), 705-715.

Dateki, M., Horii, T., Kasuya, Y., Mochizuki, R., Nagao, Y., Ishida, J., . . . Fukamizu, A. (2005). Neurochondrin negatively regulates CaMKII phosphorylation, and nervous system-specific gene disruption results in epileptic seizure. *Journal of Biological Chemistry, 280*(21), 20503-20508.

De Filippo, K., & Rankin, S. M. (2018). CXCR4, the master regulator of neutrophil trafficking in homeostasis and disease. *Eur J Clin Invest, 48*.

De Oliveira, S., Rosowski, E. E., & Huttenlocher, A. (2016). Neutrophil migration in infection and wound repair: going forward in reverse. *Nature Review Immulogy, 16*(6), 378-391.

Deng, M. H., Scott, M. J., Loughran, P., Gibson, G., Sodhi, C., Watkins, S., . . . Billiar, T. R. (2013). Lipopolysaccharide Clearance, Bacterial Clearance, and Systemic Inflammatory Responses Are Regulated by Cell Type-Specific Functions of TLR4 during Sepsis. *Journal of Immunology, 190*(10), 5152-5160.

DeWire, S. M., Ahn, S., Lefkowitz, R. J., & Shenoy, S. K. (2007). beta-arrestins and cell signaling. *Annual Review of Physiology, 69*, 483-510.

Dillon, L. M., Bean, J. R., Yang, W., Shee, K., Symonds, L. K., Balko, J. M., . . . Miller, T. W. (2015). P-REX1 creates a positive feedback loop to activate growth factor receptor, PI3K/AKT and MEK/ERK signaling in breast cancer. *Oncogene, 34*(30), 3968-3976.

Dinauer, M. C. (2016). Primary immune deficiencies with defects in neutrophil function. *Hematology-American Society of Hematology Education Program*, 43-50.

DiStasi, M. R., & Ley, K. (2009). Opening the flood-gates: how neutrophil-endothelial interactions regulate permeability. *Trends Immunol, 30*(11), 539-545.

DiVietro, J. A., Smith, M. J., Smith, B. R., Petruzzelli, L., Larson, R. S., & Lawrence, M. B. (2001). Immobilized IL-8 triggers progressive activation of neutrophils rolling in vitro on P-selectin and intercellular adhesion molecule-1. *Journal of Immunology, 167*(7), 4017-4025.

Dockrell, D. H., Marriott, H. M., Prince, L. R., Ridger, V. C., Ince, P. G., Hellewell, P. G., & Whyte, M. K. (2003). Alveolar macrophage apoptosis contributes to pneumococcal clearance in a resolving model of pulmonary infection. *Journal of Immunology, 171*(10), 5380-5388.

Dockrell, D. H., Whyte, M. K. B., & Mitchell, T. J. (2012). Pneumococcal pneumonia: mechanisms of infection and resolution. *Chest, 142*(2), 482-491.

Doherty, G. J., & McMahon, H. T. (2009). Mechanisms of Endocytosis. *Annu Rev Biochem, 78*, 857-902.

Donald, S., Hill, K., Lecureuil, C., Barnouin, R., Krugmann, S., John Coadwell, W., . . . Welch, H. C. (2004). P-Rex2, a new guanine-nucleotide exchange factor for Rac. *FEBS Lett, 572*(1-3), 172-176.

Donald, S., Humby, T., Fyfe, I., Segonds-Pichon, A., Walker, S. A., Andrews, S. R., . . . Welch, H. C. (2008). P-Rex2 regulates Purkinje cell dendrite morphology and motor coordination. *Proceedings of the National Academy of Sciences of the United States of America, 105*(11), 4483-4488.

Dong, X., Mo, Z., Bokoch, G., Guo, C., Li, Z., & Wu, D. (2005). P-Rex1 is a primary Rac2 guanine nucleotide exchange factor in mouse neutrophils. *Current Biology, 15*(20), 1874-1879.

Dooley, J. L., Abdel-Latif, D., St Laurent, C. D., Puttagunta, L., Befus, D., & Lacy, P. (2009). Regulation of inflammation by Rac2 in immune complex-mediated acute lung injury. *American Journal of Physiology-Lung Cellular and Molecular Physiology, 297*(6), L1091-L1102.

Drake, M. T., Shenoy, S. K., & Lefkowitz, R. J. (2006). Trafficking of G protein-coupled receptors. *Circ Res, 99*(6), 570-582.

Dupre-Crochet, S., Erard, M., & Nuss, O. (2013). ROS production in phagocytes: why, when, and where? *Journal of Leukococytes Biology, 94*(4), 657-670.

Eash, K. J., Greenbaum, A. M., Gopalan, P. K., & Link, D. C. (2010). CXCR2 and CXCR4 antagonistically regulate neutrophil trafficking from murine bone marrow. *Journal of Clinical Investigation, 120*(7), 2423-2431.

Eash, K. J., Means, J. M., White, D. W., & Link, D. C. (2009). CXCR4 is a key regulator of neutrophil release from the bone marrow under basal and stress granulopoiesis conditions. *Blood, 113*(19), 4711-4719.

El-Benna, J., Dang, P. M. C., & Gougerot-Pocidalo, M. A. (2008). Priming of the neutrophil NADPH oxidase activation: role of p47phox phosphorylation and NOX2 mobilisation to the plasma membrane. *Seminars in Immunopathology, 30*(3), 279-289.

El-Benna, J., Hurtado-Nedelec, M., Marzaioli, V., Marie, J. C., Gougerot-Pocidalo, M. A., & Dang, P. M. C. (2016). Priming of the neutrophil respiratory burst: role in host defense and inflammation. *Immunological Reviews, 273*(1), 180-193.

Fadok, V. A., McDonald, P. P., Bratton, D. L., & Henson, P. M. (1998). Regulation of macrophage cytokine production by phagocytosis of apoptotic and post-apoptotic cells. *Biochem Soc Trans, 26*(4), 653-656.

Fagerholm, S. C., Guenther, C., Llort Asens, M., Savinko, T., & Uotila, L. M. (2019). Beta2-Integrins and Interacting Proteins in Leukocyte Trafficking, Immune Suppression, and Immunodeficiency Disease. *Front Immunol, 10*, 254.

Faurschou, M., & Borregaard, N. (2003). Neutrophil granules and secretory vesicles in inflammation. *Microbes and Infection, 5*(14), 1317-1327.

Feng, Q. Y., Baird, D., & Cerione, R. A. (2004). Novel regulatory mechanisms for the Dbl family guanine nucleotide exchange factor Cool-2/alpha-Pix. *Embo Journal, 23*(17), 3492-3504.

Feniger-Barish, R., Ran, M., Zaslaver, A., & Ben-Baruch, A. (1999). Differential modes of regulation of CXC chemokine-induced internalization and recycling of human CXCR1 and CXCR2. *Cytokine, 11*(12), 996-1009.

Ferguson, G. J., Milne, L., Kulkarni, S., Sasaki, T., Walker, S., Andrews, S., . . . Stephens, L. (2007). PI(3)Kgamma has an important context-dependent role in neutrophil chemokinesis. *Nature Cell Biology, 9*(1), 86-91.

Ferguson, S. S. G. (2001). Evolving concepts in G protein-coupled receptor endocytosis: The role in receptor desensitization and signaling. *Pharmacological Reviews, 53*(1), 1-24.

Fiegen, D., Haeusler, L. C., Blumenstein, L., Herbrand, U., Dvorsky, R., Vetter, I. R., & Ahmadian, M. R. (2004). Alternative splicing of Rac1 generates Rac1b, a self-activating GTPase. *Journal of Biological Chemistry, 279*(6), 4743-4749.

Filippi, M. D. (2019). Neutrophil transendothelial migration: updates and new perspectives. *Blood, 133*(20), 2149-2158.

Filippi, M. D., Harris, C. E., Meller, J., Gu, Y., Zheng, Y., & Williams, D. A. (2004). Localization of Rac2 via the C terminus and aspartic acid 150 specifies superoxide generation, actin polarity and chemotaxis in neutrophils. *Nature Immunology, 5*(7), 744-751.

Filippi, M. D., Szczur, K., Harris, C. E., & Berclaz, P. Y. (2007). Rho GTPase Rac1 is critical for neutrophil migration into the lung. *Blood, 109*(3), 1257-1264.

Fillion, I., Ouellet, N., Simard, M., Bergeron, Y., Sato, S., & Bergeron, M. G. (2001). Role of chemokines and formyl peptides in pneumococcal pneumonia-induced monocyte/macrophage recruitment. *Journal of Immunology, 166*(12), 7353-7361.

Francke, F., Ward, R. J., Jenkins, L., Kellett, E., Richter, D., Milligan, G., & Bachner, D. (2006). Interaction of neurochondrin with the melanin-concentrating hormone receptor 1 interferes with G protein-coupled signal transduction but not agonist-mediated internalization. *Journal of Biological Chemistry, 281*(43), 32496-32507.

Fuchs, T. A., Abed, U., Goosmann, C., Hurwitz, R., Schulze, I., Wahn, V., . . . Zychlinsky, A. (2007). Novel cell death program leads to neutrophil extracellular traps. *Journal of Cell Biology, 176*(2), 231-241.

Fumagalli, L., Zhang, H., Baruzzi, A., Lowell, C. A., & Berton, G. (2007). The Src family kinases Hck and Fgr regulate neutrophil responses to N-formyl-methionyl-leucyl-phenylalanine. *Journal of Immunology, 178*(6), 3874-3885.

Furze, R. C., & Rankin, S. M. (2008). Neutrophil mobilisation and clearance in the bone marrow. *Immunology, 125*(3), 281-288.

Gakidis, M. A., Cullere, X., Olson, T., Wilsbacher, J. L., Zhang, B., Moores, S. L., . . . Brugge, J. S. (2004). Vav GEFs are required for beta2 integrin-dependent functions of neutrophils. *The Journal of Cell Biology, 166*(2), 273-282.

Gao, J. L., Lee, E. J., & Murphy, P. M. (1999). Impaired antibacterial host defense in mice lacking the N-formylpeptide receptor. *Journal of Experimental Medicine, 189*(4), 657-662.

Garvy, B. A., & Harmsen, A. G. (1996). The importance of neutrophils in resistance to pneumococcal pneumonia in adult and neonatal mice. *Inflammation, 20*(5), 499-512.

Ghalali, A., Wiklund, F., Zheng, H. Y., Stenius, U., & Hogberg, J. (2014). Atorvastatin prevents ATP-driven invasiveness via P2X7 and EHBP1 signaling in PTEN-expressing prostate cancer cells. *Carcinogenesis, 35*(7), 1547-1555.

Gillespie, S. H., & Balakrishnan, I. (2000). Pathogenesis of pneumococcal infection. *J Med Microbiol, 49*(12), 1057-1067.

Gillespie, S. H., Mcwhinney, P. H. M., & Kibbler, C. C. (1991). Pneumococcal Bacteremia. *Lancet, 337*(8737), 376-376.

Glogauer, M., Marchal, C. C., Zhu, F., Worku, A., Clausen, B. E., Foerster, I., . . . Kwiatkowski, D. J. (2003). Rac1 deletion in mouse neutrophils has selective effects on neutrophil functions. *Journal of Immunology, 170*(11), 5652-5657.

Godbole, A., Lyga, S., Lohse, M. J., & Calebiro, D. (2017). Internalized TSH receptors en route to the TGN induce local G(s)-protein signaling and gene transcription. *Nature Communication, 8*.

Gomez-Moreno, D., Adrover, J. M., & Hidalgo, A. (2018). Neutrophils as effectors of vascular inflammation. *European Journal Clinical Investigation, 48*.

Goodman, O. B., Jr., Krupnick, J. G., Santini, F., Gurevich, V. V., Penn, R. B., Gagnon, A. W., . . . Benovic, J. L. (1996). Beta-arrestin acts as a clathrin adaptor in endocytosis of the beta2-adrenergic receptor. *Nature, 383*(6599), 447-450.

Gordon, S. (2016). Phagocytosis: An Immunobiologic Process. *Immunity, 44*(3), 463-475.

Gordy, C., Pua, H., Sempowski, G. D., & He, Y. W. (2011). Regulation of steady-state neutrophil homeostasis by macrophages. *Blood, 117*(2), 618-629.

Graham, D. B., Robertson, C. M., Bautista, J., Mascarenhas, F., Diacovo, M. J., Montgrain, V., . . . Swat, W. (2007). Neutrophil-mediated oxidative burst and host defense are controlled by a Vav-PLC gamma 2 signaling axis in mice. *Journal of Clinical Investigation, 117*(11), 3445-3452.

Graham, D. B., Zinselmeyer, B. H., Mascarenhas, F., Delgado, R., Miller, M. J., & Swat, W. (2009). ITAM Signaling by Vav Family Rho Guanine Nucleotide Exchange Factors Regulates Interstitial Transit Rates of Neutrophils In Vivo. *PLoS One, 4*(2).

Gu, Y., Filippi, M. D., Cancelas, J. A., Siefring, J. E., Williams, E. P., Jasti, A. C., . . . Williams, D. A. (2003). Hematopoietic cell regulation by Rac1 and Rac2 guanosine triphosphatases. *Science, 302*(5644), 445-449.

Guo, R. F., & Ward, P. A. (2006). C5a, a therapeutic target in sepsis. *Recent Pat Antiinfect Drug Discov, 1*(1), 57-65.

Guthrie, L. A., Mcphail, L. C., Henson, P. M., & Johnston, R. B. (1984). Priming of Neutrophils for Enhanced Release of Oxygen Metabolites by Bacterial Lipopolysaccharide - Evidence for Increased Activity of the Superoxide-Producing Enzyme. *Journal of Experimental Medicine, 160*(6), 1656-1671.

Haataja, L., Groffen, J., & Heisterkamp, N. (1997). Characterization of RAC3, a novel member of the Rho family. *Journal of Biological Chemistry, 272*(33), 20384-20388.

Hahn, I., Klaus, A., Janze, A. K., Steinwede, K., Ding, N., Bohling, J., . . . Maus, U. A. (2011). Cathepsin G and neutrophil elastase play critical and nonredundant roles in lung-protective immunity against Streptococcus pneumoniae in mice. *Infection and Immunity, 79*(12), 4893-4901.

Hajdo-Milasinovic, A., Ellenbroek, S. I., van Es, S., van der Vaart, B., & Collard, J. G. (2007). Rac1 and Rac3 have opposing functions in cell adhesion and differentiation of neuronal cells. *Journal of Cell Science, 120*(Pt 4), 555-566.

Hakkim, A., Fuchs, T. A., Martinez, N. E., Hess, S., Prinz, H., Zychlinsky, A., & Waldmann, H. (2011). Activation of the Raf-MEK-ERK pathway is required for neutrophil extracellular trap formation. *Nature Chemical Biology, 7*(2), 75-77.

Hallett, M. B., & Lloyds, D. (1995). Neutrophil Priming - the Cellular Signals That Say Amber but Not Green. *Immunology Today, 16*(6), 264-268.

Han, J. W., Das, B., Wei, W., VanAelst, L., Mosteller, R. D., Khosravifar, R., . . . Broek, D. (1997). Lck regulates Vav activation of members of the Rho family of GTPases. *Molecular Cell Biololgy, 17*(3), 1346-1353.

Hanyaloglu, A. C., & von Zastrow, M. (2008). Regulation of GPCRs by Endocytic membrane trafficking and its potential implications. *Annual Review of Pharmacology and Toxicology, 48*, 537-568.

Haslett, C. (1999). Granulocyte apoptosis and its role in the resolution and control of lung inflammation. *Am J Respir Crit Care Med, 160*(5 Pt 2), S5-11.

Hawkins, P. T., & Stephens, L. R. (2015). PI3K signalling in inflammation. *Biochim Biophys Acta, 1851*(6), 882-897.

Hawkins, P. T., Stephens, L. R., Suire, S., & Wilson, M. (2010). PI3K signaling in neutrophils. *Curr Top Microbiol Immunol, 346*, 183-202.

Hayashi, F., Means, T. K., & Luster, A. D. (2003). Toll-like receptors stimulate human neutrophil function. *Blood, 102*(7), 2660-2669.

Heasman, S. J., & Ridley, A. J. (2008). Mammalian Rho GTPases: new insights into their functions from in vivo studies. *Nat Rev Molecular Cell Biol, 9*(9), 690-701.

Herbold, W., Maus, R., Hahn, I., Ding, N., Srivastava, M., Christman, J. W., . . . Maus, U. A. (2010). Importance of CXC chemokine receptor 2 in alveolar neutrophil and exudate macrophage recruitment in response to pneumococcal lung infection. *Infection and Immunity, 78*(6), 2620-2630.

Herrmann, J. B., Muenstermann, M., Strobel, L., Schubert-Unkmeir, A., Woodruff, T. M., Gray-Owen, S. D., . . . Johswich, K. O. (2018). Complement C5a Receptor 1 Exacerbates the Pathophysiology of N. meningitidis Sepsis and Is a Potential Target for Disease Treatment. *Mbio, 9*(1).

Herter, J., & Zarbock, A. (2013). Integrin Regulation during Leukocyte Recruitment. *Journal of Immunology, 190*(9), 4451-4457.

Herter, J. M., Rossaint, J., Block, H., Welch, H., & Zarbock, A. (2013). Integrin activation by P-Rex1 is required for selectin-mediated slow leukocyte rolling and intravascular crawling. *Blood, 121*(12), 2301-2310.

Heyworth, P. G., Shrimpton, C. F., & Segal, A. W. (1989). Localization of the 47 kDa phosphoprotein involved in the respiratory-burst NADPH oxidase of phagocytic cells. *Biochemical Journal, 260*(1), 243-248.

Hill, K., Krugmann, S., Andrews, S. R., Coadwell, W. J., Finan, P., Welch, H. C., . . . Stephens, L. R. (2005). Regulation of P-Rex1 by phosphatidylinositol (3,4,5)-trisphosphate and Gbetagamma subunits. *Journal of Biological Chemistry, 280*(6), 4166-4173.

Hill, K., & Welch, H. C. (2006). Purification of P-Rex1 from neutrophils and nucleotide exchange assay. *Methods Enzymol, 406*, 26-41.

Hoang, A. N., Jones, C. N., Dimisko, L., Hamza, B., Martel, J., Kojic, N., & Irimia, D. (2013). Measuring neutrophil speed and directionality during chemotaxis, directly from a droplet of whole blood. *Technology (Singap World Sci), 1*(1), 49.

Hodakoski, C., Hopkins, B. D., Barrows, D., Mense, S. M., Keniry, M., Anderson, K. E., . . . Parsons, R. (2014). Regulation of PTEN inhibition by the pleckstrin homology domain of P-REX2 during insulin signaling and glucose homeostasis. *Proceedings of the National Academy of Sciences of the United States of America, 111*(1), 155-160.

Hopken, U. E., Lu, B., Gerard, N. P., & Gerard, C. (1996). The C5a chemoattractant receptor mediates mucosal defence to infection. *Nature, 383*(6595), 86-89.

Hornigold K, Tsonou E., Pantarelli C, Welch HCE. (2018). P-Rex1. In S. Choi (Ed.), *Encyclopedia of Signaling Molecules* (2nd edition ed., pp. 4142-4154).

Huang, Y., Xie, Y., Jiang, H., Abel, P. W., Panettieri, R. A., Jr., Casale, T. B., & Tu, Y. (2019). Upregulated P-Rex1 exacerbates human airway smooth muscle hyperplasia in asthma. *J Allergy Clin Immunol, 143*(2), 778-781 e775.

Huang, Y., Zheng, Y., Su, Z., & Gu, X. (2009). Differences in duplication age distributions between human GPCRs and their downstream genes from a network prospective. *BMC Genomics* (Vol. 10 Suppl 1).

Hughes, J., Johnson, R. J., Mooney, A., Hugo, C., Gordon, K., & Savill, J. (1997). Neutrophil fate in experimental glomerular capillary injury in the rat - Emigration exceeds in situ clearance by apoptosis. *American Journal of Pathology, 150*(1), 223-234.

Hyun, Y. M., & Choe, Y. H. (2019). LFA-1 (CD11a/CD18) and Mac-1 (CD11b/CD18) distinctly regulate neutrophil extravasation through hotspots I and II. *Experimental & Molecular Medicine 51*(4), 39.

Hyun, Y. M., Sumagin, R., Sarangi, P. P., Lomakina, E., Overstreet, M. G., Baker, C. M., . . . Kim, M. (2012). Uropod elongation is a common final step in leukocyte extravasation through inflamed vessels. *Journal Experimental Medicine, 209*(7), 1349-1362.

Irannejad, R., Tsvetanova, N. G., Lobingier, B. T., & von Zastrow, M. (2015). Effects of endocytosis on receptor-mediated signaling. *Curr Opin Cell Biol, 35*, 137-143.

Ishiduka, Y., Mochizuki, R., Yanai, K., Takatsuka, M., Nonomura, T., Niida, S., . . . Fukamizu, A. (1999). Induction of hydroxyapatite resorptive activity in bone marrow cell populations resistant to bafilomycin A1 by a factor with restricted expression to bone and brain, neurochondrin. *Biochim Biophys Acta, 1450*(1), 92-98.

Jackson, C., Welch, H. C., & Bellamy, T. C. (2010). Control of cerebellar long-term potentiation by P-Rex-family guanine-nucleotide exchange factors and phosphoinositide 3-kinase. *PLoS One, 5*(8), e11962.

Janeway, C. A., Jr., & Medzhitov, R. (2002). Innate immune recognition. *Annual Review Immnulogy, 20*, 197-216.

Johnsson, A. K., Dai, Y., Nobis, M., Baker, M. J., McGhee, E. J., Walker, S., . . . Welch, H. C. (2014). The Rac-FRET mouse reveals tight spatiotemporal control of Rac activity in primary cells and tissues. *Cell Rep, 6*(6), 1153-1164.

Jorch, S. K., & Kubes, P. (2017). An emerging role for neutrophil extracellular traps in noninfectious disease. *Nat Med, 23*(3), 279-287.

Jordan, P., Brazao, R., Boavida, M. G., Gespach, C., & Chastre, E. (1999). Cloning of a novel human Rac1b splice variant with increased expression in colorectal tumors. *Oncogene, 18*(48), 6835-6839.

Kadioglu, A., De Filippo, K., Bangert, M., Fernandes, V. E., Richards, L., Jones, K., . . . Hogg, N. (2011). The integrins Mac-1 and alpha4beta1 perform crucial roles in neutrophil and T cell recruitment to lungs during Streptococcus pneumoniae infection. *The Journal of Immunology, 186*(10), 5907-5915.

Kaplan, M. J. (2013). Role of neutrophils in systemic autoimmune diseases. *Arthritis Res Ther, 15*(5), 219.

Kapur, R., Cooper, R., Xiao, X. L., Weiss, M. J., Donovan, P., & Williams, D. A. (1999). The presence of novel amino acids in the cytoplasmic domain of stem cell factor results in hematopoietic defects in Steel(17H) mice. *Blood, 94*(6), 1915-1925.

Karasu, E., Nilsson, B., Kohl, J., Lambris, J. D., & Huber-Lang, M. (2019). Targeting Complement Pathways in Polytrauma- and Sepsis-Induced Multiple-Organ Dysfunction. *Front Immunol, 10*.

Kay, R. R., Langridge, P., Traynor, D., & Hoeller, O. (2008). Changing directions in the study of chemotaxis. *Nature Reviews Molecular Cell Biology, 9*(6), 455-463.

Kazanietz, M. G., Barrio-Real, L., Casado-Medrano, V., Baker, M. J., & Lopez-Haber, C. (2018). The P-Rex1/Rac signaling pathway as a point of convergence for HER/ErbB receptor and GPCR responses. *Small GTPases, 9*(4), 297-303.

Keszei, M., & Westerberg, L. S. (2014). Congenital Defects in Neutrophil Dynamics. *Journal of Immunology Research*.

Khandpur, R., Carmona-Rivera, C., Vivekanandan-Giri, A., Gizinski, A., Yalavarthi, S., Knight, J. S., . . . Kaplan, M. J. (2013). NETs are a source of citrullinated autoantigens and stimulate inflammatory responses in rheumatoid arthritis. *Sci Transl Med, 5*(178), 178ra140.

Kim, C., & Dinauer, M. C. (2001). Rac2 is an essential regulator of neutrophil nicotinamide adenine dinucleotide phosphate oxidase activation in response to specific signaling pathways. *Journal of Immunology, 166*(2), 1223-1232.

Kim, C., Marchal, C. C., Penninger, J., & Dinauer, M. C. (2003). The hemopoietic Rho/Rac guanine nucleotide exchange factor Vav1 regulates N-formyl-methionyl-leucyl-phenylalanine-activated neutrophil functions. *Journal of Immunology, 171*(8), 4425-4430.

Kim, E. K., Yun, S. J., Ha, J. M., Kim, Y. W., Jin, I. H., Woo, D. H., . . . Bae, S. S. (2012). Synergistic induction of cancer cell migration regulated by Gbetagamma and phosphatidylinositol 3-kinase. *Experimental & Molecular Medicine, 44*(8), 483-491.

Kitchen, E., Rossi, A. G., Condliffe, A. M., Haslett, C., & Chilvers, E. R. (1996). Demonstration of reversible priming of human neutrophils using platelet-activating factor. *Blood, 88*(11), 4330-4337.

Klausen, P., Bjerregaard, M. D., Borregaard, N., & Cowland, J. B. (2004). End-stage differentiation of neutrophil granulocytes in vivo is accompanied by up-regulation of p27kip1 and down-regulation of CDK2, CDK4, and CDK6. *Journal Leukocyte Biology, 75*(3), 569-578.

Koh, A. L. Y., Sun, C. X., Zhu, F., & Glogauer, M. (2005). The role of Rac1 and Rac2 in bacterial killing. *Cellular Immunology, 235*(2), 92-97.

Kohler, A., De Filippo, K., Hasenberg, M., van den Brandt, C., Nye, E., Hosking, M. P., . . . Gunzer, M. (2011). G-CSF-mediated thrombopoietin release triggers neutrophil motility and mobilisation from bone marrow via induction of Cxcr2 ligands. *Blood, 117*(16), 4349-4357.

Kolaczkowska, E., & Kubes, P. (2013). Neutrophil recruitment and function in health and inflammation. *Nature Review Immulogy, 13*(3), 159-175.

Kolev, M., Le Friec, G., & Kemper, C. (2014). Complement - tapping into new sites and effector systems. *Nature Reviews Immunology, 14*(12), 811-820.

Kovacs, M., Nemeth, T., Jakus, Z., Sitaru, C., Simon, E., Futosi, K., . . . Mocsai, A. (2014). The Src family kinases Hck, Fgr, and Lyn are critical for the generation of the in vivo

inflammatory environment without a direct role in leukocyte recruitment. *Journal Experimental Medicine Med, 211*(10), 1993-2011.

Kraynov, V. S., Chamberlain, C., Bokoch, G. M., Schwartz, M. A., Slabaugh, S., & Hahn, K. M. (2000). Localized Rac activation dynamics visualized in living cells. *Science, 290*(5490), 333-337.

Kreisel, D., Nava, R. G., Li, W., Zinselmeyer, B. H., Wang, B., Lai, J., . . . Miller, M. J. (2010). In vivo two-photon imaging reveals monocyte-dependent neutrophil extravasation during pulmonary inflammation. *Proceedings of the National Academy of Sciences of the United States of America, 107*(42), 18073-18078.

Kruger, P., Saffarzadeh, M., Weber, A. N. R., Rieber, N., Radsak, M., von Bernuth, H., . . . Hartl, D. (2015). Neutrophils: Between Host Defence, Immune Modulation, and Tissue Injury. *Plos Pathogens, 11*(3).

Krupnick, J. G., & Benovic, J. L. (1998). The role of receptor kinases and arrestins in G protein-coupled receptor regulation. *Annual Review of Pharmacology and Toxicology, 38*, 289-319.

Kunisaki, Y., Nishikimi, A., Tanaka, Y., Takii, R., Noda, M., Inayoshi, A., . . . Fukui, Y. (2006). DOCK2 is a Rac activator that regulates motility and polarity during neutrophil chemotaxis. *The Journal of Cell Biology, 174*(5), 647-652.

Kunisaki, Y., Tanaka, Y., Sanui, T., Inayoshi, A., Noda, M., Nakayama, T., . . . Fukui, Y. (2006). DOCK2 is required in T cell precursors for development of Valpha14 NK T cells. *The Journal of Immunology, 176*(8), 4640-4645.

Lacy, P. (2006). Mechanisms of degranulation in neutrophils. *Allergy Asthma Clin Immunol, 2*(3), 98-108.

Lambright, D. G., Sondek, J., Bohm, A., Skiba, N. P., Hamm, H. E., & Sigler, P. B. (1996). The 2.0 A crystal structure of a heterotrimeric G protein. *Nature, 379*(6563), 311-319.

Lammermann, T., & Kastenmuller, W. (2019). Concepts of GPCR-controlled navigation in the immune system. *Immunological Reviews, 289*(1), 205-231.

Langkabel, P., Zwirner, J., & Oppermann, M. (1999). Ligand-induced phosphorylation of anaphylatoxin receptors C3aR and C5aR is mediated by G protein-coupled receptor kinases. *European Journal of Immunology, 29*(9), 3035-3046.

Laporte, S. A., Oakley, R. H., Zhang, J., Holt, J. A., Ferguson, S. S., Caron, M. G., & Barak, L. S. (1999). The beta2-adrenergic receptor/betaarrestin complex recruits the clathrin adaptor AP-2 during endocytosis. *Proceedings of the National Academy of Sciences of the United States of America, 96*(7), 3712-3717.

Lawson, C. D., Donald, S., Anderson, K. E., Patton, D. T., & Welch, H. C. (2011). P-Rex1 and Vav1 cooperate in the regulation of formyl-methionyl-leucyl-phenylalanine-dependent neutrophil responses. *The Journal of Immunology, 186*(3), 1467-1476.

Lawson, C. D., & Ridley, A. J. (2018). Rho GTPase signaling complexes in cell migration and invasion. *Journal of Cell Biology, 217*(2), 447-457.

Lefkowitz, R. J. (2013). A Brief History of G-Protein Coupled Receptors (Nobel Lecture). *Angewandte Chemie-International Edition, 52*(25), 6366-6378.

Leijh, P. C. J., Vanzwet, T. L., Terkuile, M. N., & Vanfurth, R. (1984). Effect of Thioglycolate on Phagocytic and Microbicidal Activities of Peritoneal-Macrophages. *Infection and Immunity, 46*(2), 448-452.

Lewis, J. P., Palmer, N. D., Ellington, J. B., Divers, J., Ng, M. C. Y., Lu, L. Y., . . . Bowden, D. W. (2010). Analysis of candidate genes on chromosome 20q12-13.1 reveals evidence for BMI mediated association of PREX1 with type 2 diabetes in European Americans. *Genomics, 96*(4), 211-219.

Ley, K., Laudanna, C., Cybulsky, M. I., & Nourshargh, S. (2007). Getting to the site of inflammation: the leukocyte adhesion cascade updated. *Nature Review Immulogy, 7*(9), 678-689.

Li, J., Chai, A., Wang, L., Ma, Y., Wu, Z., Yu, H., . . . Zhang, D. (2015). Synaptic P-Rex1 signaling regulates hippocampal long-term depression and autism-like social behavior. *Proceedings of the National Academy of Sciences of the United States of America, 112*(50), E6964-6972.

Li, Y. M., Baviello, G., Vlassara, H., & Mitsuhashi, T. (1997). Glycation products in aged thioglycollate medium enhance the elicitation of peritoneal macrophages. *Journal of Immunological Methods, 201*(2), 183-188.

Li, Z., Hannigan, M., Mo, Z. C., Liu, B., Lu, W., Wu, Y., . . . Wu, D. Q. (2003). Directional sensing requires G beta gamma-mediated PAK1 and PIX alpha-dependent activation of cdc42. *Cell, 114*(2), 215-227.

Li, Z., Paik, J. H., Wang, Z., Hla, T., & Wu, D. (2005). Role of guanine nucleotide exchange factor P-Rex-2b in sphingosine 1-phosphate-induced Rac1 activation and cell migration in endothelial cells. *Prostaglandins Other Lipid Mediat, 76*(1-4), 95-104.

Liang, Q., Cheng, N., Zhang, G., Liang, Y., Qian, F., Wu, D., & Ye, R. D. (2016). Identification of P-Rex1 as an anti-inflammatory and anti-fibrogenic target for pulmonary fibrosis. *Scientific Reports, 6*, 25785.

Lieschke, G. J., Grail, D., Hodgson, G., Metcalf, D., Stanley, E., Cheers, C., . . . Dunn, A. R. (1994). Mice Lacking Granulocyte-Colony-Stimulating Factor Have Chronic Neutropenia, Granulocyte and Macrophage Progenitor-Cell Deficiency, and Impaired Neutrophil Mobilisation. *Blood, 84*(6), 1737-1746.

Lin, E., Kuo, P. H., Liu, Y. L., Yu, Y. W., Yang, A. C., & Tsai, S. J. (2018). A Deep Learning Approach for Predicting Antidepressant Response in Major Depression Using Clinical and Genetic Biomarkers. *Front Psychiatry, 9*, 290.

Lindsay, C. R., Lawn, S., Campbell, A. D., Faller, W. J., Rambow, F., Mort, R. L., . . . Sansom, O. J. (2011). P-Rex1 is required for efficient melanoblast migration and melanoma metastasis. *Nature Communication, 2*, 555.

Lindsay, C. R., Li, A., Faller, W., Ozanne, B., Welch, H., Machesky, L. M., & Sansom, O. J. (2015). A Rac1-Independent Role for P-Rex1 in Melanoblasts. *Journal of Investigative Dermatology, 135*(1), 314-318.

Link, D. C. (2005). Neutrophil homeostasis - A new role for stromal cell-derived factor-1. *Immunologic Research, 32*(1-3), 169-178.

Liu, F. L., Wu, H. Y., Wesselschmidt, R., Kornaga, T., & Link, D. C. (1996). Impaired production and increased apoptosis of neutrophils in granulocyte colony-stimulating factor receptor-deficient mice. *Immunity, 5*(5), 491-501.

Liu, H. J., Ooms, L. M., Srijakotre, N., Man, J., Vieusseux, J., Waters, J. E., . . . Mitchell, C. A. (2016). PREX1 Rac-GEF Activity Promotes Breast Cancer Cell Proliferation and Tumor Growth via Activation of Extracellular-Signal-Regulated Kinase 1/2 (ERK1/2) Signaling. *Journal of Biological Chemistry*.

Liu, M. Y., Chen, K. Q., Yoshimura, T., Liu, Y., Gong, W. H., Wang, A. M., . . . Wang, J. M. (2012). Formylpeptide receptors are critical for rapid neutrophil mobilisation in host defense against Listeria monocytogenes. *Scientific Reports, 2*.

Lopez-Haber, C., Barrio-Real, L., Casado-Medrano, V., & Kazanietz, M. G. (2016). Heregulin/Erbb3 signaling enhances CXCR4-driven Rac1 activation and breast cancer cell motility via Hif-1alpha. *Molecular Cell Biol*. 36(15):2011-26

Lucato, C. M., Halls, M. L., Ooms, L. M., Liu, H. J., Mitchell, C. A., Whisstock, J. C., & Ellisdon, A. M. (2015). The Phosphatidylinositol (3,4,5)-trisphosphate-dependent Rac Exchanger 1:Ras-related C3 Botulinum Toxin Substrate 1 (P-Rex1:Rac1) Complex Reveals the Basis of Rac1 Activation in Breast Cancer Cells. *Journal of Biological Chemistry*. 290(34):20827-40.

Machesky, L. M., & Hall, A. (1997). Role of actin polymerisation and adhesion to extracellular matrix in Rac- and Rho-induced cytoskeletal reorganization. *The Journal of Cell Biology, 138*(4), 913-926.

Machesky, L. M., & Insall, R. H. (1998). Scar1 and the related Wiskott-Aldrich syndrome protein, WASP, regulate the actin cytoskeleton through the Arp2/3 complex. *Current Biology, 8*(25), 1347-1356.

Magalhaes, M. A., & Glogauer, M. (2010). Pivotal Advance: Phospholipids determine net membrane surface charge resulting in differential localization of active Rac1 and Rac2. *Journal Leukocyte Biology, 87*(4), 545-555.

Manz, M. G., & Boettcher, S. (2014). Emergency granulopoiesis. *Nature Reviews Immunology, 14*(5), 302-314.

Marriott, H. M., Jackson, L. E., Wilkinson, T. S., Simpson, A. J., Mitchell, T. J., Buttle, D. J., . . . Dockrell, D. H. (2008). Reactive oxygen species regulate neutrophil recruitment and survival in pneumococcal pneumonia. *Am J Respir Crit Care Med, 177*(8), 887-895.

Martin, C., Burdon, P. C. E., Bridger, G., Gutierrez-Ramos, J. C., Williams, T. J., & Rankin, S. M. (2003). Chemokines acting via CXCR2 and CXCR4 control the release of neutrophils from the bone marrow and their return following senescence. *Immunity, 19*(4), 583-593.

Martins-Green, M., Petreaca, M., & Wang, L. (2013). Chemokines and Their Receptors Are Key Players in the Orchestra That Regulates Wound Healing. *Adv Wound Care (New Rochelle), 2*(7), 327-347.

Massol, P., Montcourrier, P., Guillemot, J. C., & Chavrier, P. (1998). Fc receptor-mediated phagocytosis requires CDC42 and Rac1. *Embo Journal, 17*(21), 6219-6229.

Matos, P., Collard, J. G., & Jordan, P. (2003). Tumor-related alternatively spliced Rac1b is not regulated by Rho-GDP dissociation inhibitors and exhibits selective downstream signaling. *Journal of Biological Chemistry, 278*(50), 50442-50448.

Matosin, N., Fernandez-Enright, F., Fung, S. J., Lum, J. S., Engel, M., Andrews, J. L., . . . Newell, K. A. (2015). Alterations of mGluR5 and its endogenous regulators Norbin, Tamalin and Preso1 in schizophrenia: towards a model of mGluR5 dysregulation. *Acta Neuropathol, 130*(1), 119-129.

Mazaki, Y., Hashimoto, S., Tsujimura, T., Morishige, M., Hashimoto, A., Aritake, K., . . . Sabe, H. (2006). Neutrophil direction sensing and superoxide production linked by the GTPase-activating protein GIT2. *Nature Immunology, 7*(7), 724-731.

McCormick, B., Chu, J. Y., & Vermeren, S. (2019). Cross-talk between Rho GTPases and PI3K in the neutrophil. *Small GTPases, 10*(3), 187-195.

McDaniel, J. C., Roy, S., & Wilgus, T. A. (2013). Neutrophil activity in chronic venous leg ulcers-A target for therapy? *Wound Repair and Regeneration, 21*(3), 339-351.

McDonald, B., Pittman, K., Menezes, G. B., Hirota, S. A., Slaba, I., Waterhouse, C. C. M., . . . Kubes, P. (2010). Intravascular Danger Signals Guide Neutrophils to Sites of Sterile Inflammation. *Science, 330*(6002), 362-366.

McEver, R. P. (2015). Selectins: initiators of leucocyte adhesion and signalling at the vascular wall. *Cardiovascular Research, 107*(3), 331-339.

McEver, R. P., & Cummings, R. D. (1997). Role of PSGL-1 binding to selectins in leukocyte recruitment. *Journal of Clinical Investigation, 100*(11), S97-S103.

Melnicoff, M. J., Horan, P. K., & Morahan, P. S. (1989). Kinetics of Changes in Peritoneal Cell-Populations Following Acute-Inflammation. *Cellular Immunology, 118*(1), 178-191.

Metcalf, D. (2007). On hematopoietic stem cell fate. *Immunity, 26*(6), 669-673.

Michaelson, D., Silletti, J., Murphy, G., D'Eustachio, P., Rush, M., & Philips, M. R. (2001). Differential localization of Rho GTPases in live cells: regulation by hypervariable regions and RhoGDI binding. *The Journal of Cell Biology, 152*(1), 111-126.

Middleton, E. A., Weyrich, A. S., & Zimmerman, G. A. (2016). Platelets in Pulmonary Immune Responses and Inflammatory Lung Diseases. *Physiological Reviews, 96*(4), 1211-1259.

Miki, H., Suetsugu, S., & Takenawa, T. (1998). WAVE, a novel WASP-family protein involved in actin reorganization induced by Rac. *Embo j, 17*(23), 6932-6941.

Milligan, G., & Kostenis, E. (2006). Heterotrimeric G-proteins: a short history. *British Journal Pharmacology, 147*, S46-S55.

Miralda, I., Uriarte, S. M., & McLeish, K. R. (2017). Multiple Phenotypic Changes Define Neutrophil Priming. *Front Cell Infect Microbiol, 7*:217.

Miske, R., Gross, C. C., Scharf, M., Golombeck, K. S., Hartwig, M., Bhatia, U., . . . Melzer, N. (2017). Neurochondrin is a neuronal target antigen in autoimmune cerebellar degeneration. *Neurol Neuroimmunol Neuroinflamm, 4*(1), e307.

Mochizuki-Sakisaka, R., Dateki, M., Ishizuka, Y., Yanai, K., Matsuda, Y., Koga, Y., & Fukamizu, A. (2004a). Structural organization of the mouse neurochondrin gene. *International Journal of Molecular Medicine, 14*(3), 361-366.

Mochizuki-Sakisaka, R., Dateki, M., Ishizuka, Y., Yanai, K., Matsuda, Y., Koga, Y., & Fukamizu, A. (2004b). Structural organization of the mouse neurochondrin gene. *International Journal of Molecular Medicine, 14*(3), 361-366.

Mochizuki, R., Dateki, M., Yanai, K., Ishizuka, Y., Amizuka, N., Kawashima, H., . . . Fukamizu, A. (2003). Targeted disruption of the neurochondrin/norbin gene results in embryonic lethality. *Biochem Biophys Res Commun, 310*(4), 1219-1226.

Mochizuki, R., Ishizuka, Y., Yanai, K., Koga, Y., Fukamizu, A., & Murakami, K. (1999). Molecular cloning and expression of human neurochondrin-1 and -2. *Biochim Biophys Acta, 1446*(3), 397-402.

Mocsai, A. (2013). Diverse novel functions of neutrophils in immunity, inflammation, and beyond. *Journal of Experimental Medicine, 210*(7), 1283-1299.

Mocsai, A., Walzog, B., & Lowell, C. A. (2015). Intracellular signalling during neutrophil recruitment. *Cardiovascular Research, 107*(3), 373-385.

Moissoglu, K., & Schwartz, M. A. (2014). Spatial and temporal control of Rho GTPase functions. *Cell Logist, 4*(2), e943618.

Monach, P. A., Nigrovic, P. A., Chen, M., Hock, H., Lee, D. M., Benoist, C., & Mathis, D. (2010). Neutrophils in a Mouse Model of Autoantibody-Mediated Arthritis. *Arthritis and Rheumatism, 62*(3), 753-764.

Monari, C., Kozel, T. R., Bistoni, F., & Vecchiarelli, A. (2002). Modulation of C5aR expression on human Neutrophils by encapsulated and acapsular Cryptococcus neoformans. *Infection and Immunity, 70*(7), 3363-3370.

Monk, P. N., Scola, A. M., Madala, P., & Fairlie, D. P. (2007). Function, structure and therapeutic potential of complement C5a receptors. *British Journal Pharmacology, 152*(4), 429-448.

Montero, J. C., Seoane, S., Ocana, A., & Pandiella, A. (2011). P-Rex1 participates in Neuregulin-ErbB signal transduction and its expression correlates with patient outcome in breast cancer. *Oncogene, 30*(9), 1059-1071.

Montero, J. C., Seoane, S., & Pandiella, A. (2013). Phosphorylation of P-Rex1 at serine 1169 participates in IGF-1R signaling in breast cancer cells. *Cell Signal, 25*(11), 2281-2289.

Mooney, J. E., Rolfe, B. E., Osborne, G. W., Sester, D. P., van Rooijen, N., Campbell, G. R., . . . Campbell, J. H. (2010). Cellular Plasticity of Inflammatory Myeloid Cells in the Peritoneal Foreign Body Response. *American Journal of Pathology, 176*(1), 369-380.

Morikis, V. A., & Simon, S. I. (2018). Neutrophil Mechanosignaling Promotes Integrin Engagement With Endothelial Cells and Motility Within Inflamed Vessels. *Front Immunol, 9*, 2774.

Movilla, N., Dosil, M., Zheng, Y., & Bustelo, X. R. (2001). How Vav proteins discriminate the GTPases Rac1 and RhoA from Cdc42. *Oncogene, 20*(56), 8057-8065.

Mueller, H., Stadtmann, A., Van Aken, H., Hirsch, E., Wang, D., Ley, K., & Zarbock, A. (2010). Tyrosine kinase Btk regulates E-selectin-mediated integrin activation and neutrophil recruitment by controlling phospholipase C (PLC) gamma2 and PI3Kgamma pathways. *Blood, 115*(15), 3118-3127.

Muller, W. A. (2016). Transendothelial migration: unifying principles from the endothelial perspective. *Immunological Reviews, 273*(1), 61-75.

Murdoch, C., & Finn, A. (2000). Chemokine receptors and their role in inflammation and infectious diseases. *Blood, 95*(10), 3032-3043.

Murphy, P. M. (1997). Neutrophil receptors for interleukin-8 and related CXC chemokines. *Semin Hematol, 34*(4), 311-318.

Murphy, P. M., Baggiolini, M., Charo, I. F., Hebert, C. A., Horuk, R., Matsushima, K., . . . Power, C. A. (2000). International union of pharmacology. XXII. Nomenclature for chemokine receptors. *Pharmacological Reviews, 52*(1), 145-176.

Nagase, H., Miyamasu, M., Yamaguchi, M., Imanishi, M., Tsuno, N. H., Matsushima, K., . . . Hirai, K. (2002). Cytokine-mediated regulation of CXCR4 expression in human neutrophils. *Journal Leukocyte Biology, 71*(4), 711-717.

Naik, N., Giannini, E., Brouchon, L., & Boulay, F. (1997). Internalization and recycling of the C5a anaphylatoxin receptor: evidence that the agonist-mediated internalization is modulated by phosphorylation of the C-terminal domain. *Journal of Cell Science, 110*, 2381-2390.

Nathan, C. (2006). Neutrophils and immunity: challenges and opportunities. *Nature Review Immulogy, 6*(3), 173-182.

Nauseef, W. M., & Borregaard, N. (2014). Neutrophils at work. *Nature Immunology, 15*(7), 602-611.

Neves, S. R., Ram, P. T., & Iyengar, R. (2002). G protein pathways. *Science, 296*(5573), 1636-1639.

Nguyen, G. T., Green, E. R., & Mecsas, J. (2017). Neutrophils to the ROScue: Mechanisms of NADPH Oxidase Activation and Bacterial Resistance. *Front Cell Infect Microbiol, 7*, 373.

Nishikimi, A., Fukuhara, H., Su, W. J., Hongu, T., Takasuga, S., Mihara, H., . . . Fukui, Y. (2009). Sequential Regulation of DOCK2 Dynamics by Two Phospholipids During Neutrophil Chemotaxis. *Science, 324*(5925), 384-387.

Norton, L., Lindsay, Y., Deladeriere, A., Chessa, T., Guillou, H., Suire, S., . . . Stephens, L. (2016). Localizing the lipid products of PI3Kgamma in neutrophils. *Adv Biol Regul, 60*, 36-45.

Nourshargh, S., & Alon, R. (2014). Leukocyte migration into inflamed tissues. *Immunity, 41*(5), 694-707.

O'Connell, K., & E Brown, D. (2015). Practical Murine Hematopathology: A Comparative Review and Implications for Research. *Comparitive Medicine. 65*(2), 96-113.

O'Neill, S., Brault, J., Stasia, M. J., & Knaus, U. G. (2015). Genetic disorders coupled to ROS deficiency. *Redox Biology, 6*, 135-156.

Oflaherty, J. T., Rossi, A. G., Redman, J. F., & Jacobson, D. P. (1991). Tumor-Necrosis-Factor-Alpha Regulates Expression of Receptors for Formyl-Methionyl-Leucyl-Phenylalanine, Leukotriene-B4, and Platelet-Activating-Factor - Dissociation from Priming in Human Polymorphonuclear Neutrophils. *Journal of Immunology, 147*(11), 3842-3847.

Oldekamp, S., Pscheidl, S., Kress, E., Soehnlein, O., Jansen, S., Pufe, T., . . . Brandenburg, L. O. (2014). Lack of formyl peptide receptor 1 and 2 leads to more severe inflammation and higher mortality in mice with of pneumococcal meningitis. *Immunology, 143*(3), 447-461.

Oldham, W. M., & Hamm, H. E. (2008). Heterotrimeric G protein activation by G-protein-coupled receptors. *Nature Reviews Molecular Cell Biology, 9*(1), 60-71.

Page, C., & Pitchford, S. (2013). Neutrophil and platelet complexes and their relevance to neutrophil recruitment and activation. *Int Immunopharmacol, 17*(4), 1176-1184.

Paiva, C. N., & Bozza, M. T. (2014). Are reactive oxygen species always detrimental to pathogens? *Antioxid Redox Signal, 20*(6), 1000-1037.

Pan, D., Amison, R. T., Riffo-Vasquez, Y., Spina, D., Cleary, S. J., Wakelam, M. J., . . . Welch, H. C. (2015). P-Rex and Vav Rac-GEFs in platelets control leukocyte recruitment to sites of inflammation. *Blood, 125*(7), 1146-1158.

Pan, D., Barber, M. A., Hornigold, K., Baker, M. J., Toth, J. M., Oxley, D., & Welch, H. C. (2016). Norbin Stimulates the Catalytic Activity and Plasma Membrane Localization of the Guanine-Nucleotide Exchange Factor P-Rex1. *Journal of Biological Chemistry*.

Pandey, S., Mahato, P. K., & Bhattacharyya, S. (2014). Metabotropic glutamate receptor 1 recycles to the cell surface in protein phosphatase 2A-dependent manner in non-neuronal and neuronal cell lines. *Journal Neurochemistry, 131*(5), 602-614.

Pantarelli, C., & Welch, H. C. E. (2018). Rac-GTPases and Rac-GEFs in neutrophil adhesion, migration and recruitment. *European Journal of Clinical Investigation*, e12939.

Petri, B., Phillipson, M., & Kubes, P. (2008). The physiology of leukocyte recruitment: An in vivo perspective. *Journal of Immunology, 180*(10), 6439-6446.

Petty, J. M., Lenox, C. C., Weiss, D. J., Poynter, M. E., & Suratt, B. T. (2009). Crosstalk between CXCR4/Stromal Derived Factor-1 and VLA-4/VCAM-1 Pathways Regulates Neutrophil Retention in the Bone Marrow. *Journal of Immunology, 182*(1), 604-612.

Phillipson, M., Heit, B., Parsons, S. A., Petri, B., Mullaly, S. C., Colarusso, P., . . . Kubes, P. (2009). Vav1 is essential for mechanotactic crawling and migration of neutrophils out of the inflamed microvasculature. *The Journal of Immunology, 182*(11), 6870-6878.

Phillipson, M., & Kubes, P. (2019). The Healing Power of Neutrophils. *Trends Immunol*. 40(7), 635-647

Pierce, K. L., Premont, R. T., & Lefkowitz, R. J. (2002). Seven-transmembrane receptors. *Nature Reviews Molecular Cell Biology, 3*(9), 639-650.

Pillay, J., den Braber, I., Vrisekoop, N., Kwast, L. M., de Boer, R. J., Borghans, J. A. M., . . . Koenderman, L. (2010). In vivo labeling with (H2O)-H-2 reveals a human neutrophil lifespan of 5.4 days. *Blood, 116*(4), 625-627.

Pilsczek, F. H., Salina, D., Poon, K. K., Fahey, C., Yipp, B. G., Sibley, C. D., . . . Kubes, P. (2010). A novel mechanism of rapid nuclear neutrophil extracellular trap formation in response to Staphylococcus aureus. *The Journal of Immunology, 185*(12), 7413-7425.

Pitcher, J. A., Freedman, N. J., & Lefkowitz, R. J. (1998). G protein-coupled receptor kinases. *Annu Rev Biochem, 67*, 653-692.

Pitchford, S., Pan, D. X., & Welch, H. C. E. (2017). Platelets in neutrophil recruitment to sites of inflammation. *Current Opinion in Hematology, 24*(1), 23-31.

Pober, J. S., & Sessa, W. C. (2007). Evolving functions of endothelial cells in inflammation. *Nature Reviews Immunology, 7*(10), 803-815.

Poll, F., Doll, C., & Schulz, S. (2011). Rapid Dephosphorylation of G Protein-coupled Receptors by Protein Phosphatase 1 beta Is Required for Termination of beta-Arrestin-dependent Signaling. *Journal of Biological Chemistry, 286*(38), 32931-32936.

Powell, D., Tauzin, S., Hind, L. E., Deng, Q., Beebe, D. J., & Huttenlocher, A. (2017). Chemokine Signaling and the Regulation of Bidirectional Leukocyte Migration in Interstitial Tissues. *Cell Rep, 19*(8), 1572-1585.

Prado, G. N., Suzuki, H., Wilkinson, N., Cousins, B., & Navarro, J. (1996). Role of the C terminus of the interleukin 8 receptor in signal transduction and internalization. *Journal of Biological Chemistry, 271*(32), 19186-19190

Proebstl, D., Voisin, M. B., Woodfin, A., Whiteford, J., D'Acquisto, F., Jones, G. E., . . . Nourshargh, S. (2012). Pericytes support neutrophil subendothelial cell crawling and breaching of venular walls in vivo. *Journal of Experimental Medicine, 209*(6), 1219-1234.

Qian, F., Le Breton, G. C., Chen, J., Deng, J., Christman, J. W., Wu, D., & Ye, R. D. (2012a). Role for the guanine nucleotide exchange factor P-Rex1 in platelet secretion and aggregation. *Arterioscler Thromb Vasc Biol, 32*(3), 768-777.

Qian, F., Le Breton, G. C., Chen, J., Deng, J., Christman, J. W., Wu, D., & Ye, R. D. (2012b). Role for the guanine nucleotide exchange factor phosphatidylinositol-3,4,5-trisphosphate-dependent rac exchanger 1 in platelet secretion and aggregation. *Arterioscler Thromb Vasc Biol, 32*(3), 768-777.

Qin, J., Xie, Y., Wang, B., Hoshino, M., Wolff, D. W., Zhao, J., . . . Tu, Y. (2009). Upregulation of PIP3-dependent Rac exchanger 1 (P-Rex1) promotes prostate cancer metastasis. *Oncogene, 28*(16), 1853-1863.

Rabiet, M. J., Huet, E., & Boulay, F. (2007). The N-formyl peptide receptors and the anaphylatoxin C5a receptors: An overview. *Biochimie, 89*(9), 1089-1106.

Raffetseder, U., Roper, D., Mery, L., Gietz, C., Klos, A., Grotzinger, J., . . . Bautsch, W. (1996). Site-directed mutagenesis of conserved charged residues in the helical region of the human C5a receptor - Arg206 determines high-affinity binding sites of C5a receptor. *European Journal of Biochemistry, 235*(1-2), 82-90.

Reiter, E., & Lefkowitz, R. J. (2006). GRKs and beta-arrestins: roles in receptor silencing, trafficking and signaling. *Trends in Endocrinology and Metabolism, 17*(4), 159-165.

Remick, D. G., Green, L. B., Newcomb, D. E., Garg, S. J., Bolgos, G. L., & Call, D. R. (2001). CXC chemokine redundancy ensures local neutrophil recruitment during acute inflammation. *American Journal of Pathology, 159*(3), 1149-1157.

Richards, L., Ferreira, D. M., Miyaji, E. N., Andrew, P. W., & Kadioglu, A. (2010). The immunising effect of pneumococcal nasopharyngeal colonisation; protection against future colonisation and fatal invasive disease. *Immunobiology, 215*(4), 251-263.

Richardson, R. M., Marjoram, R. J., Barak, L. S., & Snyderman, R. (2003). Role of the cytoplasmic tails of CXCR1 and CXCR2 in mediating leukocyte migration, activation, and regulation. *Journal of Immunology, 170*(6), 2904-2911.

Richardson, R. M., Pridgen, B. C., Haribabu, B., Ali, H., & Snyderman, R. (1998). Differential cross-regulation of the human chemokine receptors CXCR1 and CXCR2 - Evidence for time-dependent signal generation. *Journal of Biological Chemistry, 273*(37), 23830-23836.

Ridley, A. J. (2015). Rho GTPase signalling in cell migration. *Curr Opin Cell Biol, 36*, 103-112.

Roberts, A. W., Kim, C., Zhen, L., Lowe, J. B., Kapur, R., Petryniak, B., . . . Williams, D. A. (1999). Deficiency of the hematopoietic cell-specific Rho family GTPase Rac2 is characterised by abnormalities in neutrophil function and host defense. *Immunity, 10*(2), 183-196.

Robertson, N., Rappas, M., Dore, A. S., Brown, J., Bottegoni, G., Koglin, M., . . . Marshall, F. H. (2018). Structure of the complement C5a receptor bound to the extra-helical antagonist NDT9513727. *Nature, 553*(7686), 111-+.

Rommel, F. R., Miske, R., Stocker, W., Arneth, B., Neubauer, B. A., & Hahn, A. (2017). Chorea Minor Associated with Anti-Neurochondrin Autoantibodies. *Neuropediatrics, 48*(6), 482-483.

Roos, D. (2016). Chronic granulomatous disease. *British Medical Bulletin, 118*(1), 53-66.

Rorvig, S., Ostergaard, O., Heegaard, N. H. H., & Borregaard, N. (2013). Proteome profiling of human neutrophil granule subsets, secretory vesicles, and cell membrane: correlation with transcriptome profiling of neutrophil precursors. *Journal Leukocyte Biology, 94*(4), 711-721.

Rosenfeldt, H., Vazquez-Prado, J., & Gutkind, J. S. (2004). P-REX2, a novel PI-3-kinase sensitive Rac exchange factor. *FEBS Lett, 572*(1-3), 167-171.

Rossman, K. L., Der, C. J., & Sondek, J. (2005). GEF means go: turning on RHO GTPases with guanine nucleotide-exchange factors. *Nat Rev Molecular Cell Biol, 6*(2), 167-180.

Sabroe, I., Jones, E. C., Whyte, M. K. B., & Dower, S. K. (2005). Regulation of human neutrophil chemokine receptor expression and function by activation of Toll-like receptors 2 and 4. *Immunology, 115*(1), 90-98.

Sabroe, I., Lloyd, C. M., Whyte, M. K. B., Dower, S. K., Williams, T. J., & Pease, J. E. (2002). Chemokines, innate and adaptive immunity, and respiratory disease. *European Respiratory Journal, 19*(2), 350-355.

Sabroe, I., Williams, T. J., Hebert, C. A., & Collins, P. D. (1997). Chemoattractant cross-desensitization of the human neutrophil IL-8 receptor involves receptor internalization and differential receptor subtype regulation. *Journal of Immunology, 158*(3), 1361-1369.

Sadik, C. D., Miyabe, Y., Sezin, T., & Luster, A. D. (2018). The critical role of C5a as an initiator of neutrophil-mediated autoimmune inflammation of the joint and skin. *Semin Immunol, 37*(C), 21-29.

Saffarzadeh, M., Juenemann, C., Queisser, M. A., Lochnit, G., Barreto, G., Galuska, S. P., . . . Preissner, K. T. (2012). Neutrophil extracellular traps directly induce epithelial and endothelial cell death: a predominant role of histones. *PLoS One, 7*(2), e32366.

Samanta, A. K., Oppenheim, J. J., & Matsushima, K. (1990). Interleukin-8 (Monocyte-Derived Neutrophil Chemotactic Factor) Dynamically Regulates Its Own Receptor Expression on Human-Neutrophils. *Journal of Biological Chemistry, 265*(1), 183-189.

Sander, E. E., ten Klooster, J. P., van Delft, S., van der Kammen, R. A., & Collard, J. G. (1999). Rac downregulates Rho activity: Reciprocal balance between both GTPases determines cellular morphology and migratory behavior. *Journal of Cell Biology, 147*(5), 1009-1021.

Schmitz, A. L., Schrage, R., Gaffal, E., Charpentier, T. H., Wiest, J., Hiltensperger, G., . . . Kostenis, E. (2014). A Cell-Permeable Inhibitor to Trap G alpha(q) Proteins in the Empty Pocket Conformation. *Chemistry & Biology, 21*(7), 890-902.

Schnelzer, A., Prechtel, D., Knaus, U., Dehne, K., Gerhard, M., Graeff, H., . . . Lengyel, E. (2000). Rac1 in human breast cancer: overexpression, mutation analysis, and characterization of a new isoform, Rac1b. *Oncogene, 19*(26), 3013-3020.

Schonrich, G., & Raftery, M. J. (2016). Neutrophil Extracellular Traps Go Viral. *Front Immunol, 7*.

Schumacher, M., Rommel, F. R., Ameth, B., Renz, H., Stocker, W., Windhorst, A., . . . Neubauer, B. A. (2019). Encephalopathy Associated With Neurochondrin Autoantibodies. *Journal of Child Neurology*, 883073819849773.

Segel, G. B., Halterman, M. W., & Lichtman, M. A. (2011). The paradox of the neutrophil's role in tissue injury. *Journal Leukocyte Biology, 89*(3), 359-372.

Selders, G. S., Fetz, A. E., Radic, M. Z., & Bowlin, G. L. (2017). An overview of the role of neutrophils in innate immunity, inflammation and host-biomaterial integration. *Regen Biomater, 4*(1), 55-68.

Semerad, C. L., Liu, F. L., Gregory, A. D., Stumpf, K., & Link, D. C. (2002). G-CSF is an essential regulator of neutrophil trafficking from the bone marrow to the blood. *Immunity, 17*(4), 413-423.

Sengelov, H. (1995). Complement Receptors in Neutrophils. *Critical Reviews in Immunology, 15*(2), 107-131.

Sengelov, H., Boulay, F., Kjeldsen, L., & Borregaard, N. (1994). Subcellular-Localization and Translocation of the Receptor for N-Formylmethionyl-Leucyl-Phenylalanine in Human Neutrophils. *Biochemical Journal, 299*, 473-479.

Shen, B., Delaney, M. K., & Du, X. (2012). Inside-out, outside-in, and inside-outside-in: G protein signaling in integrin-mediated cell adhesion, spreading, and retraction. *Curr Opin Cell Biol, 24*(5), 600-606.

Shenoy, S. K., & Lefkowitz, R. J. (2003). Multifaceted roles of beta-arrestins in the regulation of seven-membrane-spanning receptor trafficking and signalling. *Biochemical Journal, 375*(Pt 3), 503-515.

Shinozaki, K., Kume, H., Kuzume, H., Obata, K., & Maruyama, K. (1999). Norbin, a neurite-outgrowth-related protein, is a cytosolic protein localized in the somatodendritic region of neurons and distributed prominently in dendritic outgrowth in Purkinje cells. *Brain Res Mol Brain Res, 71*(2), 364-368.

Shinozaki, K., Maruyama, K., Kume, H., Kuzume, H., & Obata, K. (1997). A novel brain gene, norbin, induced by treatment of tetraethylammonium in rat hippocampal slice and accompanied with neurite-outgrowth in neuro 2a cells. *Biochem Biophys Res Commun, 240*(3), 766-771.

Siciliano, S. J., Rollins, T. E., & Springer, M. S. (1990). Interaction between the C5a Receptor and Gi in Both the Membrane-Bound and Detergent-Solubilized States. *Journal of Biological Chemistry, 265*(32), 19568-19574.

Siehler, S. (2009). Regulation of RhoGEF proteins by G12/13-coupled receptors. *British Journal Pharmacology, 158*(1), 41-49.

Skokowa, J., Cario, G., Uenalan, M., Schambach, A., Germeshausen, M., Battmer, K., . . . Welte, K. (2006). LEF-1 is crucial for neutrophil granulocytopoiesis and its expression is severely reduced in congenital neutropenia. *Nat Med, 12*(10), 1191-1197.

Soehnlein, O., & Lindbom, L. (2010). Phagocyte partnership during the onset and resolution of inflammation. *Nature Reviews Immunology, 10*(6), 427-439.

Sondek, J., Bohm, A., Lambright, D. G., Hamm, H. E., & Sigler, P. B. (1996). Crystal structure of a G-protein beta gamma dimer at 2.1A resolution. *Nature, 379*(6563), 369-374.

Sorkin, A., & von Zastrow, M. (2009). Endocytosis and signalling: intertwining molecular networks. *Nature Reviews Molecular Cell Biology, 10*(9), 609-622.

Sosa, M. S., Lopez-Haber, C., Yang, C., Wang, H., Lemmon, M. A., Busillo, J. M., . . . Kazanietz, M. G. (2010). Identification of the Rac-GEF P-Rex1 as an essential mediator of ErbB signaling in breast cancer. *Molecular Cell, 40*(6), 877-892.

Standish, A. J., & Weiser, J. N. (2009). Human neutrophils kill Streptococcus pneumoniae via serine proteases. *The Journal of Immunology, 183*(4), 2602-2609.

Stark, A. K., Chandra, A., Chakraborty, K., Alam, R., Carbonaro, V., Clark, J., . . . Okkenhaug, K. (2018). PI3Kdelta hyper-activation promotes development of B cells that exacerbate Streptococcus pneumoniae infection in an antibody-independent manner. *Nature Communication, 9*(1), 3174.

Stark, K., Eckart, A., Haidari, S., Tirniceriu, A., Lorenz, M., von Bruhl, M. L., . . . Massberg, S. (2013). Capillary and arteriolar pericytes attract innate leukocytes exiting through venules and 'instruct' them with pattern-recognition and motility programs. *Nature Immunology, 14*(1), 41-51.

Steinwede, K., Henken, S., Bohling, J., Maus, R., Ueberberg, B., Brumshagen, C., . . . Maus, U. A. (2012). TNF-related apoptosis-inducing ligand (TRAIL) exerts therapeutic efficacy for the treatment of pneumococcal pneumonia in mice. *Journal of Experimental Medicine, 209*(11), 1937-1952.

Stephens, L., Milne, L., & Hawkins, P. (2008). Moving towards a better understanding of chemotaxis. *Current Biology, 18*(11), R485-494.

Stevens, W. W., Taeg, S. K., Pujanauski, L. A., Hao, X. L., & Braciale, T. J. (2007). Detection and quantitation of eosinophils in the murine respiratory tract by flow cytometry. *Journal of Immunological Methods, 327*(1-2), 63-74.

Stockley, R. A., Grant, R. A., Llewellynjones, C. G., Hill, S. L., & Burnett, D. (1994). Neutrophil Formyl-Peptide Receptors - Relationship to Peptide-Induced Responses and Emphysema. *Am J Respir Crit Care Med, 149*(2), 464-468.

Stoyanov, B., Volinia, S., Hanck, T., Rubio, I., Loubtchenkov, M., Malek, D., . . . Wetzker, R. (1995). Cloning and Characterization of a G-Protein-Activated Human Phosphoinositide-3 Kinase. *Science, 269*(5224), 690-693.

Strydom, N., & Rankin, S. M. (2013). Regulation of Circulating Neutrophil Numbers under Homeostasis and in Disease. *Journal of Innate Immunity, 5*(4), 304-314.

Sugiyama, T., Kohara, H., Noda, M., & Nagasawa, T. (2006). Maintenance of the hematopoietic stem cell pool by CXCL12-CXCR4 chemokine signaling in bone marrow stromal cell niches. *Immunity, 25*(6), 977-988.

Summers, C., Rankin, S. M., Condliffe, A. M., Singh, N., Peters, A. M., & Chilvers, E. R. (2010). Neutrophil kinetics in health and disease. *Trends Immunol, 31*(8), 318-324.

Sun, C. X., Downey, G. P., Zhu, F., Koh, A. L. Y., Thang, H., & Glogauer, M. (2004). Rac1 is the small GTPase responsible for regulating the neutrophil chemotaxis compass. *Blood, 104*(12), 3758-3765.

Sungkaworn, T., Jobin, M. L., Burnecki, K., Weron, A., Lohse, M. J., & Calebiro, D. (2017). Single-molecule imaging reveals receptor-G protein interactions at cell surface hot spots. *Nature, 550*(7677), 543-+.

Suvorova, E. S., Gripentrog, J. M., Oppermann, M., & Miettinen, H. M. (2008). Role of the carboxyl terminal di-leucine in phosphorylation and internalization of C5a receptor. *Biochimica Et Biophysica Acta-Molecular Cell Research, 1783*(6), 1261-1270.

Swat, W., & Fujikawa, K. (2005). The Vav family - At the crossroads of signaling pathways. *Immunologic Research, 32*(1-3), 259-265.

Tak, T., Tesselaar, K., Pillay, J., Borghans, J. A. M., & Koenderman, L. (2013). What's your age again? Determination of human neutrophil half-lives revisited. *Journal Leukocyte Biology, 94*(4), 595-601.

Takai, Y., Sasaki, T., & Matozaki, T. (2001). Small GTP-binding proteins. *Physiological Reviews, 81*(1), 153-208.

Tan, C. M., Brady, A. E., Nickols, H. H., Wang, Q., & Limbird, L. E. (2004). Membrane trafficking of G protein-coupled receptors. *Annual Review of Pharmacology and Toxicology, 44*, 559-609.

Taut, K., Winter, C., Briles, D. E., Paton, J. C., Christman, J. W., Maus, R., . . . Maus, U. A. (2008). Macrophage Turnover Kinetics in the Lungs of Mice Infected with Streptococcus pneumoniae. *Am J Respir Cell Mol Biol, 38*(1), 105-113.

Tennenberg, S. D., & Solomkin, J. S. (1988). Neutrophil Activation in Sepsis - the Relationship between Fmet-Leu-Phe Receptor Mobilisation and Oxidative Activity. *Archives of Surgery, 123*(2), 171-175.

Tkalcevic, J., Novelli, M., Phylactides, M., Iredale, J. P., Segal, A. W., & Roes, J. (2000). Impaired immunity and enhanced resistance to endotoxin in the absence of neutrophil elastase and cathepsin G. *Immunity, 12*(2), 201-210.

Troeger, A., & Williams, D. A. (2013). Hematopoietic-specific Rho GTPases Rac2 and RhoH and human blood disorders. *Exp Cell Res, 319*(15), 2375-2383.

Tsonou E, Hornigold K., Pantarelli C, Welch HCE. (2018). P-Rex2. In S. Choi (Ed.), *Encyclopedia of Signaling Molecules* (2nd edition ed., pp. 4142-4154): Springer, Cham.

Turner, M., & Billadeau, D. D. (2002). VAV proteins as signal integrators for multi-subunit immune-recognition receptors. *Nature Review Immulogy, 2*(7), 476-486.

Tzeng, Y. S., Li, H., Kang, Y. L., Chen, W. C., Cheng, W. C., & Lai, D. M. (2011). Loss of Cxcl12/Sdf-1 in adult mice decreases the quiescent state of hematopoietic stem/progenitor cells and alters the pattern of hematopoietic regeneration after myelosuppression. *Blood, 117*(2), 429-439.

Utomo, A., Cullere, X., Glogauer, M., Swat, W., & Mayadas, T. N. (2006). Vav proteins in neutrophils are required for FcgammaR-mediated signaling to Rac GTPases and nicotinamide adenine dinucleotide phosphate oxidase component p40(phox). *The Journal of Immunology, 177*(9), 6388-6397.

Utomo, A., Hirahashi, J., Mekala, D., Asano, K., Glogauer, M., Cullere, X., & Mayadas, T. N. (2008). Requirement for Vav proteins in post-recruitment neutrophil cytotoxicity in IgG but not complement C3-dependent injury. *The Journal of Immunology, 180*(9), 6279-6287.

Van Avondt, K., & Hartl, D. (2018). Mechanisms and disease relevance of neutrophil extracellular trap formation. *Eur J Clin Invest, 48 Suppl 2*, e12919.

Vatansever, F., de Melo, W. C. M. A., Avci, P., Vecchio, D., Sadasivam, M., Gupta, A., . . . Hamblin, M. R. (2013). Antimicrobial strategies centered around reactive oxygen species - bactericidal antibiotics, photodynamic therapy, and beyond. *Fems Microbiology Reviews, 37*(6), 955-989.

Vestweber, D. (2007). Adhesion and signaling molecules controlling the transmigration of leukocytes through endothelium. *Immunological Reviews, 218*, 178-196.

Voisin, M. B., & Nourshargh, S. (2013). Neutrophil Transmigration: Emergence of an Adhesive Cascade within Venular Walls. *Journal of Innate Immunity, 5*(4), 336-347.

von Vietinghoff, S., Asagiri, M., Azar, D., Hoffmann, A., & Ley, K. (2010). Defective Regulation of CXCR2 Facilitates Neutrophil Release from Bone Marrow Causing Spontaneous Inflammation in Severely NF-kappa B-Deficient Mice. *Journal of Immunology, 185*(1), 670-678.

Wang, H., Duan, X., Ren, Y., Liu, Y., Huang, M., Liu, P., . . . Zheng, W. (2013). FoxO3a negatively regulates nerve growth factor-induced neuronal differentiation through inhibiting the expression of neurochondrin in PC12 cells. *Mol Neurobiol, 47*(1), 24-36.

Wang, H., Nong, Y., Bazan, F., Greengard, P., & Flajolet, M. (2010). Norbin: A promising central nervous system regulator. *Commun Integr Biol, 3*(6), 487-490.

Wang, H., Warner-Schmidt, J., Varela, S., Enikolopov, G., Greengard, P., & Flajolet, M. (2015). Norbin ablation results in defective adult hippocampal neurogenesis and depressive-like behavior in mice. *Proceedings of the National Academy of Sciences of the United States of America, 112*(31), 9745-9750.

Wang, H., Westin, L., Nong, Y., Birnbaum, S., Bendor, J., Brismar, H., . . . Greengard, P. (2009). Norbin is an endogenous regulator of metabotropic glutamate receptor 5 signaling. *Science, 326*(5959), 1554-1557.

Wang, H. Y., MacDonald, M. L., Borgmann-Winter, K. E., Banerjee, A., Sleiman, P., Tom, A., . . . Hahn, C. G. (2018). mGluR5 hypofunction is integral to glutamatergic dysregulation in schizophrenia. *Mol Psychiatry*.

Wang, J. (2018). Neutrophils in tissue injury and repair. *Cell and Tissue Research, 371*(3), 531-539.

Wang, J. H., Hirose, H., Du, G. H., Chong, K., Kiyohara, E., Witz, I. P., & Hoon, D. S. B. (2017). P-REX1 amplification promotes progression of cutaneous melanoma via the PAK1/P38/MMP-2 pathway. *Cancer Letters, 407*, 66-75.

Wang, Z., Dong, X., Li, Z., Smith, J. D., & Wu, D. (2008). Lack of a significant role of P-Rex1, a major regulator of macrophage Rac1 activation and chemotaxis, in atherogenesis. *Prostaglandins Other Lipid Mediat, 87*(1-4), 9-13.

Wang, Z. L., Dong, X. M., Li, Z., Smith, J. D., & Wu, D. (2008). Lack of a significant role of P-Rex1, a major regulator of macrophage Rac1 activation and chemotaxis, in atherogenesis. *Prostaglandins Other Lipid Mediat, 87*(1-4), 9-13.

Ward, R. J., Jenkins, L., & Milligan, G. (2009). Selectivity and functional consequences of interactions of family A G protein-coupled receptors with neurochondrin and periplakin. *Journal Neurochemistry, 109*(1), 182-192.

Watanabe, M., Terasawa, M., Miyano, K., Yanagihara, T., Uruno, T., Sanematsu, F., . . . Fukui, Y. (2014). DOCK2 and DOCK5 Act Additively in Neutrophils To Regulate Chemotaxis, Superoxide Production, and Extracellular Trap Formation. *Journal of Immunology, 193*(11), 5660-5667.

Weihua, Z., Haitao, R., Fang, F., Xunzhe, Y., Jing, W., & Hongzhi, G. (2019). Neurochondrin Antibody Serum Positivity in Three Cases of Autoimmune Cerebellar Ataxia. *Cerebellum*.

Weiss, S. J. (1989). Tissue destruction by neutrophils. *New England Journal Medicine, 320*(6), 365-376.

Weisser, S. B., van Rooijen, N., & Sly, L. M. (2012). Depletion and reconstitution of macrophages in mice. *J Vis Exp*(66), 4105.

Welch, H. C. (2015). Regulation and function of P-Rex family Rac-GEFs. *Small GTPases, 6*(2), 49-70.

Welch, H. C., Coadwell, W. J., Ellson, C. D., Ferguson, G. J., Andrews, S. R., Erdjument-Bromage, H., . . . Stephens, L. R. (2002). P-Rex1, a PtdIns(3,4,5)P3- and Gbetagamma-regulated guanine-nucleotide exchange factor for Rac. *Cell, 108*(6), 809-821.

Welch, H. C., Condliffe, A. M., Milne, L. J., Ferguson, G. J., Hill, K., Webb, L. M., . . . Stephens, L. R. (2005). P-Rex1 regulates neutrophil function. *Current Biology, 15*(20), 1867-1873.

Wennerberg, K., & Der, C. J. (2004). Rho-family GTPases: it's not only Rac and Rho (and I like it). *Journal of Cell Science, 117*(Pt 8), 1301-1312.

Wennerberg, K., Rossman, K. L., & Der, C. J. (2005). The Ras superfamily at a glance. *Journal of Cell Science, 118*(5), 843-846.

Wieland, C. W., Florquin, S., Maris, N. A., Hoebe, K., Beutler, B., Takeda, K., . . . van der Poll, T. (2005). The MyD88-dependent, but not the MyD88-independent, pathway of TLR4 signaling is important in clearing nontypeable Haemophilus influenzae from the mouse lung. *Journal of Immunology, 175*(9), 6042-6049.

Williams, D. A., Tao, W., Yang, F. C., Kim, C., Gu, Y., Mansfield, P., . . . Boxer, L. (2000). Dominant negative mutation of the hematopoietic-specific Rho GTPase, Rac2, is associated with a human phagocyte immunodeficiency. *Blood, 96*(5), 1646-1654.

Wolf, M., Delgado, M. B., Jones, S. A., Dewald, B., Clark-Lewis, I., & Baggiolini, M. (1998). Granulocyte chemotactic protein 2 acts via both IL-8 receptors, CXCR1 and CXCR2. *European Journal of Immunology, 28*(1), 164-170.

Wong, C. Y. A., Jiang, H. H., Abel, P. W., Scofield, M. A., Xie, Y., Wei, T. T., & Tu, Y. P. (2016). Phorbol myristate acetate suppresses breast cancer cell growth via down-regulation of P-Rex1 expression. *Protein & Cell, 7*(6), 445-449.

Wong, C. Y. A., Wuriyanghan, H., Xie, Y., Lin, M. F., Abel, P. W., & Tu, Y. P. (2011). Epigenetic Regulation of Phosphatidylinositol 3,4,5-Triphosphate-dependent Rac Exchanger 1 Gene Expression in Prostate Cancer Cells. *Journal of Biological Chemistry, 286*(29), 25813-25822.

Wright, H. L., Thomas, H. B., Moots, R. J., & Edwards, S. W. (2013). RNA-Seq Reveals Activation of Both Common and Cytokine-Specific Pathways following Neutrophil Priming. *PLoS One, 8*(3).

Xu, Y., Li, Z., Yao, L., Zhang, X., Gan, D., Jiang, M., . . . Wang, X. (2017). Altered Norbin Expression in Patients with Epilepsy and a Rat Model. *Scientific Reports, 7*(1), 13970.

Xue, R., Lynes, M. D., Dreyfuss, J. M., Shamsi, F., Schulz, T. J., Zhang, H., . . . Tseng, Y. H. (2015). Clonal analyses and gene profiling identify genetic biomarkers of the thermogenic potential of human brown and white preadipocytes. *Nat Med, 21*(7), 760-768.

Yang, J., Zhang, L., Yu, C., Yang, X. F., & Wang, H. (2014). Monocyte and macrophage differentiation: circulation inflammatory monocyte as biomarker for inflammatory diseases. *Biomark Res, 2*(1), 1.

Yang, N., Higuchi, O., Ohashi, K., Nagata, K., Wada, A., Kangawa, K., . . . Mizuno, K. (1998). Cofilin phosphorylation by LIM-kinase 1 and its role in Rac-mediated actin reorganization. *Nature, 393*(6687), 809-812.

Yipp, B. G., Petri, B., Salina, D., Jenne, C. N., Scott, B. N. V., Zbytnuik, L. D., . . . Kubes, P. (2012). Infection-induced NETosis is a dynamic process involving neutrophil multitasking in vivo. *Nat Med, 18*(9), 1386-+.

Yoo, S. K., Deng, Q., Cavnar, P. J., Wu, Y. I., Hahn, K. M., & Huttenlocher, A. (2010). Differential Regulation of Protrusion and Polarity by PI(3)K during Neutrophil Motility in Live Zebrafish. *Developmental Cell, 18*(2), 226-236.

Yoshimura, T., Matsushima, K., Tanaka, S., Robinson, E. A., Appella, E., Oppenheim, J. J., & Leonard, E. J. (1987). Purification of a Human Monocyte-Derived Neutrophil Chemotactic Factor That Has Peptide Sequence Similarity to Other Host Defense Cytokines. *Proceedings of the National Academy of Sciences of the United States of America, 84*(24), 9233-9237.

Yoshizawa, M., Kawauchi, T., Sone, M., Nishimura, Y. V., Terao, M., Chihama, K., . . . Hoshino, M. (2005). Involvement of a Rac activator,P-Rex1, in neurotrophin-derived signaling and neuronal migration. *Journal Neuroscience, 25*(17), 4406-4419.

Zarbock, A., Ley, K., McEver, R. P., & Hidalgo, A. (2011). Leukocyte ligands for endothelial selectins: specialized glycoconjugates that mediate rolling and signaling under flow. *Blood, 118*(26), 6743-6751.

Zhang, X., Glogauer, M., Zhu, F., Kim, T. H., Chiu, B., & Inman, R. D. (2005). Innate immunity and arthritis - Neutrophil Rac and toll-like receptor 4 expression define outcomes in infection-triggered arthritis. *Arthritis and Rheumatism, 52*(4), 1297-1304.

Zhao, T., Nalbant, P., Hoshino, M., Dong, X., Wu, D., & Bokoch, G. M. (2007). Signaling requirements for translocation of P-Rex1, a key Rac2 exchange factor involved in chemoattractant-stimulated human neutrophil function. *Journal Leukocyte Biology, 81*(4), 1127-1136.

Appendix A - Supplementary Figures

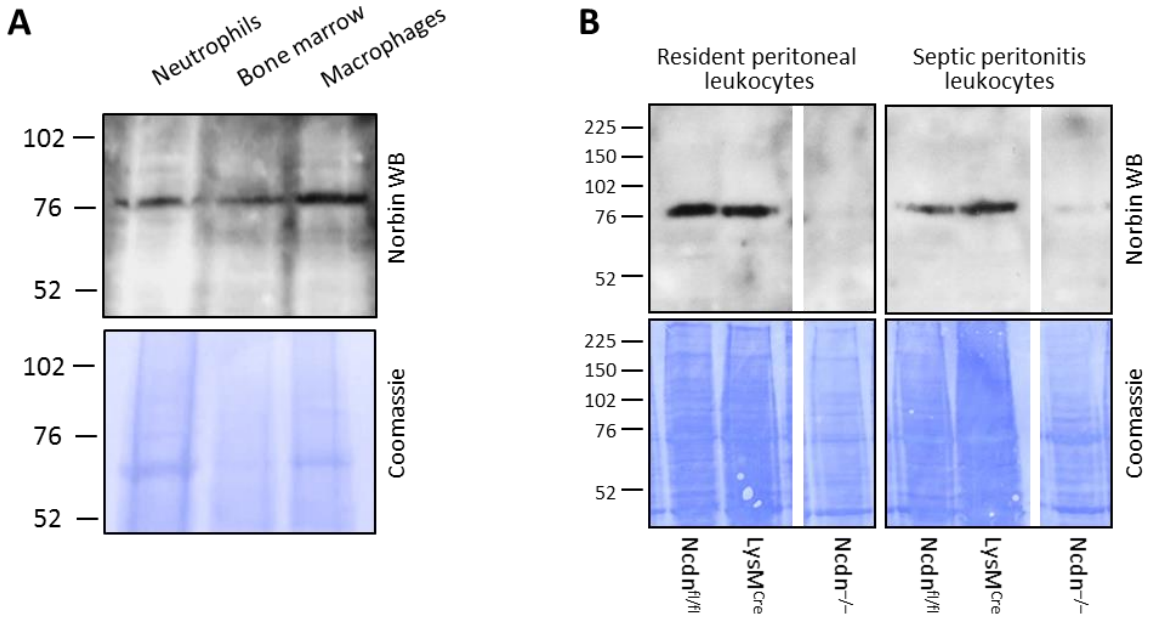

Supplementary Figure 1: Expression of Norbin in the myeloid cell lineage and deletion in peritoneal leukocytes of Ncdn$^{-/-}$ mice

(A) Norbin is expressed in neutrophils. Total lysates of bone marrow cells, macrophages and neutrophils isolated from adult wild-type mice (100 µg tissue per lane) were western blotted for Norbin expression using Norbin C1 antibody and protein loading assessed by coomassie staining.

(B) Norbin is deleted in myeloid cells. Mature neutrophils and monocyte/macrophages were isolated from peritoneal exudates of Ncdn$^{fl/fl}$ (floxed Norbin), LysM^{Cre} (myeloid Cre) and Ncdn$^{-/-}$ (myeloid Norbin KO) mice before and after LPS stimulation (Sigma, 25 µg.kg^{-1}, prepared in sterile saline to a final volume of 200 µL) for 4 h. Total cell lysates were subjected to Western blotting with Norbin C1 antibody and equal protein loading was assessed by coomassie staining. The western blots (WBs) of Ncdn$^{fl/fl}$, LysM^{Cre} lysates showed a 79 kDa band that was efficiently deleted from Ncdn$^{-/-}$ lysates. Previous PhD student, Dr Dingxin Pan, generated the data from this figure. Panel A is adapted from (Pan et al., 2016), panel B is unpublished.

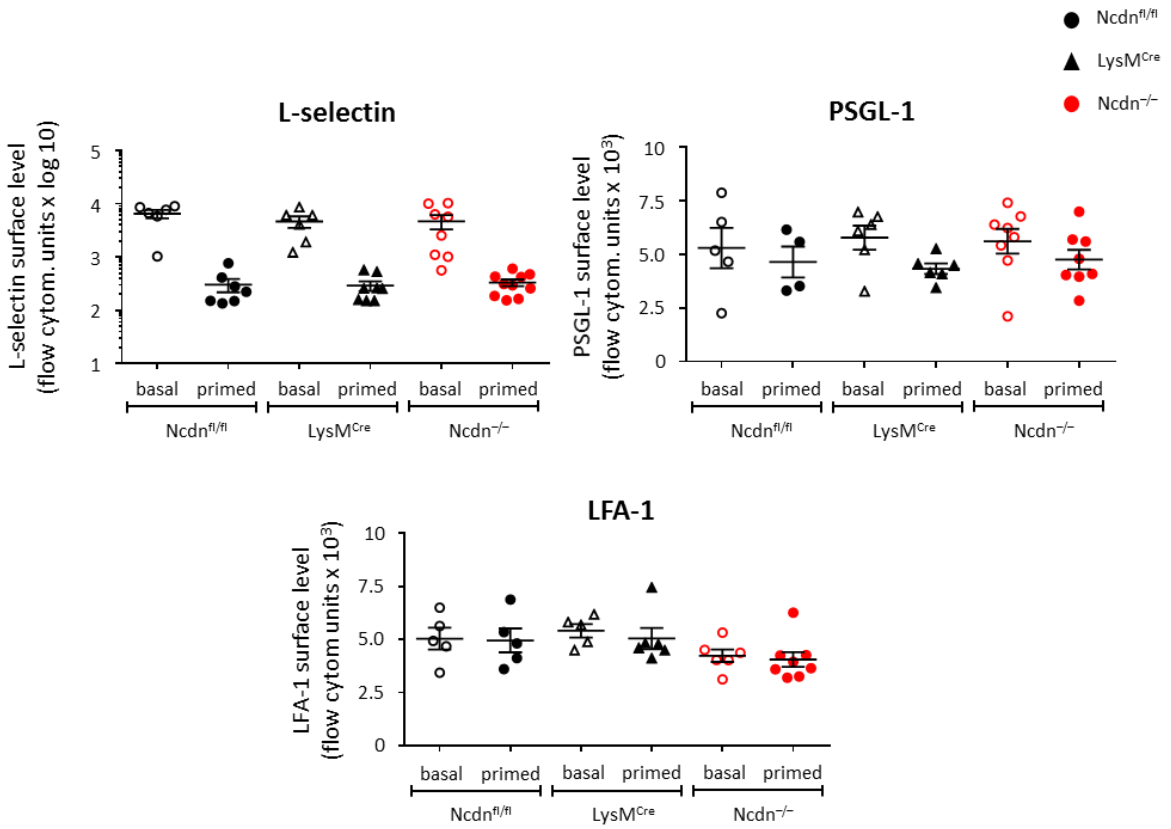

Supplementary Figure 2: Norbin-deficient neutrophils have normal cell surface levels of integrins
Bone marrow cells from Ncdn$^{fl/fl}$, LysM^{Cre} and Ncdn$^{-/-}$ mice were primed with 20 ng.mL^{-1} murine TNFα and 40 ng.mL^{-1} GM-CSF for 45 min at 37°C, or left on ice (basal), before being transferred onto ice and stained to investigate the level of L-selectin, PSGL-1 and LFA-1 integrins on the neutrophil surface by flow cytometry. Neutrophils were detected by their scatter characteristics and BV510-Ly6G antibody staining and the various integrin identified by the signal of the appropriate antibody staining. All conditions were assessed in parallel. Each dot is the mean of one experiment. Data are mean ± SEM of 4-8 independent experiments. Statistical significance was assessed using two-way Anova with Sidak's multiple comparisons test. Previous PhD student, Dr Dingxin Pan, generated the data from this figure.

Appendix B - Publications